THEME II

SEISMIC BEHAVIOUR OF STRUCTURAL CONCRETE LINEAR ELEMENTS (BEAMS, COLUMNS) AND THEIR CONNECTIONS

COMPORTEMENT SISMIQUE DES ELEMENTS STRUCTURAUX LINEAIRES (POUTRES, POTEAUX) ET DE LEURS JONCTIONS

Reporter
Rapporteur

Vitelmo BERTERO
University of California
Berkeley, Calif., USA

ANALYTICAL STUDY OF R/C MATERIAL HYSTERESIS

A. Emin AKTAN
Middle East Technical University
Ankara, Turkey

U. ERSOY
Middle East Technical University
Ankara, Turkey

SUMMARY

Analytical section responses were generated for reinforced concrete column specimens tested and reported by a number of authors. Different hysteresis models for the materials were incorporated, varying a number of parameters. Comparison of analytical and experimental responses led to an assesment of material hysteresis in generating column section response.

RESUME

Les réactions des sections sont produties analytiquement pour des spécimens de colonnes en beton armé qui avaient été auparavant étudiés empiriquement par des auteurs différents. Les différents modéles d'hysteresis pour les matériaux sont traités en variant certains paramétres. La comparaison des réactions analytiques et experimentales aboutit a une évaluation de l'hysteresis des matériaux dans le cas des réactions des sections de colonnes.

INTRODUCTION

The main purpose of this study is to investigate the required sophistication and basic parameters of the material hysteresis models in generating hysteretic response of reinforced concrete column crossections. An analytical assessment of material hysteresis through column section response is considered appropriate since experimental data is available, the methodology is well established and bond is not directly involved as in member response. Any information gained through such an investigation can be extrapolated to material response in analysis problems involving different stress configurations.

A multi-linear hysteresis model for steel and two hysteresis models for concrete are constructed with the information provided by tests and studies on material behavior by Aktan (1973), Hognestad (1955), Kent (1971), Smith (1955) and Karsan (1969). The finite-filament technique, proposed by Aktan (1974) was incorporated in conjunction with these material hysteresis models to generate column section response.

A significantly more detailed presentation of the study presented in this paper is contained in Reference 4 by Ersoy (1976).

MATERIAL HYSTERESIS MODELS

Steel (Fig. 1)

The elastic-strain hardening plastic initial loading paths in both directions constitute the envelopes for strain reversals. Unloading slopes in tension or compression are equal to the modulus of elasticity until a line through the origin and parallel to the plastic paths are intercepted. Unloading continues linearly with a smaller slope termed as the Bauschinger slope.

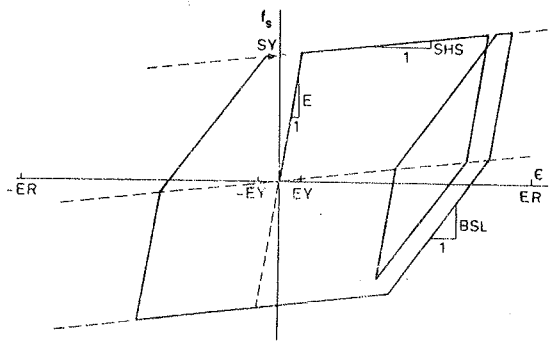

Fig. 1 Steel Hysteresis Model

The multi-linear model has only the Bauschinger slope as a hysteresis parameter. The yield stress and strain as well as the strain hardening slope are characteristics of the monotonic strain behavior. This model is considered to have practical advantages over the Ramberg-Osgood representation as the significantly more complicated Ramberg-Osgood model has three hysteresis

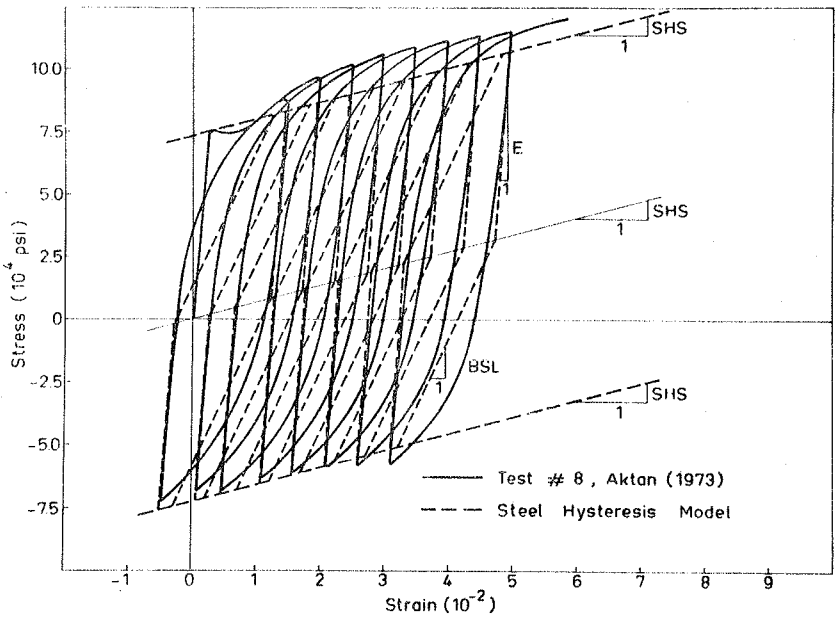

Fig. 2 Comparison of Steel Hysteresis Model With Test # 8, Aktan (1973)
(1psi = 0.07 kgf per cm^2)

parameters which need to be determined by regression techniques applied to test results. Borrowing this information to apply to material with different virgin properties does not necessarily result in a better simulation of section response compared to that provided by the multi-linear model. The proposed steel hysteresis model is checked against coupon test #8 reported by Aktan (1973) in Fig. 2. The Bauschinger slope is observed to be approximately 20% of the modulus of elasticity for this specimen.

Concrete Hysteresis Model 1 (Fig. 3)

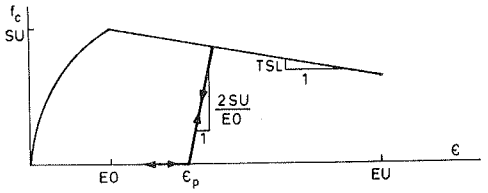

Fig. 3 Concrete Hysteresis Model 1

The envelope up to maximum stress is the parabola defined by Hognestad (1955), followed by a linear descending portion which is determined as a function of confinement in accordance with the expressions provided by Kent (1971). Loading and unloading paths are linear, with a slope equal to the initial tangent to the parabola. No tensile stress capacity is assumed.

Concrete Hysteresis Model 2 (Fig. 4)

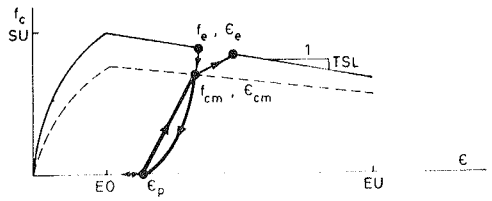

Fig. 4 Concrete Hysteresis Model 2

The envelope curve is the exponential expression proposed by Smith (1955) up to maximum stress. The descending linear portion is identical to model 1.

A common point curve parallel to the envelope curve is defined after Karsan (1969). Stable hysteresis is assumed for stress levels below the common point curve, the ordinates of which are 0.75 times the ordinates of the envelope curve.

Unloading paths are second degree parabolas. Reloading paths are bi-linear, the change in slope occurring at the common point. For envelope strains less than thrice the strain at maximum stress, the envelope, common point and cracking strains for unloading and reloading are related by the expressions provided by Karsan (1969). For larger strains, the reloading and unloading paths are parallel to those at thrice the strain at maximum stress.

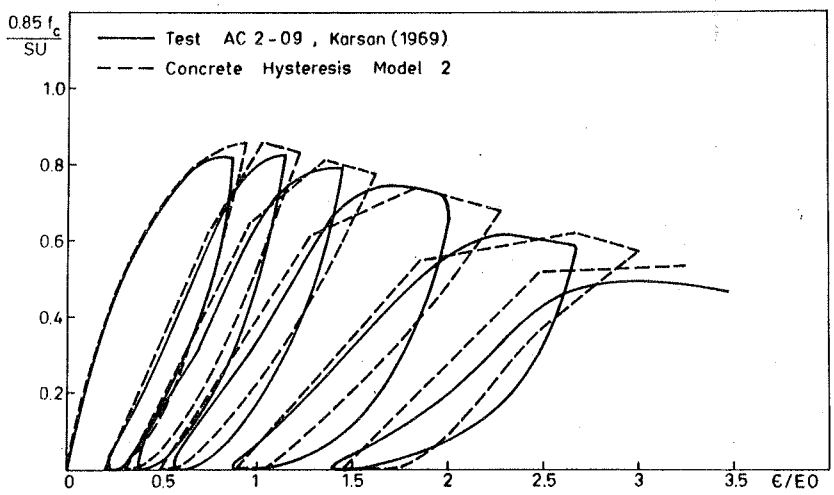

Fig. 5 Concrete Hysteresis Provided by Model 2 Compared with Test AC2-09, Karsan (1969)

The hysteresis provided by this model is compared to test AC2-09 reported by Karsan (1969) in Fig.5. The strain history in the simulated response is slightly changed from the test history to enable a direct comparison of the actual and simulated energy dissipation during cycling.

SECTION HYSTERESIS

To investigate the reflection of material hysteresis on section response, the moment-curvature hysteresis of column crossections tested by Aoyama (1964), Wight (1973) and Ersoy (1976) were simulated by the finite-filament technique. This technique, proposed by Aktan (1974), discretises the section into filaments of different materials. The case studies and material hysteresis data used to generate the analytical responses are summarized in Table 1.

TABLE 1. - MATERIAL HYSTERESIS DATA FOR ANALYTICAL SECTION HYSTERESIS

Figure Number	Designation for Analytical Hysteresis	Concrete Hysteresis Model Used	Envelope for Unconfined Concrete				Envelope for Confined Concrete				Steel			
			SU in psi	EO	EU	TSL in psi	SU in psi	EO	EU	TSL in psi	SY in psi	EY	SHS in psi	BSL in psi
6	1	2	4885	.002	.004	6.5×10^5	4885	.002	.012	2.6×10^5	4.9×10^4	.0017	5×10^5	5×10^6
6	2	2	4885	.002	.004	6.5×10^5	4885	.002	.012	2.6×10^5	4.9×10^4	.0017	1×10^6	17×10^6
7	1	2	4860	.0025	.005	6×10^5	4860	.0025	.022	0.7×10^5	7.3×10^4	.0025	1×10^6	5×10^6
7	2	2	4860	.0025	.005	6×10^5	4860	.0025	.022	0.7×10^5	7.3×10^4	.0025	1×10^6	15×10^6
8	1	2	4885	.002	.004	19×10^5	4885	.002	.012	2.6×10^5	4.9×10^4	.0017	1×10^6	17×10^6
8	2	1	4885	.002	.004	19×10^5	4885	.002	.012	2.6×10^5	4.9×10^4	.0017	1×10^6	29×10^6
9	-	2	2286	.002	.007	3.7×10^5	2286	.002	.04	0.4×10^5	4.9×10^4	.0017	-	-
10	1	2	2286	.002	.007	3.7×10^5	2286	.002	.04	0.4×10^5	4.9×10^4	.0017	-	-
10	2	1	2286	.002	.007	3.7×10^5	2286	.002	.04	0.4×10^5	4.9×10^4	.0017	-	-
11	-	2	3780	.0025	.005	2×10^5	3780	.0025	.016	1.8×10^5	7.3×10^4	.0025	1×10^6	5×10^6

Note : 1 psi = 0.07 kgf per cm^2

Aoyama column specimen A-2 (1964) with 27.5% of its balanced axial force was selected for the first case study (Fig. 6). The strain hardening and Bauschinger slopes of the steel model were the parameters that were different in the two analytical responses.

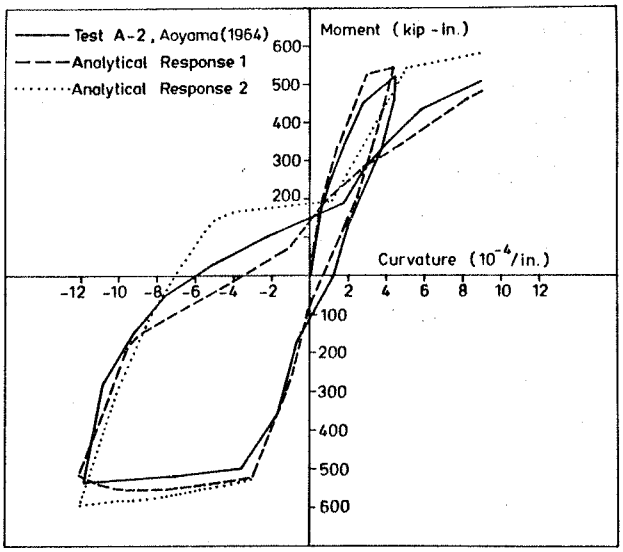

Fig. 6 Analytical and Experimental Responses, Specimen A-2, Aoyama (1964) (1 kip-in. = 1151 kgf-cm, 1 in. = 2.54 cm)

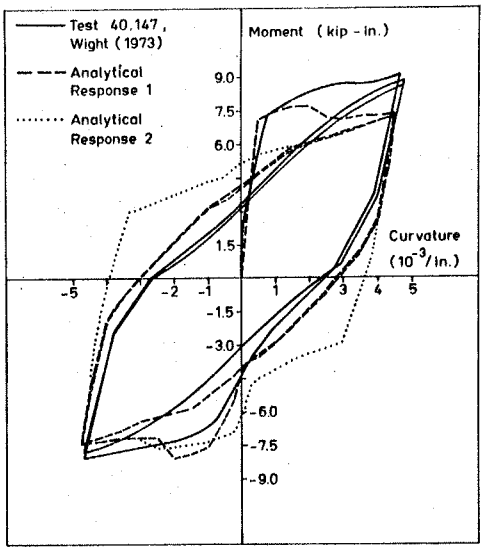

Fig. 7 Analytical and Experimental Responses, Specimen 40.147, Wight (1973) (1 kip-in. = 1151 kgf-cm, 1 in. = 2.54 cm)

In Fig. 7, the response of Wights specimen 40.147 (1973) is used to compare the two analytical responses with the Bauschinger slope as the only variable. This specimen was subjected to 45% of its balanced axial force. Both figures demonstrate that the Bauschinger slope of the steel hysteresis model is a significant variable, governing the response at the zero moment region. The strain hardening slope affects the post yield response in the maximum moment region.

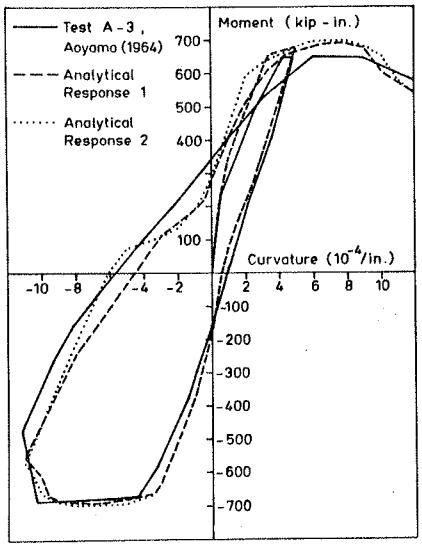

Fig. 8 Analytical and Experimental Responses, Specimen A-3, Aoyama (1964) (1 kip-in. = 1151 kgf-cm, 1 in. = 2.54 cm)

The experimental and analytical responses of the Aoyama specimen A-3 (1964), subjected to 50% of its balanced axial force, are presented in Fig.8. In analytical response 2, the simpler concrete hysteresis model was used. Furthermore, in this response, the Bauschinger slope of steel was assigned the extreme value of the modulus of elasticity. Response at the zero moment region does not appear to be as sensitive to this parameter as in the previous cases due to the increased axial force level. Furthermore, any advantage of the more sophisticated concrete hysteresis in analytical response 1 is not apparent.

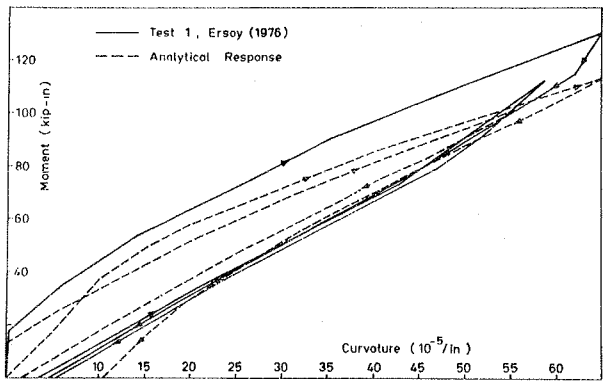

Fig 9 Analytical and Experimental Responses, Specimen 1, Ersoy (1976) (1 kip-in. = 1151 kgf-cm, 1 in. = 2.54 cm)

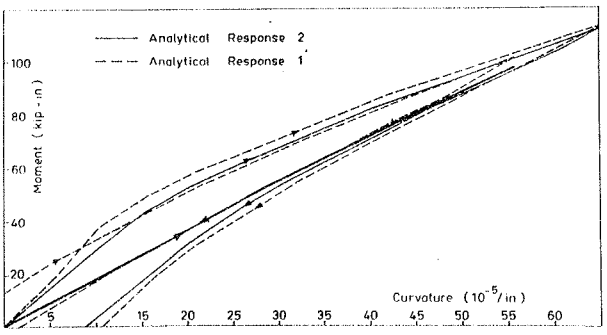

Fig. 10 Analytical Responses, Specimen 1, Ersoy (1976) (1 kip-in. = 1151 kgf-cm, 1in = 2.54cm)

Ersoy specimen 1 (1976), with an axial force 83% of balanced was used to compare the two concrete hysteresis models. First two cycles of the section hysteresis in the positive moment-curvature region are compared to the analytical response obtained with the more sophisticated concrete model 2 in Fig. 9. Section steel remained elastic during these cycles, enabling a direct evaluation of the energy dissipation characteristics of the concrete model. The responses obtained by the different concrete hysteresis models are compared in Fig.10. The more idealized model does not result in energy dissipation in the second cycle.

CONCLUSIONS

Reinforced concrete column section response can be analytically generated by the multi-linear steel model and the idealized concrete model 1 with reasonable accuracy. Use of the significantly more expensive concrete model 2 does not appear feasible unless axial force levels approaching the balanced force are present.

The Bauschinger slope and the properties of the descending linear portion of the concrete envelope curve were observed to be the parameters affecting analytical simulation of the section response significantly.

REFERENCES

1. Aktan, A.E., Karlsson, B.I., and Sozen, M.A., "Stress-strain Relationships of Reinforcing Bars Subjected to Large Strain Reversals", Civil Engineering Studies, Structural Research Series, No. 397, University of Illinois at Urbana-Champaign, Urbana, Ill., June, 1973.

2. Aktan, A.E., Pecknold,David, A., and Sozen, M.A., "R/C Column Earthquake Response in Two Dimensions", Journal of the Structural Division, ASCE, No. ST10, Proc. Paper 10864, October, 1974, pp. 1999-2015.

3. Aoyama, H., "Moment-curvature Characteristics of Reinforced-Concrete Members Subjected to Axial Load and Reversals of Bending", Proceedings of the International Symposium on Flexural Mechanics of Reinforced Concrete, ACI, ASCE, Miami, Florida, Nov., 1964, pp. 183-205.

4. Ersoy, U., and Aktan, A.E., "Response of Reinforced Concrete Beam-Column Connections under Earthquake Effects", Project No. MAG-379, Turkish Scientific and Research Council, Civil Engineering Research Group, Ankara, Turkey, May, 1976 (in Turkish, with a 30 p. abridged version in English).

5. Hognestad, E., Hanson, N.W., and McHenry, D., "Concrete Stress Distribution in Ultimate Strength Design", ACI Journal Proceedings V.52, No.4, Dec., 1955, pp. 455-479.

6. Karsan, I. Demir, and Jirsa, James, O., "Behavior of Concrete under Compressive Loadings", Journal of the Structural Division, ASCE, Vol. 95, No. ST12, Proc. Paper 6935, December 1969, pp. 2543-2563.

7. Kent, Dudley Charles, and Park, Robert, "Flexural Members with Confined Concrete", Journal of the Structural Division, ASCE, No. ST7, Proc. Paper 8-43, July 1971, pp. 1969-1990.

8. Smith, G.M., and Young, L.E., "Ultimate Theory in Flexure by Exponential Function", ACI Journal, Proceedings V. 52, No.3, Nov., 1955, pp. 349-359.

9. Wight, J.K., and Sozen, M.A., "Shear Strength Decay in Reinforced Concrete Columns Subjected to Large Deflection Reversals", Civil Engineering Studies, Structural Research Series No. 403, University of Illinois at Urbana-Champaign, Urbana, Ill., August, 1973.

NUMERICAL STUDIES OF THE BEHAVIOUR OF A REINFORCED CONCRETE BEAM ELEMENT UNDER REPEATED LOADINGS

D. CAPECCHI
Comitato Nazionale
per l'Energia Nucleare
Rome, Italy

V. CIAMPI
Ist. di Scienza delle Costruzioni
University of Rome
Rome, Italy

F. VESTRONI
Ist. di Scienza delle Costruzioni
University of L'Aquila
L'Aquila, Italy

SUMMARY

A numerical model has been developed in order to predict the behaviour of reinforced concrete members subjected to axial load and alternate bending.

Based on an accurate, but as far as possible simple, description of the constituent materials' hysteretic behaviour, the numerical procedure allows the calculation, for any assigned history of curvature χ, under fixed axial load N, of the corresponding flexural moment M and axial deformation ε.

The model response, compared with available experimental results, has been found to reproduce satisfactorily the important characteristics of the inelastic hysteretic behaviour.

An extensive numerical investigation is in progress, the purpose of which is to define the influence of the model's various parameters on the overall behaviour and which it is felt should provide deeper insight into the meaning of ductility for cyclically loaded deteriorating systems and into the parameters influencing this ductility.

Finally a simple dynamic model is derived and its response to prescribed accelerograms examined and commented.

RESUME

On développe une méthode numérique pour la description du comportement des poutres en béton armé soumises à force axial et flexion alterne. La méthod se base sur une description précise, quoique la plus simple possible, du comportement hystérétique des matériaux constituants et elle permet le calcul, pour une hystoire donnée de la courbure χ, sous une charge normale N fixée, du moment flechissant M et de la deformation axiale ε.

La réponse du modèle, comparée à des resultats d'expériences disponibles, s'est révèleé capable de reproduir d'une façon satisfaisante les caractères principaux du comportement inélastique hystérétique.

On développe maintenant une recherche numérique systématique, dont le but est de définir l'influence des nombreux paramètres du modèle sur le comportement d'ensemble, et qui devra fournir des informations sur la notion de ductilité pour les systèmes soumis à chargements cycliques avec endommagement et sur les paramètres qui influencent cette ductilité.

On passe enfin à un modèle dynamique simple et on examine et on discute la réponse à des accélérogrammes donnés.

1. INTRODUCTION

The safety of structures in seismic zones depends primarily on the vertical elements; more generally, at least for relatively simple structures, the type of the response can be considered as related to the time evolution of the structural reaction of the columns.

Since it is incorrect to assume that structures should resist the strongest earthquakes while remaining in the elastic range, it is important to have available an accurate representation of the non-elastic behaviour of the elements which are subjected to axial force and cyclic bending.

This explains the large number of experiments which have recently been dedicated to the study of the behaviour of r.c. members.

These studies have shown that this behaviour is strongly dependent on the load path. Its main characteristics are a continuous variation of the stiffness and a decrease in the value of the strength, which correspond to a certain amount of deterioration.

Many authors have demonstrated that the seismic response of deteriorating systems is much different from that of bilinear hysteretic systems even when the models adopted to describe the former are rather simplified; moreover while the first aspect of deterioration (the stiffness degradation) has received much more attention, the second (the strength deterioration) has been taken into consideration only recently.

At the same time models have been developed which describe the behaviour of r.c. members subjected to repeated loads. In some of these the force displacement relationship is directly modelled through analytical laws and deterioration is controlled by certain parameters which are empirically related to the physical causes of degradation; in others the force-displacement relationship is the result of the analysis of a section in which the time evolution of each layer is followed, on the basis of laws which appropriately describe, for steel and concrete, the behaviour of the two materials under cyclic strains.

The model proposed here belongs to this second category. Its general characteristics are analized synthetically and the dependence of the behaviour on the principal parameters which define it, is put into evidence.

The model has shown itself able to reproduce, both qualitatively and quantitatively, the main features of the behaviour of a r.c. element subjected to repeated intense loads.

Thus it is possible to utilize this numerical tool for a sufficiently extensive, yet economical, investigation of r.c. members with different mechanical characteristics, obtaining results which can complement those obtained experimentally.

Based on the same hysteretic behaviour, a numerical model for studying the dynamic response of simple r.c. structures has been also derived and tested. Its relative simplicity is hoped to allow certain characteristics of the response of realistic deteriorating systems to be evidenced, as result of extensive numerical analyses.

2. MECHANICAL MODEL

A model is to be developed which will represent the behaviour of a r.c. beam element subjected to compression and alternating bending.

Since attention is focused only on critical regions, a beam element of limited dimension is considered, which has constant generalized stresses (M,N) and strains (u/l, θ/l) as indicated in fig.1a. According to these hypotheses the force-displacement relationship of the element can be obtained from the analysis of the behaviour of a single section.

Under the usual assumptions of linear variation in strain across a section and of no bond failure between concrete and steel, the use of the appropriate σ-ε relationships for the two materials and equilibrium conditions

resolve the problem.

For the purpose of numerical analysis the beam section is discretized into concrete and steel layers, as shown in fig.1b. The numerical procedure follows an incremental formulation based on the displacement method; at each step the incremental equilibrium equations are satisfied by an iterative process based on a modified secant method.

As for the constitutive relationships of the materials, sufficiently accurate laws are assumed. Care is taken to represent also phenomena connected with the longitudinal dimension of the element which does not appear specifically in the model.

Concrete model

The uniaxial stress-strain relationship for concrete is described in fig.2, 3.

The main features of the relationship can be summarized as follows:

- The envelope curve is that suggested by Kent and Park (1971). It is as is known a 'modified' relation which accounts for factors related to the longitudinal dimension such as the ratio of the volume of the stirrups to the volume of the concrete core. Three branches define the envelope curve: a parabolic ascending branch, a linear falling branch, a horizontal branch. This last indicates a residual stress which the confined concrete can offer also for high values of strain in the range $\varepsilon_{br\,1}$ - $\varepsilon_{br\,2}$. For unconfined concrete the curve is interrupted either at the strain ε_{br} (a) or at the intersection of the falling linear branch with the zero stress axis (b).
- The cyclic behaviour is described by two distinct unloading and reloading stiffness moduli, which are both a decreasing function of the maximum escursion into the compressive plastic strain range. Since during the unloading zero stress is reached (point 4), complete loss of stiffness is assumed (the model therefore disregards the tensile strength of concrete). As loading reverses at point 6 and moves back into the compressive strain range, elastic stiffness is regained only after point A is passed and loading proceeds elastically with a different modulus until reaching the envelope curve. Thereafter the envelope curve is followed.
  More detail can be found in Capecchi et al. (1979).

Reinforcing steel model

For the uniaxial σ-ε relationship of the reinforcing steel, the expression suggested by Giuffrè and Pinto (1970) is used because of its advantages with respect to the classic Ramberg-Osgood formula. In fact the equation

$$\sigma^* = b\,\varepsilon^* + \frac{(1-b)\varepsilon^*}{(1+\varepsilon^{*R})^{1/R}}$$

explicitly expresses stresses as a function of strains and accounts simply for workhardening through the slope parameter b. It also allows an accurate representation of the reversal curves through the parameter R which can be varied depending on the magnitude of the maximum excursion in the plastic range (fig.4).

A set of additional rules is needed for the application of the hysteresis law when a general strain history is given, in order to avoid the necessity of storing the parameters of all the reversal curves.

The simple set of rules suggested by Jennings (1968), which leads to the definition of a minimum curve and a maximum curve, besides a skeleton curve, is used here. It has proved to be sufficiently accurate in this case.

3. ANALYSIS OF THE MODEL BEHAVIOUR

The influence on the model behaviour of the various parameters which de-

fine it will now be discussed, analizing the model response to an imposed history of cyclic deformations at fixed axial load, just as is done in an experimental test.

Typical M-θ diagrams obtained from numerical tests are presented in fig. 6. As can be noticed all the main aspects of the experimentally observed behaviour are reproduced.

In particular:

1) the reduction of stiffness with increasing amplitude of inelastic deformation;
2) the reduction of strength at fixed amplitude of deformation;
3) the dependence of the loop's shape on such parameters as the elastic modulus and the ultimate stress of the concrete, the volume of the stirrups, the average compressive stress on the section, the percentage of the reinforcing steel.

On the basis of the limited number of numerical tests carried out until now it is already possible to make some considerations about the influence of certain parameters:

- Slope of the falling branch of the envelope curve of concrete. In Fig.7 results are presented which refer to two cases differing only in the slope of the falling branch. Increasing slope produces larger deterioration effects: in case (b) the continuous strength reduction during cycles produces collapse, while in case (a) the loops tend to become stable.
- Value of the average compressive stress (σ_m). In fig.8 three cases are presented in which only σ_m is varied (20÷40÷60 kg/cm^2). The shape of the loop modifies continuously and the element presents a less and less ductile behaviour. During cycles of variable amplitude collapse occurs at lower number of cycles, for increasing σ_m.
- 'Nominal' value of the ultimate strain of concrete ε_{br}. This value is influenced, as is known, by the distribution and the volume of the stirrups, as well as by the mechanical material properties. An increase in the value of this parameter improves the model behaviour in general, but it is decisive only in the cases in which the deterioration is primarily related to the breakage of the external layers, as occurs in the case of fig.9 in which ε_{br} assumes the values 12‰ (a), and 6‰ (b) respectively.
- P-Δ effect. In order to analize these effects reference is made to the simple column of fig.1c. The restoring force of this model has been simply deduced from the M-θ relationship, furnished by the presented model, under the assumption that the deformation of the column is all concentrated in the critical region (plastic hinge). For a section depth which is only 1/10 of the height of the column, the diagram of the lateral restoring force versus horizontal displacement is presented in fig.10a. When the P-Δ effect is taken into account the diagram is that of fig.10b.
The case of a very slender column is presented here in order to make the phenomenon more evident. For less slender columns the geometric effect is less marked but the danger of its coupling with the physical deterioration remains.

4. SEISMIC RESPONSE OF A SIMPLE STRUCTURAL MODEL

Although much more numerical work is to be done for a better understanding of the mechanical behaviour of the r.c. beam element, it has seemed worthwhile to start, at the same time, an investigation of the dynamic response, under seismic actions, of a simple structure (fig.5).

The restoring force-displacement relationship f(x) for the structure can be derived again from the M-θ relationship considering the column deformation as concentrated at the column's ends.

The equation of motion can be written:

$$\ddot{x} + 2\nu\omega_o \dot{x} + \frac{1}{m} f(x) - \beta \frac{g}{H} = \ddot{x}_G$$

where ν is the fraction of linear viscous damping, ω_o the 'nominal' circular frequency of the structural model, f(x) the restoring force, β=N/mg a coefficient which accounts for geometric effects. In order to test the dynamic model two recorded accelerograms have been considered (fig.11):

Excitation 1 Forgaria-Cornino 15.9.76, NS (Friuli) Exc.1
Excitation 2 Taft 21.07.52, N 69 W Exc.2

The response of some of these first tests is presented here. In fig.12 three structural cases are considered in which the columns' height and depth and the percentage of reinforcing steel, are held constant, while the mass (and consequently the average compressive stress σ) and the slope E_2/E_1 of the falling branch of the envelope curve of concrete are changed. The typical response is described through the time history of the displacement and the cyclic diagram of the restoring force.

The two responses (a) and (b) are substantially different and in particular collapse occurs in the latter while in the former stable hysteretic loops are obtained. In case (c) a high degree of deterioration is reached even though collapse does not occur. In fig.13 the numerical response of the structural model under excitation 2 is presented. The P-Δ effect (story height 4 m, section depth 0.25 m) is considered, or not considered, respectively in case (b) and (a). After an almost identical initial behaviour case (b) is shown to diverge rapidly, up to collapse.

CONCLUDING REMARKS

It is obviously difficult to draw complete conclusions from the analyses carried out so far. Much more numerical work is needed in this direction.

Is is useful here to point out again that the principal aim of this work is not so much to improve and better define a physical model (especially from the quantitative point of view), as to use the model itself as an investigative tool. In fact the proposed model is capable of accurately representing the behaviour of r.c. elements, while at the same time beeing relatively simple to use. This simplicity is also due to the limited number of easily controlled parameters, with clear physical meaning, on which the model's behaviour depends.

Thus it is expected that extensive numerical tests will provide more information about the real behaviour, under repeated loads, of r.c. elements and will also lead to a better understanding of their ductility characteristics.

As for the dynamic analyses, it is expected that certain problems, which arise in the study of structures whose collapse, strongly history-dependent, is not easily definable with a single overall control parameters, such as ductility, will be clarified.

REFERENCES

Atalay, B. and Penzien, J., 'Inelastic cyclic behaviour of reinforced concrete flexural members', Sixth Word Conf. Earth. Engr., New Delhi, 1977.

Bertero, V.V., 'Experimental studies concerning reinforced, prestressed and partially prestressed concrete structures and their elements', AIPC,Sym. on Resistance and Ultimate Deformability of Structures Acted on Well Defined Repeated Loads', Lisboa, 1973.

Capecchi, D., Ciampi, V. and Vestroni, F., 'A model for reinforced concrete beam element under axial load and alternate bending', 1979 (to be published).

Chopra, A.K. and Kan, C., 'Effects of stiffness degradation on ductility requirements for multistory buildings', Earth. Engr. and Struc. Dyn., Vol. 2, 1973.

Giuffrè, A. and Pinto, P.E., 'Reinforced concrete behavior under strong repeated loadings' (in italian), G. Genio Civile, N.5, 1970.

Imbeault, F.A. and Nielsen, N.N., 'Effect of Degrading Stiffness on the respon se of Multistory Frames Subjected to Earthquakes', Fifth World Conf. on Earth. Engr., Rome, 1975.

Iwan, D., W., 'The earthquake response of strongly deteriorating systems including gravity effects', Sixth Europ. Conf. Earth. Engr., Dubrovnik, 1978.

Jennings, P.C., 'Response of simple yielding structures to earthquake excitation', California Ist. of Technology, Pasadena, California, June 1963.

Kent, D.C. and Park, R., 'Flexural members with confined Concrete', J. of Str. Div., ASCE, Vol.97, July, 1971.

Mahin, S.A. and Bertero, V.V., 'Reliability of inelastic design methods for seismic-resistant structures',Sixth Europ. Conf. Earth. Engr., Dubrovnik, 1978.

Parducci, A. and Samuelli Ferretti, A., 'Reinforced concrete behavior under strong repeated loadings' (in italian), G. Genio Civile, N.5, 1970.

Popov, E.P. and Bertero, V.V., 'Model of cyclic inelastic flexural behavior of reinforced concrete members', SMIRT, K3/14, S.Francisco, 1977.

Popov, E.P., Bertero, V.V. and Viwathanatepa, S., 'Analytic and experimental hysteretic loops for r/c subassemblages' Fifth Europ. Conf. Earth. Engr., Istanbul, 1975.

Sozen, M.A., 'Hysteresis in structural elements', App. Mech. in Earth. Eng., Vol. 8, 1974.

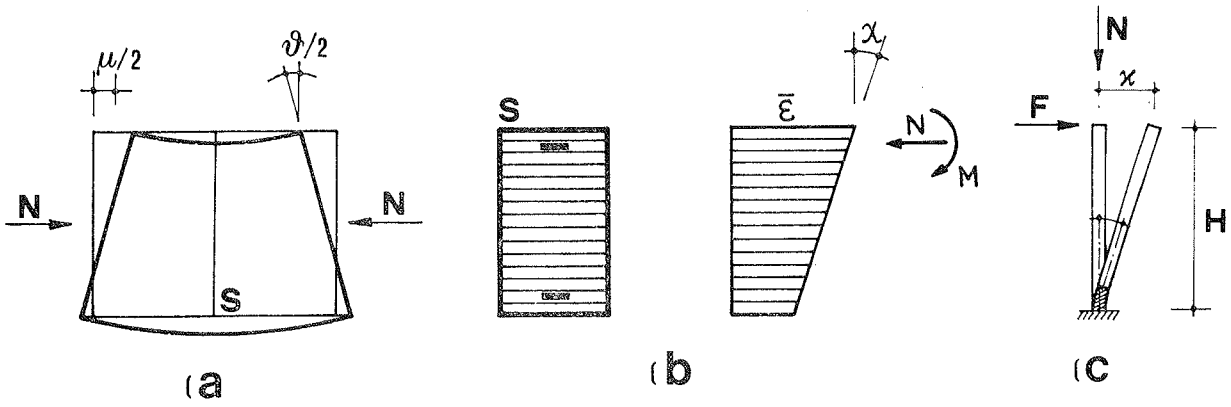

Fig.1

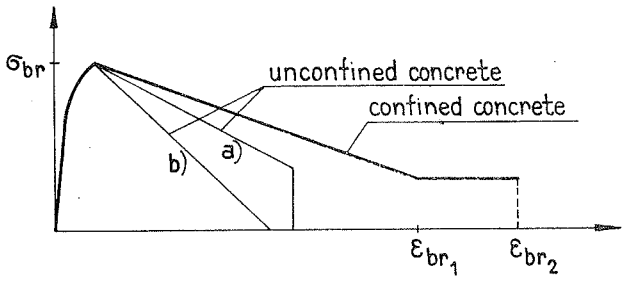

Fig.2

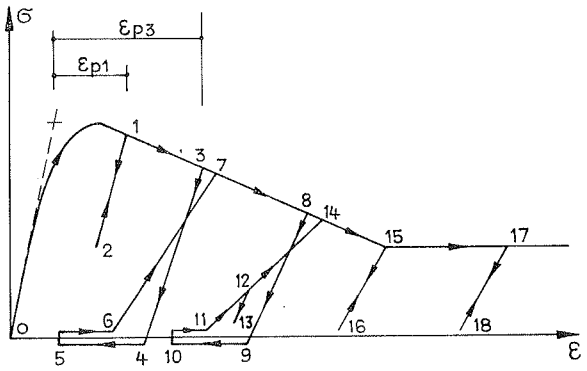

Fig.3

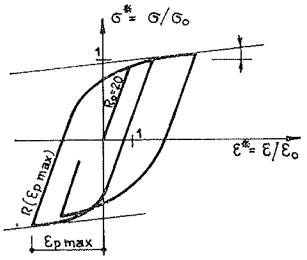

Fig.4

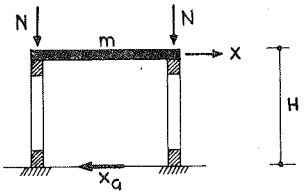

Fig.5

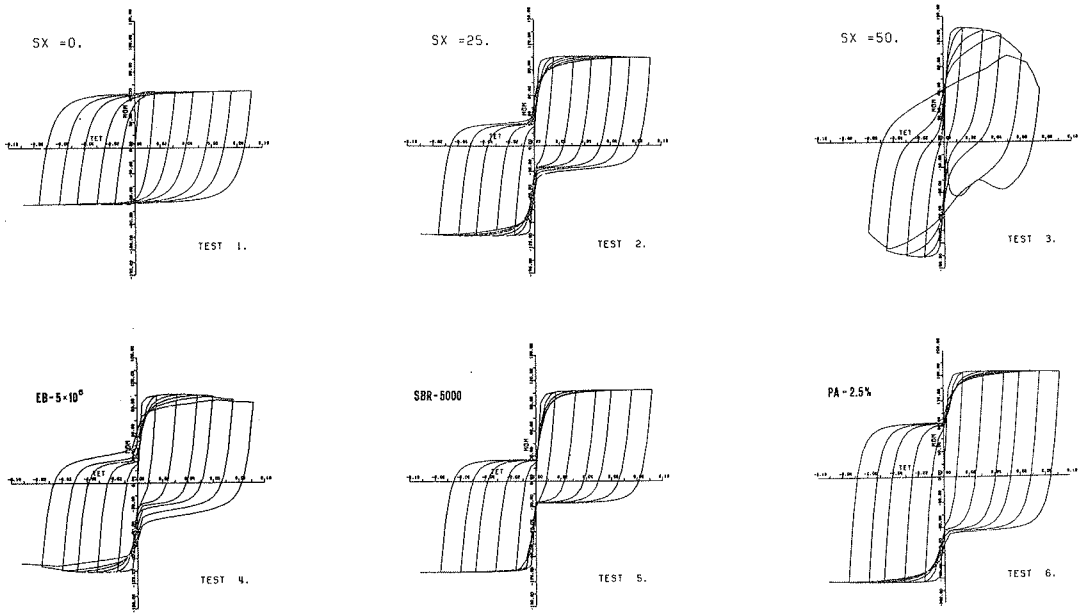

Fig.6

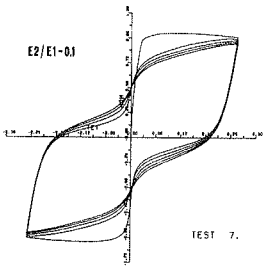

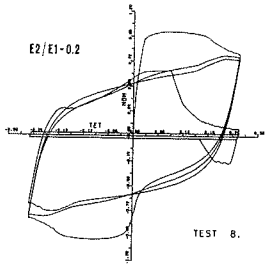

Fig.7

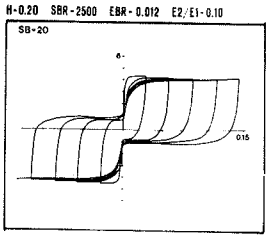

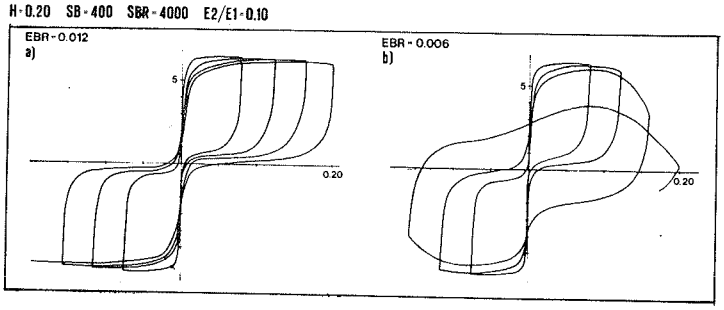

Fig.9

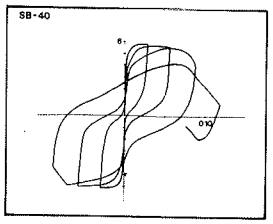

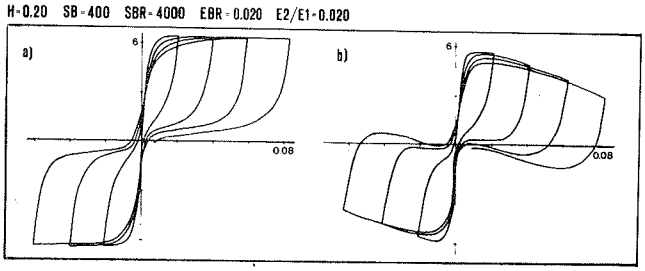

Fig.10

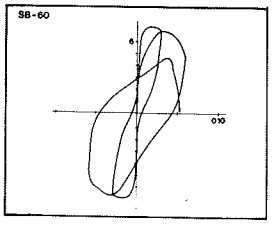

Fig.8

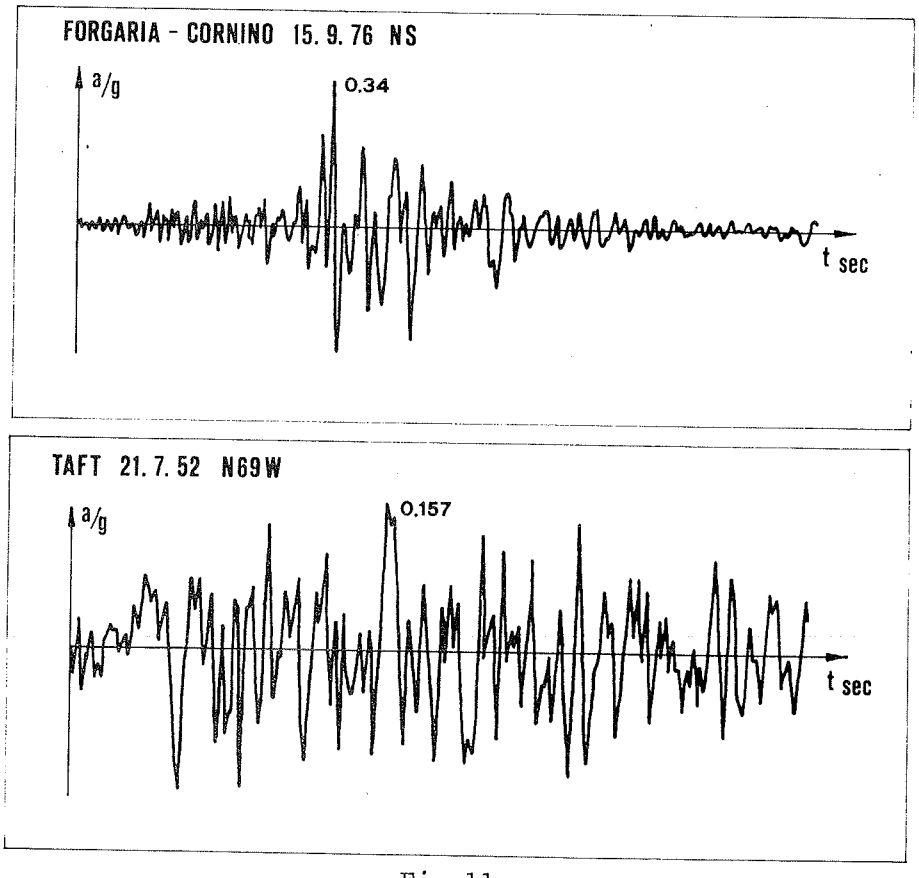

Fig.11

a)

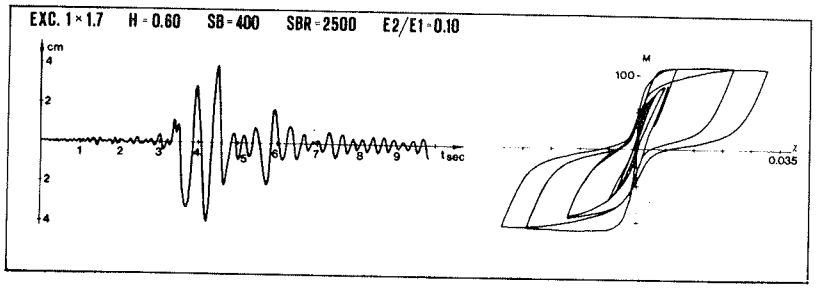

b)

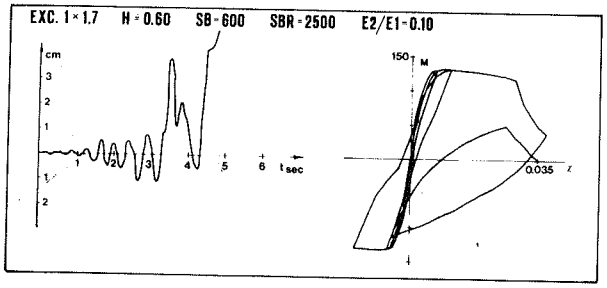

c)

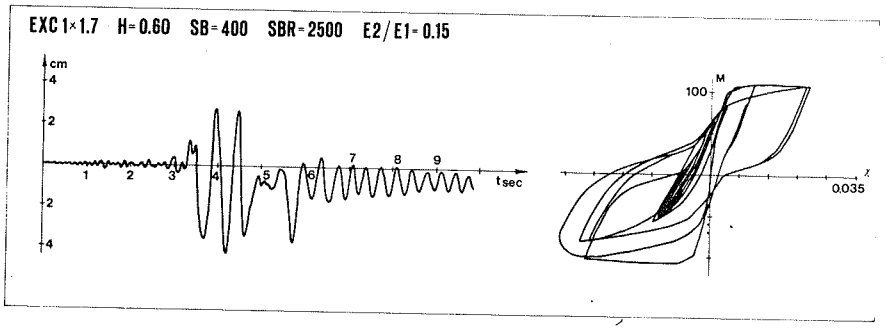

Fig.12

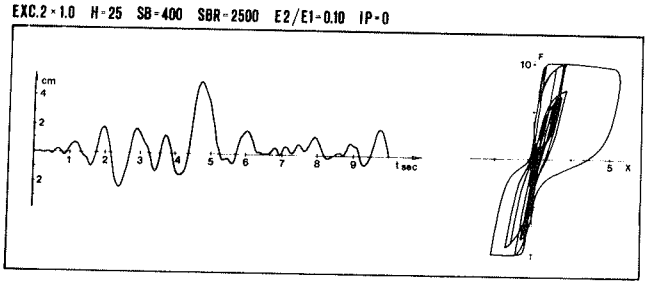

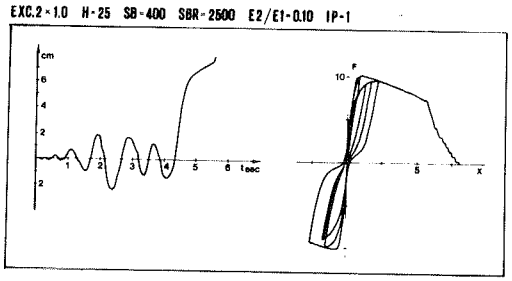

Fig.13

DUCTILITE DE POTEAUX EN FLEXION COMPOSEE SOUS CHARGES ALTERNEES

Michel KAVYRCHINE
C.E.B.T.P. - Service d'Etude des Structures
Saint-Remy-lès-Chevreuse, France

Alain GRELAT
C.E.B.T.P. - Service d'Etude des Structures
Saint-Remy-lès-Chevreuse, France

RESUME

Des poteaux en béton armé, de 200 x 250 mm de section, ont été essayés sous charge normale constante, (avec deux niveaux de charge) sous dix cycles de flexion alternée, suivie par une rupture finale à vitesse de déformation contrôlée. Ils avaient la même armature longitudinale et des cadres d'espacement et d'épaisseur de recouvrement différents.

Lorsque le rapport de la force maximale exercée à chaque cycle à la force maximale de l'essai de rupture ne dépassait pas 0,9, on a obtenu après un premier cycle où l'énergie dépensée était plus importante, une stabilisation relative de l'énergie dépensée à chaque cycle. L'augmentation de l'espacement des cadres a favorisé, pour une contrainte de compression relativement élevée une rupture finale par le béton avec une énergie de rupture plus faible que dans les autres cas.

SUMMARY

Columns in reinforced concrete, with a section of 200 x 250 mm have been tested under a constant normal force (with two levels of force), under ten cycles of alternate flexion followed by a final failure at a controled speed of deformation. They had the same longitudinal reinforcement, and links of different spacing and concrete covering.

When the ratio of the maximum force in a cycle to the maximum force at failure test was not higher than 0,9, after a first cycle of higher energy, a relative stabilisation of cycle energy was obtained. A higher spacing of links induced, for a relatively high compressive stress, a final failure by the concrete, with a failure energy lesser than in the other cases.

1 - INTRODUCTION

Des travaux faits au Service d'Etude des Structures du C.E.B.T.P. à Saint-Rémy-lès-Chevreuse (voir Kavyrchine (1977) et (1978))ont porté sur l'étude de poutres en béton armé sous sollicitations dynamique ou statique en flexion simple au-delà de la sollicitation ultime. Les essais présentés dans la présente Communication (financés conjointement par la Direction des Affaires Economiques et Internationales au Ministère de l'Equipement et par l'Union Technique Interprofessionnelle du Bâtiment et des Travaux Publics) introduisent en plus l'effet d'une force de compression longitudinale et l'effet de cycles de flexion alternée.

2 - DESCRIPTION DES CORPS D'EPREUVE

Chacun des poteaux essayés avait pour dimensions 200 mm de large, 250 mm de haut, 2700 mm de long, avec deux axes transversaux d'appui espacés de 2500 mm. Ils étaient tous armés longitudinalement par 4 aciers Tor de 14 mm de diamètre. L'armature transversale était formée de cadres en acier doux de 6 mm de diamètre, d'espacement variable(50,100 ou 150mm) Une partie des pièces essayées avait un recouvrement normal d'environ 25 mm (les aciers longitudinaux étaient alors placés à des entr'axes de 130 par 180 mm) et une autre partie avait des cadres affleurant la surface du béton (les aciers longitudinaux étaient alors placés à des distances entre axes de 170 et 220 mm) (voir figure 2).

Le tableau 1 ci-dessous donne les principales caractéristiques de leur ferraillage, la résistance et le module d'Young mesurés sur cylindre au jour de l'essai, l'âge du béton au jour de l'essai.

TABLEAU 1

Corps d'épreuve	Recouvrement béton	Espacement cadres mm	Résistance béton MPa	Module d'Young MPa	Age à l'essai jours
KT 1	normal	50	32,3	35,3	28
KT 2	normal	50	32,9	35,9	31
			38	39,3	46
KT 3	nul	50	34,7	37,4	37
KT 4	nul	50	32,5	37,3	36
KT 5	normal	150	32,4	36,0	32
KT 6	normal	150	31,2	38,5	28
KT 7	nul	150	27,5	35,6	28
KT 8	nul	150	22,7	33,8	29
KT 9	nul	100	23,6	33,5	29

Des corps d'épreuve de même section et même armature que les poteaux de 600 mm de long ont été réalisés avec un béton de même qualité que celui des poteaux, pour des essais de compression simple, à vitesse de déformation constante (environ 1000.10^{-6} par minute).

3 - METHODE D'ESSAI

Le montage d'essai est représenté sur la figure 1.
Après la mise en place de la poutre, on appliquait la force normale horizontale, dont l'intensité (mesurée à l'aide d'un dynamomètre) était maintenue constante pendant la suite de l'essai. Deux niveaux de charge normale ont été ainsi réalisés : 440 KN et 221 KN (soit 8,8 MPa et 4,4 MPa de compression). On réalisait ensuite dix cycles de chargement alternés entre deux forces limites de sens opposé et égales en valeur absolue. La valeur de la force transversale maximum Pc de chaque cycle représentait une fraction importante de la charge transversale ultime pouvant être supportée par la pièce (voir tableau 3).

Après la réalisation des dix cycles à forces maximales limitées, on procédait à un chargement de déformation contrôlée jusqu'à l'épuisement complet de la résistance de la pièce.

La flèche au milieu de la poutre était enregistrée en continu en fonction de la charge, directement sur table traçante, pendant l'essai. Plusieurs flèches, rotations, déformations locales des armatures et du béton, étaient en outre mesurées à chaque étape de chargement.

4 - RESULTATS DES ESSAIS

La courbe charge flèche enregistrée pendant l'essai montrait une stabilisation des cycles; après le premier cycle, qui était plus large que les autres, montrant une dépense d'énergie initiale plus forte, les cycles n° 2 à 10 étaient étroits et presque superposables, (voir figure 3). Des fissures de flexion apparaissaient au cours du premier cycle, et s'ouvraient au cours des cycles successifs, sans modification notable de leur aspect.

Le tableau 2 montre l'évolution de l'énergie dépensée dans un cycle et de la déformation totale mesurée entre chacune des positions extrêmes de la pièce. La dernière colonne donne le rapport entre la charge maximum appliquée à chaque cycle et la charge maximum atteinte lors de l'essai de rupture.

Le cas de la pièce KT 8 est particulier : la résistance ultime a été pratiquement atteinte au cours du premier cycle, où la courbe de montée en charge montre un palier horizontal sous la charge maximum Pc. L'énergie dépensée au cours des différents cycles est donc nettement plus importante que pour les autres pièces et ne se stabilise pas.

On peut constater,sur le tableau 2 que la surface du premier cycle correspondant à l'ouverture des fissures des deux côtés de la poutre fléchie est nettement plus grand que pour les cycles suivants, où l'énergie dépensée ne décroit que lentement. L'énergie dépensée au cours du premier cycle est elle-même assez faible pour les pièces KT 2 et KT 5 où le rapport Pc/Pu est d'environ 2/3. De manière générale, on note une tendance à l'accroissement de l'énergie dépensée au cours d'un cycle et de l'amplitude de la déformation en fonction du rapport Pc/Pu.
L'amplitude de la déformation croit lentement et progressivement avec les cycles.

TABLEAU 2 : $\frac{\text{énergie par cycle (joules)}}{\text{amplitude cycle (mm)}}$

N° du cycle	1	2	3	6	10	Pc/Pu
KT 1	630 joules	150	130	110	110	0,81
	14,8 mm	15,7	15,7	16,8	17,3	
KT 2	130	110	70	70	60	0,63
	8,7	11,1	10,7	10,7	11,0	
KT 3	430	210	220	210	210	0,92
	18,8	18,0	20,0	20,5	21,8	
KT 4	480	190	160	150	130	0,76
	13,2	13,7	13,8	14,6	14,9	
KT 5	150	110	90	90	80	0,66
	9,3	9,8	9,8	10,3	10,7	
KT 6	310	150	120	110	90	0,84
	14,0	15,0	15,4	16	16,5	
KT 7	420	240	220	200	190	0,78
	15,0	15,3	15,6	16,5	16,8	
KT 8	1020	560	740	640	710	1,00
	26,6	27,0	26,5	31,1	32,7	
KT 9	570	390	330	320	330	0,82
	17,3	18,3	19,0	20,5	21,7	

Au cours de l'essai de rupture final, les fissures existantes se développaient, de nouvelles fissures apparaissaient. Le forme de la rupture et de la courbe charge flèche de cet essai final, poussé jusqu'à destruction de la force portante de la poutre, dépendaient de la constitution de la pièce, comme indiqué plus loin.
Les courbes flèche charge, à rupture, sont données sur les figures 4,5,6 et 7.

Le tableau 3 ci-dessous rappelle les valeurs des forces appliquées au cours de chaque essai, et donne la forme de la rupture ainsi que l'énergie totale de destruction de la pièce, calculée d'après le travail accompli par la force transversale (aire sous la courbe charge flèche).
La figure 8 donne des photos de rupture par les aciers (KT 3) et le béton (KT 5).

TABLEAU 3

Corps d'épreuve	Force normale N K Newtons	Force transversale maximum		Mode de rupture finale	Energie de destruction joule
		cycle Pc KN	à rupture Pu KN		
KT 1	221	79	98	acier	4800
KT 2	441	79	125	acier	5100
KT 3	221	99	108	acier	4500
KT 4	441	99	131	acier	6100
KT 5	441	79	120	béton	3400
KT 6	221	78	93	acier	5400
KT 7	441	98	125	béton	3800
KT 8	221	98	98	acier + béton	4400
KT 9	441	98	120	béton	4300

L'influence de l'espacement des cadres est nette, dans le cas de la force de compression la plus élevée, en ce qui concerne le mode de rupture final (obtenu par le béton uniquement pour les espacements les plus élevés) et en ce qui concerne l'énergie de destruction. Cette dernière est d'environ 5600 joules pour N = 441 KN et des cadres serrés à 50 mm et de 3600 joules pour N = 441 KN, et des cadres espacés de 150 mm. Pour des cadres espacés de 100 mm les résultats sont proches de ceux obtenus avec des cadres espacés de 150 mm(mais la résistance du béton est relativement faible dans ce cas).

Pour la force de compression la plus faible, l'influence des cadres apparait dans la forme de la courbe charge flèche, mais la rupture des aciers intervenant trop tôt pour que l'énergie de destruction soit importante. Dans le cas des cadres serrés on peut se référer à d'autres essais pour constater l'effet des armatures transversales : dans Kavyrchine (1978), on trouvera pages 109 et 110 l'aspect après rupture, et les courbes flèche charge de deux poutres de 15 x 24 cm armées de 2 Tor 16 mm longitudinaux, l'une avec des cadres espacés de 10 cm dans un cas et l'autre sans cadres : l'énergie de destruction est plus faible quand il n'y a pas de cadres.

Les courbes déformation contrainte de deux prismes de référence KT 13 et KT 17 sont données sur la figure 9. Resserrer les armatures transversales augmente le raccourcissement ultime (le sommet de la courbe passe de 2.2 à $2.3.10^{-3}$ à 3.2 ou $3.8.10^{-3}$ mais surtout la branche descendante est fortement relevée : pour les prismes sans enrobage, on passe pour 14,7 MPa (soit approximativement la moitié de la contrainte de rupture), de $7.5.10^{-3}$ à $22.5.10^{-3}$. Des résultats analogues ont été obtenus sur des cylindres armés de cerces (voir Kavyrchine (1978), figure 10, page 104).

La modification proposée par Kent et Park, pour la courbe contrainte-déformation du béton en fonction de la présence d'armatures transversales (voir Park et Paulay 1975, page 28) nous donne pour les prismes sans enrobage et pour une contrainte moitié de la contrainte de rupture, un raccourcissement du béton égal à $6.9.10^{-3}$ pour les cadres espacés de 150 mm et $13.6.10^{-3}$ pour les cadres à 50 mm; dans notre cas, ces valeurs théoriques sont donc conservatrices.

5 - CONCLUSION

Les essais en flexion composée sur des poteaux en béton armé, avec divers espacements de cadres et divers recouvrements de béton sur la cage d'armatures, ont mis en évidence l'influence de l'espacement des cadres sur la forme de la rupture finale et sur la courbe charge flèche au-delà du moment résistant maximum.

La destruction par épuisement de la résistance du béton en compression a été obtenue pour la compression la plus élevée et des espacements de cadres de 100 ou 150 mm. Les valeurs les plus basses de destruction totale correspondant à des espacements de 150 mm combinés avec la compression la plus élevée.

Au cours des dix cycles successifs de chargement faits au début de chaque essai, on a constaté une fissuration sur les deux côtés tendus successivement par la flexion,avec une dépense d'énergie d'autant plus importante que la sollicitation était élevée au cours du premier cycle. La fissuration n'évoluait pratiquement plus au cours des neuf cycles suivants, pendant lesquels l'amplitude de la déformation croissait lentement; l'énergie dépensée à chaque cycle avait une valeur nettement plus faible que celle du premier cycle, pour une force appliquée égale à 80 % environ de la force ultime, et elle décroissait lentement avec le nombre de cycles. Nous n'avons eu de dégradation importante par des cycles successifs que si la force appliquée à chaque fois était voisine de la force ultime.

REFERENCES

M. KAVYRCHINE - Effets de choc sur le béton armé. Annales ITBTP N° 356 décembre 1977. Série Béton N° 173.

M. KAVYRCHINE - (présentation de)
Bétons légers et normaux, comportement et résistance structurelle, Chapitre III de Recherches sur les structures en béton. Annales ITBTP N° 360 - avril 1978.
Série Béton N° 177

R. PARK . T. PAULAY - Reinforced Concrete Structures. John Wiley-1975.

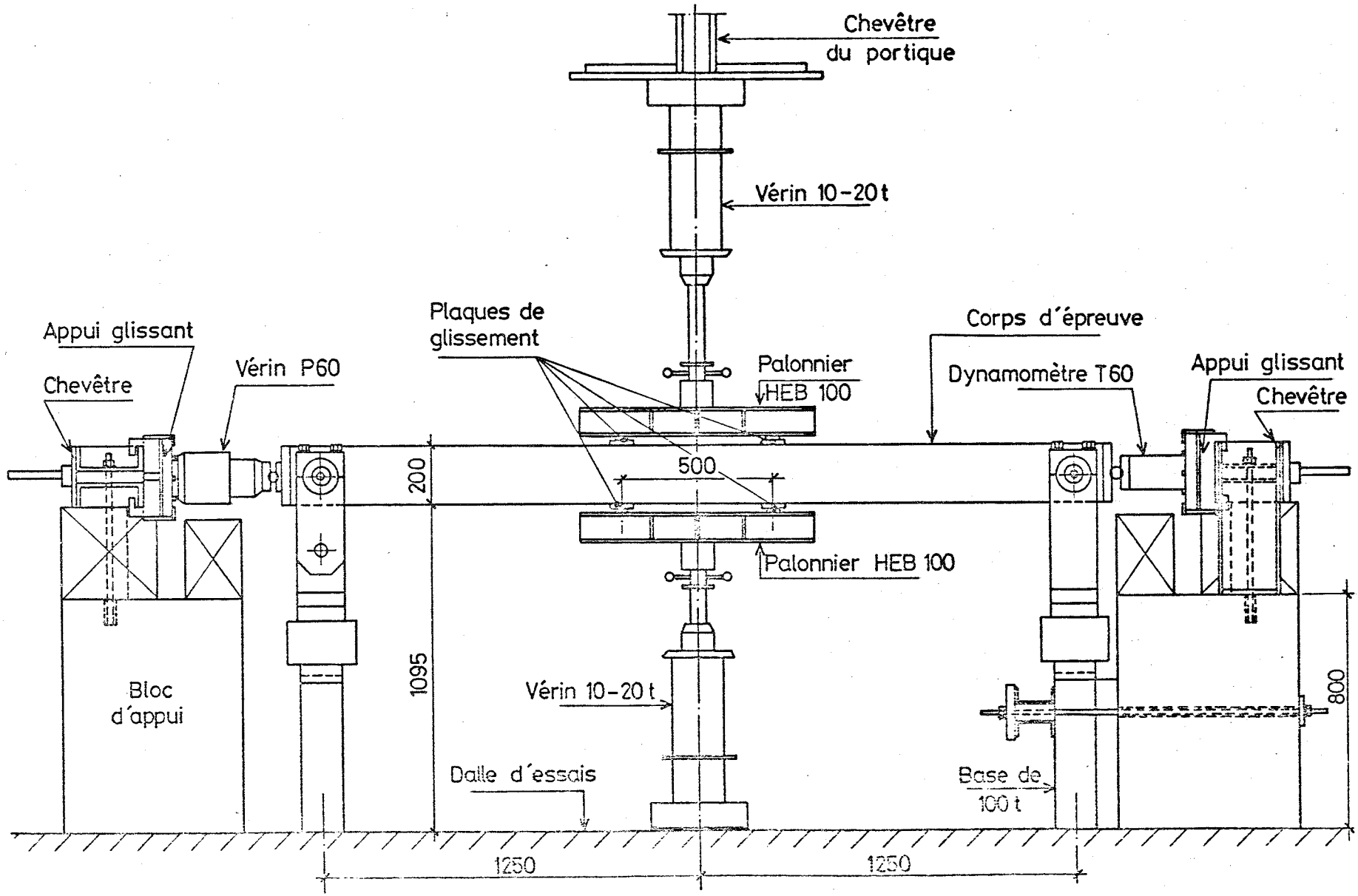

Figure 1 - Montage d'essai

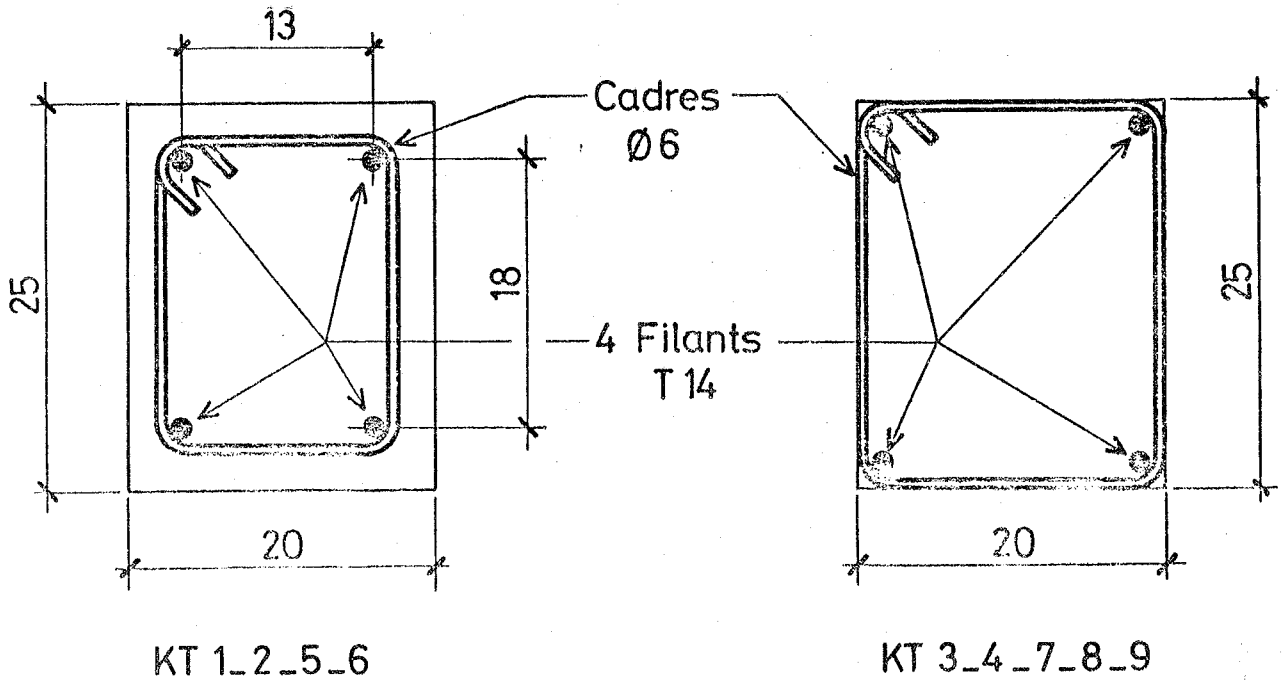

Figure 2 - Coupes transversales des corps d'épreuve

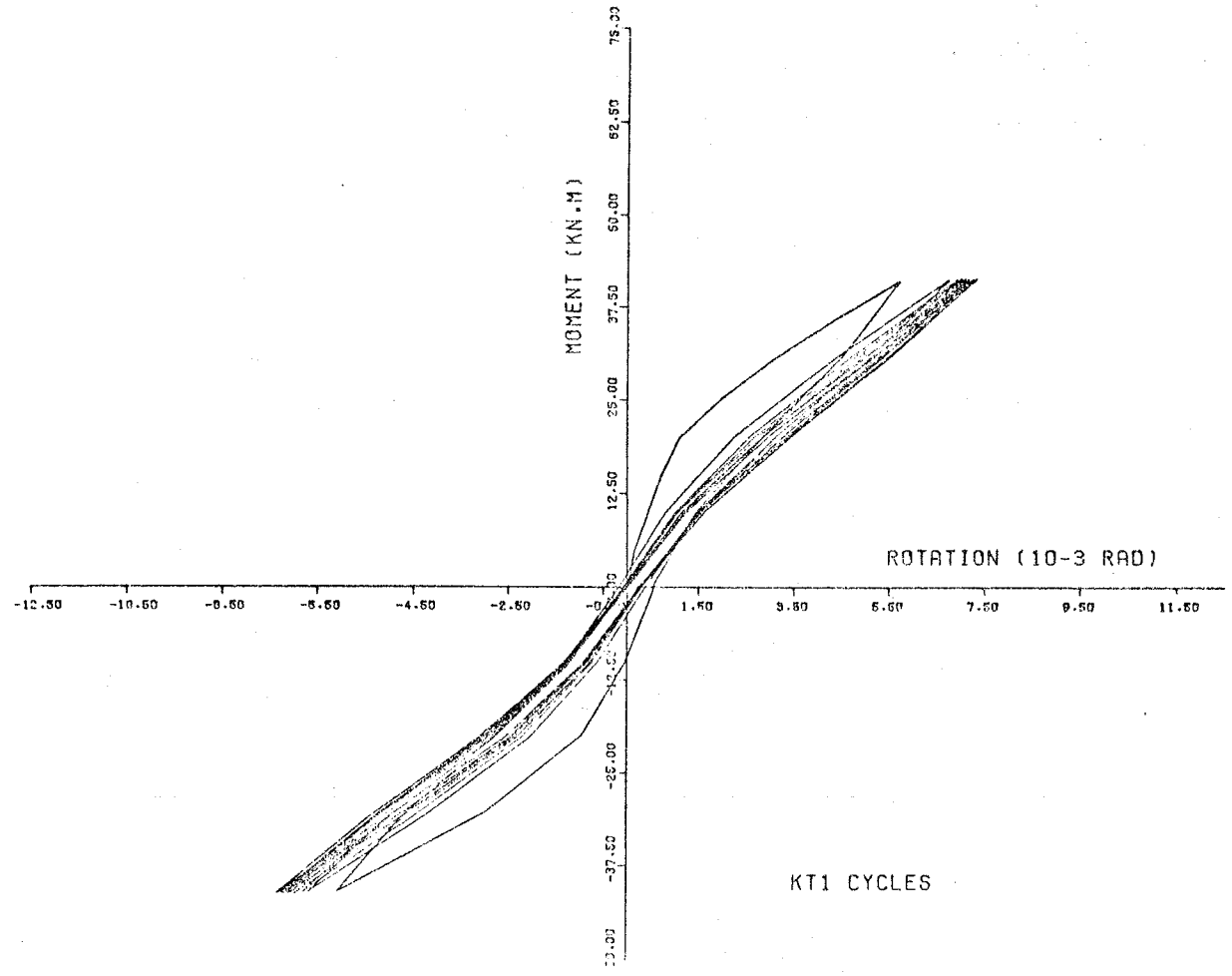

Figure 3 - Cycles moment rotation (KT 1)

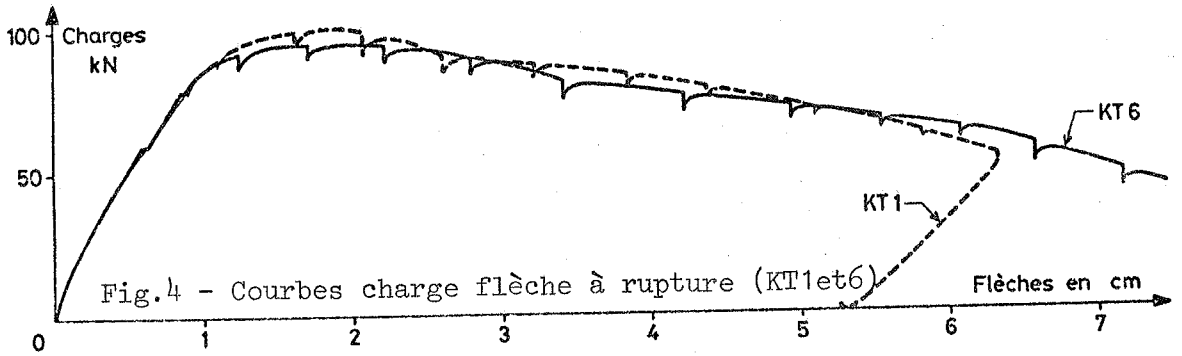

Fig.4 - Courbes charge flèche à rupture (KT1et6)

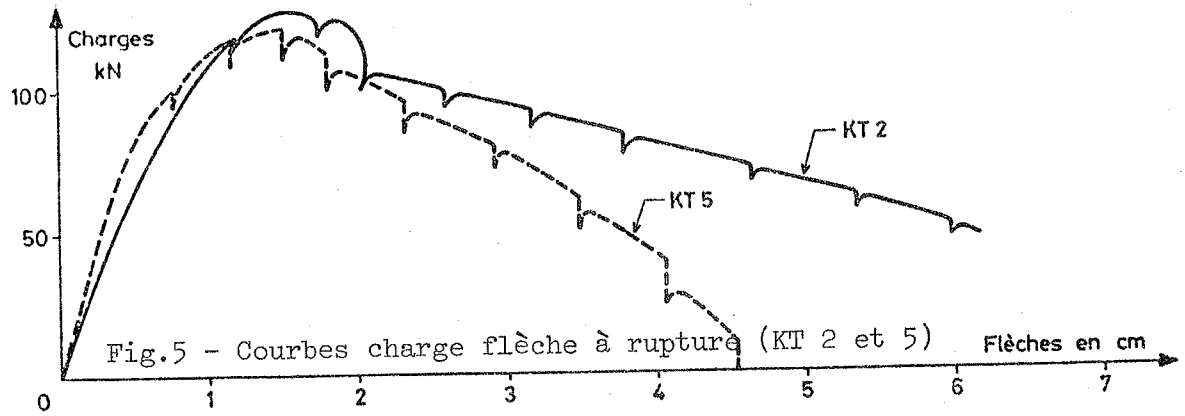

Fig.5 - Courbes charge flèche à rupture (KT 2 et 5)

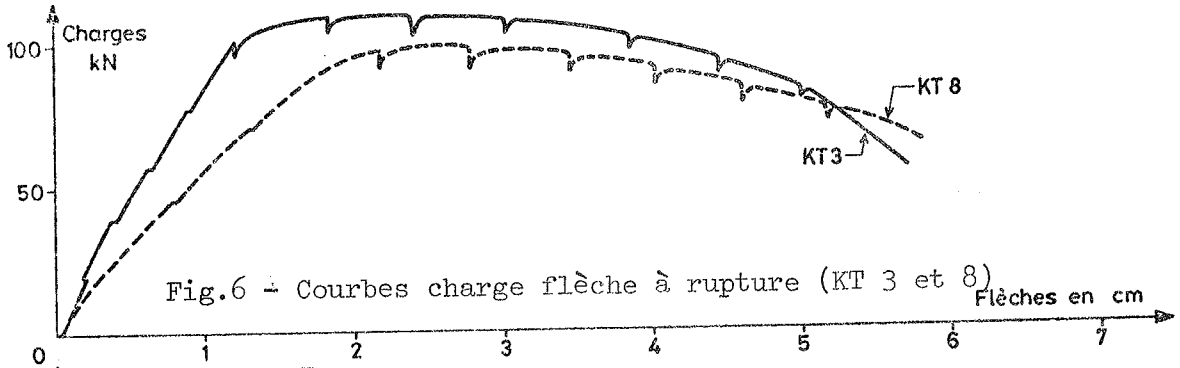

Fig.6 - Courbes charge flèche à rupture (KT 3 et 8)

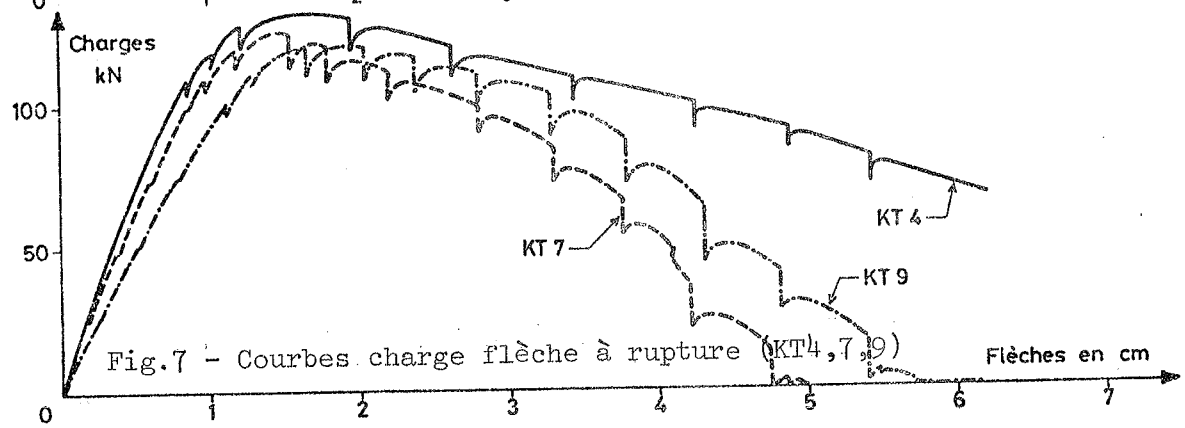

Fig.7 - Courbes charge flèche à rupture (KT4,7,9)

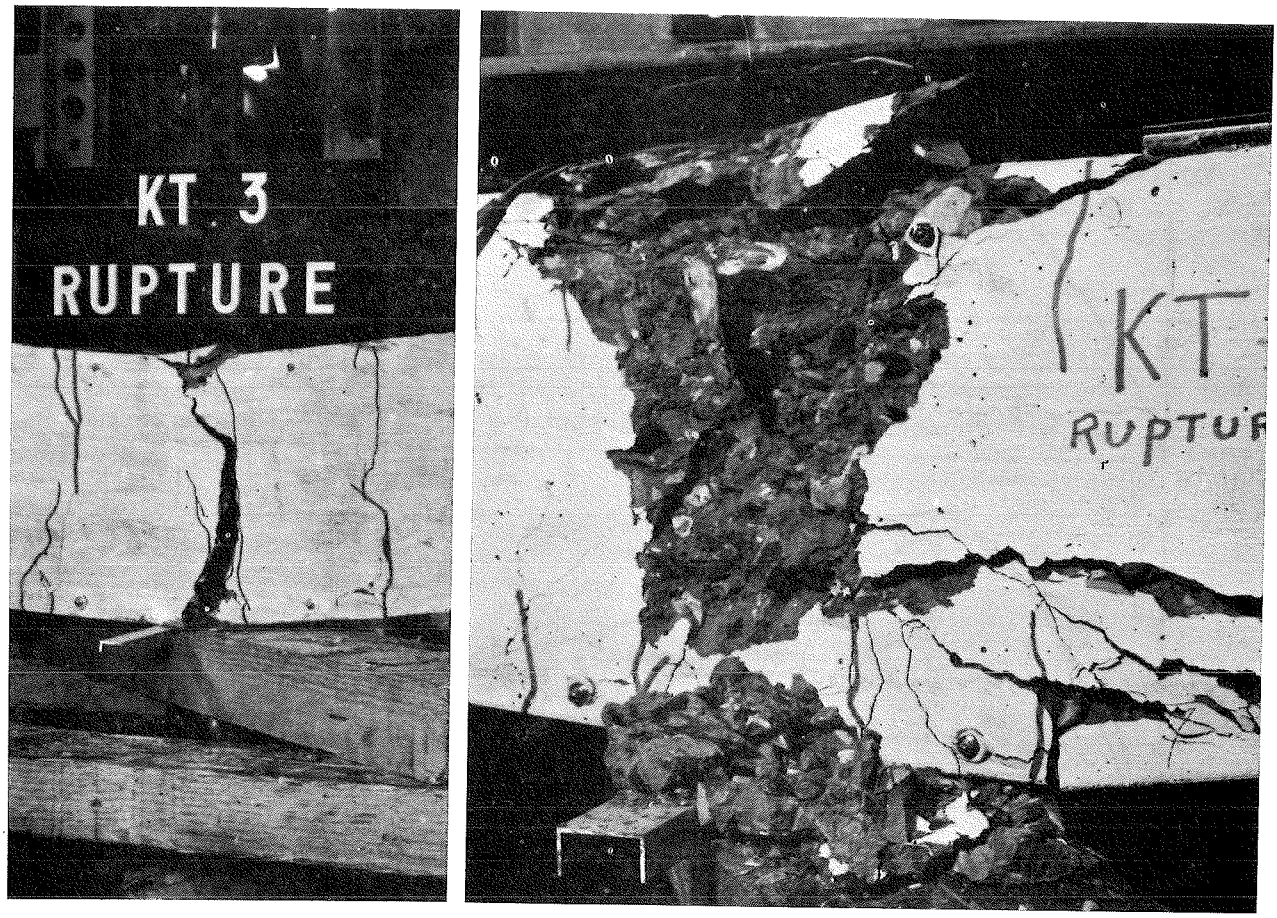

Fig.8 - Photos de rupture (KT 3 et KT 5)

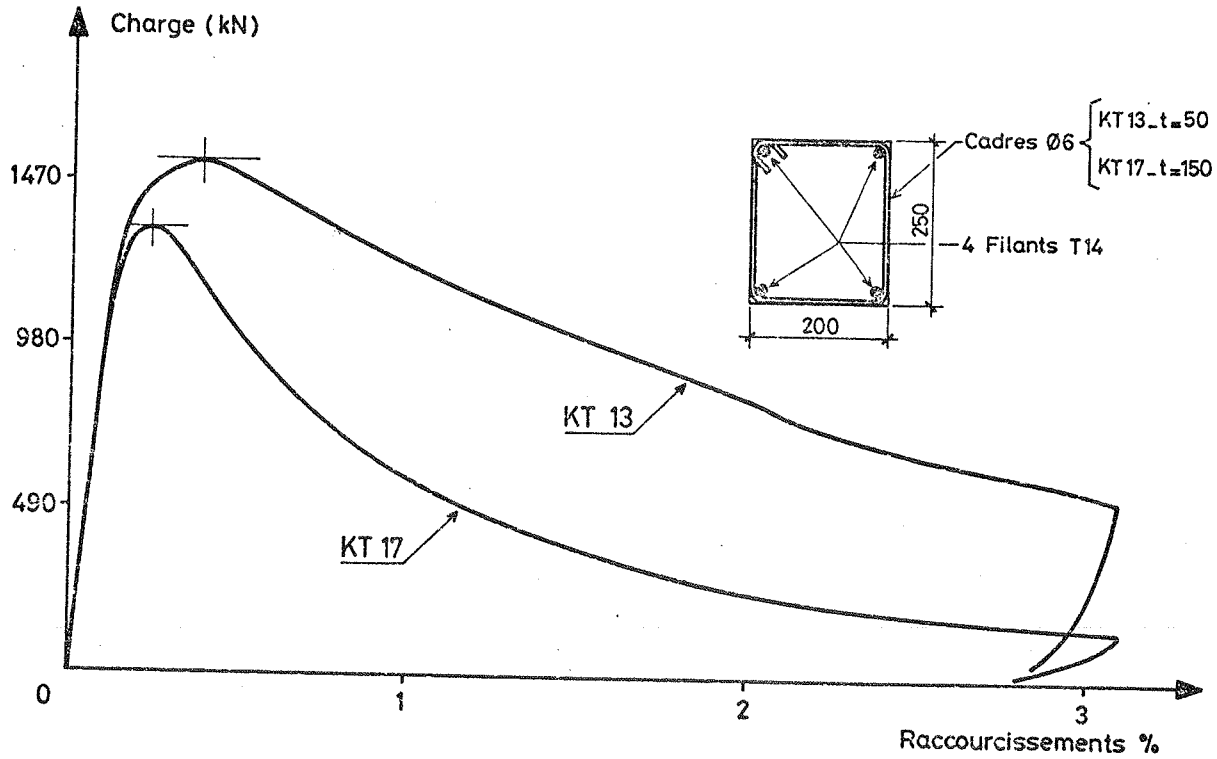

Fig.9 - Courbes contrainte déformation sur prismes (KT 13 et KT 17)

STUDY OF THE BENDING BEHAVIOUR OF REINFORCED CONCRETE COLUMNS UNDER CHANGING AXIAL FORCE

Shizuo HAYASHI
Tokyo Institute of Tecnology
Tokyo, Japan

Seiji KOKUSHO
Tokyo Institute of Technology
Tokyo, Japan

Eiji TERAMOTO
Technical Official, Financial Bureau,
Tokyo, Japan

Tooru OSANAI
Tokyo Institute of Technology
Tokyo, Japan

SUMMARY

This paper describes the experimental and analytical results carried out to investigate the influence of changing axial force on the restoring force characteristics of reinforced concrete columns. Test specimens are 20cm x 20cm cross section, 180cm simple span and 1% ratio of tensile reinforcement. Each specimen is tested under tow-point loading and subjected to pure bending moment and axial force in the test length. Parameters are the loading paths of lateral load and axial force. The moment-curvature relation in the test length is analyzed using the results of the bond tests which are carried out about specimens of the same cross section of foregoing bending test specimens. The restoring force characteristics of reinforced concrete columns are much influenced by changing axial force working columns, and the results of analysis in consideration of the bond between concrete and tensile reinforcement agree with the results of the bending tests very well.

SOMMAIRE

Etude de résistance à la flexion de colonnes en béton armé soumis à une charge axiale changeante Ce texte se charge de décrire les résusltats d'analyse et d'expériences poursuivies dans le but de connaître l'importance de l'influence d'une force axiale changeante sur les caractéristiques de force restitutive sur des colonnes en béton armé. Les échantillons utilisés pour les essais sont des sectioncroisées de 20 × 20 cm d'une envergure de 180 cm et possédant un rapport de 1 % de renforcement à la traction. Chaque échantillon est soumis à un essai sous une charge appliquée à deux endroits et soumis à un moment de torsion simple et une force axiale au cours de l'essai en longueur. Les paramètres représentent les passages de charge du moment de torsion et de la force axiale. Le rapport du moment de courbure au cours de l'essai en longueur est analysé en utilisant les résultats des essais de flexion qui sont effectués sur des échantillons possédant une coupe croisée identique des échantillons utilisés pour les essais mentionnés précédemment. Les caractéristiques de force restitutive des colonnes en béton armé sont notamment influencées par le changement de la force axiale travaillant sur chanque colonne. Les résultats de l'analyse tenant compte de la flexion entre le béton et le renforcement à la tension sont conformes aux résultats de résistance à lz flexion.

INTRODUCTION

The restoring force characteristics of reinforced concrete columns are influenced by magnitude of axial force. During an earthquake, not only lateral force but also axial force of columns changes every moment. However, experimental data of the influence of changing axial force on the restoring force characteristics are few. This paper describes the experimental and analytical results carried out to investigate the influence of changing axial force on the yield moment, on the maximum moment and on the moment-curvature relationship of reinforced concrete columns.

BENDING TESTS SET-UP

The proportions and reinforcement details of bending tests are shown in Fig.1. Test specimens consist of 11 specimens of 20cm x 20cm cross section, 180cm simple span. Tensile and compressive reinforcements consist of 3 deformed bars, respectively. They are 13 mm in diameter and have the lateral lugs. The load paths of the lateral load (P) and axial force (N) of specimens are shown in Fig.2. 5 specimens are tested under loading condition of constant axial force and increasing lateral load. 5 specimens are tested under loading condition that axial force and lateral load increase or decrease by turns. One is tested under loading condition that axial force and lateral load increase or decrease at the same time.

The loading arrangement is shown in Fig.3. Eash specimen is tested under two-point loading and subjected to pure bending moment and axial force in the test length of 65cm between loading points. The measuring arrangement of deflection by dial gages is shown in Fig.4.

The average moment (M) in the test length is calculated from the sum of P x 40cm and N x $\bar{\delta}$, where $\bar{\delta}$ is the average deflection in the test length measured by dial gages from No.3 to No.9. The average curvature in the test length is calculated from deflection measured by dial gages No.3, No.6 and No.9.

The mechanical properties of materials are shown in Table 1.

RESULTS OF BENDING TESTS

The relationships between average moment and average curvature of specimens N-00.02-V, N-04.00-V and N-00.02-VY are shown in Fig.5, Fig.6 and Fig.7, respectively. When axial force increases under constant lateral load, curvature decreases a little. And then lateral load increases under the constant axial force, relationship between moment and curvature draws toward that of the specimen tested under loading condition of the constant axial force and increasing only lateral load. When axial force decreases under constant lateral load, curvature increases according to decreasing of axial force and comes up to the curvature of the specimen tested under the constant axial force. The yield moment is not influenced by load paths if the axial force is the same when the yielding of tensile reinforcement occurs.

ANALYSIS (1) (NO CONSIDERATION OF THE BOND)

In this analysis of bending test results, it is assumed that the section remains plane after deformation.

The models of the stress-strain relationship of reinforcement and concrete used in analysis (1) are shown in Fig.8 and Fig.9. The analytical results of specimens N-00.02-V, N-04.00-V and N-00.02-VY are shown in Fig.10, Fig.11 and Fig.12, respectively.

Several interesting points are pointed out in the results of analysis (1). After cracking, the curvature obtained by analysis (1) is greater than that of the experiments. When axial force increases under constant lateral load, the curvature decreases and comes up to the curvature of the specimen under loading condition of the constant axial force and increasing only lateral load. The results of analysis (1) do not agree with the experimental results on these points so well. When axial force decreases under constant lateral load, the results of analysis (1) agree with the experimental results. However, when bending moment decreases under constant axial force, the relationships between moment and curvature are linear.

In analysis (1), we consider that concrete can not bear the tensile stress after cracking and that bending cracks occur in all tensile zone. In actual facts, however, bending cracks occur at intervals and concrete between cracks works through the bond between reinforcement and concrete. For this reason, the results obtained by analysis (1) do not agree with that of experiments so well.

RESULTS OF BOND TESTS

In order to investigate behavior of concrete between cracks through the bond between reinforcement and concrete, bond tests were carried out under loading condition of repeated axial compression and tension. The proportions and reinforcement details are shown in Fig.13. The cross section is the same of the specimens of foregoing bending tests.

The mecanical properties of materials are shown in Table 2.

The relationship between the axial force and the axial strain obtained by one of bond tests is shown in Fig.14 The dot-dash line in Fig.14 is the relationship between axial force and axial strain of reinforcement, and the dotted line in Fig.14 is relationship between axial force and axial strain of concrete. The remains, which are obtained by taking the forces of reinforcement and concrete from the total force of test result, are shown in Fig.15. These curves can be regarded as the relationship between strain and force which is depends on concrete between cracks through the bond between reinforcement and concrete.

The idearization of the relationship between force depending on bond and strain is shown in Fig.16.

ANALYSIS (2) (IN CONSIDERATION OF THE BOND)

In this analysis, it is assumed that the force depending on the bond shown in Fig.16 works on the section at the position of the reinforcement besides the forces depending on concrete and on reinforcement shown in Fig. 8 and Fig. 9.

The analytical results of the specimen N-00.02-V, N-04.00-V and N-00.02-VY are shown in Fig.17, Fig.18 and Fig.19, respectively. And the examples of the comparison of the analytical results with the experimental results are shown in Fig.20 and Fig.21.

In respect of the curvature after bending cracking, the results of the analysis (2) agree with those of the bending tests better than the analysis (1). And when axial force increases under constant lateral load, the curvature obtained by analysis (2) decreases a little and agrees with the result of bending test better than that of analysis (1). When the lateral load decreases or increases under constant axial force, the relationship between moment and curvature obtained by the analysis (2) agrees with that of bending test better than that obtained by the analysis (1).

CONCLUSIONS

The results of the experimental tests and analyses are as follows;

(1) The yield moment is not influenced by load paths if the axial force is the same when the yielding of tensile reinforcement occurs.

(2) When axial force increases under constant lateral load, curvature decreases a little. And when lateral load increases under the constant axial force, the relationship between moment and curvature draws towards that of the specimen tested under loading condition of the constant axial force and increasing only lateral load.

(3) When axial force decreases under constant lateral load, curvature increases according to decreasing of axial force and comes up to the curvature of the specimen tested under the constant axial force.

(4) Concrete between cracks works through the bond between concrete and reinforcement, and the force in apearance depending on the bond can be modified as shown in Fig.16.

(5) Analysis in consideration of the bond between concrete and reinforcement agrees with the experimental results very well.

This paper describes a method of analysis in consideration of the bond between concrete and reinforcement and shows that the results of this analysis agree with the experimental results very well. Therefore, additional studies are necessary to apply this analytical method to columns which are subject to shear force, bending moment and axial force at the same time.

ACKNOWLEGMENTS

The authors wish to thank KOBE STEEL, LTD. and NETSUREN CO., LTD. for provision of reinforcing bars.

REFERENCES

(1) H.Muguruma, S.Morita, K.Tomita, "Stress Distribution in Reinforced Concrete Beams with Flexural Cracks", Transaction of the A.I.J. No.220, Oct., 1972.

(2) S.Kokusho, S.Hayashi, E.Teramoto, "An Experimental Study on the Bending Behavior of Reinforced Concrete Members under Changing Axial Force, Part 1 and Part 2", Proc. of the A.I.J., Oct., 1975.

(3) S.Kokusho, S.Hayashi, T.Osanai, "An Experimental Study on the Bending Behavior of Reinforced Concrete Members under Changing Axial Force, Part 3 and Part 4", Proc. of the A.I.J., Oct., 1978.

(4) S.Tani, S.Soda, "Dynamic Analysis of Reinforced Concrete Frame Subjected to Earthquake Excitation in Both the Horizontal and the Vertical Directions", Proc. of the 5th Japan Earthquake Engineering Symposium, Nov., 1978.

Table 1 Mechanical properties of materials used in bending tests

Steel Bar			
	$s\sigma y$ (kg/cm^2)	$s\sigma max$ (kg/cm^2)	Elongation (%)
D13	3,820	5,570	25.6
6ϕ	3,950	4,390	27.2
Concrete			
$c\sigma B$ (kg/cm^2)	$c\varepsilon B$ ($\times 10^{-6}$)	cE (kg/cm^2)	$c\sigma t$ (kg/cm^2)
298	2,500	2.08×10^5	27.2

Table 2 Mechanical properties of materials used in bond tests

Steel Bar			
	$s\sigma y$ (kg/cm^2)	$s\sigma max$ (kg/cm^2)	Elongation (%)
D13	4,230	6,443	27.7
6ϕ	3,820	4,400	27.8
Concrete			
$c\sigma B$ (kg/cm^2)	$c\varepsilon B$ ($\times 10^{-6}$)	cE (kg/cm^2)	$c\sigma t$ (kg/cm^2)
337	3,600	1.77×10^5	24.3

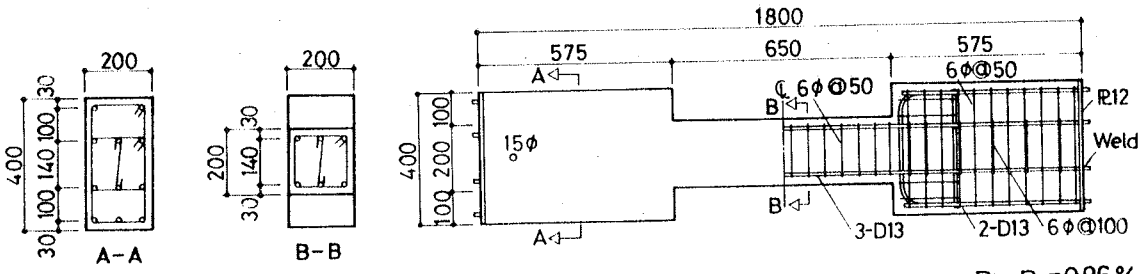

Fig.1 Test specimen of bending test unit:mm $P_t = P_c = 0.96\%$ $P_w = 0.85\%$

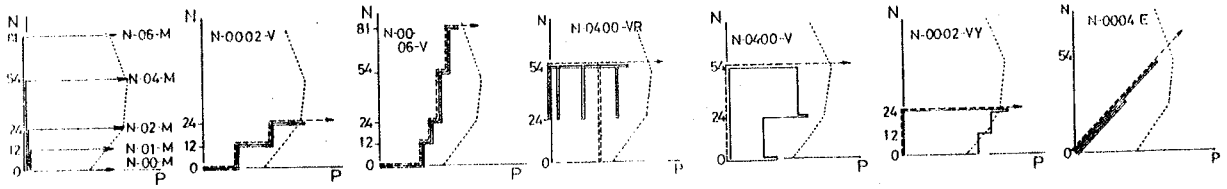

Fig.2 Load paths of specimens

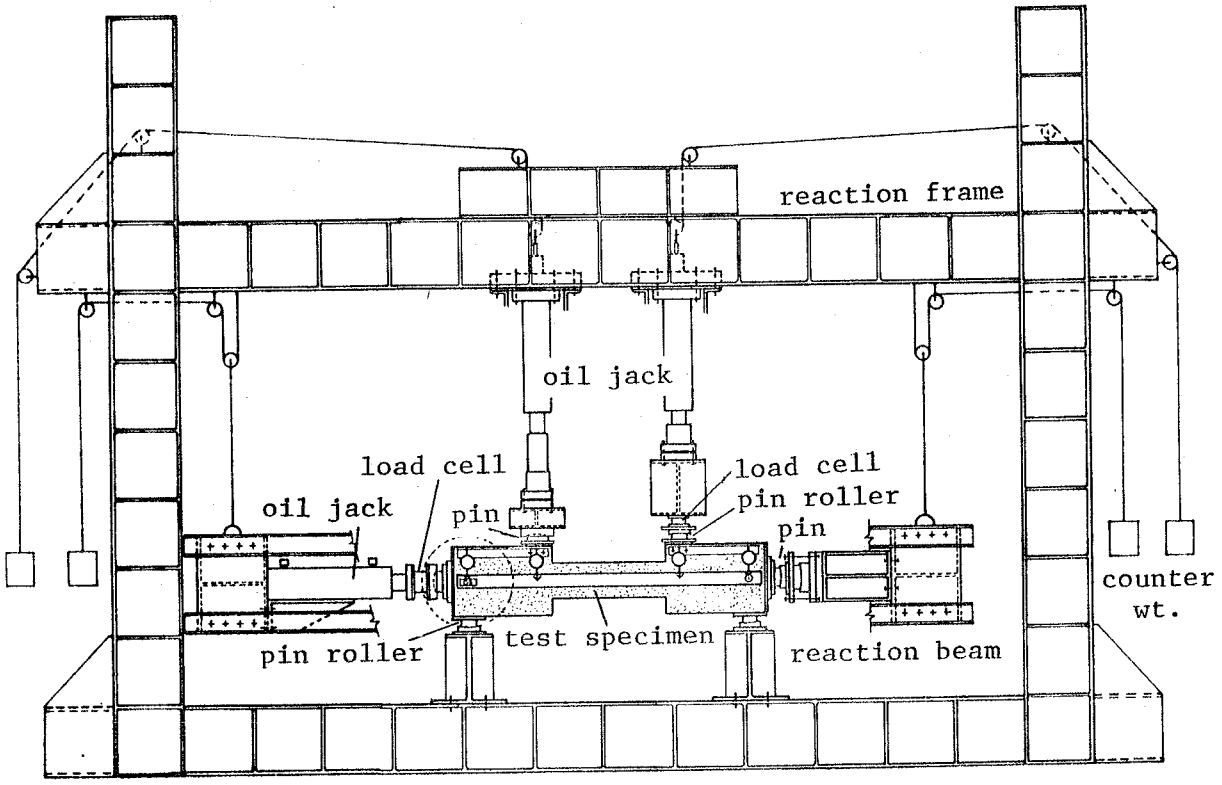

Fig.3 Loading arrangement

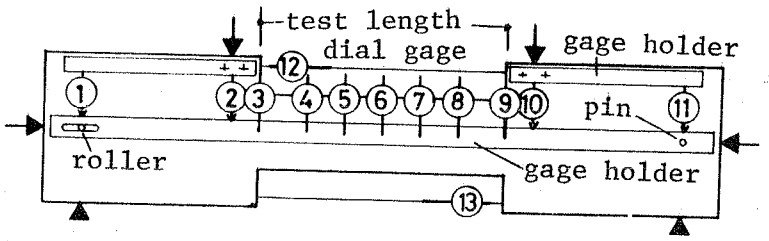

Fig.4 Measuring arrangement of deflection

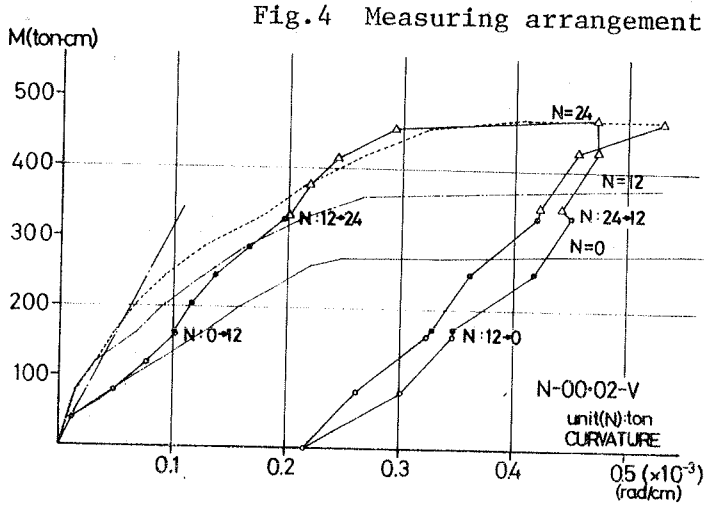

Fig.5 Relationship between moment and average curvature of N-00.02-V from bending test

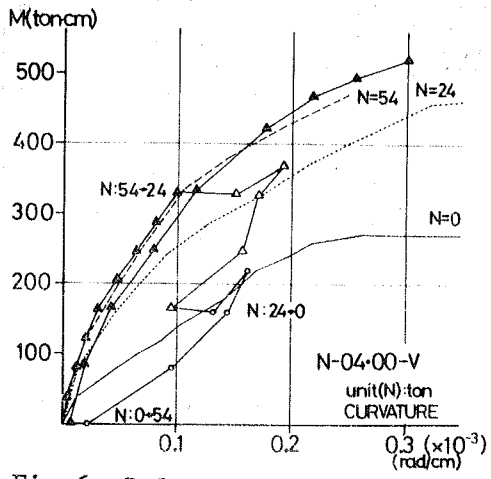

Fig.6 Relationship between moment and average curvature of N-04.00-V from bending test

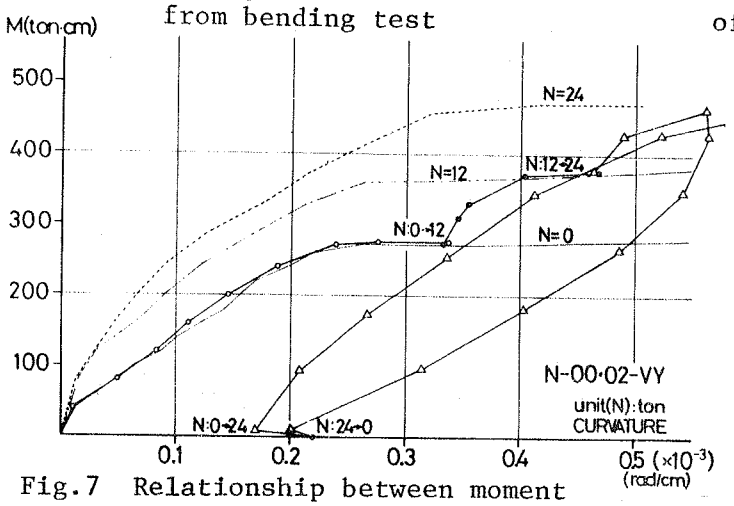

Fig.7 Relationship between moment and average curvature of N-00.02-VY from bending test

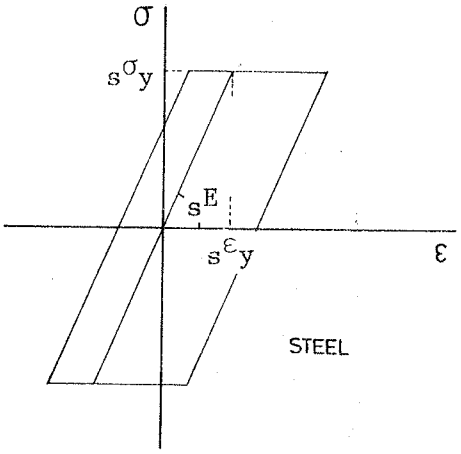

Fig.8 Model of reinforcement used in analysis

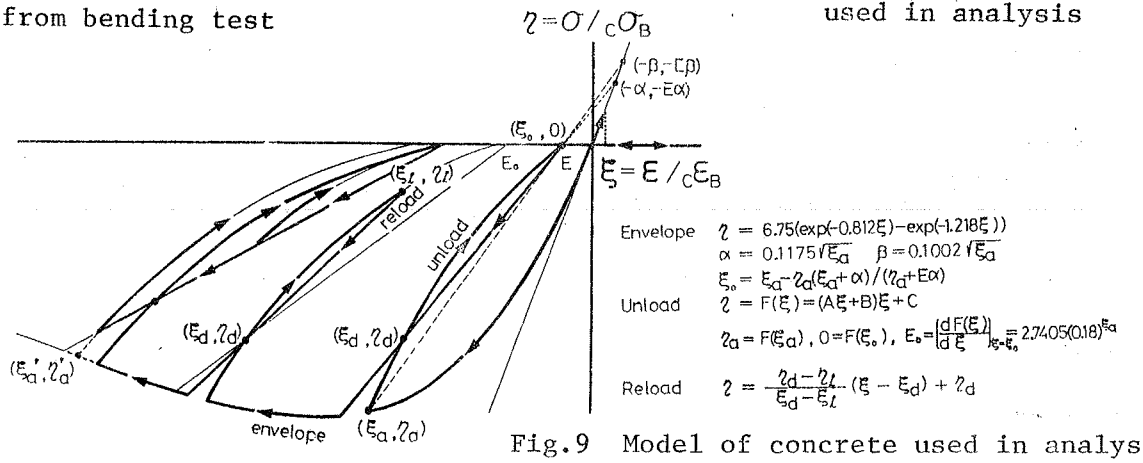

Fig.9 Model of concrete used in analysis

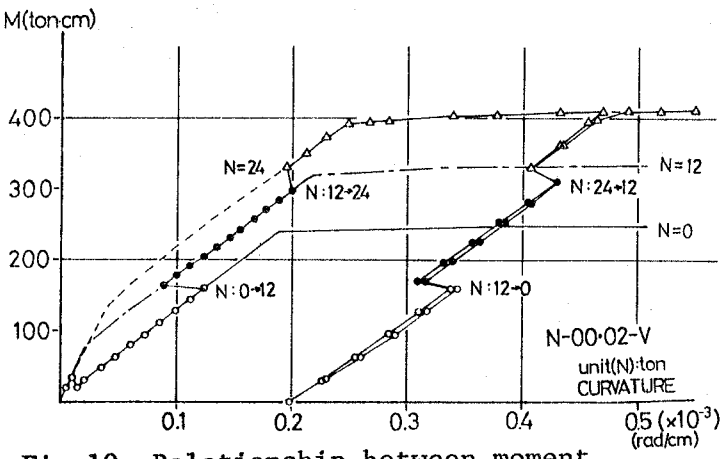

Fig.10 Relationship between moment and curvature of N-00.02-V from analysis(1)

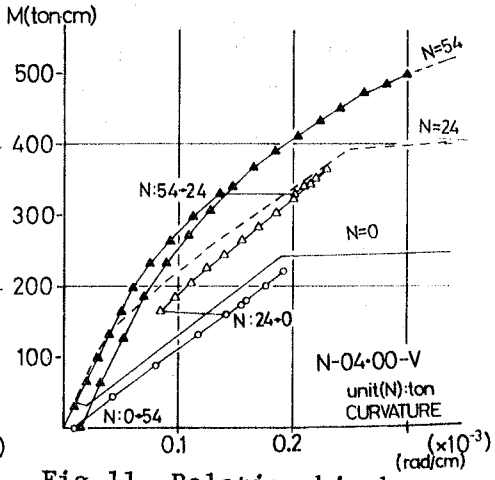

Fig.11 Relationship between moment and curvature of N-04.00-V from analysis(1)

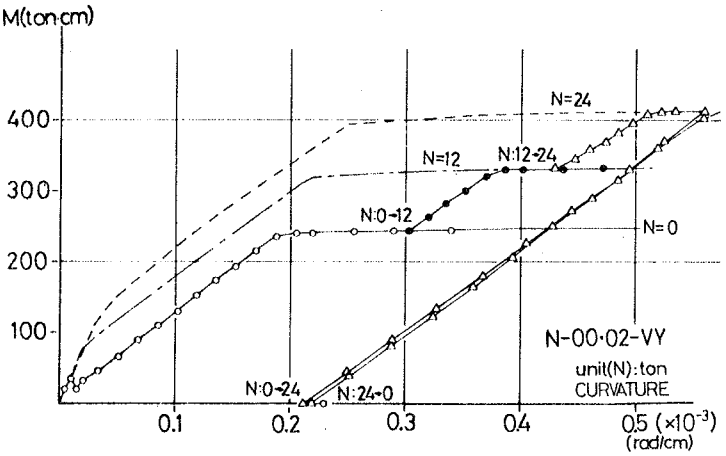

Fig.12 Relationship between moment and curvature of N-00.02-VY from analysis(1)

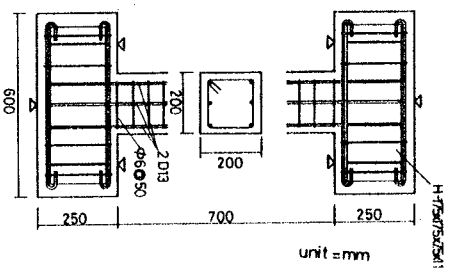

Fig.13 Test specimen of bond test

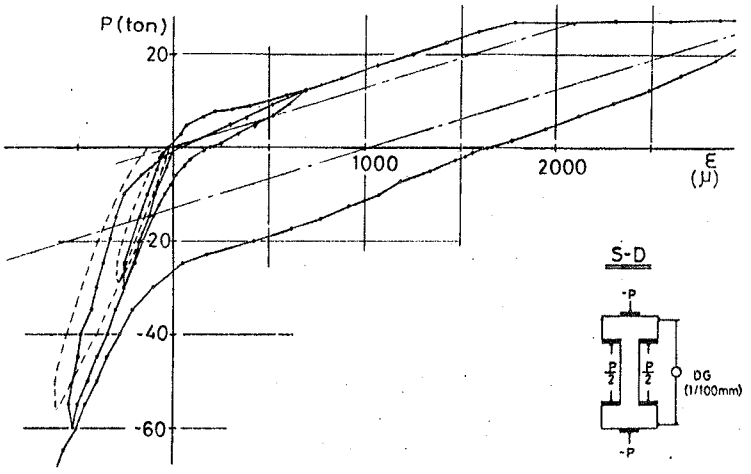

Fig.14 Relationship between axial force and axial strain of bond test

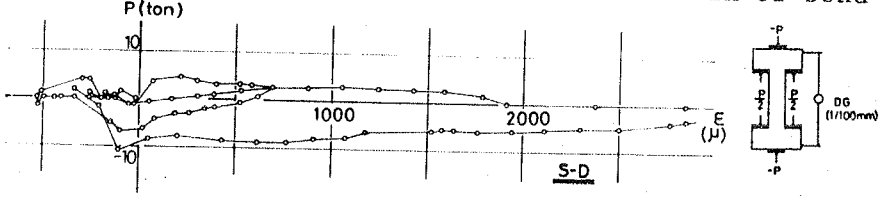

Fig.15 Relationship between strain and force depending on the bond

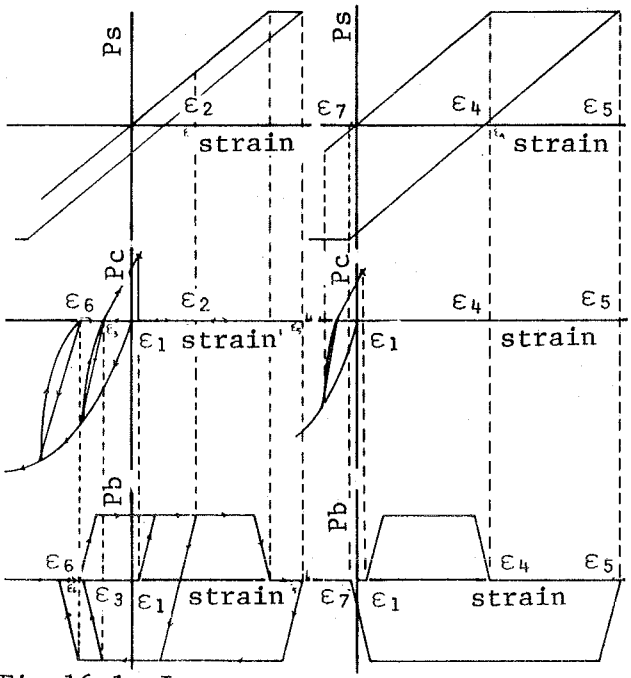

Fig.16-1 In case that crack is closed before reinforcing bar yield in compression

Fig.16-2 In case that reinforcing bar yield in compression before crack is closed

Fig.16 Idearization of the relationship between strain and force depending on the bond

Ps: force of reinforcing bar
Pc: force of concrete at posiyion of the reinforcing bar
Pb: force depended on the bond
strain: strain at position of the reinforcing bar

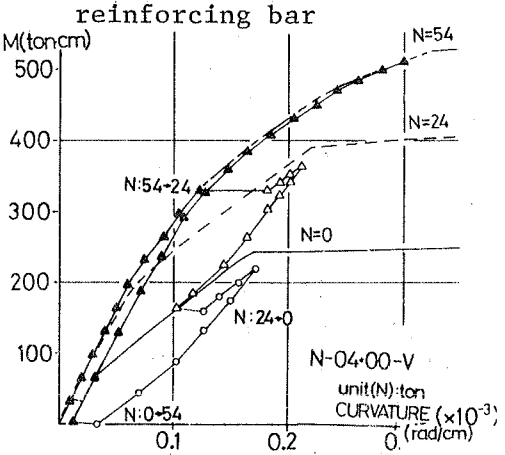

Fig.18 Relationship between moment and curvature of N-04.00-V from analysis(2)

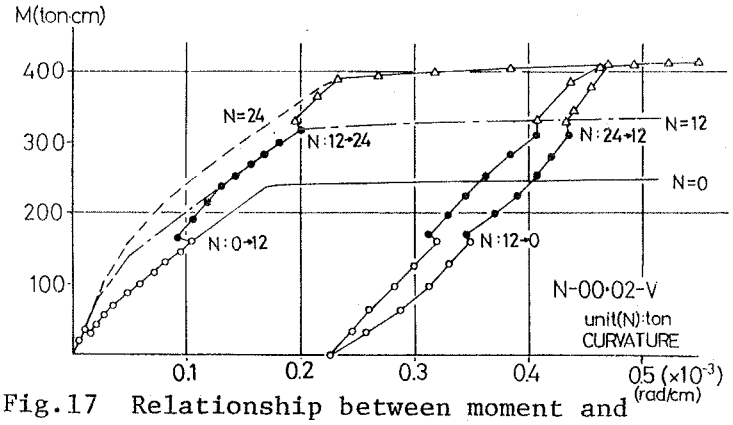

Fig.17 Relationship between moment and curvature of N-00.02-V from analysis(2)

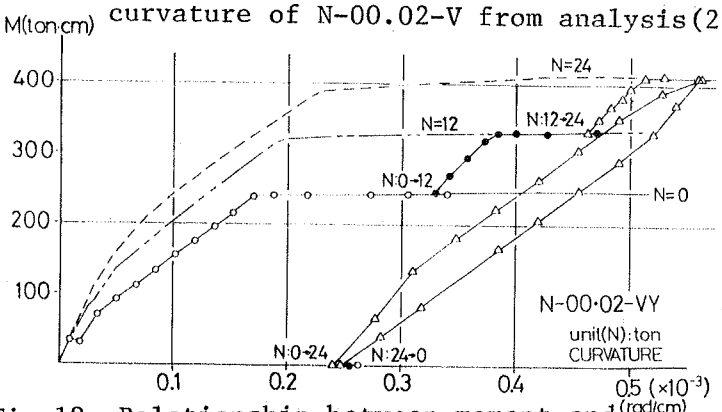

Fig.19 Relationship between moment and curvature of N-00.02-VY from analysis(2)

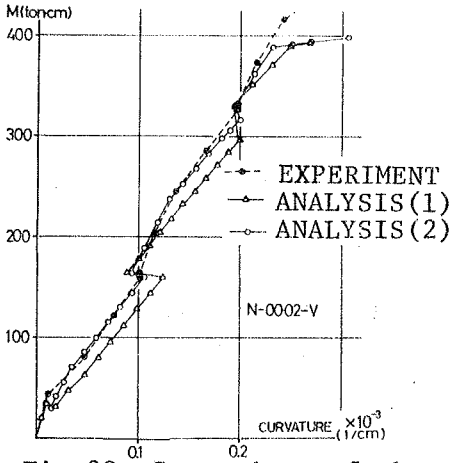

Fig.20 Comparison of the analyzed results with the experimental result

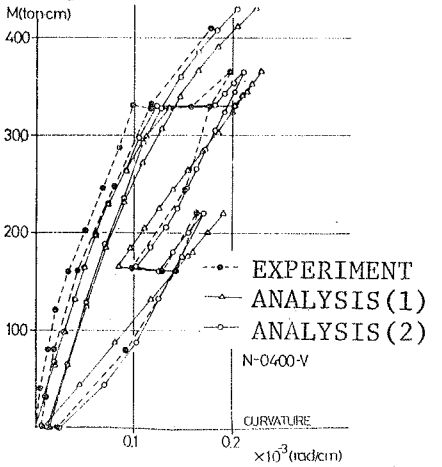

Fig.21 Comparison of the analyzed results with the experimental result

THE INFLUENCE OF AXIAL LOAD ON THE RESPONSE OF COLUMNS UNDER BIDIRECTIONAL LOADINGS

H. RAMIREZ
The University of Texas at Austin
Texas, U.S.A.

J.O. JIRSA
The University of Texas at Austin
Texas, U.S.A.

SUMMARY

The purpose of this investigation was to examine experimentally the influence of axial load on the behavior of reinforced concrete short columns under bidirectional cyclic lateral deformations.

L'objet de ce programme de recherche a été d'examiner l'influence d'une force axiale sur le comportement de colonnes courte soumisses à deformationscycliques bi-latérales.

INTRODUCTION

It has been shown in previous analytical studies [1,2,3] that the response of a structure to ground motion may be adversely influenced if lateral motion in both orthogonal directions is considered. Experimental data are needed in order to incorporate the effect of multidirectional forces in the analysis and design of R/C buildings for earthquakes. Some experimental work has been reported [4,5] on R/C members subjected to cyclic biaxial bending in which flexural failures were produced. While flexural deformations are preferable in any structure subjected to large earthquake ground motions, it is not always possible to proportion the members to ensure such behavior. The examination of the influence of bidirectional lateral loading histories on short columns failing in shear has been reported [6] for series of tests in which the specimen geometry was constant, no axial load was imposed and the only variable was the lateral history. The purpose of this study is to extend the previous work and to examine experimentally the influence of axial loads on short columns under cyclic lateral deformations. In all the tests, the specimen geometry is the same as in the previous work [6]. Two basic lateral deformation histories are used in combination with different levels of axial tension and compression as well as alternate application of both. Future work is planned on specimens with different geometry.

Test Specimen

The test specimen is shown in Fig. 1. The test specimen is considered to be a short column framing into rigid floors which are simulated by large

end blocks. The longitudinal reinforcement consists of eight 19 mm bars with 90° hooks anchored in the end blocks. Transverse reinforcement is fabricated from 6 mm deformed bars spaced at 65 mm and designed with the criterion of dealing with a column that might not perform satisfactorily under the imposed loads, but representing typical practice in column design. The nominal yield strength of the reinforcement is 420 MPa. The nominal strength of the concrete is 35 MPa.

Test Setup

A schematic elevation view of the test setup is shown in Fig. 2 (similar arrangement in the orthogonal direction). The lateral loads are applied with 670 kN servo-controlled actuators and the vertical load with a 1330 kN servo-controlled actuator. Three paired positioning actuators are used to control the rotation of the top end in each plane. The loading frame and hydraulic loading system are anchored to the floor-wall reaction system built at The University of Texas at Austin. Details on the characteristics and operation of the loading apparatus are described in Ref. 7.

Lateral Deformation Histories

Two basic lateral deformation histories are used. History U, with cyclic lateral deformations in only one direction, is shown in Fig. 3. History B, with alternate cyclic lateral deformations in both orthogonal directions, is shown in Fig. 4. Three cycles at each peak lateral deformation level of one, two, three, and four times an initial value are considered: a total of twelve continuous cycles for History U and twenty-four cycles, groups of three cycles at each level in each direction, for History B. The value for the initial deformation is used as 5 mm, representing approximately the displacement producing yield in the main tension reinforcement when no axial load is present.

Axial Load Variations and Test Schedule

Axial load variations are selected with the intention to develop basic information that might be useful for further experimental studies. In order to study the effect of constant compression, constant tension and alternate tension and compression, axial loads are held constant in some tests and variable in others. Because no data have been reported regarding cyclic lateral loads in combination with axial tension, three levels of axial tension are included and only one of compression. The upper limit for tension axial force is represented by the force required to produce yield in the vertical reinforcing bars. Regardless of the fact that this case may not be realistic, it is considered because it represents a point of reference. The other two levels of tension correspond to one-fourth and one-half of that upper limit. The level of axial compression used produced an average stress based in the core area of 8.4 MPa. The complete test schedule for the study is listed in Table 1. Tests 1 to 5 form a group in which the effect of the axial load level is varied and only the loading history U is used. In a more limited way, tests 7 to 9 form a similar group when History B is considered. In the last two tests, alternate application of axial loads is studied. Test ATC-U is included to simulate loads induced by an earthquake on an exterior column in which tension alternating with compression occurs in the first stage of the event where afterwards only compression is present. This may be the case arising in a reinforced concrete frame building with stiff but low-strength filler walls. The application sequence of axial force in relation with the History U is shown in Fig. 5. Test ATC-B is included to

simulate loads induced by an earthquake on an exterior column of a slender R/C building in which tension alternating with compression occurs for deformations in one direction, and only compression for deformations in the orthogonal direction. The sequence of application of axial force in relation to History B is shown in Fig. 6.

DESCRIPTION OF TEST RESULTS

Lateral loads, as well as loads in the positioning actuators, are monitored. Lateral translations of the top end block and vertical displacements of top and bottom end blocks are measured. Strains in the transverse and longitudinal reinforcement are measured at the locations indicated in Fig. 1. Crack patterns are marked at all load stages. Lateral displacements are not large enough to cause an increase in moment due to eccentricity of column load.

A qualitative analysis is performed based on comparisons of the data from different tests. It includes a study of the effect of constant compression, constant tension, and alternate application of both. Envelopes of peak normalized shear are used to summarize behavior. The envelopes are the curves uniting peak values in the hysteretic curves, test 00-U is shown in Fig. 7.

Influence of Compression

Fig. 8 compares the peak normalized shear, $V/A_c \sqrt{f'_c}$ (V in kN, A_c = 0.0625 m^2, and f'_c in Pa), envelopes for first and last peaks in the north direction for tests 00-U, 00-B, 120C-U, and 120C-B. In this figure the monotonic curve is also shown for comparison. Note that the behavior of 00-U is approximately the same as for monotonic loading. In 120C-U and 120C-B, applied shear first increases for levels of deformation up to $2\Delta_i$ and after that a high rate of shear deterioration is exhibited. The effect of lateral alternate deformations in the orthogonal direction is reflected by a more drastic shear deterioration after the $2\Delta_i$ level. Figure 9 compares the progressive strain in a tie for test 00-U and 120C-U. In 00-U, the tie remains below the yield, while a similar tie in 120C-U reaches yield at $2\Delta_i$ level.

Influence of Tension

In Fig. 10, the envelopes of first and last peaks of normalized shear for tests with constant tension and History U are presented. The required shear to attain certain deformation decreases as the level of tension increases but less shear deterioration is observed. Figure 11 shows the progressive strain in a tie for the same tests. This figure shows that the required level of lateral deformation to produce yield in the tie increases as the level of tension increases. Comparing envelopes of shear in the north direction (Fig. 12) of tests 50T-B, 00-B, and 120C-B shows that the presence of tension reduces the shear deterioration when alternate lateral (bidirectional) deformations are imposed.

Influence of Alternating Tension and Compression

The first and last peaks for tests ATC-U are compared with those of tests 120C-U and 100T-U in Fig. 13. For peaks to the north at Δ_i level in which tension is applied, both applied shear and stiffness reduce more than that observed in 100T-U (constant level of tension instead of alternate).

However, for higher levels of deformation, in which compression is applied, the behavior of ATC-U approximates that of 120C-U. For peaks to the south, ATC-U approximates the behavior of 120C-U for all deflection levels.

Figure 14 shows the envelopes in the NS direction of loading for test ATC-B as compared with 50T-B and 120C-B. Peaks to the north show similar behavior but lower strength in relation to 50T-B (same level of tension applied in different sequence). This is due to the mode of application of tension and the presence of compression in the orthogonal direction in ATC-B. For peaks to the south, test ATC-B shows similar behavior to 120C-B but less shear deterioration is noted.

CONCLUSIONS

Based on the data presented here, the following general trends were observed.

1. The level and mode of application of axial loads affects the behavior. The amount of transverse reinforcement was not sufficient to permit flexural failures in any of the specimens tested. However, it was effective in providing some confinement.

2. Constant compression accelerated shear deterioration. Constant tension decreased shear deterioration but at the same time substantially reduced the shear capacity and the stiffness.

3. The application of tension alternating with compression influences the response mainly at the peaks where the tension is present.

4. The response appears to be governed by the confining action of the ties. The efficiency of the ties to confine the core decreases with compressive axial load, with the number of cycles at a deformation level and with the presence of lateral deformations in the perpendicular direction.

ACKNOWLEDGMENT

The support of the National Science Foundation through Grants ENV75-00192 and ENV77-20816 for this work is gratefully acknowledged.

REFERENCES

1. Pecknold, D. A. W., and Sozen, M. A., "Calculated Inelastic Structural Response to Uniaxial and Biaxial Earthquake Motions," Paper No. 223, Fifth World Conference on Earthquake Engineering, Rome, 1973.

2. Takizawa, H., "Biaxial and Gravity Effects in Modeling Strong-Motion Response of RC Structures," Sixth World Conference in Earthquake Engineering, New Delhi, 1977, pp. 3-49 to 3-54.

3. Selna, L. G., and Lawder, J. H., "Biaxial Inelastic Frame Seismic Behavior," SP-53, American Concrete Institute, Detroit, 1977, pp. 439-461.

4. Okada, T., et al., "Restoring Force of Reinforced Concrete Columns under Biaxial Load Reversals with Constant Axial Load," Architectural Institute of Japan, Paper Nos. 2506, 2507, and 2508, 1976.

5. Takiguchi, K., and Kokusho, S., "Hysteretic Behavior of RC Members Subjected to Biaxial Bending Moments," Sixth World Conference on Earthquake Engineering, New Delhi, 1977, pp. 11-250.

6. Maruyama, K., Ramirez, H., and Jirsa, J. O., "Behavior of Reinforced Concrete Columns under Biaxial Lateral Loading," Sixth European Conference on Earthquake Engineering, Dubrovnik, 1978.

7. Jirsa, J. O., Maruyama, K., and Ramirez, H., "Development of Loading Systems and Initial Tests--Short Columns under Bidirectional Loading," CESRL Report No. 78-2, Civil Engineering Structures Research Laboratory, Department of Civil Engineering, The University of Texas at Austin, September 1978.

TABLE 1 TEST SCHEDULE

No.	Mark	Lateral History	f'_c (MPa)	Axial Load	
				Mode	Level
1	120C-U	U	31	Constant Compression	530 kN (120 K)
2	00-U	U	34	No axial load	Zero
3	50T-U	U	35	Constant Tension	220 kN(50 K) 1/4 Yield
4	100T-U	U	39	Constant Tension	445 kN(100 K) 1/2 Yield
5	200T-U	U	40	Constant Tension	890 kN(200 K) Yield Level
6	120C-B	B	41	Constant Compression	530 kN (120 K)
7	00-B	B	41	No Axial Load	Zero
8	50T-B	B	32	Constant Tension	220 kN (50 K)
9	ATC-U	U	32	Alternate	445 kN(100 K) Tension 530 kN (120K) Compression
10	ATC-B	B	34	Alternate	220 kN (50 K) Tension 530 kN(120 K) Compression

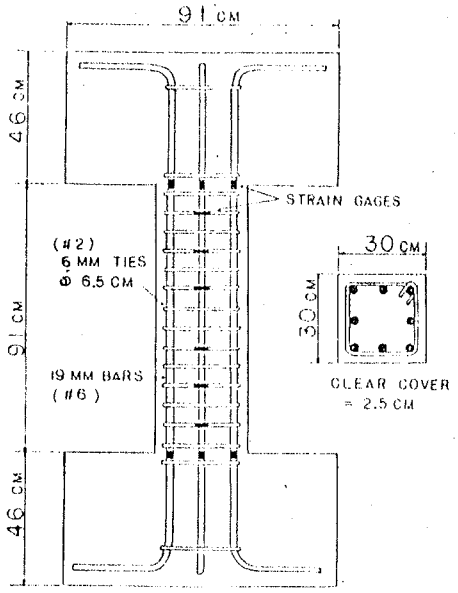

Fig. 1 Test Specimen

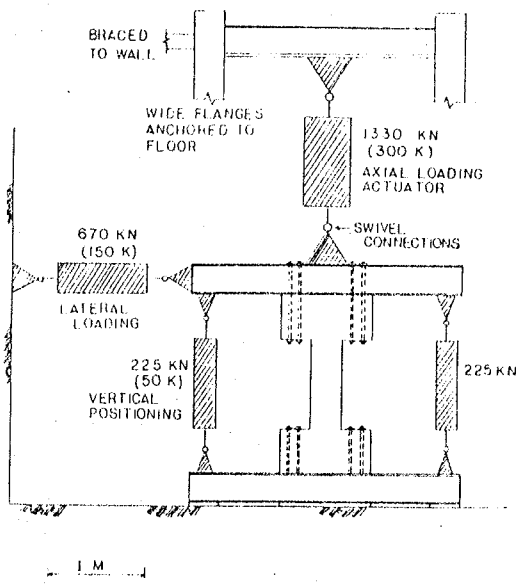

Fig. 2 Elevation of Test Setup

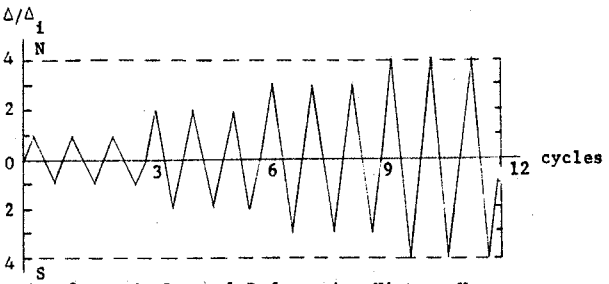

Fig. 3 Basic Lateral Deformation History U

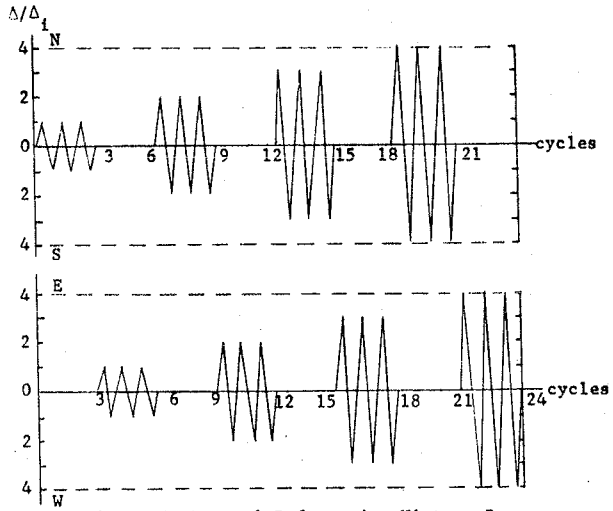

Fig. 4 Basic Lateral Deformation History B

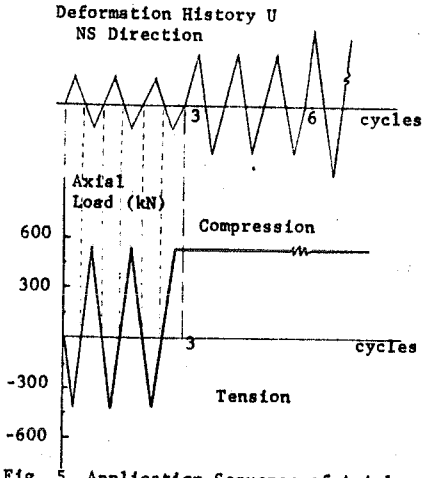

Fig. 5 Application Sequence of Axial Loads, Test ATC-U

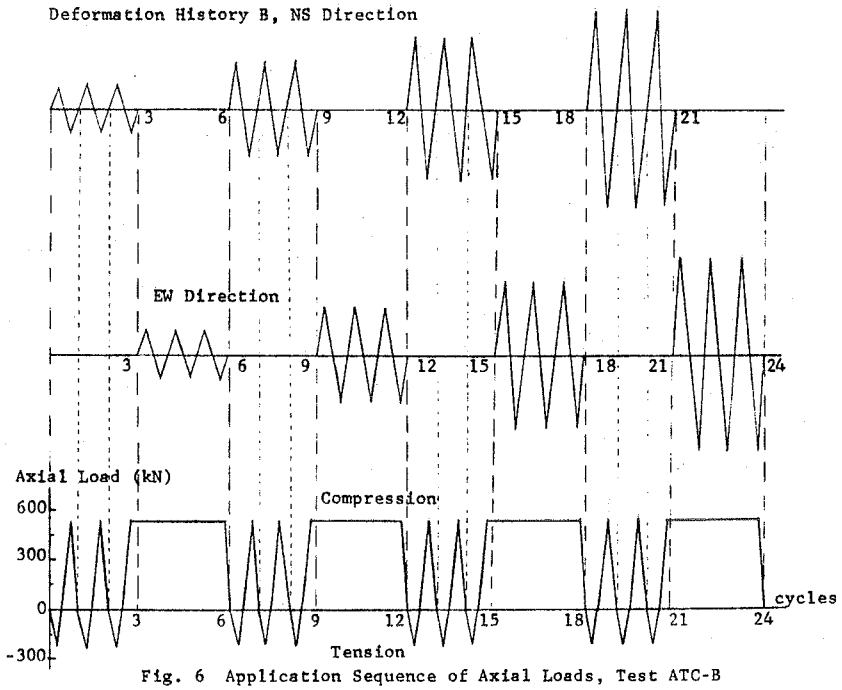

Fig. 6 Application Sequence of Axial Loads, Test ATC-B

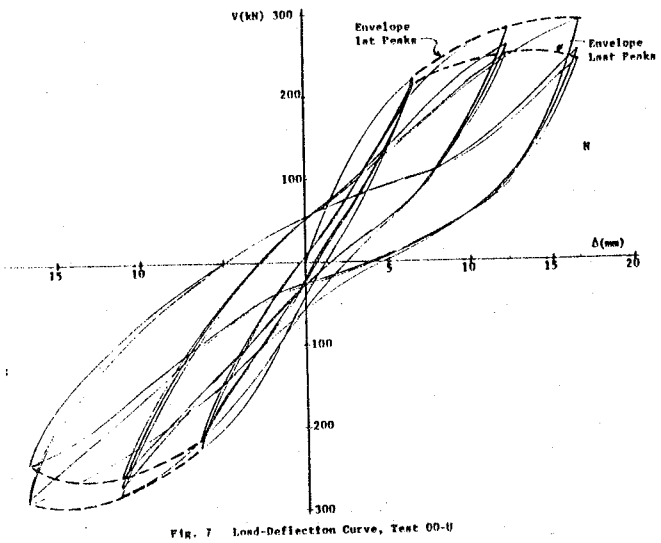

Fig. 7 Load-Deflection Curve, Test 00-U

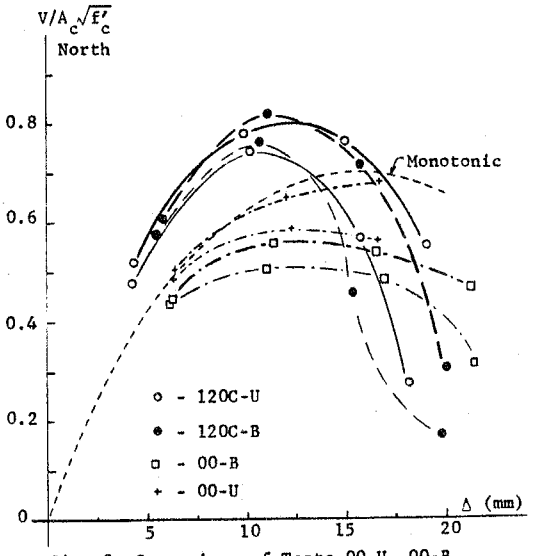

Fig. 8 Comparison of Tests 00-U, 00-B, 120C-U, and 120C-B

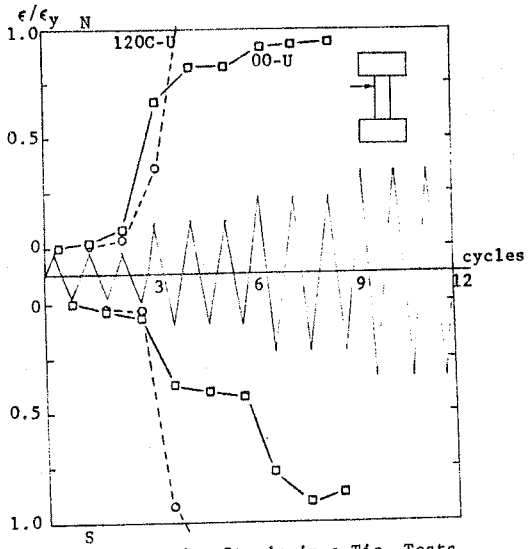

Fig. 9 Progressive Strain in a Tie, Tests 00-U and 120C-U

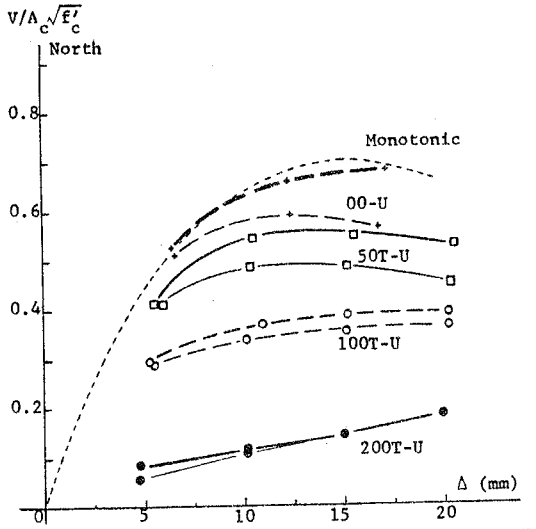

Fig. 10 Tests with Constant Tension and History U

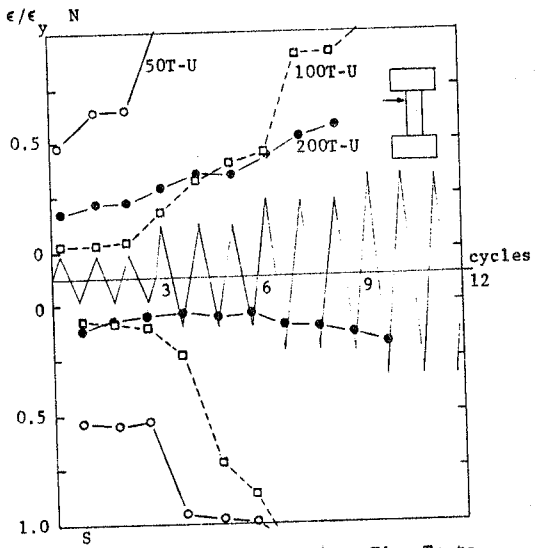

Fig. 11 Progressive Strain in a Tie, Tests with Constant Tension and History U

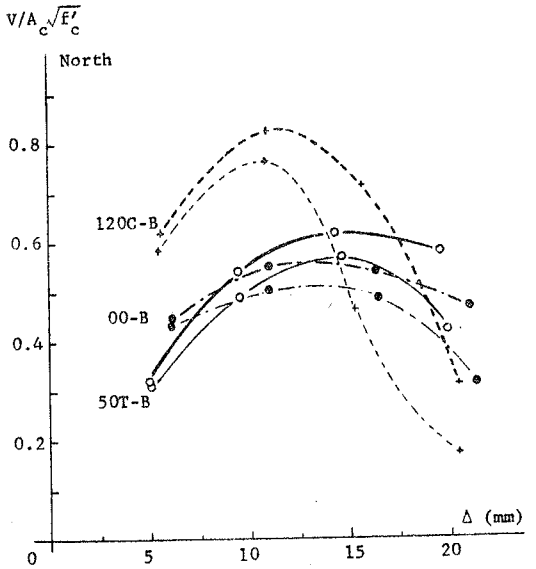

Fig. 12 Comparison of Tests 50T-B, 00-B, and 120C-B - NS Direction

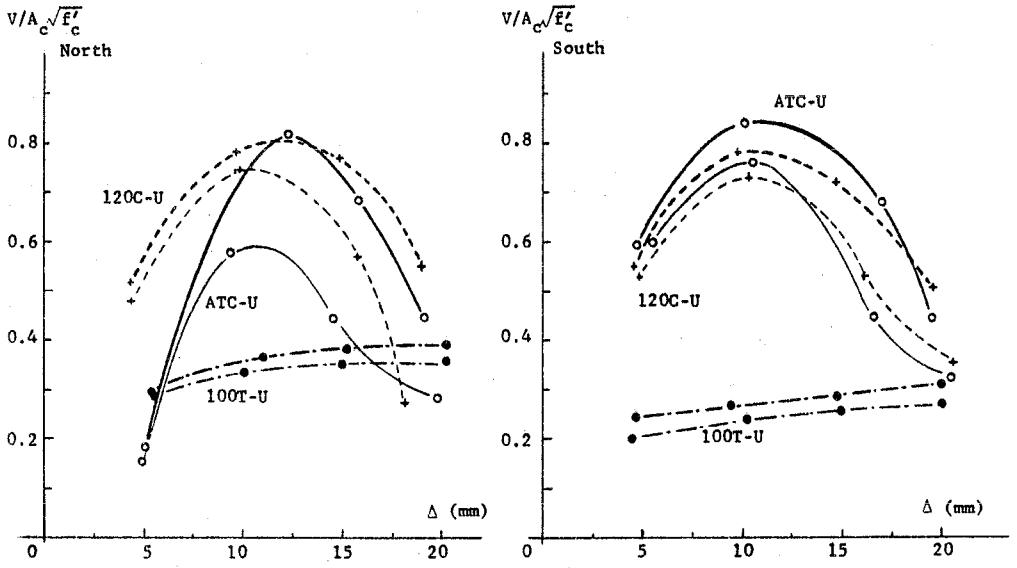

Fig. 13 Test ATC-U Compared with Tests 100T-U and 120C-U

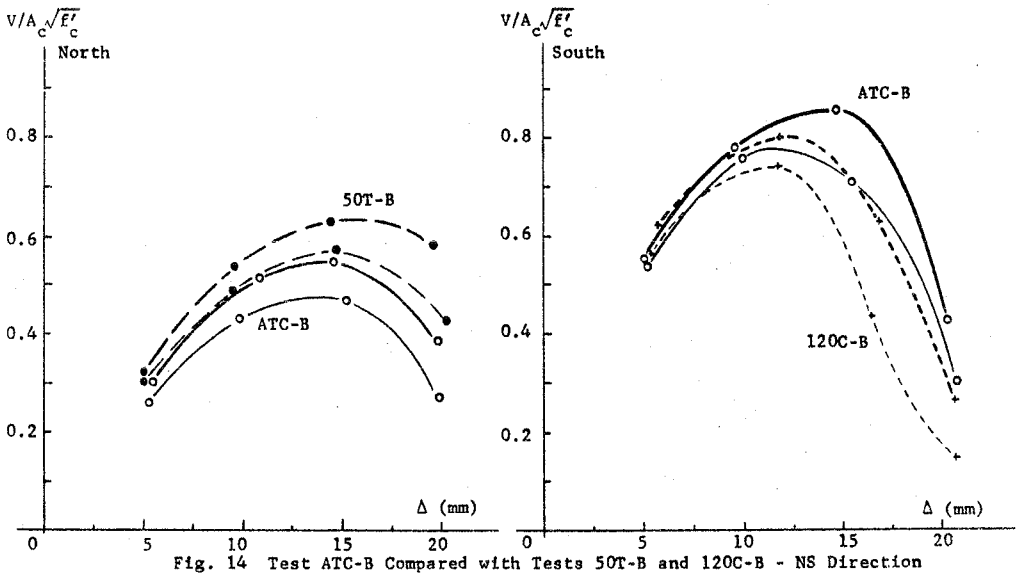

Fig. 14 Test ATC-B Compared with Tests 50T-B and 120C-B - NS Direction

INELASTIC BEHAVIOUR OF REINFORCED CONCRETE MEMBERS SUBJECTED TO BI-AXIAL BENDING MOMENTS

Katsumi KOBAYASHI
Tokyo Institute of Technology
Tokyo, Japan

Seiji KOKUSHO
Tokyo Institute of Technology
Tokyo, Japan

Katsuki TAKIGUCHI
Nagoya Institute of Technology
Nagoya, Yapan

SUMMARY

This study was planned as the first fundamental step to make clear the inelastic behavior of reinforced concrete columns subjected to bi-directional horizontal forces and axial force. This paper deals with static tests of twenty-six specimens subjected to bi-axial bending moments and with analysis of the test results.

In the experiments, loading and measuring arrangements were newly developed, by which two bending moments about two axes were applied independently. By the experiments, moment-curvature hysteretic relations of reinforced concrete sections subjected to bi-axial bending moments were obtained. The experimental results were followed by sectional analysis.

In the analysis, cross sections were partitioned into small elements. It was assumed that each element was uni-axially stressed and that Bernoulli's principle could be applied. In this analysis, uni-axial non-stationary stress-strain hysteresis rules of concrete and reinforcing bar were postulated according to recent experimental studies on them. Experimental and analytical results coincide quite well.

RESUME

C'est une étude qui a été réglée dans une première pas pour faire la rechérche sur le condition inélastique de la colonne en béton armé qui supporte deux forces à l'horizontal et l'axial direction.

Ce sujet est à l'examan statique par vingt-six matières qui supportent les moments de deux axes courbes et à l'analyse des resultats.

Dans le experience, on a inventé d'arranger les lochs de force d'augmentation et d'installer autrement deux moments courbe autour de deux axes.

De cela, on a trouvé des relations pourcentages courbes des moments des sections en béton armé qui supportent les moments deux axes courbes.

Ce résultat a été poursuivi par l'analyse après: lorsque le sections ont été partagés à chaque éléments petites qui ont supporté une axes, le Principe Brenouille peux supposer à application. Les relations de force et courbe ont été fixés sur béton armé à l'expression en consultant les études d'experience recent. Cet experience coincide parfaitement avec les resultats de ses analyses.

INTRODUCTION

It is necessary to study the three-dimensional behavior of reinforced concrete structure during an actual earthquake, in order to design aseismically such structures. This study was planned as the first fundamental step to make clear the inelastic behavior of reinforced concrete columns subjected to bi-directional horizontal forces and axial force. Now, there are only a few data about hysteretic behaviors of reinforced concrete sections subjected to bi-axial bending moments, though the behaviors should be clarified for reasonable aseismic design of reinforced concrete columns. The main purpose of this study is to obtain fundamental data about hysteretic behaviors of reinforced concrete sections subjected to bi-axial bending moments by experiments and numerical analysis. As for details of this study, the papers by Takiguchi et al.[2][3][4](1975, 1976) could be referred.

EXPERIMENT

Three series of experiments named B series, 10B series and 15B series were carried out.

In B series, fourteen specimens with 10cm square cross section were tested. Five of them were tested under the loading condition of constant bending moment about one axis named axis-2 and monotonically increasing deformation about the other axis named axis-1 orthogonal to axis-2. Five more specimens were tested under the loading condition of constant bending moment about axis-2 and reversed cyclic bending moment about axis-1. Reversed cyclic bending moment was applied by a rule of incremental deformation amplitude loading. Another four specimens were tested under the more complicated loading condition.

In 10B series, six specimens with 10cm square cross section were tested under the loading condition of constant bending moment about axis-2 and reversed cyclic deformation with constant amplitude about axis-1.

In 15B series, six specimens with 15cm square cross section were tested under the same loading condition as that of 10B series.

Table 1 Mechanical Properties of Concrete and Reinforcing Bar

	Reinforcing Bar	Yield Strength kg/cm^2	Tensile Strength kg/cm^2	Elongation %
B Series	D 10	3117	4572	28.1
	6 ϕ	2746	3626	25.6
10B and 15B Series	D 10	2782	4206	29.6
	6 ϕ	4904*	5012	—

* 0.2% proof stress

		← Test Period →		
B Series	Age of Concrete	30 days	41 days	72 days
	Compressive Strength kg/cm^2	255	273	248
	Splitting Tensile Strength kg/cm^2	22.7	—	22.1
10B and 15B Series	Age of Concrete	28 days	39 days	48 days
	Compressive Strength kg/cm^2	184	206	214
	Splitting Tensile Strength kg/cm^2	21.2	21.0	23.0

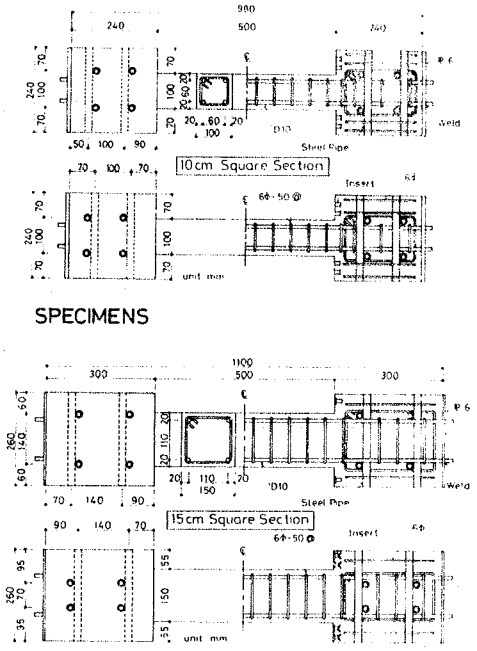

Fig. 1 Specimens

As shown in Fig.1, all specimens were reinforced with four deformed bars of 10mm nominal diameter in longitudinal direction. Mechanical properties of concrete and of reinforcing bars used in the specimens are shown in Table 1.

With respect to loading and measuring in this experiments, the system and practical apparatus are shown in Fig.2, Fig.3 and Fig.4. By the loading system, small axial force $N=M_1/LL_1+M_2/LL_2$ is loaded to the specimen concurrently with bending moment, where M_1 and M_2 are bending moments about axis-1 and axis-2 respectively, and LL_1 and LL_2 are eccentric distances. To be exact, after large deformation the specimen is subjected to small shearing forces and small torsional moment, too, by deforming effect.

End rotations ϕ_1 and ϕ_2 and end moments M_1 and M_2 of the specimen were measured in the experiments. ϕ/L, where L is the length of the tested part of the specimen, means average curvature of the specimen.

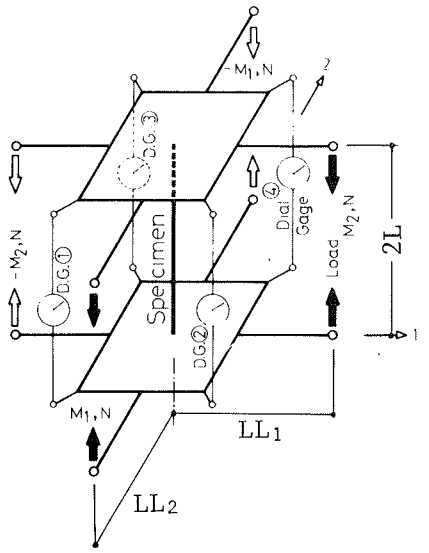

Fig. 2 Loading and Measuring System

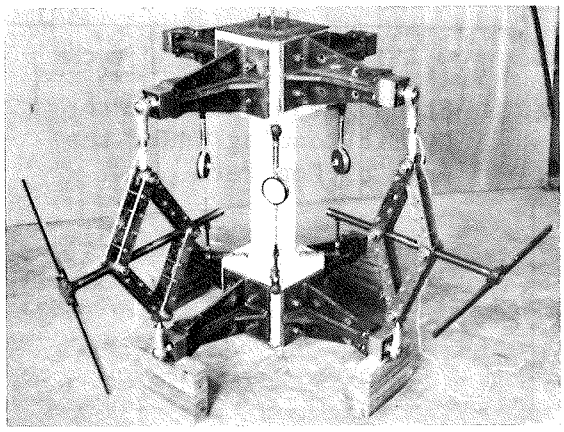

Fig. 4 Test Arrangements for the Specimen with 10cm Square Cross Section

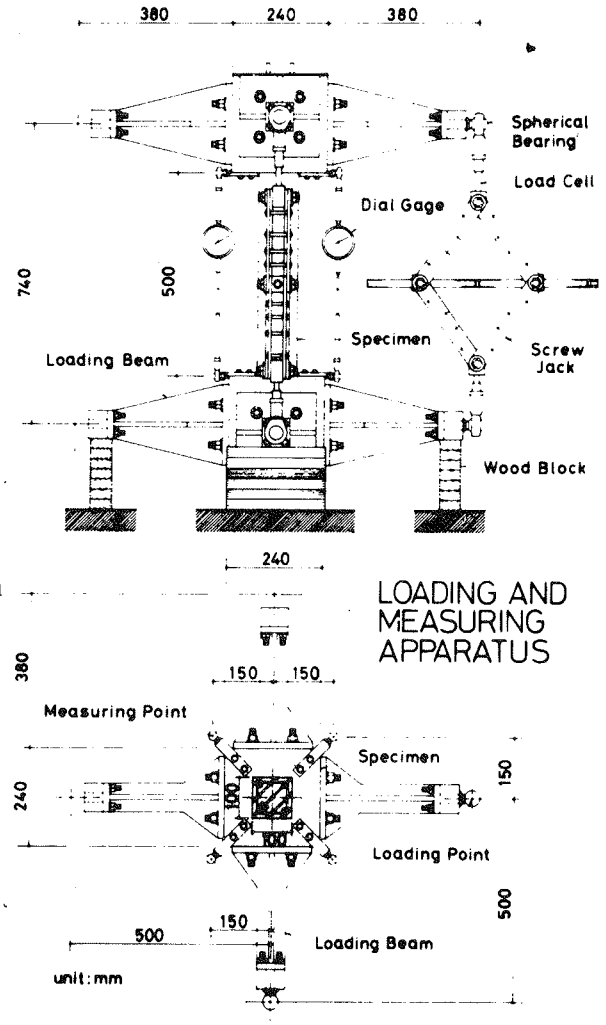

Fig. 3 Loading and Measuring Apparatus for the Specimen with 10cm Square Cross Section

ANALYSIS

In the analysis of this study, as shown in Fig.5 reinforced concrete section was partitioned into small elements which were assumed to be stressed uni-axially and to be independent each other. Then, Bernoulli's

principle i.e. the section remains plane after deformation was applied.

Confining effect of core concrete was not taken into consideration in the analysis.

Stress-strain hysteresis rule of concrete was postulated according to recent experimental studies on it, as shown in Fig.6. Relations between α and ξ_a, between β and ξ_a and between ξ_o and ξ_a are shown in Fig.7, where ξ_a is the strain at a reversal point on the envelope curve normalized by ${}_c\varepsilon_B$, the parameter α is for calculation of the residual strain ξ_o normalized by ${}_c\varepsilon_B$ and β is for determination of the point D (ξ_d, η_d). In Fig.6, ${}_c\sigma_B$ is compressive strength of concrete and ${}_c\varepsilon_B$ is compressive strain at ${}_c\sigma_B$. E is initial tangent modulus of ξ-η envelope curve. Fig.8 shows stress reduction due to cyclic loading according to the postulated rule of concrete.

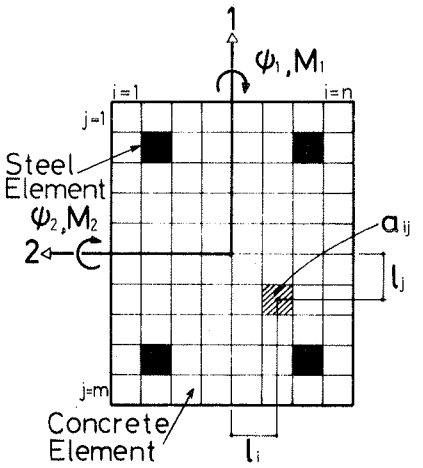

Fig. 5 Partitioning of R.C. Cross Section

Stress-strain hysteresis rule of reinforcing bar was postulated according to the experimental study by Yokoo et al.[7][8](1977), as shown in Figs.9-(1) through 9-(4). The virgin curve consists of linear elastic part, yield plateaus and strain-hardening curves of Ramberg-Osgood type [Fig.9-(1)].

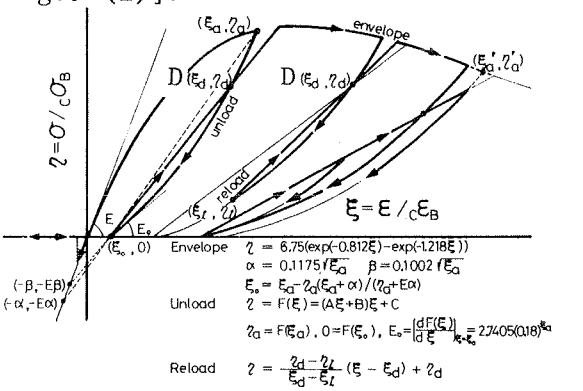

Fig. 6 Postulated Stress-Strain Hysteresis Rule of Concrete

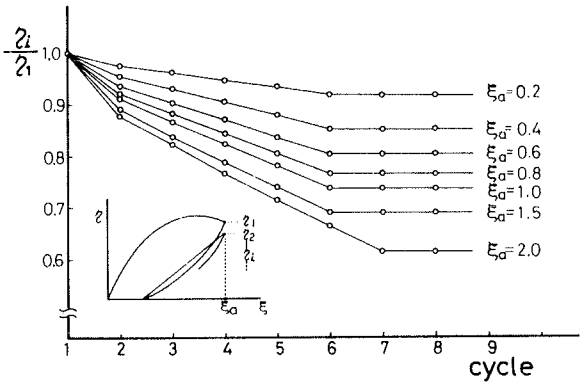

Fig. 8 Stress Reduction due to Cyclic Loading Under the Rule of Concrete

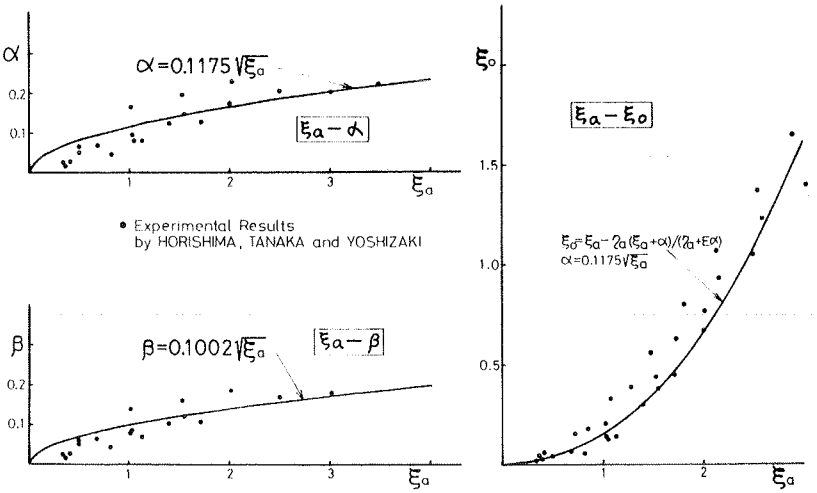

Fig. 7 Relations between α and ξ_a, between β and ξ_a and between ξ_o and ξ_a

Each general half cycle curve emanating from one reversal point to the next is represented by a pair of Ramberg-Osgood type equations. Their parameters a and r are dependent upon the maximum preceding stress amplitude normalized by yield stress σy [Fig.9-(2)]. In the case that the reversal point is on a yield plateau, a half cycle curve consists of three parts. Three parts are a nonlinear curve represented by a pair of Ramberg-Osgood type equations, secondary yield plateau and a strain-hardening curve of Ramberg-Osgood type. Parameters a and r appeared in the Ramberg-Osgood equations are dependent upon the magnitude of summed up plastic strain on the preceding yield plateaus [Fig.9-(3)]. There must be a supplementary rule. If the i-th curve is to intersect with (i-2)-nd curve, the i-th curve shall be regarded as having return to the (i-2)-nd curve and the latter shall take over the role of the i-th curve [Fig.9-(4)].

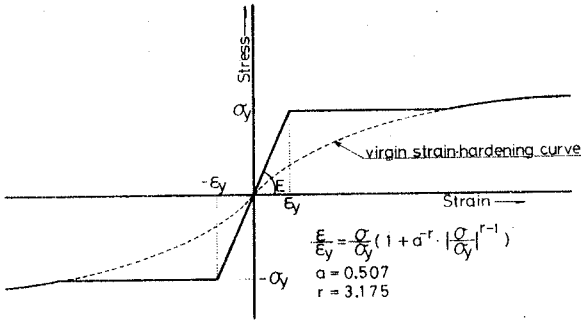

Fig. 9-(1) Virgin Curve

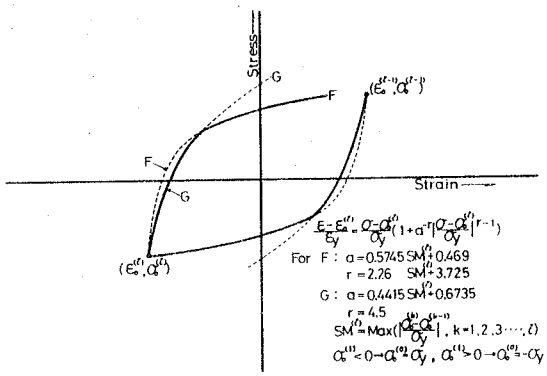

Fig. 9-(2) General Curve

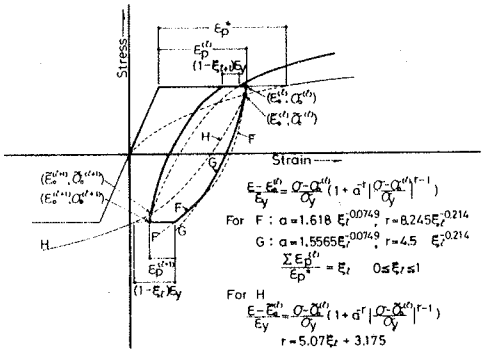

Fig. 9-(3) Curve Emanating From Yield Plateau

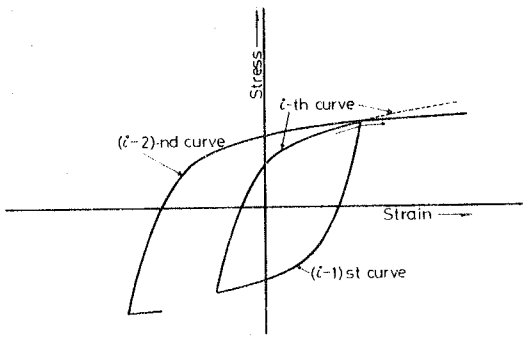

Fig. 9-(4) Return Phenomena

By Bernoulli's principle, incremental strain $\Delta\varepsilon_{ij}$ of (i,j) element is led from incremental strain $\Delta\varepsilon_o$ at the centroid of section, incremental curvature $\Delta\psi_1$ and $\Delta\psi_2$ about axis-1 and axis-2 respectively, and coordinates 1_i and 1_j of the centroid of element.

$$\Delta\varepsilon_{ij} = \Delta\varepsilon_o + \Delta\psi_1 \cdot 1_i - \Delta\psi_2 \cdot 1_j \qquad \cdots\cdots(1)$$

By postulated hysteresis rules of concrete and of reinforcing bar incremental stress $\Delta\sigma_{ij}$ of (i,j) element is determined from the incremental strain $\Delta\varepsilon_{ij}$.

$$\Delta\sigma_{ij} = \Delta\sigma_{ij}(\Delta\varepsilon_{ij}) \qquad \cdots\cdots(2)$$

Equilibrium equations for incremental axial force and incremental bending moments are as follows.

$$\Delta N = -\sum_{i=1}^{n}\sum_{j=1}^{m} \Delta\sigma_{ij} \cdot a_{ij} \qquad \cdots\cdots(3\text{-}1)$$

$$\Delta M_1 = \sum_{i=1}^{n} \sum_{j=1}^{m} \Delta\sigma_{ij} \cdot a_{ij} \cdot l_i \qquad \cdots\cdots(3\text{-}2)$$

$$\Delta M_2 = -\sum_{i=1}^{n} \sum_{j=1}^{m} \Delta\sigma_{ij} \cdot a_{ij} \cdot l_j \qquad \cdots\cdots(3\text{-}3)$$

From equations (1), (2) and (3-1) through (3-3), the incremental relation between ($\Delta\psi_1$, $\Delta\psi_2$, $\Delta\varepsilon_o$) and (ΔM_1, ΔM_2, ΔN) can be obtained.

In Fig.10, Partitioning of cross sections of the analyzed specimens are shown. Input data on mechanical properties of concrete and reinforcing bars are shown in Table 2.

Table 2 Input Data on Mechanical Properties of Concrete and Reinforcing bars

Reinforcing Bar (D10)		
	$s\sigma_y$ (kg/cm²)	sE (kg/cm²)
B series	3117	2.1×10^6
10B,15B series	2782	2.1×10^6
Concrete		
	$c\sigma_B$ (kg/cm²)	$c\varepsilon_B$
B series	259	2409×10^{-6}
10B,15B series	201	2116×10^{-6}

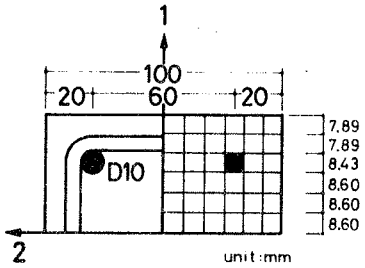

PARTITIONING OF CROSS SECTION

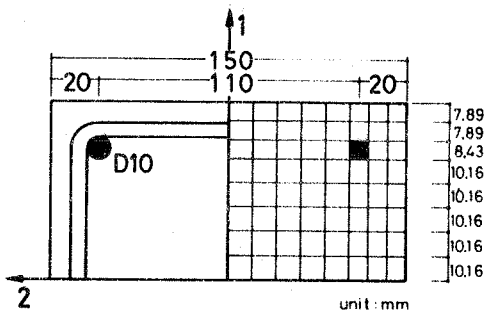

Fig. 10 Partitioning of Analyzed Cross Section

RESULT

As the results of this study, in regard to four specimens, M_1-ϕ_1/L, M_2-ϕ_2/L and ϕ_1/L-ϕ_2/L curves obtained by these experiments and M_1-ψ_1, M_2-ψ_2 and ψ_1-ψ_2 curves obtained by the above mentioned analysis are shown in Figs.11-(1) through 11-(4).

Restoring force characteristics about axis-1 and deformation about axis-2 became stable during cyclic loading with constant deformation amplitude about axis-1 when both constant bending moment about axis-2 and constant deformation amplitude about axis-1 were small. On the other hand, constant bending moment about axis-2 had considerable influence on the restoring force characteristics about axis-1 and deformation about axis-2 became very large during cyclic loading.

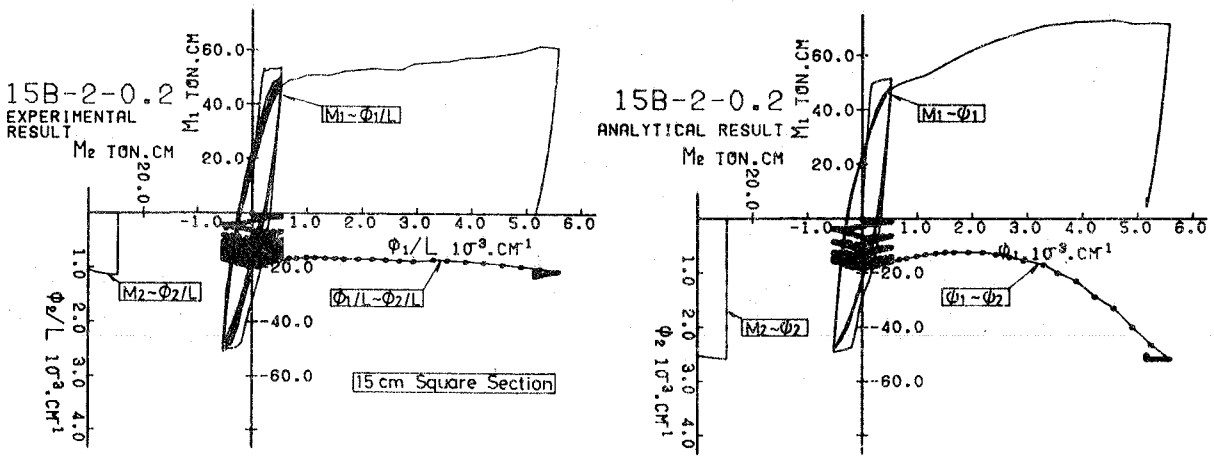

Fig. 11-(1) Experimental and Analytical Results of 15B-2-0.2 in 15B Series

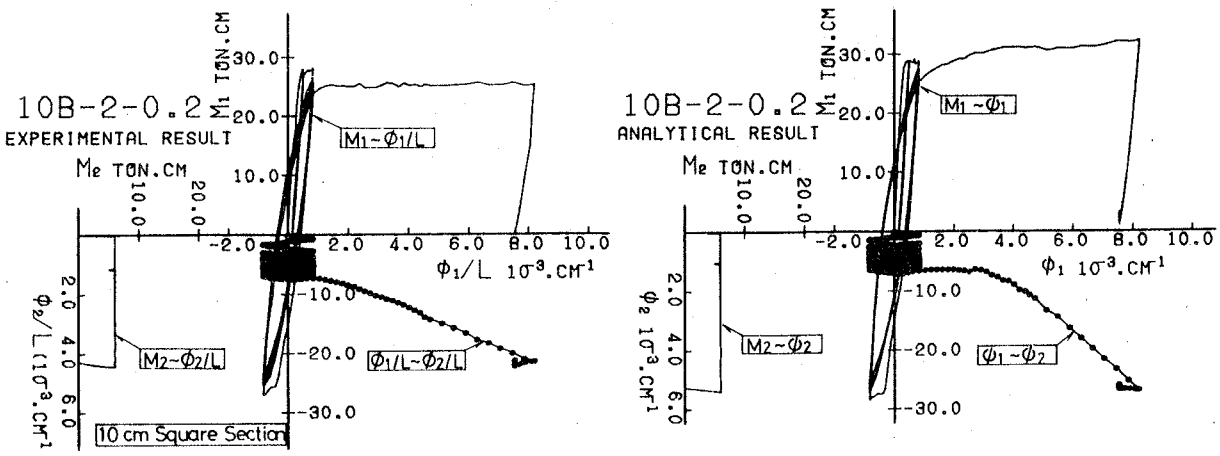

Fig. 11-(2) Experimental and Analytical Results of 10B-2-0.2 in 10B Series

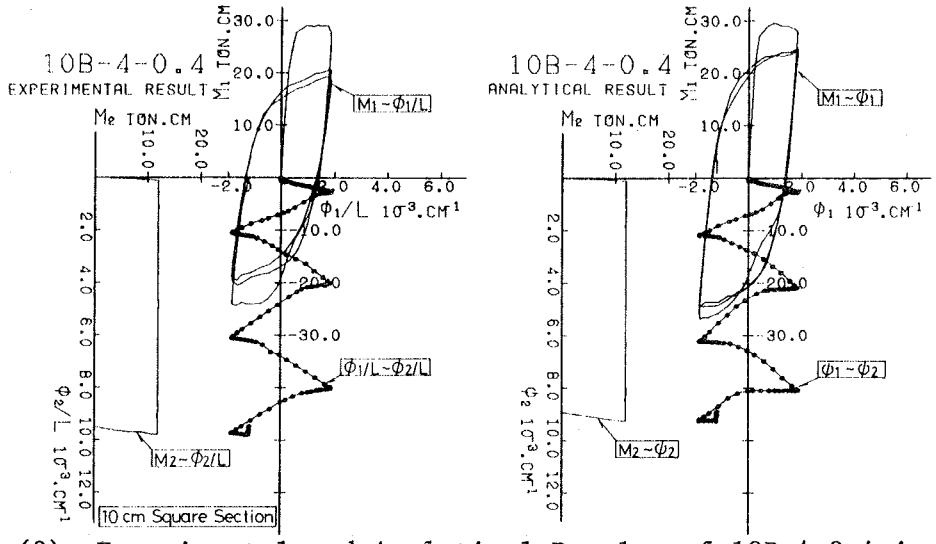

Fig. 11-(3) Experimental and Analytical Results of 10B-4-0.4 in 10B Series

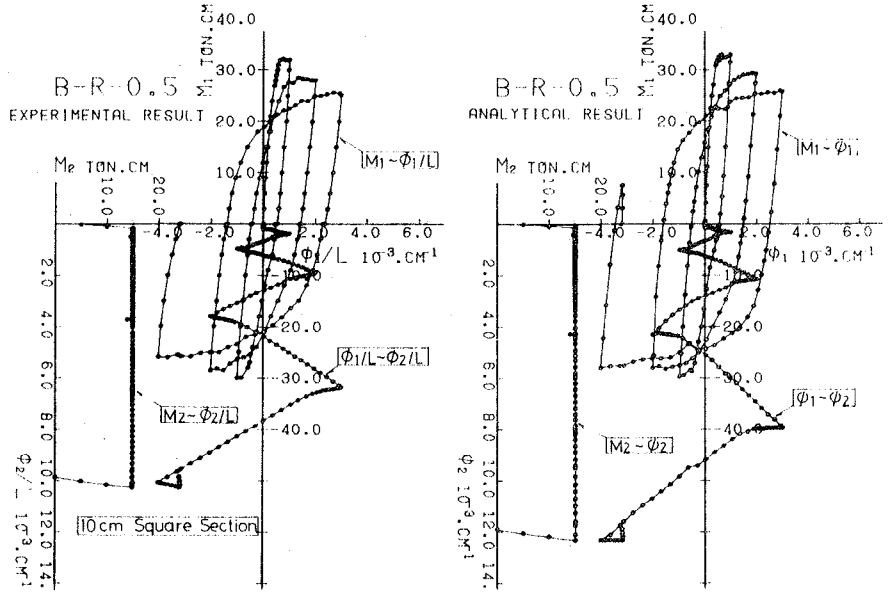

Fig. 11-(4) Experimental and Analytical Results of B-R-0.5 in B Series

CONCLUSION

In the experiments, loading and measuring arrangements were newly

developed and some fundamental data about hysteretic behaviors of reinforced concrete sections subjected to bi-axial bending moments were obtained. It was noticed that their behaviors were different from uni-axial hysteretic behaviors apparently.

In order to generalize the inelastic behaviors obtained in the experiments, the sectional analysis was carried out. The cross section was partitioned into small elements. It was assumed that each element was uni-axially stressed and that Bernoulli's principle could be applied. In this analysis, uni-axial non-stationary stress-strain hysteresis rules of concrete and reinforcing bar were postulated according to recent experimental studies on them. Experimental and analytical results coincide quite well.

As a result, it is clarified that bi-axial hysteretic behaviors would be able to be investigated by this analytical method based on the characteristics of materials.

ACKNOWLEDGEMENT

The writers wish to thank professor Tsuneyoshi Nakamura of Kyoto University for his valuable advice about stress-strain hysteresis rule of reinforcing bar.

The writers wish to thank The Technical Research Institute, Taisei Corporation for provision of experimental data about stress-strain relations of concrete.

This study received the grant in aid for scientific research from the Ministry of Education, Science and Culture of Japan. The writers wish to thank the Ministry.

REFERENCES

(1) H,Takizawa and H.Aoyama; Biaxial Effect in Modelling Earthquake Response of R/C Structures; Earthquake Engineering and Structural Dynamics Vol.4 1976

(2) K.Takiguchi, S.Kokusho and K.Okada; Experiments on Reinforced Concrete Columns Subjected to Bi-axial Bending Moments I; Transaction of Architectural Institute of Japan (A.I.J.) No.229 March 1975

(3) K.Takiguchi, S.Kokusho and K.Okada; Experiments on Reinforced Concrete Columns Subjected to Bi-Axial Bending Moments II; Trans. of A.I.J. No.247 Sept. 1976

(4) K.Takiguchi, S.Kokusho and K.Kobayashi; Analysis of Reinforced Concrete Sections Subjected to Bi-axial Bending Moments; Trans. of A.I.J. No.250 Dec. 1976

(5) S.Otani and C.S.Tang; Behavior of Reinforced Concrete Columns under Biaxial Lateral Load Reversals -(I) Pilot Test-; University of Tronto Feb. 1978

(6) T.Okada, M.Seki and S.Asai; Response of Reinforced Concrete Columns to Bi-directional Horizontal Force and Constant Axial Force; SEISAN-KENKYU, Monthly Journal of Institute of Industrial Science, University of Tokyo Vol.29 No.5 May 1977

(7) Y.Yokoo, T.Nakamura, T.Komiyama and Y.Kawada; Non-Stationary Hysteretic Uniaxial Stress-Strain Relations of a Wide-Flange Steel Part I: Experimental Investigation; Trans. of A.I.J. No.259 Sept. 1977

(8) Y.Yokoo and T.Nakamura; Non-Stationary Hysteretic Uniaxial Stress-Strain Relations of a Wide-Flange Steel Part II: Empirical Formulae; Trans. of A.I.J. No.260 Oct 1977

BEHAVIOUR OF REINFORCED CONCRETE COLUMNS UNDER SIMULATED BIAXIAL EARTHQUAKE LOADS

Shunsuke OTANI
University of Toronto
Toronto, Canada

V. Wai-To CHEUNG
University of Toronto
Toronto, Canada

SUMMARY

The effect of biaxial lateral loading on the hysteretic behaviour of reinforced concrete columns is studied through laboratory experiment. Three pairs of columns have been tested. One column of each pair was tested under uniaxial lateral loading, while the other under biaxial lateral load reversals.

Diagonal cracks, flexural cracks, crushing and spalling of shell concrete was observed on all four faces of the biaxially loaded columns. The final failure modes of a pair of uniaxially and biaxially loaded specimens were similar. Loading and resulting damage in the transverse direction reduced the stiffness of a biaxially loaded column in the longitudinal direction. However, the overall hysteretic characteristics of a pair of uniaxially and biaxially loaded columns were similar.

L'etude du comportement hysteretique des colonnes en beton arme, sous l'effet de charges bidirectionnelles, est entreprise a l'aide d'essais de laboratoire. La premiere colonne de chaque paire etait soumise a un chargement lateral unidirectionnel, tandis que la seconde subissait des efforts lateraux bidirectionnels et alternes.

Fissurations, ecrasement, et ecaillage du beton furent observes sur toutes les faces des colonnes soumises a des charges bidirectionnelles. Les modes finals de rupture, pour les deux specimens de chaque paire, etaient semblables. Les degats dus a l'action transversale reduisaient la rigidite principale des colonnes a chargement bidirectionnel. Cependant, les caracteristiques hysteretiques etaient essentiellement les memes pour une paire de colonnes, que la colonne soit soumise a un effort unidirectionnel ou bidirectionnel.

INTRODUCTION

The earthquake motion is not limited to one horizontal direction. Consequently, columns of a framed structure must resist lateral forces in the two horizontal directions simultaneously. The methods to estimate the strength of reinforced concrete column sections under monotonically increasing compression and biaxial bendings have been studied by many investigators on the basis of the flexural theory or on the basis of static experiments to failure. The strength and deformability under monotonically

increasing loads are not sufficient performance criteria of the reinforced concrete under earthquake motion because the stiffness and strength of the reinforced concrete depends on a strain history.

Innumerable experiments have been carried out on reinforced concrete columns under axial and uniaxial lateral load reversals. Recent experimental studies on the behaviour of reinforced concrete members under biaxial lateral load reversals reported a significant reduction in resistance and stiffness compared to reinforced concrete members under uniaxial lateral load reversals (Okada et al, 1976).

OUTLINE OF EXPERIMENTAL WORK

The behaviour of reinforced concrete columns subjected to a series of static biaxial lateral load reversals is examined. The test specimens

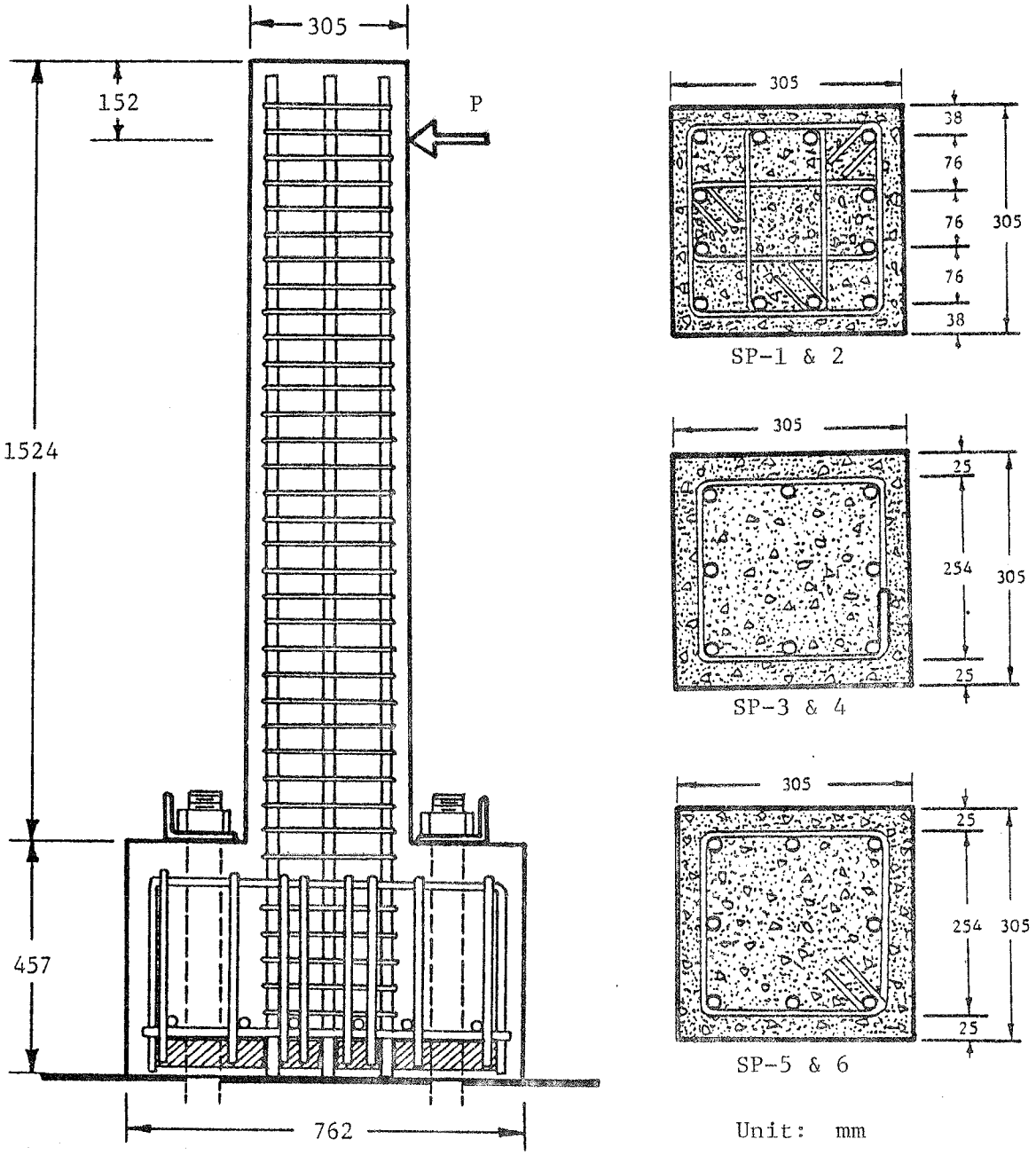

Fig. 1: Arrangement of Reinforcement in Specimen

represent a portion of a first storey column between the foundation and the inflection point of the column. No axial load was applied to the specimens in order to simplify the experiment. Three pairs of columns have been tested. Each pair of columns were constructed using the same materials and specifications. Odd-numbered columns of each pair were tested under uniaxial lateral load reversals, and even-numbered specimens under biaxial lateral load reversals.

The arrangement of longitudinal and transverse reinforcement is shown in Fig. 1. In specimens SP-1 & 2, three different shape ties, made of No. 3 bars, were placed at the same level with an interval of 127 mm. Square ties made of No. 3 bars in specimens SP-3 & 4 were welded at the splice and then heat treated. The bars were extended at least 76 mm beyond the 135° bend in specimens SP-5 & 6. The shear resisting capacities as evaluated by the ACI Standard 318-77 (1977) using a capacity reduction factor are 2.3, 1.6, and 1.1 times the shear corresponding to the calculated flexural capacity (without capacity reduction factor) for specimens SP-1 & 2, SP-3 & 4, and SP-5 & 6, respectively.

The properties of the concrete and the reinforcement are listed in Table 1.

Table 1: Material Properties

	Specimens 1&2	Specimens 3&4	Specimens 5&6
(a) Concrete			
Compressive Strength	34.2 MPa	31.7 MPa	22.7 MPa
Splitting Tensile Strength	3.5 MPa	3.3 MPa	2.7 MPa
(b) Longitudinal Reinforcement			
Number and Size	12 - No. 6	8 - No. 7	8 - No. 7
Yield Stress	454 MPa	441 MPa	464 MPa
Ultimate Stress	782 MPa	696 MPa	689 MPa
(c) Lateral Reinforcement			
Number and Size	3 - No. 3	1 - No. 3	1 - No. 2
Interval	127 mm	53 mm	51 mm
Yield Stress	510 MPa	500 MPa	303 MPa

The loading system for biaxial lateral loading is schematically shown in Fig. 2.

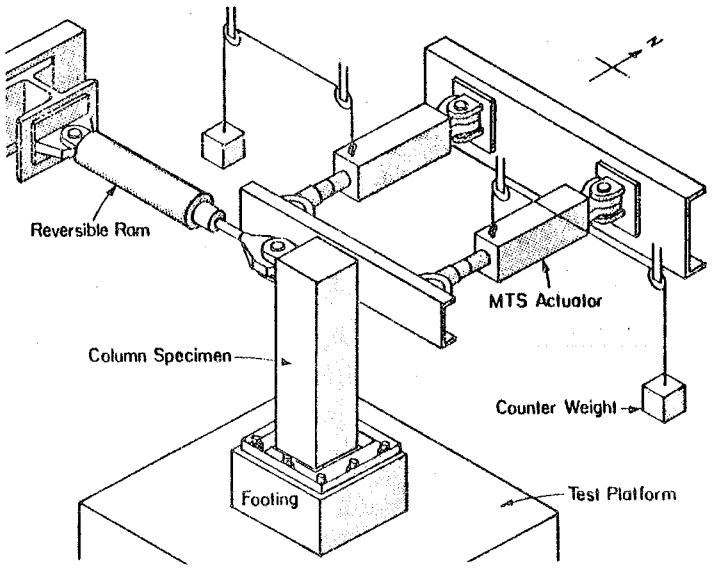

Fig. 2: Loading System for Biaxial Tests

Typical loading programs used in test SP-5 & 6 are illustrated in Fig. 3. The yielding was defined by the tensile yielding of the second layer reinforcement from the extreme tensile fibre of the section under monotonically increasing load. Only flexural deformation was considered in calculating the yield deflection.

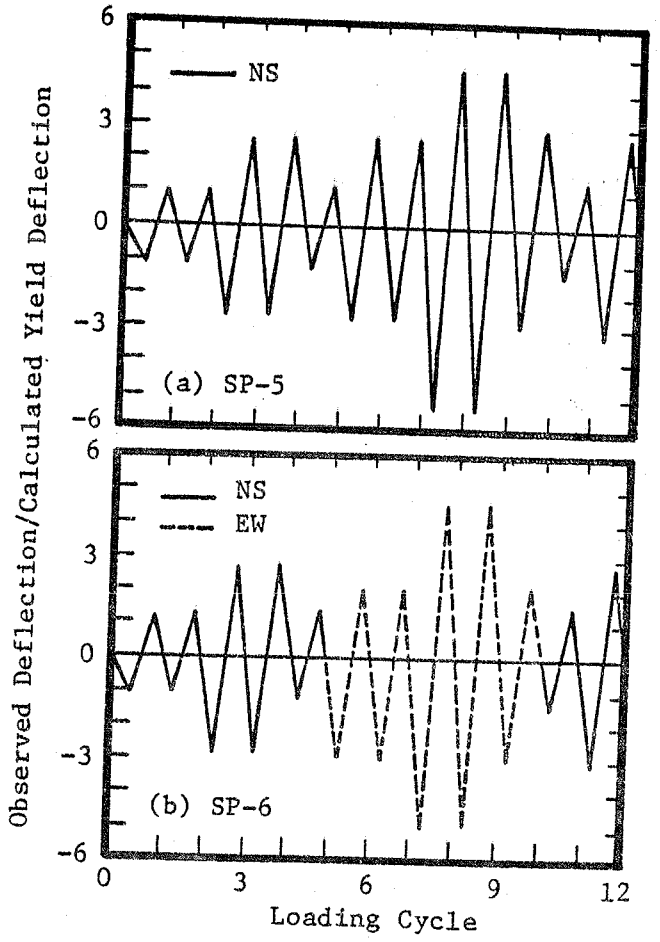

Fig. 3: Typical Loading Programs

OBSERVED BEHAVIOUR

General Observations

All specimens developed horizontal flexural and diagonal shear cracks along the entire height of a column, followed by tensile yielding of the longitudinal reinforcement, and compressive crushing of concrete at the base of the columns. X-shaped diagonal shear cracks appeared on all four faces of the biaxially loaded specimens, whereas diagonal cracks appeared on the two faces parallel to the load direction in the uniaxially loaded specimens. Similarly, crushing and spalling of shell concrete was observed on all four faces of the biaxially loaded specimens. Although diagonal cracks were observed on the column faces, the behaviour of the specimens was dominantly in flexure. The deterioration in stiffness and resistance due to shear was not detected until the last stage of a test.

Specimens SP-1 & 2 failed by the fracture of longitudinal reinforcement at a location where a piece of metal was welded near the critical section. The ductility factors for specimens SP-1 & 2 were 4.1 and 3.0, respectively.

Failure of specimens SP-3 & 4 was due to buckling of the longitudinal reinforcement near the base after spalling of shell concrete and extensive

cracking in the core of section. Note that the shear resisting capacity provided was 1.6 times the shear corresponding to the calculated ultimate moment at the base. Furthermore, the spacing of ties was reduced to one-half over a distance equal to twice the effective depth from the top face of the column footing. Ductility factors for specimens SP-3 & 4 were 8.2 and 9.8, respectively.

Specimens SP-5 & 6 had the least shear resisting capacity of the three pairs. After separation and spalling of shell concrete outside the longitudinal reinforcement cage, the core concrete was also broken into pieces due to flexural cracks, crushing of concrete and diagonal shear cracks. The resistance of the two specimens was lost through the disintegration of the core concrete. Ductility factors attained were 4.8 for the two specimens. The last four specimens (SP-3 through SP-6) were provided with the same amount of longitudinal reinforcement, whereas the lateral reinforcement ratios of SP-3 & 4 were more than twice that of SP-5 & 6. By far smaller ductility factors for specimens SP-5 & 6 than those for specimens SP-3 & 4 must be attributable to the difference in the amount of lateral reinforcement at the critical region provided in the two pairs of specimens. Fig. 4 shows crack patterns observed in specimens SP-5 & 6 at approximately the same load stage.

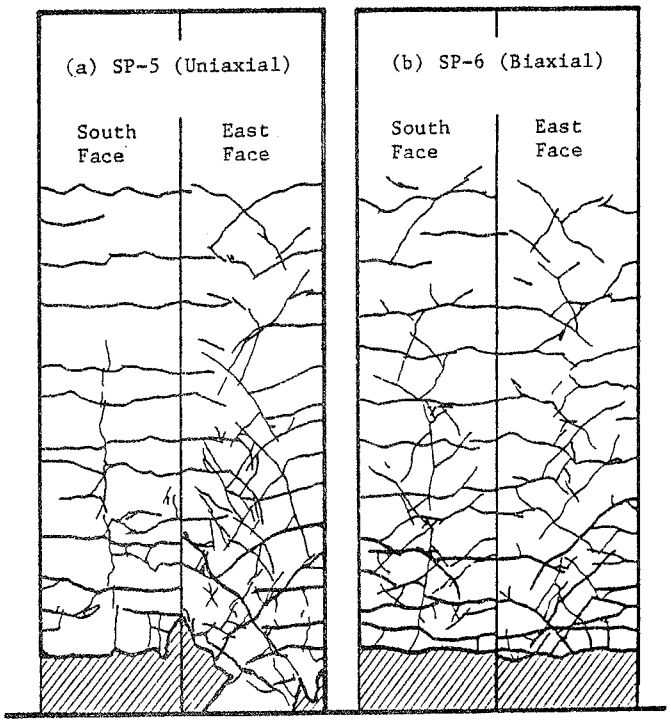

Fig. 4: Observed Crack Patterns Before Failure

Stiffness Reduction Under Uniaxial Loading

Lateral deflections at the point of loading were measured by ± 127 mm linear variable differential transformers. The stiffness of a test specimen was reduced with increasing damage as summarized below.

(a) Stiffness changed due to flexural cracking of concrete and tensile yielding of the longitudinal reinforcement;

(b) When a deflection reversal was repeated at the same newly attained maximum amplitude, the stiffness in the second cycle was noticeably lower than that in the first cycle, although the resistance at the peak displacement were almost identical. This can be observed in Fig. 5, which shows the load-deflection relationship observed during the first 5 cycles of uniaxial load test SP-5. The displacement amplitude in the third cycle was repeated in the fourth cycle. Note a distinct reduction in stiffness in load cycle 4, but also note comparable resistance at the peak displacement. This reduction in stiffness is attributable to the formation of additional flexural cracks and a reduced stiffness of the longitudinal reinforcement due to the Bauschinger effect.

(c) Average stiffness of a complete cycle (peak-to-peak stiffness) decreased with a previous maximum amplitude. In Fig. 5, displacement amplitude of cycle 5 was reduced to an amplitude comparable to cycle 2. Note a significant reduction in stiffness in cycle 5 compared to the stiffness in cycles 1 and 2. The peak-to-peak stiffness in cycle 5 was close to that in cycles 3 and 4.

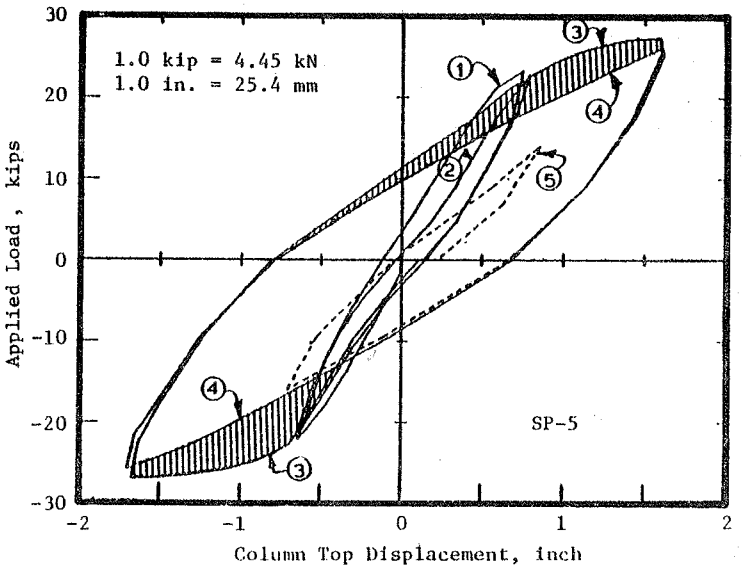

Fig. 5: Reduction in Stiffness in Uniaxial Loading Test

Effect of Transverse Loading

The behaviour of specimen 4, subjected to biaxial loading, is examined to study the effect of transverse loading on the hysteretic characteristics. The tensile yielding of longitudinal reinforcement was observed in cycle 12 in NS direction. After loading cycle 13, repeating the same amplitude as in cycle 12, the forced displacement was applied in EW direction, causing first yielding in EW direction in cycle 16. The displacement amplitudes in cycle 12 (NS) and cycle 16 (EW) were comparable. Note that the stiffness in cycle 16 is much less than that in cycle 12. This stiffness reduction was attributable to the damage caused by loading in NS direction.

After two displacement reversals (cycles 19 and 20) at an amplitude 4.5 times the calculated yield displacement as shown in Fig. 6(b), the specimen was subjected to a forced displacement reversal (cycle 22) in NS direction at the amplitude used in cycle 13 (previous maximum amplitude in NS direction). The stiffness in cycle 22 was significantly reduced from the stiffness in cycle 13 as demonstrated by a dashed line in Fig. 6(a). This stiffness reduction is a direct result of

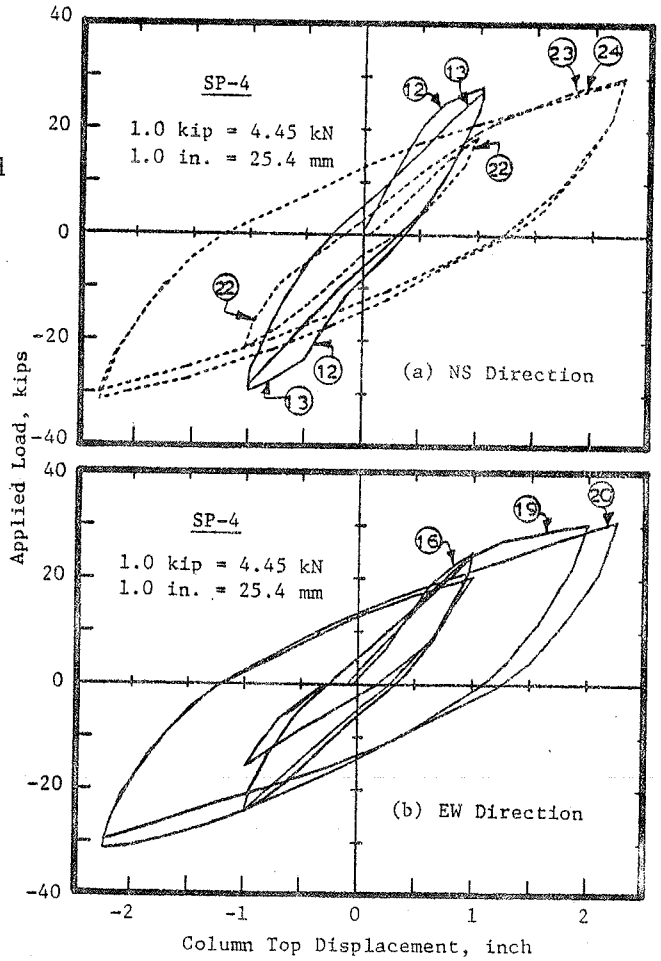

Fig. 6: Effect of Transverse Loading on Stiffness

damage caused during loading in the transverse loading. Note that subsequent loading cycles 23 and 24 did not show a sign of failure.

Does the biaxial lateral load reversal cause a substantial stiffness reduction which may not be detected by a uniaxial lateral load reversal test? The force-deflection relation curves observed during tests on specimens SP-5 and SP-6 are compared for this purpose. Both specimens were subjected to the same number of load cycles and also similar displacement histories as shown in Fig. 3. Figure 7(a) shows the force-deflection curves of specimen SP-5. The hysteresis loops in NS and EW directions of specimen SP-6 are combined and plotted in Fig. 7(b). The general shapes of the two curves in Fig. 7(a) and (b) are quite similar, indicating the hysteretic characteristic obtained through uniaxial lateral load reversals can provide a good index to judge the performance under biaxial lateral load reversals. A slightly larger maximum load was observed from specimen SP-6.

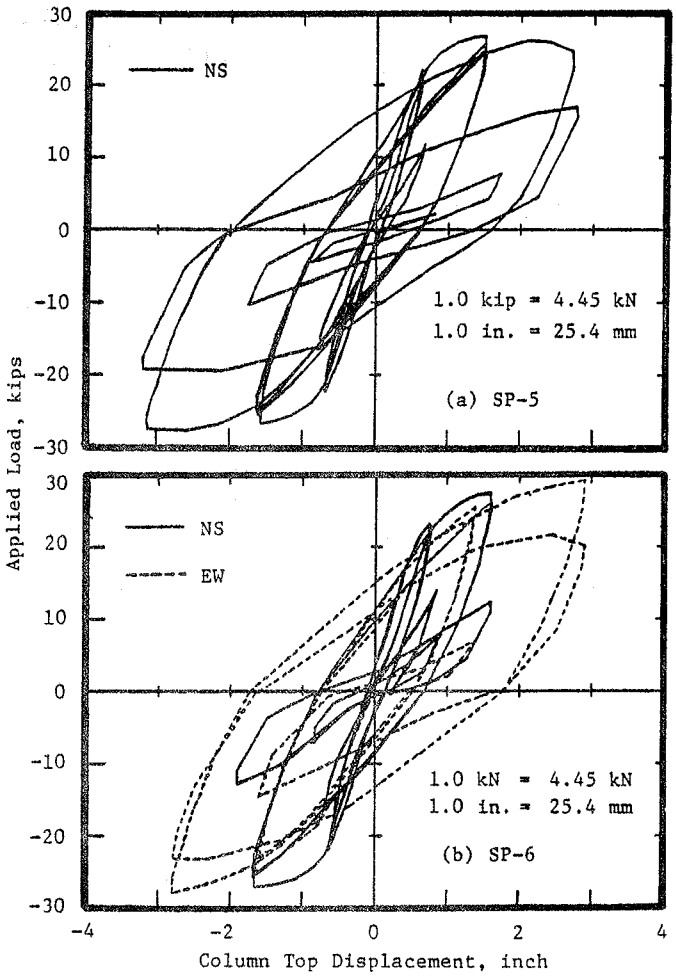

Fig. 7: Hysteretic Characteristics of of Uniaxially and Biaxially Loaded Columns

CONCLUDING REMARKS

The effect of biaxial lateral loading on the hysteretic behaviour of reinforced concrete columns was experimentally investigated. Under biaxial lateral loading, diagonal cracks, flexural cracks, crushing and spalling of shell concrete was observed on all four faces of a column before failure.

The final modes of failure of a pair of identically constructed columns were similar subjected to either uniaxial or biaxial lateral load reversals. The overall hysteretic characteristics of such a pair of columns were similar.

Loading and resulting damage in the transverse direction reduced significantly the stiffness of a biaxially loaded column in the longitudinal direction.

ACKNOWLEDGMENT

The study was supported by the Connaught Fund of the University of Toronto, and by the National Research Council Grants. The assistance of

C.S. Tang, former graduate assistant, H.P. Tang and H.F.T. Chong, former undergraduate students, is deeply appreciated.

REFERENCE

ACI Committee 318, Building Code Requirements for Reinforced Concrete (ACI 318-77), American Concrete Institute, Detroit, December, 1977.

Okada, T., Seki, M., and Asai, S., "Response of Reinforced Concrete Columns to Bi-Directional Horizontal Force and Constant Axial Force", Bulletin, Earthquake Resistant Structure Research Centre, Institute of Industrial Science, University of Tokyo, No. 10, December, 1976, pp. 30-36.

Otani, S., and Tang, C.S., "Behaviour of Reinforced Concrete Columns Under Biaxial Lateral Load Reversals - (I) Pilot Test -", Publication 78-03, Department of Civil Engineering, University of Toronto, Toronto, February, 1978.

EXPERIMENTAL STUDIES OF ULTIMATE SHEAR STRENGTH AND DEFORMATION CAPACITY IN REINFORCED CONCRETE MEMBERS WITH HIGH TENSION SHEAR REINFORCEMENT

Masashi FUKUHARA
Institute of Technology
Tokyo, Japan

Seiji KOKUSHO
Architectural Institute of Japan
Tokyo, Yapan

Tetsumitsu EIGAWA
Architectural Institute of Japan
Tokyo, Japan

SUMMARY

This paper describes the results of experimental studies concerning reinforced concrete beams and columns with a high tension shear reinforcement which 0.2% proof stress is about $14^t/cm^2$.

Thirty three specimens of beams subjected to bending moment and shear force were tested in experimental study A, and six specimens of columns subjected to bending moment, shear force and axial load were tested in experimental study B. Loadings were applied in anti-symmetrically in both studies. In study A, type of loading was monotonic, and in study B, the alternative loading of more than forty cycles was conducted after flexural tensile yielding of longitudinal reinforcement by means of a special loading system as shown in Fig.13.

The results of study A provide an information on the mechanism of shear failure and represent the equations concerning the effectiveness of high tension shear reinforcement in resisting shear. The results of study B indicate the effectiveness of high tension shear reinforcement in deformation capacity after flexural tensile yielding of longitudinal reinforcement.

RESUME

Ce texte décrit les résultats obtenus à la suite d'études expérimentales concernant les poutres en béton arméet des colonnes hautement renforcées contres les forces de cisaillement et dont la résistance de 0.2% est d'environ $14^t/cm^2$.

Trente trois sortes de poutres soumises à un moment fléchissant et à une tension de cisaillementont fait l'objet d'un etude spéciale au cours de l'étude expérimentale A et six sortes de colonnes soumises à un moment fliéchissant et une charge axiale ont fait l'objet d'une étude expérimentale B. Les charges ont été appliqué par méthode anti-symétrique au cours des deux études expérimentales. Au cours de l'étude A, le type de charge est monotonique tandis qu'au cours de l'étude B, la charge alternative de plus de quarante cycles est accomplie par déformation fléchissante de renforcement longitudinal par l'intermédiaire d'un système de charge spécial comme le montre la figure 13.

Lesrésultats de l'étude A fournissent des renseignements sur le mécanisme de panne cisaillement et représente l'équation qui se rapporte à l'efficacité de renforcement aux tensions élevée de cisaillement. Les resultats de l'étude B indiquent une efficacité de renforcement aux tensions élevées de capacité de déformation de déformation fléchissante de renforcement longitudinal.

INTRODUCTION

Recent research works regarding the effectiveness of shear reinforcement

have been primarily devoted to members with the ordinary shear reinforcement which yield stress was about $4t/cm^2$. Although several investigations have included the members with high tension shear reinforcement, the factors affecting ultimate shear strength in beams and deformation capacity after flexural tensile yielding in columns have not been studied systematically.

It can be considered that the principal effectiveness of shear reinforcement in beams and columns were two cases as following i) and ii).

i) to increase ultimate shear strength

ii) to increase deformation capacity after flexural tensile yielding of longitudinal reinforcement

Two experimental studies have been carried out to investigate those effectinevess of high tension shear reinforcement in reinforced concrete beams and columns since 1974. One is the experimental study A to investigate the effectiveness in resisting shear using the specimens of beams, and the other is the experimental study B to investigate the effectiveness in deformation capacity in columns.

It appears of practical importance to obtain information on those effectiveness of high tension shear reinforcement in beams and columns. This was the primary purpose of these experimental studies.

EXPERIMENTAL STUDY A

SPECIMENS AND PROPERTIES OF MATERIALS

Specimens were designed to investigate the effectiveness of high tension shear reinforcement, which 0.2% proof stress was about $14t/cm^2$as shown in Fig. 5, in resisting shear.

Thirty three specimens were tested as shown in Table 1. The primary factors were yield stress of shear reinforcement ($_w\sigma_y$), shear reinfocement ratio (p_w), shear span ratio(a/D), and the lap joint of spiral as shown in Fig.7. All specimens had the same section (b x D = 18cm x 40cm)and the same amount of longitudinal reinforcement ($p_t = p_c = 2.99\%$) as shown in Fig.1.

High tension shear reinforcement in this experimental study were the heat treated steel called "ULUBON". The compressive concrete strength from 10cm x 20cm cylinders was $281kg/cm^2$in the case of a/D = 1.0 and 2.0,and was $324kg/cm^2$ in the case of a/D = 1.5 as shown in Table 3.

PROCEDURE

Loading was carried out in an anti-symmetrical method as shown in Fig.4, and the type of loading was monotonic. Shear force(V) was measured by the load cell between the jack and the specimen, and the relative deformation(δ) was measured by the electric gages as shown in Fig.3.

Strains of shear reinfocement were measured by wire strain gages to investigate the mechanism of shear failure.

EXPERIMENTAL RESULTS

1) FAILURE MODES

Experimental results are summarized in Table 2. Failure modes were of two kinds as shown in Fig.8, one was the shear compression type (symbol SC) and the other was the flexure type (symbol FSC) after flexural tensile yielding of logitudinal reinforcement.

2) EFFECTIVENESS OF HIGH TENSION SHEAR REINFORCEMENT

The difference between ultimate shear stress of specimens with shear reinforcement (v_u) and that of specimen without shear reinforcement ($v_{upw=0}$) will be used as a measure of the effectiveness of shear reinforcement. This increment of stress ($v_u - v_{upw=0}$), was plotted against p_w in Fig.9 for SC failure groups. As shown in Fig.9, the effectiveness of high tension shear reinforcement was more than that of the ordinary shear reinforcement under the same value of p_w.

3) FUNCTION OF SHEAR REINFORCEMENT

The relation between shear force (V) and the relative deformation (δ), and the relation between shear force (V) and stress of shear reinforcement ($_w\sigma$) substituted for strain measured by wire strain gages are illustrated in Fig. 10 (a) through (e) in increasing order of $p_w \cdot {}_w\sigma_y$. Figs.10 indicate the function of shear reinforcement as following i), ii) and iii)

i) After the first inclined crack, this $_w\sigma$ increased remarkably.

ii) Relation between additional shear force and additional stress of shear reinforcement after the first inclined crack was almost linear.

iii) Yielding of shear reinforcement were found in specimens that $p_w \cdot {}_w\sigma_y$ was less than about 40kg/cm^{2}as shown in Fig.10 a) through c),and on the other hand, in the case of $p_w \cdot {}_w\sigma_y$ was not less than about 40kg/cm^2, beams failed in shear before yielding of shear reinfocement as shown in Fig.10 d) and e).

4) RELATION BETWEEN $\{v_u - v_{upw=0}\}$AND $p_w \cdot {}_w\sigma_y$

In Fig.12, $\{v_u - v_{upw=0}\}$ is plotted against $p_w \cdot {}_w\sigma_y$. The relation between $\{v_u - v_{upw=0}\}$ and $p_w \cdot {}_w\sigma_y$ could be represented by two straight lines: one with a slope extending to about $p_w \cdot {}_w\sigma_y = 45kg/cm^2$ and the other with a slope extending from $p_w \cdot {}_w\sigma_y = 45kg/cm^2$. This change in slope appears to correspond to a change in behavior of shear reinforcement as shown in 3)-iii). Then, dividing data into group of yielding and group of no yielding of shear reinforcement, two lines could represent those two groups by regression analysis as following Eq.(1) and Eq.(2).

in the case of yielding, $\{v_u - v_{upw=0}\} = 0.69p_w \cdot {}_w\sigma_y + 10.0$ - - - (1)

in the case of no yielding, $\{v_u - v_{upw=0}\} = 0.05p_w \cdot {}_w\sigma_y + 41.6$ - - -(2)

The intersection of Eq.(1) and Eq.(2) is $p_w \cdot {}_w\sigma_y = 49kg/cm^2$, Eq.(1) and Eq.(2) could be represented more generally as following Eq.(3) and Eq.(4).

for $0 < p_w \cdot {}_w\sigma_y \leq 49kg/cm^2$, $\{v_u - v_{upw=0}\} = 0.69p_w \cdot {}_w\sigma_y + 10.0$ - - - (3)

for $49kg/cm^2 < p_w \cdot {}_w\sigma_y \leq 160kg/cm^2$, $\{v_u - v_{upw=0}\} = 0.05p_w \cdot {}_w\sigma_y + 41.6$ - - (4)

where

$2.6t/cm^2 \leq {}_w\sigma_y \leq 14t/cm^2$, $1 \leq a/D \leq 2$, $281kg/cm^2 \leq {}_c\sigma_b \leq 324kg/cm^2$

5) LAP JOINT

Fig.11 shows the relation between shear stress (v) and the relative deformation (δ) of specimens with and without lap joint. the behavior of specimen with lap joint was as same as the specimen without the lap joint.

CONCLUSION

Based on the experiment reported herein, the following conclusions can be drawn.

1) In the case of that $p_w \cdot {}_w\sigma_y$ was less than about 40kg/cm^2, beams failed in shear after yielding of shear reinforcement. On the other hand, in the case of that $p_w \cdot {}_w\sigma_y$ was larger than about 45kg/cm^2, failed in shear before yielding of shear reinforcement{See Fig.10}

2) Experimental equations(3) and (4) concerning the effectiveness of shear reinforcement included high tension in resisting shear were represented by the regression analysis.

3) The beam with lap joint indicates the behavior as same as that without lap joint.{ See Fig.11}

EXPERIMENTAL STUDY B

SPECIMENS AND PROPERTIES OF MATERIALS

Specimens were designed to investigate the effectiveness of high tension shear reinforcement in deformation capacity after flexural tensile yielding of longitudinal reinforcement.

Six specimens were tested as shown in Table 5. The primary factors are shear reinforcement ratio (p_w) and yield stress of shear reinforcement ($_w\sigma_y$). All specimens had the same shear span ratio (a/D = 1.5), the same section(b x D = 25cm x 25cm), the same amount of longitudinal reinforcement ($p_t = p_c = 0.61\%$) as shown in Fig.15, and axial compressive stress (σ_0 = 26.3kg/cm^2). The compressive concrete strength from 10cm x 20cm cylinders and yield stress of shear reinforcement ($_w\sigma_y$) are shown in Table 5.

PROCEDURE

Loading was carried out in an anti-symmetrical method by means of a special loading system as shown in Fig.13. The alternatively reversal loading of more than forty cycles as shown in Fig.16 were conducted after flexural tensile yielding of longitudinal reinforcement.

Shear force (V) were measured by the load cell and the relative deformation (δ) were measured by electric gages as shown in Fig.14.

EXPERIMENTAL RESULTS

1) FAILURE MODES

The failure modes of all specimens had tendency as following i) and ii).

i) After the first flexural crack formed at the end of specimen and presently formed at distance of about 25cm from the end in tension side, the later crack bent over toward compression zone near the end of specimen, at higher load, the flexural tensile reinforcement yielded.

ii) After flexural tensile yielding, the deformation was increased,and shear force decreased gradually. The relation between shear force and the deformation of specimen No.6 is illustrated in Fig.17.

2) BEHAVIOR UNDER ALTERNATIVE LOADING

The relation between $V/V_{y(cal)}$* and the number of alternative loading after flexural tensile yielding are shown in Fig.18 through 21. Those Fig.18,19,20 and 21 indicate the effectiveness of shear reinforcement in deformation capacity after flexural tensile yielding as following i), ii) and iii).

i) $V/V_{y(cal)}$ in specimens with high tension shear reinforcement subjected to alternative loading was more than in specimens with ordinary shear reinforcement, in both cases of p_w = 0.6% and 0.26% as shown in Fig.18 and 19.

ii) $V/V_{y(cal)}$ in the case of small spacing of shear reinforcement were more than large spacing under the same value of p_w and $p_w \cdot {}_w\sigma_y$ as shown in Fig.20.

iii) The specimen with high tension shear reinforcement of p_w less than half of the ordinary, and of smaller spacing than the ordinary could obtain the deformation capacity as much as with the ordinary shear reinforcement as shown in Fig.21.

CONCLUSION

Based on the experiment reported herein, the following conclusions can be drawn.

In order to increase the deformation capacity after flexural tensile yielding of longitudinal reinforcement, it is important to use the shear reinforcement of higher yield stress than the ordinary one and to narrow down the spacing of shear reinforcements. Saying it differently, by using the high tension shear reinforcement of narrow spacing and slender steel in stead of the ordinary shear reinforcement, it may be possible to reduce the amount of shear reinforcement.

ACKNOWLEDGMENT

The authers wish to thank NETSUREN CO., LTD. for this experiment.

---

* : calculated shear strength at yielding by using the e-function method.

REFERENCE

A ACI Standard Building Code requirements for Reinforced Concrete (ACI. 318-71)

B Shear and Diagonal Tension, Report of ACI-ASCE Commitee 326, 1962

C M.J. Haddin and A.H. Mattock: Stirrup Effectiveness in Reinforced Concrete Beams with Axial Force, Journal of the Structural Division, Proceeding of the American Society of Civil Engineers, September 1971

D A.H. Mattock: Diagonal Tension Cracking in Concrete Beams with Axial Force, Journal of the Structural Division, Proceeding of the American Society of Civil Engineers, September 1971

E G.N.J. Kani: The Riddle of Shear Failure and its Solution, ACI Journal, Vol 61, No.4, April 1964

F J.A. Hofbeck, I.O. Ibrahim and A.H. Mattock: Shear Transfer in Reinforced Concrete, ACI Journal, February 1969

G R.P. Kennedy: A Statistical Analysis at the Shear Strength of Reinforced Concrete Beams, Stanford University, 1967

H Recommendation for International Code of Practice for Reinforced Concrete, by C.E.B.,1964

I British Standard Code of Practice for The structural use of concrete, British Standards Institution 1972

Table 1. List of Beams

Series(1);a/D=1.0,(2);a/D=1.5,(3);a/D=2.0

(Series) -No	Symbol	Dia-Pitch (mm-mm)	p_w*1 (%)	$_w\sigma_y$*2 (t/cm²)	$p_w \cdot {}_w\sigma_y$ (kg/cm²)	Form
(1)-1		0- 0	0	-	-	-
(1)-2	●	6-160	0.19	3.52	6.69	135°
(1)-3	○	6-160	0.19	13.88	26.37	135°
(1)-4	○	6-160	0.19	13.88	26.37	s
(1)-5	○	6-160	0.19	13.88	26.37	sL*3
(1)-6	●	6-114	0.26	3.52	9.15	135°
(1)-7	○	6-114	0.26	13.88	36.09	s*4
(1)-8	●	6- 89	0.34	3.52	11.97	135°
(1)-9	○	6- 89	0.34	13.88	47.19	s
(1)-10	○	6- 62	0.49	13.88	68.01	s
(1)-11	○	9-146	0.47	14.22	66.83	s
(1)-12	○	9- 62	1.12	14.22	159.26	s
(2)-1		0- 0	0	-	-	-
(2)-2		0- 0	0	-	-	-
(2)-3	▲	6-120	0.28	2.55	7.14	135°
(2)-4	▲	6-120	0.28	2.55	7.14	s
(2)-5	△	6-120	0.28	13.49	37.77	135°
(2)-6	△	6-120	0.28	13.49	37.77	s
(2)-7	▲	6- 60	0.56	2.55	14.28	135°
(2)-8	▲	6- 60	0.56	2.55	14.28	s
(2)-9	△	6- 60	0.56	13.49	75.54	135°
(2)-10	△	6- 60	0.56	13.49	75.54	s
(2)-11	▲	9- 90	0.75	2.60	19,50	135°
(2)-12	△	9- 90	0.77	13.98	107.65	s
(2)-13	▲	9- 60	1.13	2.60	29.38	135°
(2)-14	△	9- 60	1.15	13.98	160.77	s
(2)-15	△	6-120	0.29	6.87	19.92	s
(3)-1		0- 0	0	-	-	-
(3)-2	■	6-160	0.19	3.52	6.69	135°
(3)-3	□	6-160	0.19	13.88	26.37	s
(3)-4	■	6-114	0.26	3.52	9.15	135°
(3)-5	□	6-114	0.26	13.88	36.09	s
(3)-6	□	6- 62	0.49	13.88	68.01	s

*1 : p_w=shear reinforcement ratio

*2 : $_w\sigma_y$=yield stress or 0.2% proof stress of shear reinforcement

*3 : sL=Lap joint as shown in Fig.A-7

*4 : s= spiral

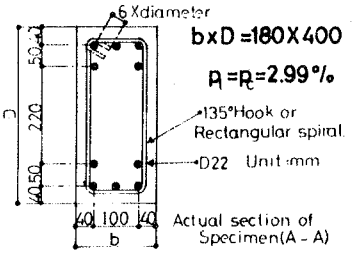

Fig.1 Actual Section

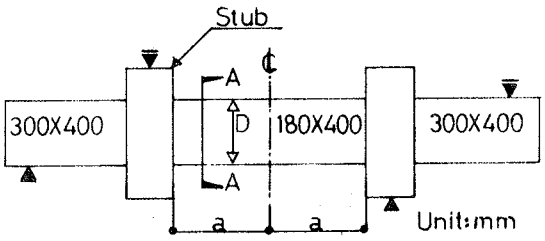

Fig.2 Specimen

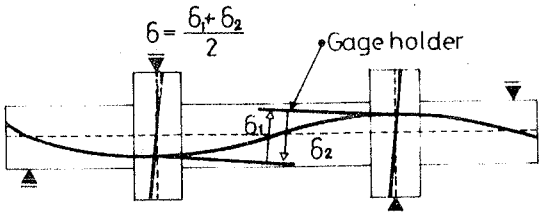

Fig.3 Measuring Method

Table 2. Experimental Results

unit; kg/cm²

(Series) No	Failure Modes*1	v_c*2	v_u*3	$v_u - v_u(p_w=0)$ *4
(1)-1	SC	9.3	15.8	0
(1)-2	SC	12.3	27.5	11.7
(1)-3	SC	10.7	42.6	26.8
(1)-4	SC	12.3	42.6	26.8
(1)-5	SC	15.4	47.9	32.1
(1)-6	SC	18.6	32.3	16.5
(1)-7	SC	18.6	52.9	37.1
(1)-8	SC	15.4	34.3	18.5
(1)-9	SC	12.3	54.5	38.7
(1)-10	SC	15.4	63.3	47.5
(1)-11	SC	15.4	58.6	42.8
(1)-12	SC	18.6	70.4	54.6
(2)-1	SC	10.9	17.0	0.3
(2)-2	SC	10.8	16.4	-0.3
(2)-3	SC	10.8	33.0	16.3
(2)-4	SC	7.9	29.8	13.1
(2)-5	SC	8.1	46.3	29.6
(2)-6	SC	7.9	50.9	34.2
(2)-7	SC	10.8	38.6	21.9
(2)-8	SC	10.8	38.6	21.9
(2)-9	FSC	9.3	58.6	-
(2)-10	FSC	13.9	58.4	-
(2)-11	SC	15.4	42.4	25.7
(2)-12	FSC	9.3	59.2	-
(2)-13	SC	12.3	50.9	34.2
(2)-14	FSC	9.3	63.7	-
(2)-15	SC	9.3	43.2	26.5
(3)-1	SC	9.3	13.1	0
(3)-2	SC	9.3	23.2	10.1
(3)-3	FSC	9.3	38.9	-
(3)-4	SC	9.3	29.3	16.2
(3)-5	FSC	9.3	41.7	-
(3)-6	FSC	12.3	47.1	-

*1 SC: shear compression failure
FSC: flexural failure

*2 v_c: shear stress at first inclined crack

*3 v_u: ultimate stress

*4 $v_u - v_u(p_w=0)$: effectiveness of shear reinforcement in resisting shear

Table 3. Concrete

unit: kg/cm²

Series	$_c\sigma_b$*1	$_c\sigma_t$*2	$_cE(1/4)\times10^5$
(1),(3)	281	22	2.85
(2)	324	30	2.24

*1 : $_c\sigma_b$=compressive strength (10 x 20 cm cylinder)

*2 : $_c\sigma_t$=split-cylinder tensile strength

Table 4. Reinforcement

Series	bars (mm)	σ_y*1 (kg/cm²)	$\sigma_{s\,max}$ (kg/cm²)	ε_y*2 ($\times 10^{-6}$)
(1)	D22	3.5	5.5	1811
	6 N	3.4	5.3	1548
(3)	6 H	13.9	15.2	8210
	9 H	14.2	15.4	8515
(2)	D22	3.8	6.1	1980
	6 N	2.6	3.3	1200
	6 H	6.9	8.0	5280
	6 H	13.5	15.0	8350
	9 N	2.6	3.5	1240
	9 H	14.0	15.2	7790

*1 : yield stress or 0.2% proof stress

*2 : yield strain or 0.25 proof strain

D : deformed bar ,N :ordinary , H :high tension

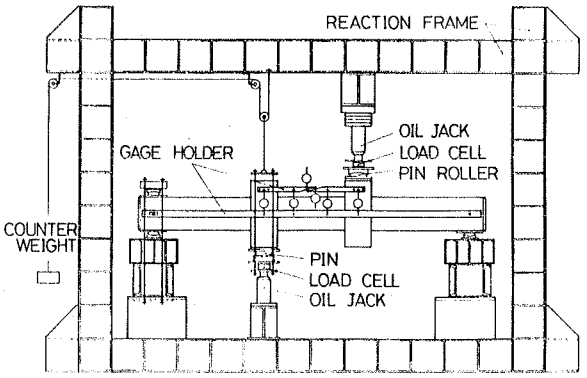

Fig.4 Loading Arrangement

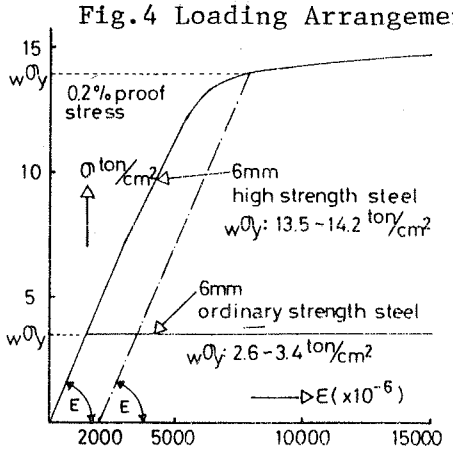

Fig.5 σ- ε Curve

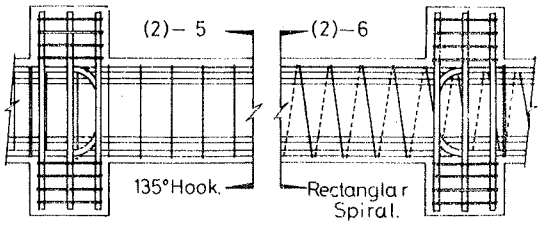

Fig.6 Form of shear Reinforcement

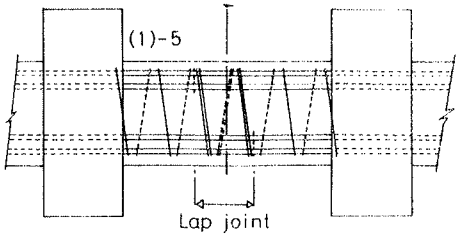

Fig.7 Lap Joint

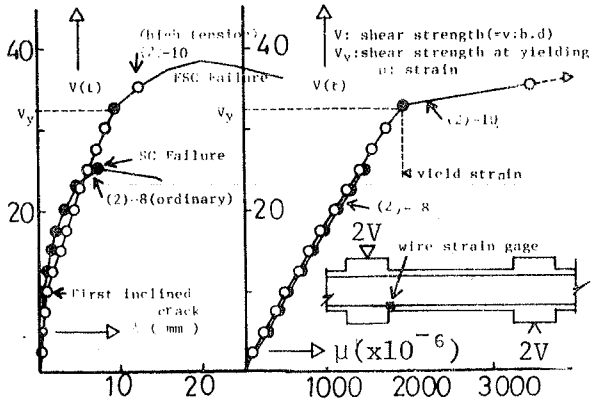

Fig.8 Failure Modes

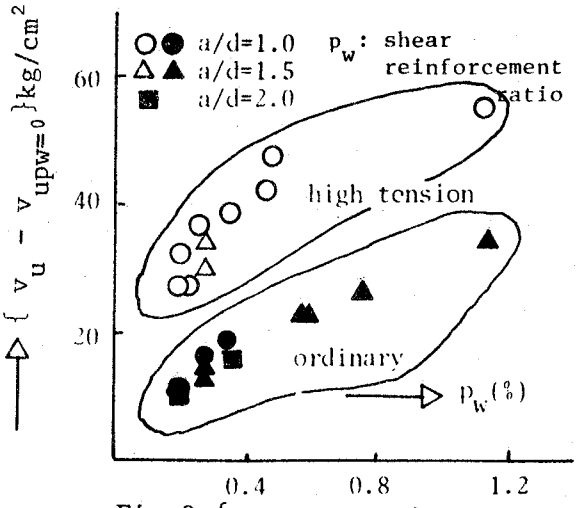

Fig.9 $\{v_u - v_{upw=0}\}$ and p_w

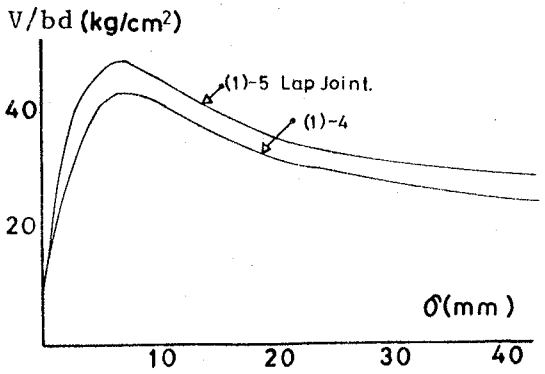

Fig.11 v - δ Curve with and without Lap Joint

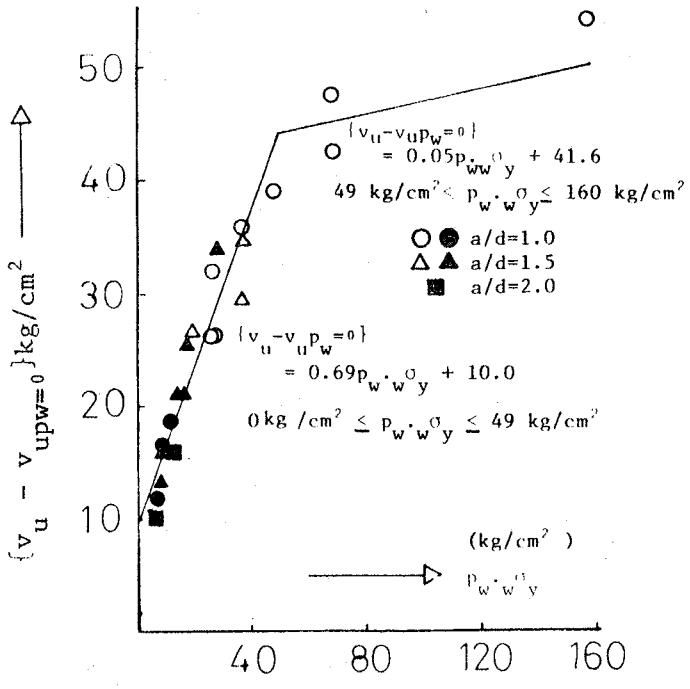

Fig.12 $\{v_u - v_{upw=0}\}$ and $p_w \cdot_w \sigma_y$

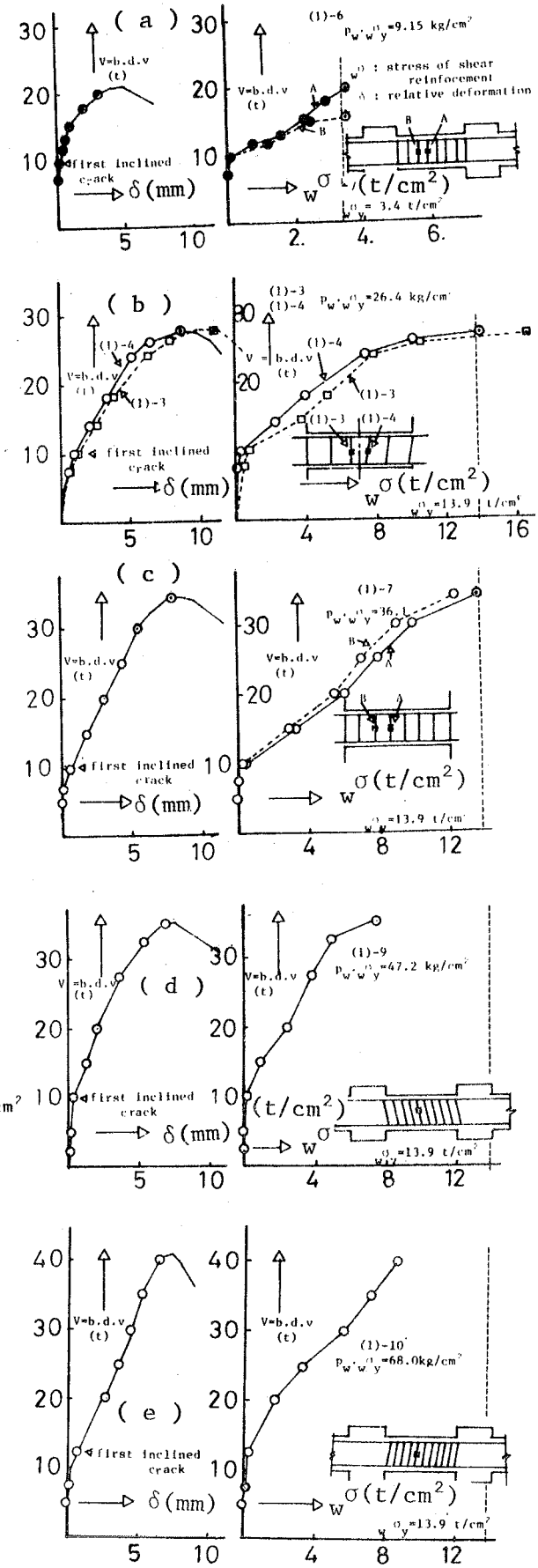

Fig.10 (V - δ) and (V - $_w\sigma$)

Table 5 List of Columns

No	symbol	$_w\sigma_y$ (kg/cm^2)	dia-pitch (mm - mm)	p_w (%)	$p_w \cdot {}_w\sigma_y$ (kg/cm^2)
1	135^0	3.91	9 - 83	0.60	23.3
2	△ 135^0	3.36	6 - 83	0.26	9.2
3	⊖spiral	13.9	6 - 83	0.26	36.4
4	⊕spiral	13.4	5 - 58	0.26	35.2
5	●spiral	13.9	7 -125	0.26	36.4
6	○spiral	14.2	9 - 83	0.60	84.6

$_c\sigma_b$=226kg/cm^2(compressive concrete strength)

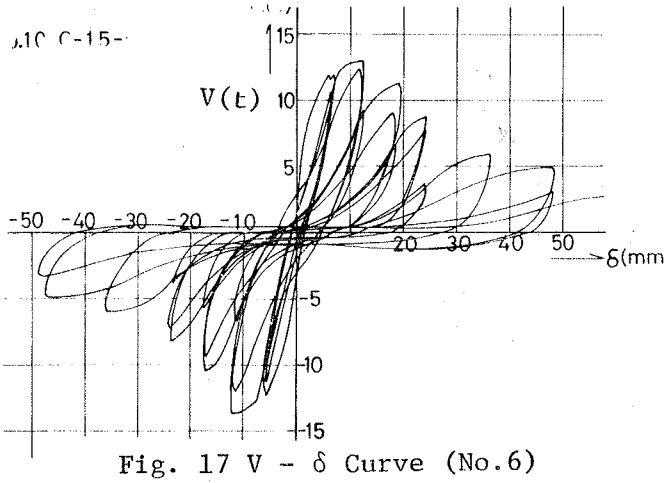

Fig. 17 V - δ Curve (No.6)

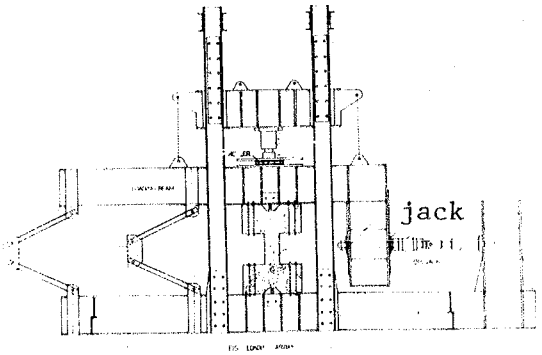

Fig. 13 Loading Arrangement

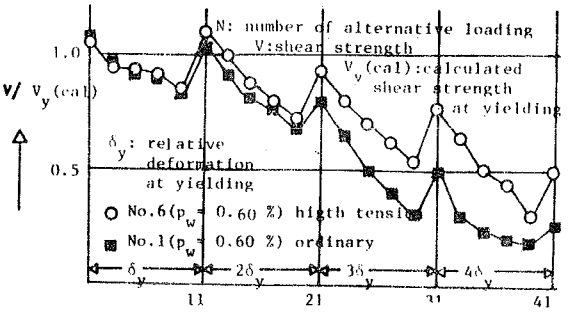

Fig. 18 V/V_y(cal) and N (No1, No6)

σ_0= 26.3kg/cm^2

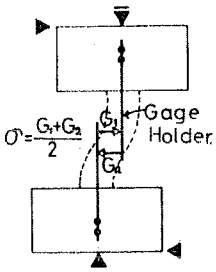

unit:mm

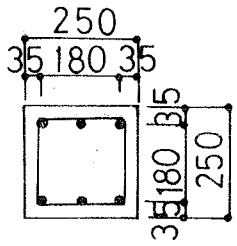

3-D13 $p_t=p_c$=0.61%

Fig. 14 Measuring Method

Fig. 15 Section of Column

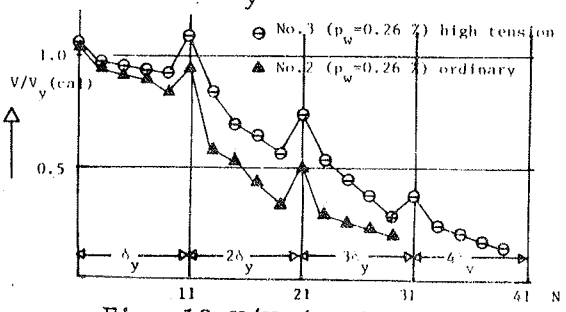

Fig. 19 V/V_y(cal) and N (No2, No3)

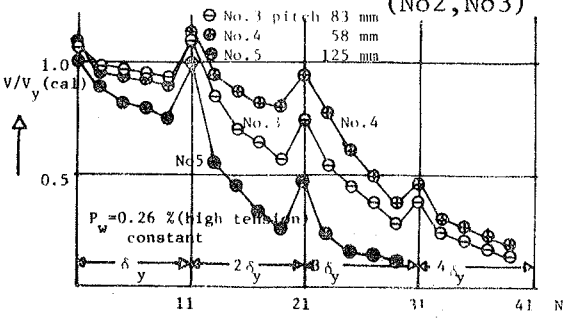

Fig. 20 V/V_y(cal) and N (No3, No4, No5)

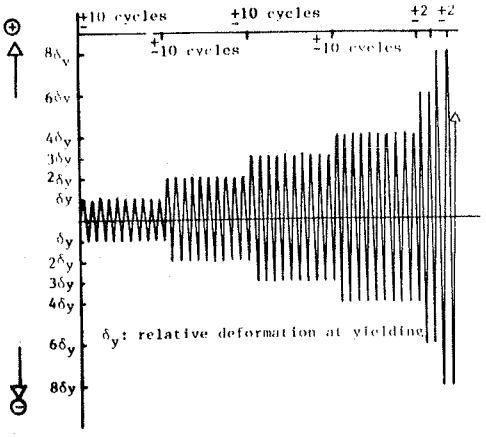

Fig. 16 Loading Procedure

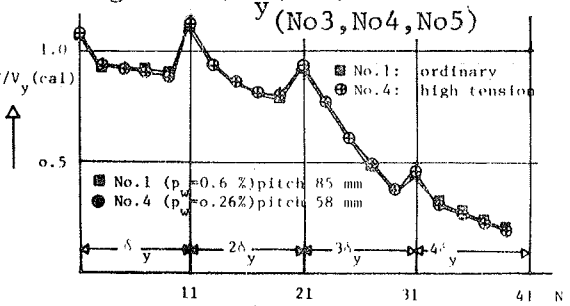

Fig. 21 V/V_y(cal) and N (No1, No4)

SHEAR EFFECTS ON PLASTIC HINGES OF EARTQUAKE RESISTING REINFORCED CONCRETE FRAMES

Thomas PAULAY
University of Canterbury
Christchurch, New Zealand

Ian N. BULL
Morrison Coopers & Partners
Wellington, New Zealand

SUMMARY

Wide full depth cracks that develop across plastic hinge regions of beams which are subjected to reversed cyclic loading, may be responsible for significant loss of energy dissipation. The primary causes of the phenomenon are sliding displacements which result in the grinding of crack interfaces, bond loss along and possibly buckling of the principal flexural bars because shear transfer is enforced mainly by dowel action across these bars. Different ways of detailing, by which improved performance may be obtained, are briefly discussed. It is shown how satisfactory response can be obtained also in beams in which plastic hinges have been deliberately relocated away from column faces. The superior performance of plastic hinge zones with diagonal reinforcement is demonstrated. Nominal shear stress levels are suggested, beyond which the use of diagonal shear reinforcement, to control shear sliding, should be made mandatory.

RÉSUMÉ

De larges crevasses de toute la profondeur, qui se développent au travers des parties à charnière plastique des poutres qui sont soumises à des charges cycliques inversées pourraient être responsables pour une perte importante de dispersion d'énergie. Les causes premières de ce phénomène sont les déplacements qui glissent et qui finissent par ronger les parois internes, par perdre la liaison le long des barres de courbure principales et peut-être même par les tordre; - car la transmission de la force de cisaillement se fait, en grande partie, par une action similaire à celle du goujon, à travers ces barres. On discutera brièvement des moyens de détailler les renforcements qui donneront de meilleurs résultats. On montrera aussi comment une réponse satisfaisante peut être obtenue dans les poutres dont les charnières plastiques ont été déplacées, à dessein, loin des têtes de colonne. On démontre aussi le comportement superieu des zones de charnière plastique avec renforcement diagonal. On propose les niveaux de tension de cisaillement au delà desquels, l'utilisation de renforcement diagonal devrait être rendu obligatoire, pour controler les glissements de cisaillements.

INTRODUCTION

It is generally recognized that a realistic means, by which the response of ductile reinforced concrete frames to large earthquake excitations can be contained within practical limits, is hysteretic damping. Therefore a frame should dissipate significant energy in a stable manner during its inelastic

response. Stability in this context refers to the maintenance of reasonably constant and high level of lateral load resistance during several large reversed cycles of inelastic displacements, with as little loss of stiffness as possible after each such cycle. Therefore the design and detailing of potential plastic hinges warrants particular attention.

In the analytical assessment of the inelastic dynamic response of frames, beam behaviour is often modelled as shown by curve 1 in Fig. 1. Such perfectly elastic-plastic load-displacement relationship is unattainable in reinforced concrete plastic hinges. In steel beams a nonlinear moment-rotation relationship, characterised by Bauschinger effect, such as shown by curve 2 in Fig. 1, is usually observed. When internal forces, such as tension, compression and shear, in the plastic hinge of a reinforced concrete member are transferred predominantly by reinforcing steel, a response similar to that of a steel beam, i.e. curve 2 in Fig. 1, will be approached. Such response represents the optimum realistic energy dissipation, as measured by the area under the load-displacement curve during an inelastic displacement excursion.

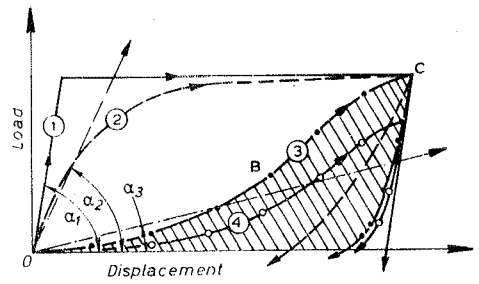

FIG. 1 - Idealized, optimal and degrading displacement response of a beam during an inelastic pulse.

When during large displacement reversals significant portions of the internal member forces are to be transferred by the concrete, both strength and stiffness degradation will occur. The largest single cause for these two detrimental phenomena is the shear force that needs to be resisted. For reasons to be discussed subsequently, one quadrant of a complete typical hysterisis loop may take the form of curve 3 in Fig. 1. Clearly the energy dissipation and hence hysteretic damping, expressed by the shaded area in Fig. 1, is distinctly less than in the previous cases. A plastic hinge, that followed in a particular cycle the load-displacement path along curve 3, is likely to trace curve 4 in the following displacement cycle. The resistance offered by the member at any displacement will now be less than in the previous cycle. The straight lines radiating from the origin of Fig. 1 may be taken as a measure of the average stiffness, tan α, associated with each load path. Most well designed reinforced concrete members will exhibit load-displacement relationships that will lie between curves 2 and 3 of Fig. 1.

SHEAR EFFECTS IN PLASTIC HINGES

Distinct stages of the somewhat idealized behaviour of a conventionally reinforced plastic hinge region are illustrated in Fig. 2. In this example it is assumed that the top and the bottom flexural reinforcement is approximately equal. If the shear force is significant, extensive diagonal cracking will develop in the first inelastic load cycle. (Fig. 2a). Adequate web (stirrup) reinforcement will, however, without exceeding yield strain, transfer the shear forces. Upon load reversal significant moment will need to be applied before the previously formed large tension crack will close. Fig. 2b shows the stage when the bottom reinforcement has already yielded in tension but the top bars have not yet yielded sufficiently in compression for the crack to close. At this stage, when a wide full depth crack has developed at the support, a significant shear force need be transferred across that crack. Shear transfer by aggregate interlock-action will be reduced and therefore the major part of the shear will need be transferred by dowel action

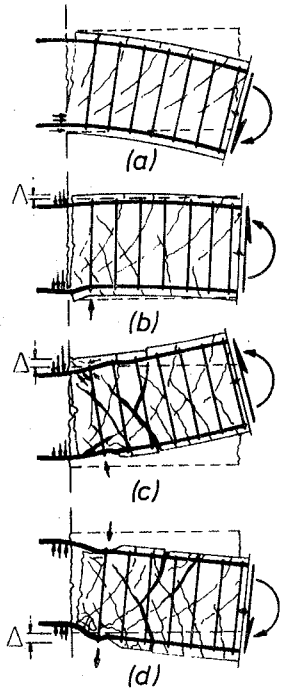

FIG. 2 - Significant stages if the development of a plastic hinge during reversed cyclic loading.

of the top and bottom flexural bars. (Fig. 2b). As both the top and the bottom bars have yielded, appreciable shear (dowel) displacement will be involved in dowel shear transfer, leading to a reduction in stiffness of the beam so represented by the range O-B along curves 3 in Fig. 1.

Further increase of shear load will result in further sliding displacement, Δ , till the critical crack closes at the top of the beam, as seen in Fig. 2c. At this stage shear can be transferred also across the concrete compression zone. The shear displacement, Δ , that has occurred before the closure of the crack, results in uneven bearing in the newly formed concrete compression zone. Consequently at a relatively low nominal compression stress level grinding of the concrete at the crack interfaces will occur because of the lack of fit and the frictional shear load. The range B - C along curve 3 in Fig. 1, illustrates this stage of the response.

After several large inelastic load cycles, residual plastic tensile strains accumulate in the flexural reinforcement, and therefore the beam becomes longer. The shear may then need to be transferred entirely by dowel action, as is shown in Fig. 2d. Large dowel displacements, loss of cover and the deterioration of concrete around compression bars may eventually lead to their buckling. Clearly at this stage a beam cannot develop its original flexural or shear capacity.

The degree and the rate of deterioration will be dependent on the relative magnitude of shear, as measured by the nominal shear stress

$$v = V/bd \qquad (1)$$

where V = shear force, b = width of web, d = effective depth of section, and also on the magnitude of inelastic deformations that have been imposed on the plastic hinge zone during the preceding load cycle or cycles. It is evident from the works of Bertero et al. (1974)(1975) and Scribner and Wight (1978) that in this respect conventionally reinforced beams can be placed in three broad groups:

(a) A large number of inelastic load cycles can be carried by a beam without serious deterioration in energy dissipating capacity when the maximum nominal shear stress does not exceed about $0.3\sqrt{f'_c}$ MPa.*

(b) When $0.3 < v/\sqrt{f'_c} < 0.5$, serious degradation of energy dissipating capacity must be expected. The transition from one range to another is not distinct.

(c) When nominal shear stresses in excess $0.5\sqrt{f'_c}$ MPa are to be transferred during reversed cyclic loading, a premature failure of the plastic hinge in a conventionally reinforced beam due to sliding shear is to be expected.

---

* The term $\sqrt{f'_c}$ is to be in MPa, where f'_c is the compression cylinder strength of the concrete in MPa.

If a plastic hinge is to dissipate significant energy, while maintaining a reasonably stable resistance during cyclic displacements, either the nominal shear stress across the plastic hinge must be limited, or special detailing must be employed to control shear displacements.

THE CONTROL OF SHEAR DEFORMATIONS

To illustrate a number of possible alternatives in the detailing for the control of sliding shear displacements, the example of a simple cantilever, shown in Fig. 3 will be used. Conventional beam detailing, as shown in Fig. 3a should be adequate when the nominal shear stresses cannot exceed $0.3\sqrt{f'_c}$. When the shear stress is in excess of $0.2\sqrt{f'_c}$ noticeable pinching in the hysterisis loops will, however, become evident.

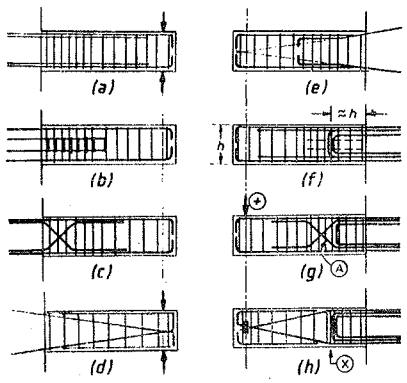

FIG. 3 - Alternatives in the detailing of potential plastic hinge regions.

Some improvement in the response will result if intermediate bars, placed between the top and bottom flexural reinforcement, are employed, as shown in Fig. 3b. However, these bars should not significantly increase the flexural capacity of the beam. In addition to providing some dowel resistance, such bars assist in the development of several smaller full depth cracks. Thereby shear transfer by aggregate interlock action will be enhanced. Scribner and Wight (1978) found, however, that the improvement in energy dissipation was not very significant.

One of the most effective ways to control sliding shear displacements is by the use of diagonal bars, as shown in Fig. 3c. Such bars contribute to both the diagonal tensile and the sliding shear strength and they may be designed to resist the major proportion of, if not the entire shear force to be transferred across the potential full depth crack in the plastic hinge zone. The behaviour of plastic hinges reinforced in such a way are discussed subsequently when the detail of Fig. 3g is examined. A similar arrangement of diagonally bent bars was used by Bertero, Popov and Wang (1974), who demonstrated its effectiveness. The response of such beams may be considered to be the optimum obtainable for reinforced concrete members.

When a beam is short and relatively deep, it may be more convenient to use diagonal reinforcement only to transfer moments and shear forces simultaneously. All other reinforcement serves secondary purposes only. Such an arrangement is shown in Fig. 3d. Park and Paulay (1975) described a similar arrangement that has been used extensively in coupling beams of tall shear wall structures. In these, diagonal bars intersect at midspan where the point of contraflexure of the loaded beam occurs. The excellent response of such beams has also been identified by Barney, Shiu, Rabbat and Fiorato (1976). Diagonal bars must be suitably supported laterally to ensure that buckling of the compression bars can not interfere with the excellent response.

With longer and shallower beams a single set of diagonals, as shown in Fig. 3d, may not provide sufficient moment of resistance against gravity loading at midspan. For such spandrel beams the previous arrangement may be slightly modified, as shown in Fig. 3e. It must be realised, however, that yielding, extending over the inclined portion of the flexural bars, may penetrate into the splice zone. Therefore generous transverse (stirrup)

reinforcement is required there to improve bond transfer. The observed excellent response of such a beam was reported by Paulay and Spurr (1977).

RELOCATED PLASTIC HINGES

The ultimate cause of failure, particularly at interior beam-column joints, adequately reinforced for shear, is often due to the slippage of the beam bars. Yield penetration from beam plastic hinges, immediately adjacent to the column, reduces the effective embedment length of the beam bars and eventually a breakdown of the bond resistance may result. Primarily to eliminate such a bond failure it has been suggested by Bertero et al. (1974) and Bull (1978) that in such cases the plastic hinge in the beam could be removed away from the column face. Fig. 3f shows the typical detailing of such a plastic hinge. The flexural reinforcement is abruptly reduced at a short distance from the column face in such a way that when the flexural overstrength* of the hinge is developed, tensile stresses in the beam bars at the column face can attain only the nominal yield strength. Thereby the beam section adjacent to the beam-column joint remains elastic. Therefore satisfactory anchorage of these bars can be provided within a joint. This will also considerably improve the behaviour of beam-column joints.

In a recent experimental program the behaviour of such relocated plastic hinges, which have been subjected to rather large shear stresses ($v_{max} \simeq 0.5 \sqrt{f'_c}$ MPa), has been studied by Bull (1978). The aim of the investigation was: (a) to observe the effect of sliding shear on energy dissipation in a plastic hinge, (b) to measure strain variations along flexural bars of the beam, which should show whether, with the selected position of the critical section (Fig. 3f), yielding would occur at the face of the column. All three tests, shown somewhat simplified in Figs. 3f, 3g and 3h, exhibited very satisfactory performance with respect to this second aim. It appears that the critical section of the plastic hinge need not be located further from the beam face than the approximate depth of the beam (Fig. 3f).

The response of Unit 1, in terms of tip deflection and the applied load P to theoretical strength P_u^* ratio, is given in Fig. 4. Four 20mm diameter intermediate bars crossed the critical section of the 500mm deep beam at the positions shown by the broken line in Fig. 3f. It is believed that these

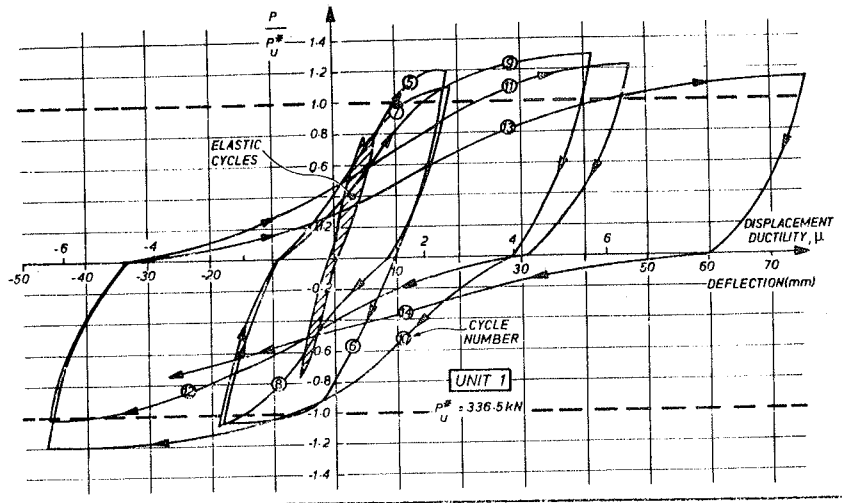

FIG. 4 - Load-displacement response of a beam with a conventionally reinforced relocated plastic hinge, detailed as in Fig. 3f.

*Flexural overstrength is assumed to develop when, as a result of very large tensile strains, the flexural reinforcement enters the strain hardening range. For mild steel the effective overstrength is normally taken as 1.25 times the specified yield strength.

dowel bars resulted in the very satisfactory energy dissipation capacity of this beam, which is normally not attainable at this high level of nominal shear stress. The beam failed by sliding shear in the 14th semicycle, after it sustained a displacement ductility of 10 in the previous cycle. Fig. 5 shows the beam at this stage.

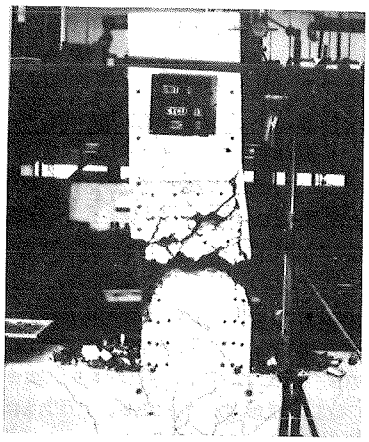

FIG. 5 - Failure of a beam by a sliding shear.

Fig. 3g is a sketch of Unit 2 in which it was attempted to control sliding shear by diagonal bars in the plastic hinge zone. The theoretical combined contribution of the two sets of diagonal bars to transverse shear resistance was approximately equal to the shear force that could be developed at flexural overcapacity. It was found, however, that this high shear resistance did not develop during the test. The excellent response of this beam is presented in Fig. 6. Unit 2 is shown at the end of the test in Fig. 7.

In Unit 3, shown in Fig. 3h, the principles explained in connection with the detailing illustrated in Fig. 3d, were studied. As expected, with progressive cyclic loading, yielding developed over the entire inclined portion of the bars. The response of the beam and its displacement history, which was similar to those applied to the other two units, is presented in Fig. 8. Particular attention was paid to the proportioning of stirrup-

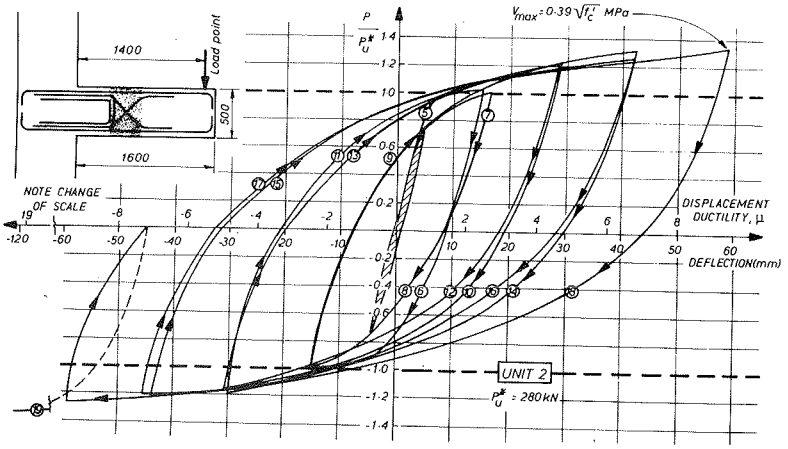

FIG. 6 - Load-displacement response of a beam diagonally reinforced in the plastic hinge.

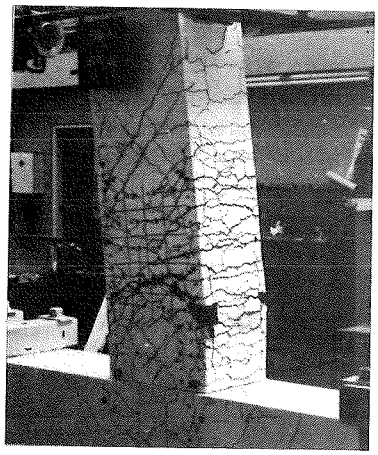

FIG. 7 - Unit 2 with diagonally reinforced plastic hinge at the termination of the test.

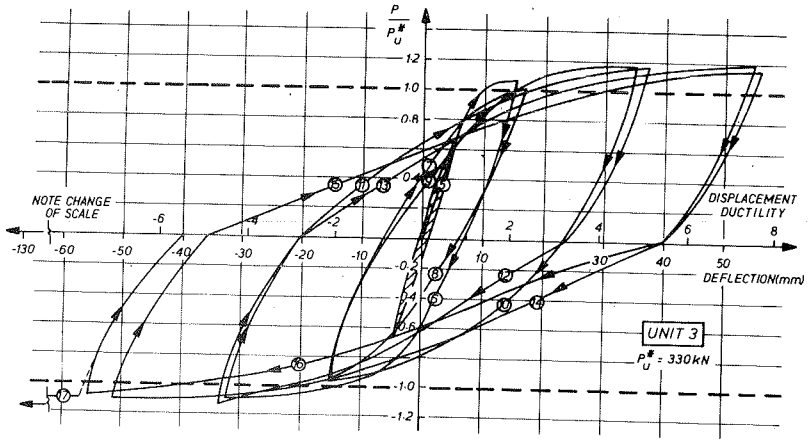

FIG. 8 - Load-displacement response of a beam with full diagonal reinforcement as in Fig. 3h.

ties, fitted to the diagonal bars at the bend, to prevent buckling of these main bars when they are subjected to compression. In spite of this precaution some yielding of these special ties, located at the position marked X in Fig. 3h, has occurred. As a result a gap developed at the inside of the bend of the main diagonal bars and due to uneven bearing eventually local crushing of the concrete has occurred. The resulting shear displacements caused some loss of energy dissipation, as may be seen when Figs. 6 and 8 are compared.

CONCLUSIONS AND RECOMMENDATIONS

1) From experimental information it is evident that shear forces, to be transferred across plastic hinges of members of earthquake resisting frames, may adversely affect both the strength and the energy dissipating ability of such members.

2) The major cause of strength and stiffness degradation and the consequent loss of energy dissipation in such members is the development of wide, full depth cracks in the plastic hinge zones.

3) When the nominal shear stress is relatively small, i.e. $v_u < 0.3\sqrt{f'_c}$ MPa, conventional stirrup shear reinforcement, resisting the entire shear force, will ensure that tolerable loss of energy dissipation will occur in the plastic hinges.

4) Intermediate longitudinal bars, placed in the web of a beam between the principal flexural reinforcement, will improve energy dissipation of the member, because it will assist in the formation of a larger number of smaller full depth cracks. Larger diameter short intermediate bars, which should not contribute significantly to the flexural strength of the member, are likely to be more efficient because of their more effective contribution as dowels.

5) When nominal shear stresses in excess of approximately $0.3\sqrt{f'_c}$ MPa were required to be transferred, various arrangements of diagonal reinforcement were found to result in optimal seismic member performance. The skilful use of diagonal bars can ensure that the seismic response of a reinforced concrete beam is as good as that of a steel beam.

6) When the anchorage of the beam flexural reinforcement becomes critical, particularly at interior beam-column joints, the relocation of the potential plastic hinges in the beams, away from the column faces, should be considered. This will result in the need for less joint shear reinforcement. The control of shear distortions by proper detailing of relocated plastic hinges should be as summarized in the previous points. The primary aim of such beam detailing is to ensure that tensile yielding along beam bars does not penetrate into the joint core during cyclic reversed loading.

7) The critical nature of shear forces with respect to the performance of a potential plastic hinge will not only depend on the absolute magnitude of the nominal shear stress to be sustained, but also on the relative magnitude of the shear forces which may act in opposite directions. In most tests reported, the magnitudes of the reversed shear forces applied were approximately of the same order. Cyclic shear forces, however, are likely to be less detrimental when reversal does not occur because the grinding of the crack interfaces is then much less severe. It is suggested, therefore, that in order to minimize the loss of energy dissipation in potential plastic hinges due to seismic shear effects:

(a) The nominal shear stress that should be assumed to be developed in a

beam, in which the top and bottom flexural reinforcement may be subjected to yielding and in which only conventional stirrup shear reinforcement is used, should not exceed at the attainment of the flexural overstrength capacity

$$v_u = 0.3\ (2 + r)\ \sqrt{f'_c} \qquad (2)$$

where r is the algebraic ratio of the maximum shear force developed at the plastic hinge section when the bottom flexural reinforcement is yielding, to the maximum shear force induced at the same section when the top beam reinforcement is yielding. Its value is limited thus: $-1 < r < 0$.

(b) If the computed shear stress exceeds the value given by Eq. (2), at least 75% of the shear force should be resisted at every section of the plastic hinge region by diagonal reinforcement across the web.

(c) The entire shear force should be resisted by diagonal reinforcement if the shear stress exceeds one and one half times the value given by Eq. (2).

(d) For the purpose of these recommendations the plastic hinge should be assumed to extend by d from the face of the support or from a similar cross section where maximum yielding due to reversed loading is expected.

(e) When diagonal bars cross a section in two directions, the transverse components of the diagonal tension and compression steel forces may be considered together.

(f) The shear stress in a member should not exceed $0.8\sqrt{f'_c}$ MPa, unless the member is designed to carry the load by diagonal reinforcement over its entire span.

ACKNOWLEDGEMENTS

The financial support for the experimental work, provided by the University of Canterbury, and the invaluable contribution of the technician staff of its Department of Civil Engineering is gratefully acknowledged.

REFERENCES

Barney, G.B., Shiu, K.N., Rabbat, B.G. and Fiorato, A.E., "Earthquake Resistant Structural Walls - Tests of Coupling Beams", Progress Report, Portland Cement Association, Research and Development Laboratories, Skokie, 1976, 136 pp.

Bertero, V.V., Popov, E.P. and Wang, T.Y., "Hysteretic Behaviour of Reinforced Concrete Flexural Members with Special Web Reinforcement", Report No. EERC 74-9, Earthquake Engineering Research Center, University of California, Berkeley, 1974, 134 pp.

Bertero, V.V. and Popov, E.P., "Hysteretic Behaviour of Ductile Moment-Resisting Reinforced Concrete Frame Components", Report No. EERC 75-16, Earthquake Engineering Research Center, University of California, Berkeley, 1975, 71 pp.

Bull, I.N., "The Shear Strength of Relocated Plastic Hinges", M.E. Report No. 78/11, Department of Civil Engineering, University of Canterbury, New Zealand, 1978, 113 pp.

Park, R., and Paulay, T., "Reinforced Concrete Structures", John Wiley & Sons, New York, 1975, 769 pp.

Paulay, T., and Spurr, D., "Simulated Seismic Loading on Reinforced Concrete Frame - Shear Wall Structures", Sixth World Conference on Earthquake Engineering, New Delhi, 1977, Vol.3, pp. 221-226.

Scribner, C.F., and Wight, J.K., "Delaying Shear Strength Decay in Reinforced Concrete Flexural Members Under Large Load Reversals", Report UMEE 78R2, Department of Civil Engineering, The University of Michigan, 1978, 241 pp.

ROTATIONAL CAPACITY OF PLASTIC HINGE IN REINFORCED LIGHTWEIGHT CONCRETE BEAMS

Igor TERTEA
Polytechnic Institute of
Cluj-Napoca, Romania

Traian ONET
Polytechnic Institute of
Cluj-Napoca, Romania

SYNOPSIS

A theoretical and experimental investigation is reported of the rotational capacity of hinging regions in lightweight aggregate concrete beams. The results of 131 beams tests are analyzed. The variables in the tests were: shape of cross section, yield point stress of reinforcement, amount of longitudinal tension and compression reinforcement.

RÉSUMÉ

On présente le calcul et les vérifications expérimentales concernant la rotation plastique des éléments fléchis en béton léger armé. Les 131 poutres essayées mettent en évidence l'influence des paramètres suivants: la forme de la section transversale, la nature de l'acier, le pourcentage de l'armature tendue et de l'armature comprimée.

INTRODUCTION

The present investigation has been stimulated by the extension of lightweight aggregate concrete utilization for multi-storey buildings. The advantage of reducing the dead weight is positive for the evaluation of the inertial forces in case of seismic actions, especially in the non-linear dynamic analysis of structures. The rotation capacity of plastic hinge is directly related to ductility and it becomes

evident in the consequent analysis for reinforced lightweight concrete bent elements.

ASSUMPTIONS

a) At commencement of yield of the reinforcement, the concrete compressive stresses vary with a second degree parabola (Fig.1a);

b) At ultimate moment (Fig.1b) the concrete compressive stresses vary with a third degree parabola, having the maximum value f'_c;

c) Tensile stresses of the concrete may be neglected;

d) The strain in the concrete may be assumed directly proportional to the distance from the neutral axis both at commencement of steel yield and at ultimate moment (Fig.1c);

e) The stress in tension reinforcement at ultimate moment may be obtained multiplying the yield point stress by a behaviour coefficient m_s shown in Fig.2;

f) The stress in compression reinforcement may be obtained from the strain diagram considering $m_s = 1$.

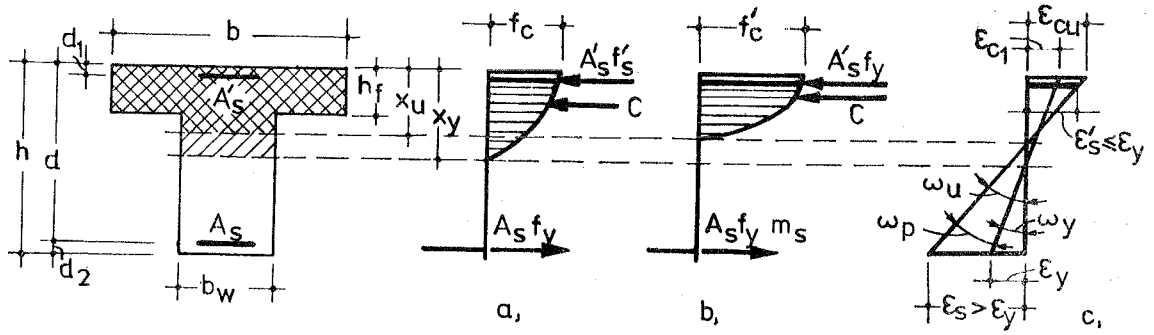

Fig.1. Conditions at yield of tension reinforcement (a) at ultimate moment (b) and strain distribution diagram (c).

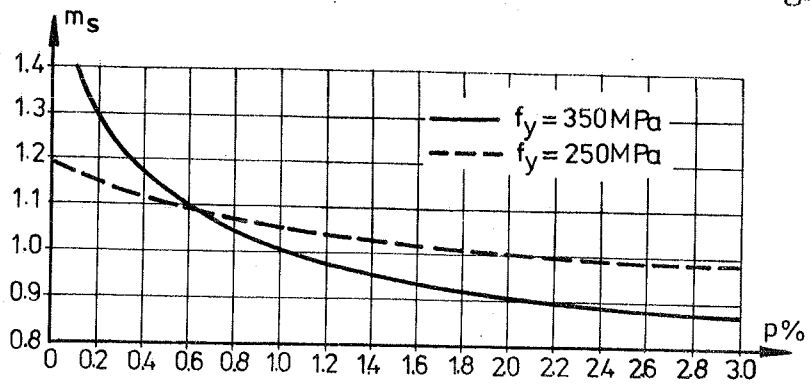

Fig.2. Variation of behaviour coefficient m_s.

CALCULATING EQUATIONS

T sections. The capacity of plastic rotation (θ_p) represents the difference between the rotation at failure (θ_u) and the rotation at commencement of tension reinforcement yield (θ_y), i.e.:

$$\theta_p = \theta_u - \theta_y \tag{1}$$

Using the specific rotations (ω) and the equivalent length of plastic hinge (ℓ_p), Eq.1 may be written:

$$\theta_p = \omega_p \ \ell_p = (\omega_u - \omega_y)\,\ell_p = \left(\frac{\varepsilon_{cu}}{k_u} - \frac{\varepsilon_{cl}}{k_y}\right)\frac{\ell_p}{d} \tag{2}$$

where

$$k_y = \frac{x_y}{d} \qquad \text{and} \qquad k_u = \frac{x_u}{d} \tag{3}$$

The relative position of neutral axis at yield (k_y) and failure (k_u) moment may be determined from the equilibrium of forces getting to the Eq.(4),(5) and (6):

$$k_y = 0.75\left[r_1 + n'(p+p')\right]\left\{-1 + \sqrt{1 + \frac{2.67\left[n'(p+r_3p') + 0.5r_1r_2\right]}{\left[r_1 + n'(p+p')\right]^2}}\right\} \tag{4}$$

$$k_u = 1.33\,(pm_s - p')\,\frac{f_y}{f'_c} - r_1\,, \tag{5}$$

if $f'_s = f_y$

$$k_u = \frac{2}{3}\,(p_1 - p'_1 - r_1) + \sqrt{\left[\frac{2}{3}\,(p_1 - p'_1 - r_1)\right]^2 + \frac{4}{3}\,r_3p'_1}\,, \tag{6}$$

if $f'_s < f_y$. Above we noted:

$$p_1 = pm_s\,\frac{f_y}{f'_c}\,, \qquad p'_1 = p'\,\frac{\varepsilon_{cu}}{\varepsilon_y}\,\frac{f_y}{f'_c} \tag{7}$$

$$\varepsilon_y = 0.002 + \frac{f_y}{E_s} \tag{8}$$

$$r_1 = \frac{b-b_w}{b_w}\,\frac{h_f}{d}\,; \quad r_2 = \frac{h_f}{d}\,; \quad r_3 = \frac{d_1}{d} \tag{9}$$

$$p = \frac{A_s}{b_w d} \quad ; \qquad p' = \frac{A'_s}{b_w d} \tag{10}$$

$$n' = \frac{E_s}{E_c}\left(1 + \frac{p}{200} f_y\right)(1 + v\varphi) \leq 6\,\frac{E_s}{E_c} \tag{11}$$

The variation of plastic rotation capacity with reinforcement ratio for two yield point stresses of steel is shown in Fig.3

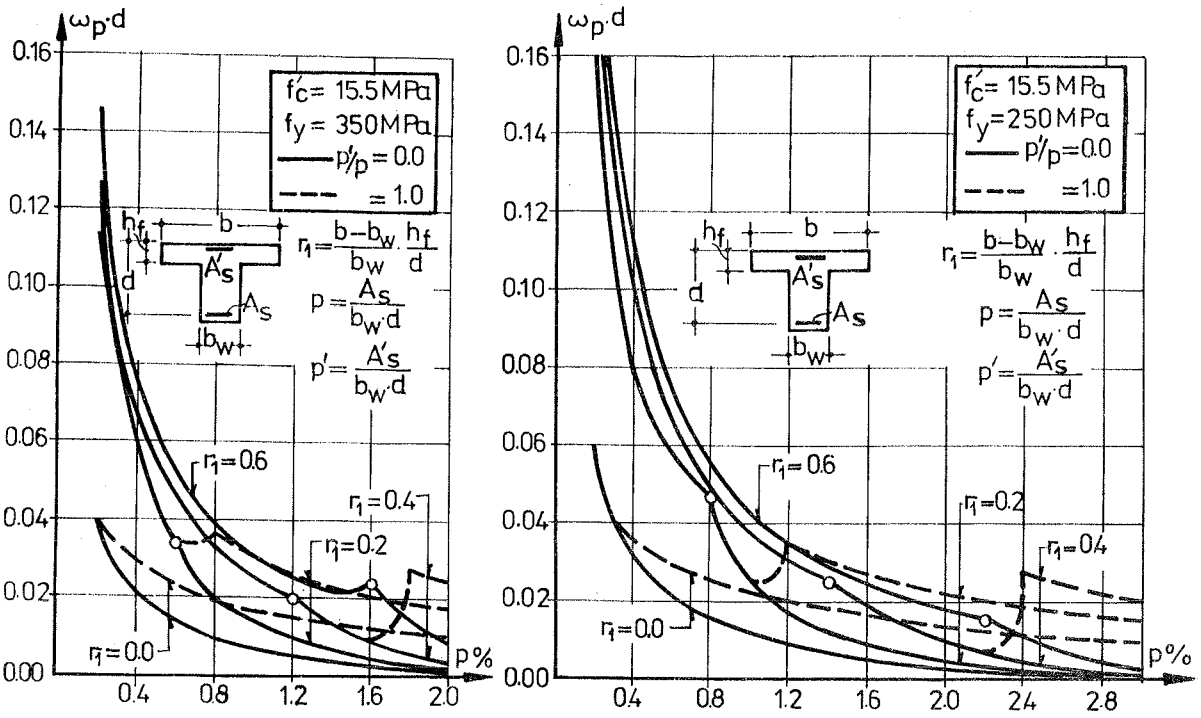

Fig.3. Variation of plastic rotation with the reinforcement ratios p and p' for T beams.

Rectangular sections. The capacity of plastic rotation is determined using Eq.(2) in which

$$k_y = 0.75\, n'(p+p')\left[-1 + \sqrt{1 + \frac{2.67(p+r_3 p')}{n'(p+p')^2}}\right] \tag{12}$$

$$k_u = 1.33(pm_s - p')\,\frac{f_y}{f'_c} \tag{13}$$

if $f'_s = f_y$, and

$$k_u = \frac{2}{3}(p_1 - p_1') + \sqrt{\left[\frac{2}{3}(p_1 - p_1')\right]^2 + \frac{4}{3} r_3 p_1'} \qquad (14)$$

if $f_s' < f_y$.

In Fig.4 is shown the variation of plastic rotation with tension reinforcement ratio and the amount of compressive reinforcement, for two qualities of steel.

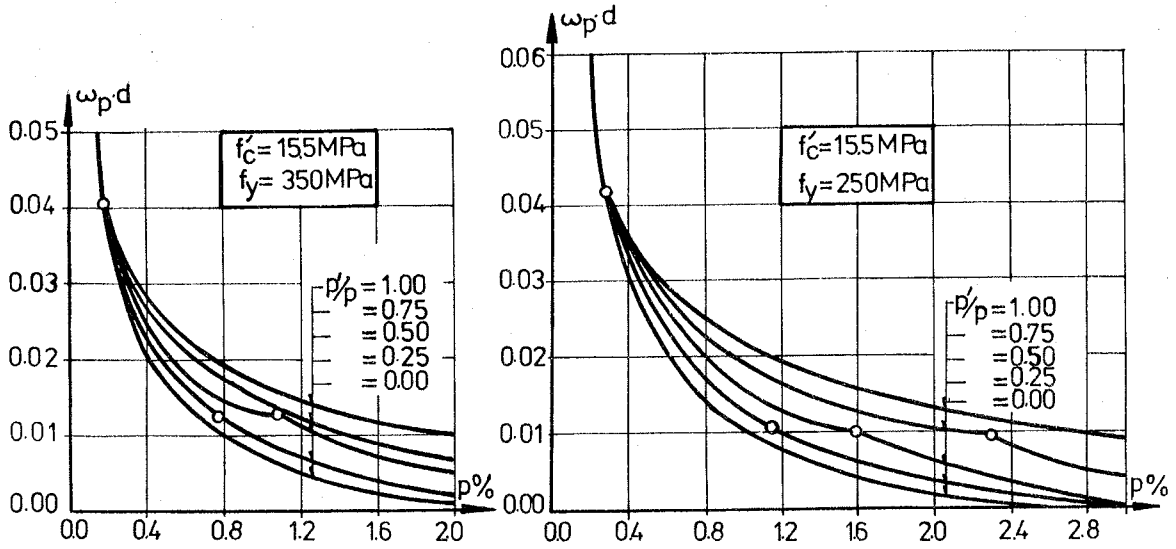

Fig.4. Variation of plastic rotation with the reinforcement ratios p and p', for rectangular beams.

EXPERIMENTAL TESTS

115 rectangular and 16 T- shaped beams were tested.The amount of tension reinforcement was ranged between 0.07 and 2.87 %. All specimens were with a span between supports of 300 cm and were tested with equal loads applied at each one third of span. The characteristic value of compressive strength of a lightweight aggregate (expanded clay) concrete was 15.5 MPa.

Tests results pointed out a linear variation of compressive strain of concrete (ε_{cl}) at commencement of the tension reinforcement yield with the reinforcement ratio, as shown by Fig.5. At ultimate moment the average value of the compressive strain of lightweight concrete may be considered $\varepsilon_{cu} = 4.5$ ‰ .

For T - beams the ratio between calculated and experimental values of plastic rotation capacity vary between 0.70 and 1.23.

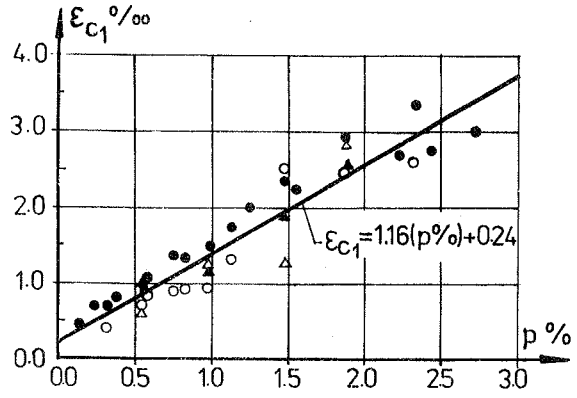

Fig.5. Variation of compressive strain of concrete at yield moment.

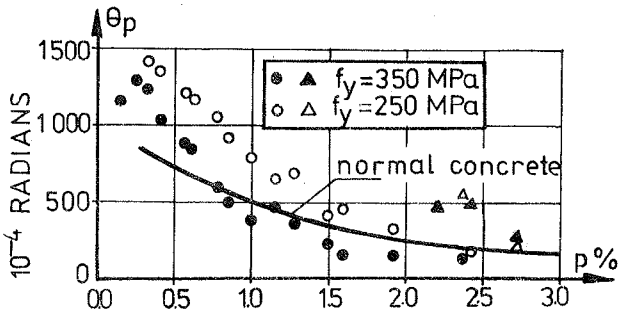

Fig.6. Experimental values of plastic rotation of light-weight concrete.

For rectangular simple reinforced beams, the experimental values of the plastic rotation capacity are represented by Fig.6 in comparison with the values obtained by J.C.Maldague [1] for normal concrete.

Statistically processing the test results of rectangular beams led to following laws concerning the variation of plastic rotation capacity with the reinforcement ratio and yield point stress:

$$\theta_p = 0.367\ p^{-0.919}, \text{ for } f_y = 350 \text{ MPa} \qquad (15)$$

$$\theta_p = 0.616\ p^{-1.135}, \text{ for } f_y = 250 \text{ MPa} \qquad (16)$$

The influence of compressive reinforcement ratio on plastic rotation capacity of rectangular beams is represented by the curves series in Fig.7 where the test results are also given.

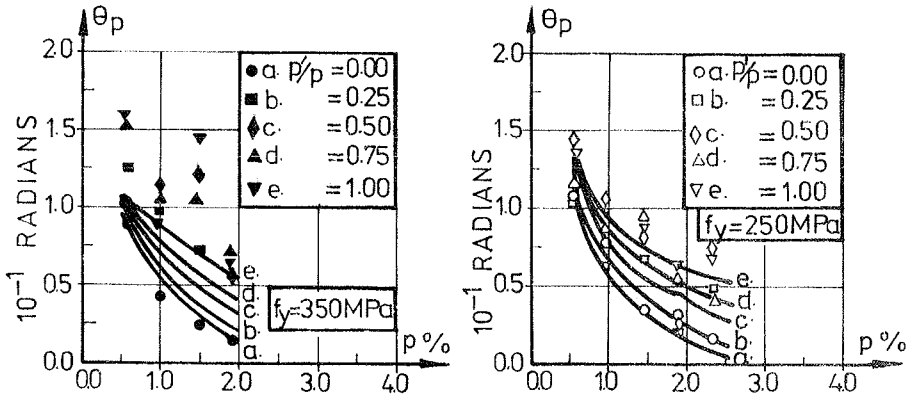

Fig.7. Comparison of calculated and measured plastic rotation for double-reinforced rectangular beams.

CONCLUSIONS

Study of factors influencing the plastic rotation capacity of lightweight reinforced concrete bent elements led to the following conclusions:

- The plastic rotation capacity increases with the decrease of yield point stress of steel and with the increase of concrete quality.

- The plastic rotation capacity increases with the decrease of tension reinforcement ratio and with the increase of compression reinforcement ratio.

- The provision of a flange in the compression zone of beams is advantageous for the plastic rotation capacity.

Qualitatively considered, the above conclusions are similar with those in normal concrete beams.

- The structural lightweight aggregate (expanded clay) concrete, having the compressive strength between 20 and 30 MPa, presents higher plastic rotation capacity than normal concrete at the same reinforcement amount. This finding may be of particular interest in dynamic analysis of structures for seismic loadings.

APPENDIX - Notations

E_c - modulus of elasticity of concrete;

E_s - modulus of elasticity of reinforcing steel;

f_c - compressive strength of concrete at commencement of tension reinforcement yield;

f'_c - ultimate strength of concrete;

f_s - stress in tension reinforcement;

f'_s - stress in compression reinforcement;

f_y - yield point stress of tension and compression reinforcement;

k_y - relative depth of neutral axis at yield of tension reinforcement;

k_u - relative depth of neutral axis at ultimate moment;

m_s - behaviour coefficient of tensile reinforcement;

v - ratio of long-time loading to the total one;

ε_{cl} - maximum concrete compressive strain at commencement of tension reinforcement yield;

ε_{cu} - maximum concrete compressive strain at ultimate strength;

φ - characteristic of long-time strains of concrete.

REFERENCES

1. Maldague,J.C., "Détermination expérimentale des lois moments - courbures des poutres en béton armé", Annales ITBTP, No.209, 1965.

2. Oneţ,T., "Contribuţii la studiul articulaţiei plastice în elementele din beton uşor armat", Studii şi Cercetări de Mecanică Aplicată, No.1, tom.33, 1974.

3. Tertea,I., Oneţ,T., "Ruperea elementelor încovoiate din beton uşor de granulit, armate cu bare netede şi cu profil periodic", Studii şi Cercetări de Mecanică Aplicată, No.6, tom.30, 1971.

4. Tertea,I., Oneţ,T., "Considérations concernant la formation des articulations plastiques dans les éléments fléchis en béton armé d'argile expansée", Symposium on Plastic Analysis of Structures, Jassy 6-8 september, 1972, Romania.

REINFORCED CONCRETE BEAMS UNDER REVERSED CYCLIC TORSIONAL LOADING

Michael P.COLLINS
University of Toronto
Toronto, Canada

Sithambaram CHOCKALINGAM
University of Toronto
Toronto, Canada

SUMMARY

Three nominally identical reinforced concrete beams were subjected to three different histories of pure torsional loading. The first was loaded monotonically to failure, the second was subjected to repeated applications of non-alternating torsion, while the third was loaded under reversed cyclic torsion.

The observed response of these three beams is discussed and compared with the predictions of the compression field theory. The significant deterioration in the ability of the concrete to resist reversed cyclic diagonal compression is demonstrated.

RÉSUMÉ

Trois poutres en béton armé, nominalement identiques, ont été soumises à trois cas différents de chargement en torsion pure. La première poutre fut soumise a un chargement monotone jusqu'a la rupture, la deuxieme a des efforts de torsion répétés dans le même sens, et la troisième à une torsion cyclique alternative.

Le comportement de ces trois poutres fait le sujet d'une discussion, puis d'une comparaison avec les prédictions de la théorie du champ de compression. La détérioration sensible de la capacité du béton à supporter des efforts périodiques alternatifs de compression diagonale est mise en évidence.

INTRODUCTION

To date nearly all studies aimed at predicting the behaviour of reinforced concrete structures under seismic action have restricted their attention to two-dimensional structures. The state-of-the-art has now reached the stage where it is appropriate to give consideration to the three-dimensional nature of actual structures. Tests on model three-dimensional structures, (Wilby, 1975), have demonstrated that for the typical slab-beam-column reinforced concrete building, the torsional response of the beams has a significant influence on the overall behaviour of the structure.

A research programme at the University of Toronto aims to contribute to the understanding of the behaviour of three-dimensional structures by

developing rational models capable of predicting the response of reinforced concrete members subjected to any combination of the six possible internal stress resultants (i.e. torsion, vertical moment, lateral moment, axial load, vertical shear and lateral shear). This paper will concentrate on describing just one phase of this long term programme in which the response of reinforced concrete members under repeated pure torsion, both alternating and non-alternating, was studied.

EXPERIMENTAL PROGRAMME

Three nominally identical beams, R1, R2 and R3, were loaded in pure torsion using the test rig described in Fig. 1.

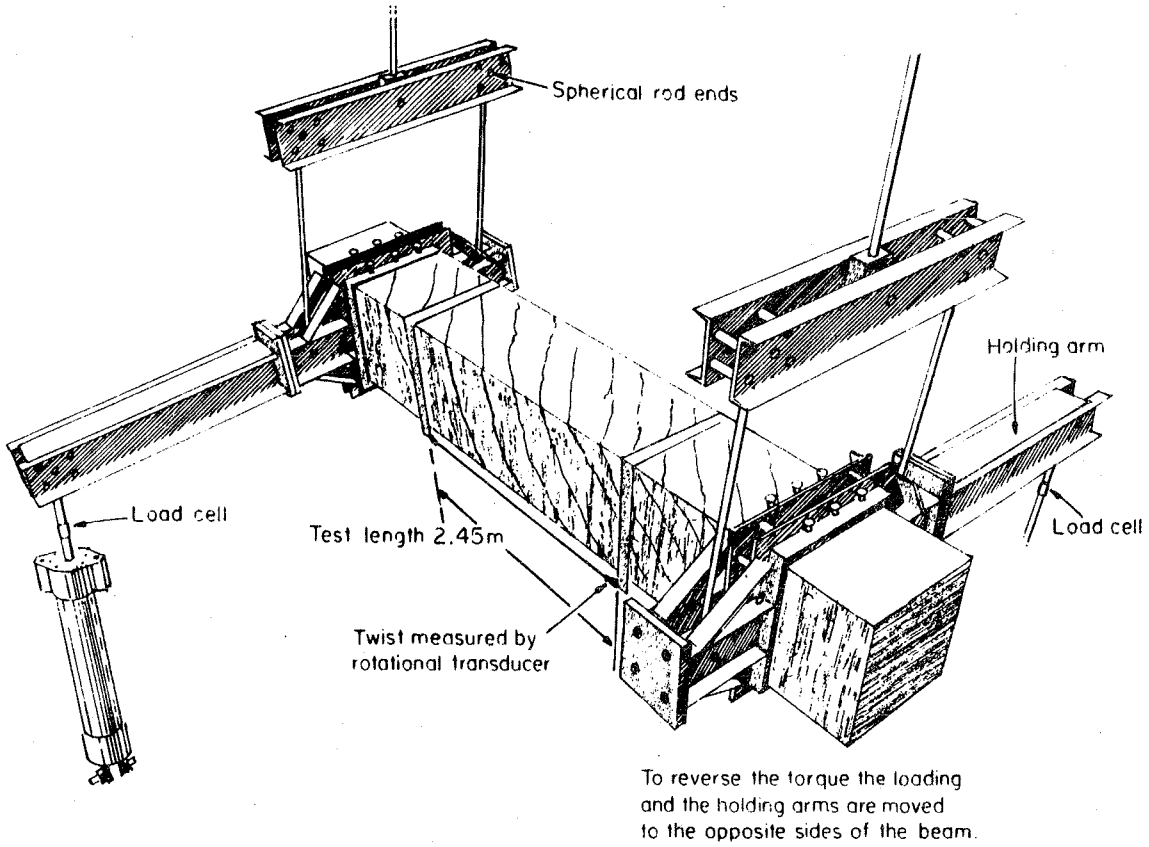

Fig. 1: Torsional Test Rig

All three beams were square and hollow with cross-sectional properties as shown in Fig. 2. The hoops had centre-to-centre dimensions of 340 mm by 340 mm, were made from #3 bars (properties given in Fig. 3), and were anchored with 105° bends with 16 bar diameter extensions.

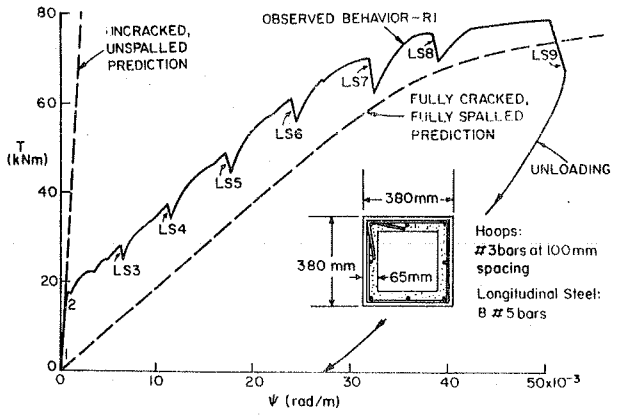

Fig. 2: Torque-Twist Response of Beam R1 - Monotonic Loading

The longitudinal steel consisted of #5 bars, the properties of which are described in Fig. 3. A separate batch of ready-mixed concrete with a maximum aggregate size of 10 mm was used to cast each of the beams.

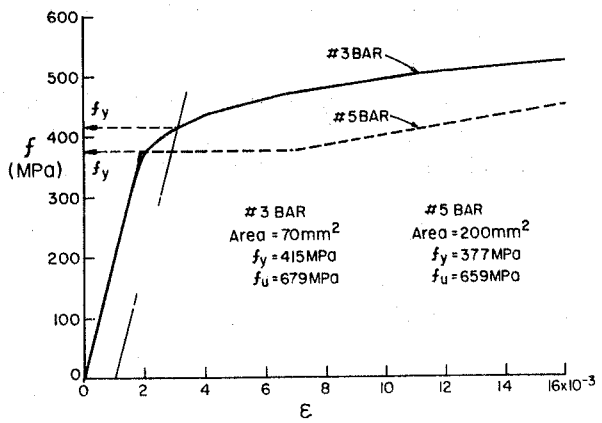

Fig. 3: Characteristics of the Reinforced Used

Beam R1 was loaded monotonically to failure, beam R2 was tested under repeated applications of unidirectional torsional moments, while beam R3 was tested under repeated applications of torsion alternating in direction. The specific loading histories will be described in more detail in the sections below.

BEAM R1 - MONOTONIC LOADING

Beam R1 was tested 67 days after casting at which time the concrete cylinder strength, f'_c, was 34 MPa. The continuously recorded torque-twist curve for this beam is reproduced in Fig. 2. During the test the movement of the loading jack was stopped a number of times to enable strain readings to be taken. These readings took approximately half an hour to complete. The relaxation of torsion that occurred during the reading time at each load stage can be seen in Fig. 2.

Also shown in Fig. 2 are two predicted torque-twist relationships for beam R1. One, the uncracked prediction, is based on Bredt's equation for thin walled elastic beams and on assuming the shear modulus of the concrete, G, to be 500 f'_c. The other prediction is based on the compression field theory, Mitchell and Collins (1974), which assumes that the concrete is fully cracked (i.e. no contribution of concrete tensile stresses). In calculating this prediction it was assumed that the concrete cover outside the hoop centreline had spalled off. Further the concrete stress-strain curve was assumed to be parabolic with the peak stress, f'_c, being reached at a strain of 2.3×10^{-3} (this value was determined from the cylinder tests). For the steel the stress-strain characteristics shown in Fig. 3 were used.

It can be seen (Fig. 2) that prior to diagonal cracking, which occurred at 17 kNm, the beam followed closely the elastic prediction. After cracking the observed torque-twist curve became approximately parallel to the fully cracked prediction but remained some distance above it. At any particular twist the measured strains were in good agreement with those predicted by the compression field theory. For example, at a twist of 32×10^{-3} rad/m (which corresponds to load stage 7) the theory would predict that the tensile strain in the hoop steel, ε_h, would equal 1.87×10^{-3}, the tensile strain in the longitudinal steel, ε_ℓ, would equal 1.31×10^{-3} and the diagonal compressive strain in the concrete, ε_d, would equal 1.25×10^{-3}. At load stage 7 the 24 hoop strain readings (gauge length = 200 mm) gave a maximum value for ε_h of 2.56×10^{-3}, a minimum value of 1.27×10^{-3} and an average value of 1.98×10^{-3}. The 20 longitudinal steel strain readings (gauge length = 200 mm) gave a maximum value for ε_ℓ of 1.90×10^{-3}, a minimum value of 0.75×10^{-3} and an average value of 1.33×10^{-3}. The 40 diagonal concrete strain readings (gauge length = 100 mm) gave a maximum value

for ε_d of 2.09 x 10^{-3}, a minimum value of 0.72 x 10^{-3} and an average value of 1.14 x 10^{-3}.

The maximum torque applied to beam R1 was 78 kNm at which stage the load began to gradually drop. For this beam the diagonal compression field theory predicts an ultimate torsional capacity of 79 kNm.

BEAM R2 - REPEATED NON-ALTERNATING LOADING

The testing of beam R2 started 18 days after casting, at which time the concrete cylinder strength, f'_c, was 37 MPa. This beam was subjected to repeated applications of predetermined levels of torsional moment. Increasing the applied torque from zero to the predetermined level and then unloading back to zero was described as one cycle of loading. The torque-twist response of the beam produced by these load cycles is described in Fig. 4.

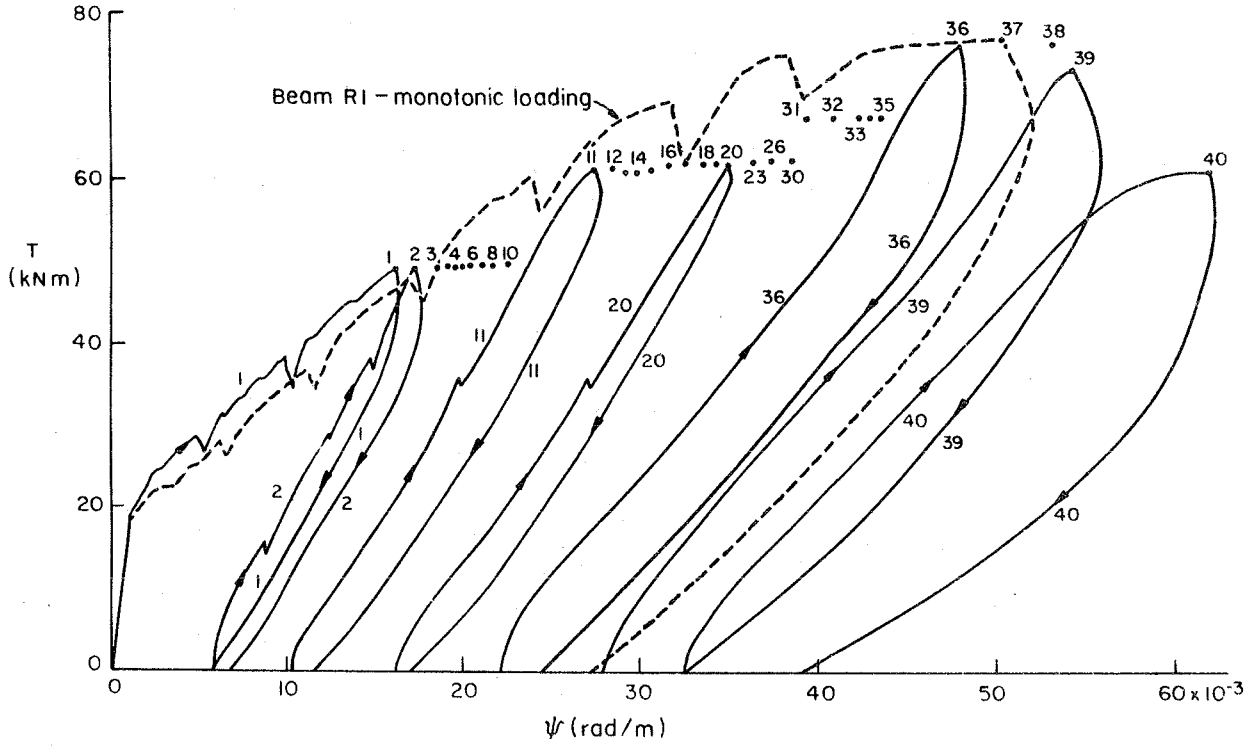

Fig. 4: Torque-Twist Response of Beam R2 - Repeated Non-Alternating Loading

As can be seen in Fig. 4, the predetermined level of torque for the first 10 cycles was 49 kNm. In the loading phase of the first cycle the behaviour of the beam was very similar to that of beam R1 (the torque-twist curve of R1 is also shown in Fig. 4), except that diagonal cracking occurred at a somewhat higher torque (18 kNm). After unloading to zero torque considerable strains and deformations still existed in the member. Thus at the end of cycle 1 the average tensile strain in the hoop steel, ε_h, was 0.19 x 10^{-3}, the average tensile strain in the longitudinal steel, ε_ℓ, was 0.15 x 10^{-3}, while the average diagonal compressive strain in the concrete, ε_d, was 0.22 x 10^{-3}. Due to the fact that the cracks did not completely close the beam was, in effect, at this stage "prestressed" with the steel being in tension and the concrete being in compression. Thus when the torque was again applied in cycle 2 the initial stiffness of this

"prestressed" beam was nearly equal to the elastic, uncracked torsional stiffness. Once the cracks reopened the stiffness dropped rapidly after which the torque-twist response became nearly linear as the torque returned to the previous level. With each cycle of loading the strains and deformations increased but with a smaller increase for each successive cycle. By the end of cycle 10 the average strains at zero torque had increased to 0.32×10^{-3} for ε_h, 0.29×10^{-3} for ε_ℓ and 0.34×10^{-3} for ε_d.

For cycles 11 through 30 the beam was taken to a torque of 61 kNm. At this load level the torque-twist loops became narrower as cycling progressed (compare cycle 20 and cycle 11 in Fig. 4).

Five load cycles (31 to 35) were performed at a torque of 67 kNm and then in cycle 36 the torque was increased to 76 kNm. The capacity of the beam was exhausted in cycle 39 as it was not possible to again reach 76 kNm. The test was completed 32 days after casting at which time the concrete cylinder strength was 38 MPa.

BEAM R3 - REVERSED CYCLIC LOADING

The testing of beam R3 started 57 days after casting at which time the concrete cylinder strength was 37 MPa. Once again increasing the torque from zero to a predetermined level and then unloading back to zero was described as one cycle of loading. For this beam the direction of the torque applied in each cycle was alternated (odd numbered cycles have positive torque, even numbered cycles have negative torque). The observed torque-twist response for the beam is summarized in Fig. 5.

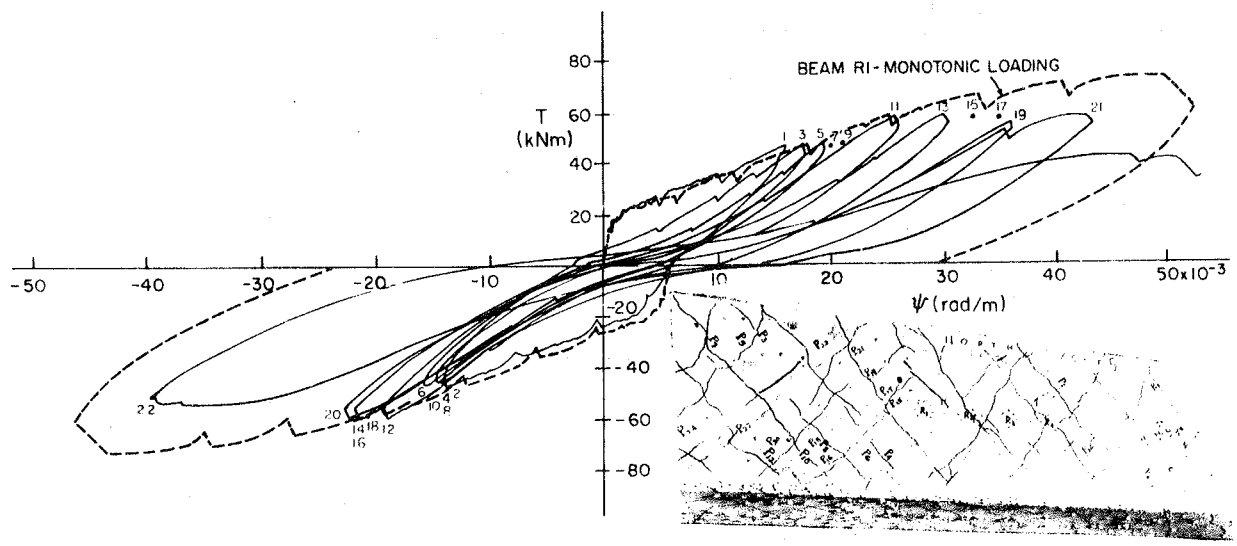

Fig. 5: Torque-Twist Response of Beam R3 - Reversed Cyclic Loading

For beam R3 as for R2, the predetermined level of torque for the first 10 cycles was 49 kNm. As expected during the first cycle the behaviour was essentially identical to that of R2 (cracking occurred at 19 kNm). Under the reversed torsion, in the second cycle, the second set of diagonal cracks (see photograph in Fig. 5) began to form at a torque of -19 kNm. Thus the pre-existing cracks did not reduce the torque required to produce cracks in the other direction. The pre-existing cracks did, however, reduce the "uncracked" torsional stiffness by about 60%. After the third cycle the

torque-twist loops became noticeably "pinched" with large deformations occurring at low torques due to the need in each cycle to first close the cracks formed in the previous cycle. The peak-to-peak torsional stiffness of the loops decreased from 3.3×10^3 kNm^2 for the loop formed by cycles 1 and 2 to 2.8×10^3 kNm^2 for the loop formed by cycles 9 and 10. It is of interest to note that the predicted uncracked stiffness (Fig. 2) is 34.5×10^3 kNm^2 while the predicted cracked stiffness (Fig. 2) is 1.9×10^3 kNm^2.

After cycle 10 the predetermined level of torque was set at 61 kNm. For cycles 11 to 20 this predetermined torsional magnitude was reached. During this cycling the peak-to-peak torsional stiffness of the loops decreased to 2.2×10^3 kNm^2. It was noticed that at this stage in the life of the beam the pattern of steel strains at any particular twist was quite similar to the pattern observed in the monotonically loaded beam at the same twist. Thus at the peak of cycle 15 (twist equals 32×10^{-3} rad/m) the maximum value for ε_h was 3.52×10^{-3}, the minimum value was 1.27×10^{-3} and the average was 1.92×10^{-3}, while the maximum value for ε_ℓ was 1.90×10^{-3}, the minimum was 0.70×10^{-3} and the average was 1.15×10^{-3} (compare these values with those reported above for R1 at load stage 7).

During cycle 21 difficulty was experienced in reaching the predetermined torque level, however a torsion of 63 kNm was finally applied. By this stage the deformations had become concentrated at a few of the cracks leading to a much wider scatter in the recorded steel strains (ε_h: - max. = 4.69×10^{-3}, min. = 1.46×10^{-3}, avg. = 2.34×10^{-3}; ε_ℓ: - max. = 4.60×10^{-3}, min. = 0.55×10^{-3}, avg. = 1.50×10^{-3}). When the torsion was reversed in cycle 22 it was not possible to increase its magnitude beyond -57 kNm. Cycle 23 was the last cycle applied with the maximum torque reached being 45 kNm. The test was completed 124 days after casting at which stage the concrete cylinder strength was 43 MPa.

DISCUSSION OF TEST RESULTS

The torsional capacity of the monotonically loaded beam, R1, was accurately predicted by the compression field theory (see Table 1). However, as this theory ignores the contribution of tensile stresses in the concrete (in particular the "tension stiffening" of the reinforcement by the surrounding concrete) it overestimated the deformations.

Table 1: Behaviour at Ultimate

Beam	f'_c (MPa)	Avg. Crack Spacing (mm)	Ultimate Torque (kNm) Observed	Predicted	Observed / Predicted
R1	34	95	78	79	0.99
R2	38	70	76	81	0.94
R3	43	85	63	82	0.77

The repeated application of unidirectional torques in the case of beam R2 caused more cracks to form (see Table 1) destroyed much of the tension stiffening effect, and hence took the deformations close to or even somewhat beyond (+ 10%) those predicted by the compression field theory. This repeated loading caused only a small reduction (about 5%) in the capacity of the beam.

The repeated opening and closing of the diagonal cracks in the case of beam R3 (reversed cyclic loading) caused a significant reduction in torsional capacity (see Table 1). The beam failed at a torque which was only 77% of the predicted monotonic capacity. It is estimated that the average diagonal concrete stress at failure was about 23 MPa (i.e. 0.53 f'_c).

CONCLUDING REMARKS

The experiments described in this paper demonstrate that the repeated application of unidirectional torques cause a significant increase in twist but only a small reduction in ultimate torsional capacity. Further they show that reversed cyclic torsion will cause a significant increase in twist and a significant reduction in torsional capacity.

The torque-twist curve for a monotonically loaded beam provides an approximate envelope to the torque-twist curves for otherwise identical repeatedly loaded beams both alternating and non-alternating.

The complete torque-twist curve for a beam subjected to reversed cyclic torsion can be predicted by the compression field theory if the appropriate stress-strain characteristics are known. In particular the stress-strain response of concrete diagonally cracked in both directions is required. Experiments currently underway at the University of Toronto are designed to produce information in this area.

ACKNOWLEDGEMENTS

The research reported in this paper was made possible by a grant from the National Research Council of Canada, which is gratefully acknowledged. Thanks are also extended to the Steel Company of Canada for providing the reinforcing steel.

REFERENCES

Mitchell, D., and Collins, M.P., "Diagonal Compression Field Theory - A Rational Model for Structural Concrete in Pure Torsion," American Concrete Institute Journal, Vol. 71, Aug. 1974, pp. 396-408.

Wilby, G.K., "Response of Concrete Structures to Seismic Motions," Ph.D. Thesis, Department of Civil Engineering, University of Canterbury, 1975.

STUDY ON LOW-CYCLE FATIGUE STRENGTH OF POST-TENSIONED UNBONDED PRESTRESSED CONCRETE BEAMS

Hiroshi MUGURUMA
Kyoto University
Kyoto, Japan

SUMMARY: Low-cycle flexural fatigue tests were carried out on 22 unbonded prestressed concrete beams and the fatigue strength as well as the failure mode were compared with those from corresponding 22 bonded beams. Test results showed that the beams were failed in fatigue crushing of concrete in compression zone at midspan section, excepting 4 unbonded and 5 bonded beams failed in fracture of prestressing steel bar at anchorage end or at midspan section. However, no obvious differences in fatigue strength were recognized between unbonded and corresponding bonded beams without regard to the failure mode.

RESUME: Des essais de fatigue à flexion de bas cycle furent effectués sur vingt deux poutres en béton précontraint par non-adhérence. La résistance à la fatigue et le mode de rupture furent comparés entre les vingt deux autres poutres en béton précontraint par adhérence et les premières qui se correspondent. Il fut obvervé que les pourtres ont cédé en leur partie médiane à cause du broyage de fatigue de béton, à l'exception de quatre pourtres par non-adhérence et cinq poutres par adhérence qui ont cédé en leur partie médiane ou aux extrémités d'ancrage, à cause de la fatigue de l'acier précontraint. Cependant, quelque soit le mode de cession, aucune différence remarquable n'apparut pas entre la résistance de fatigue de poutre par adhérence et celle de poutre par non-adhérence qui correspondent aux premières.

1 INTRODUCTION

The use of unbonded tendons for beams and girders is only occasionally because of a doubt for the safety against the fracture of tendon or tendon-anchorage assembly under repeated high-over cyclic loads due to the seismic action[1),2)]. Several cyclic loading test results on unbonded beams were presented by H. W. Chung[3)], Y. Miyamoto, et al[4)], or T. Brϕndum-Nielsen[5)]. However, these tests were mainly carried out under the cyclic loadings having relatively medium maximum load level, for instance, from the design working load to 75 % of the static flexural strength of beam. In this study, to obtain the basic information on the asismic behaviour of unbonded member the low-cycle flexural fatigue tests were carried out on 22 unbonded and corresponding 22 bonded beams prestressed by 1-ϕ17 mm dia. post-tensioning steel bar. Maximum load levels of applied cyclic loadings are from 60 to 90 % of static ultimate strength, where minimum load level is about 5 %. The test results on the unbonded beams were compared with those on bonded beams in terms of fatigue strength, failure mode and stress fluctuation in prestressing bar at anchorage end and at midspan section, etc.

2. TEST SPECIMENS

The dimensions of unbonded and bonded beams used in the tests are 15 x 18 cm in cross section and are 90, 126 or 162 cm in length as shown in Fig.1. The beams were prestressed by 1-ϕ17 mm dia. post-tensioned steel bar in the constant eccentricity of 3 cm. The bar used in the unbonded specimen is coated with bitumastics, while non-coated one in the bonded beams is grouted by cement paste after prestress transfer. As the end anchorage system, rolled thread-nut anchorage with steel bearing plate was used, which is commonly used in Japan as the end anchorage of post-tensioning steel bar. In addition, the shear reinforcements necessary to prevent the shear failure under cyclic loadings were provided in the shear span of beams.

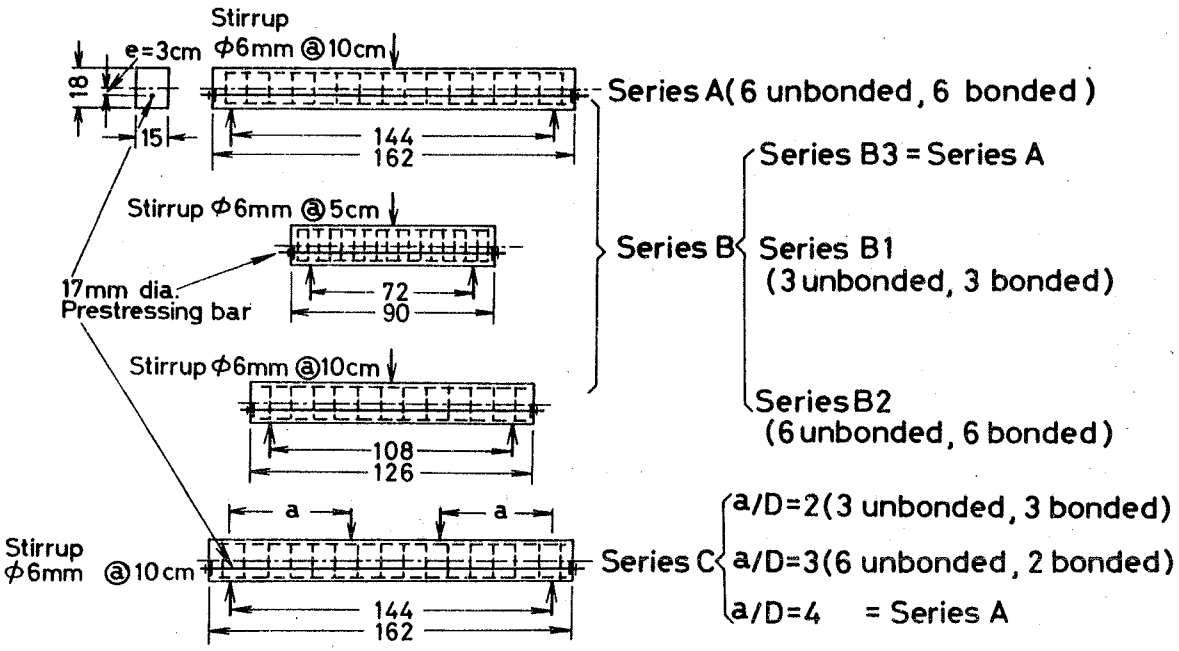

Fig.1 Test specimens

High-early strength portland cement, river sand and crushed stone gravel were used for concrete. The mix porportion of concrete was 1 : 1.62 : 2.60 by weight with the water-cement ratio of 37 %. In Table 1, the properties of concrete at 28 days as well as at the age of cyclic high-over loading tests are listed.

Table 1. Properties of concrete and neat cement grout

Materials and test series		At 28 days			At the age of beam test			
		Compressive strength in kg/cm^2	Tensile strength in kg/cm^2	Elastic modulus in kg/cm^2	Test ages in months	Compressive strength in kg/cm^2	Tensile strength in kg/cm^2	Elastic modulus in kg/cm^2
Concrete	A	593	42.8	384,000	3 - 6	574 - 611	35.1 - 43.9	327,000 - 357,000
	B	547	43.2	329,000	3 - 11	532 - 594	39.5 - 43.0	315,000 - 323,000
	C	495	31.1	355,000	4 - 7	512 - 536	36.7 - 38.6	311,000 - 326,000
Neat cement grout		Compressive strength in kg/cm^2			At 7 days			213 - 245
					At 28 days (at the age of beam tests)			254 - 280

In Table 2, mechanical properties of ϕ 17 mm dia. prestressing bar used in the tests are summarized with those of anchorage assembly. It can be seen from Table 2 that the end anchorage assembly shows the yield strength as similar as that of original part of bar, while the tensile strength becomes smaller than that of original part.

Table 2. Properties of 17mm dia. prestressing bar

	Yield strength in kg/mm^2	Tensile strength in kg/mm^2	Elongation in %
Ordinary part	134	142	11
Threaded part	133	135	Not measured
Specified value	>110	>125	>5

Test specimens were cast in the wooden mould in diving three series as shown in Fig. 1. After casting, they were wet-cured until 28 days. At 28 days before tests, the bonded beams were prestressed in the nominal prestressing force of 22.5 tons and were immediately grouted by neat cement paste having the water-cement ratio of 45%, where the expansive admixture was added for preventing the shrinkage. The compressive strengths of neat cement grout at the age of beam tests are also listed in Table 1. After decreasing the transferred prestress due to the creep and shrinkage of concrete and relaxation of prestressing bar, the effective prestressing force in bonded beams becomes 19.25 tons (84.6 kg/mm^2) in average at the test age, which corresponds to the stress of 63 % of the actual yield strength or that of 60 % of the actual tensile strength of bar listed in Table 2. Referring to such value in bonded beams, the nominal prestressing force of 20 tons was transferred into the each unbonded beam just before loading test. The prestressing force actually transferred into the unbonded beams was 20.26 tons (89.03 kg/mm^2) in average, which is 66 % of yield strength or 63 % of the tensile strength of bar.

3. TEST PROCEDURE

Low-cycle fatigue loading tests were carried out at the different ages from 3 to 11 months in dividing into three series. In Series A and C, the beams of 162 cm in length were used. In Series A, the concentrated load was applied at the center of beam as shown in Fig. 1, while two-point loads were applied in Series C for obtaining the effects of the shear span length upon the low-cycle fatigue behaviour of beams. In Series B, three different lengths of beams, that is, 90, 126 and 162 cm, respectively, were tested by concentrated load.

The first unbonded and corresponding bonded beam in each series were loaded monotonically to obtain the static ultimate flexural moment as well as the initial cracking moment. Remaining beams were tested under cyclic loads with the maximum load levels from 60 to 90 % of static ultimate flexural strength, where the static initial cracking strength obtained from monotonic loading tests was 55 % of ultimate strength. The minimum load level was kept in 5 % of static flexural strength in each beam during cyclic loadings. The loading speed was controlled as 200 cycles per minite in average. The fluctuation of tensile force in prestressing steel bar due to cyclic loadings was measured at the midspan section as well as at the anchorage ends.

4. TEST RESULTS AND DISCUSSIONS

(a) Fatigue Strength and Failure Mode

Fatigue strenths obtained from the cyclic loading tests on unbonded beams in each series are shown in Fig. 2 in comparison with those obtained from corresponding bonded beams, where the number of loading cycles after failure are plotted against the maximum load levels of cyclic loadings. The load cycles sustained until the fracture were varried from 500 to more than 2,000,000 cycles as shown in Fig. 2, where less fatigue load cycles correspond to larger maximum load level of cyclic loadings.

The fatigue failure was caused mainly by crushing of concrete in compression zone near midspan section without regard to unbonded or bonded. Only 4 unbonded beams were failed by the fracture of prestressing bar at anchorage end, while 5 bonded beams by the fracture of bar near midspan section or at anchorage end. Such failure mode mainly appeared in the beam having the loading condition of relatively smaller shear span length, say, in the case of shear span-depth ratio less than 3 in this study. Also, it is apparent from Fig. 2 that it was concentrated in the case of maximum load level from 65 to 75 % of the static beam strength in Series B and about 80 % in Series C.

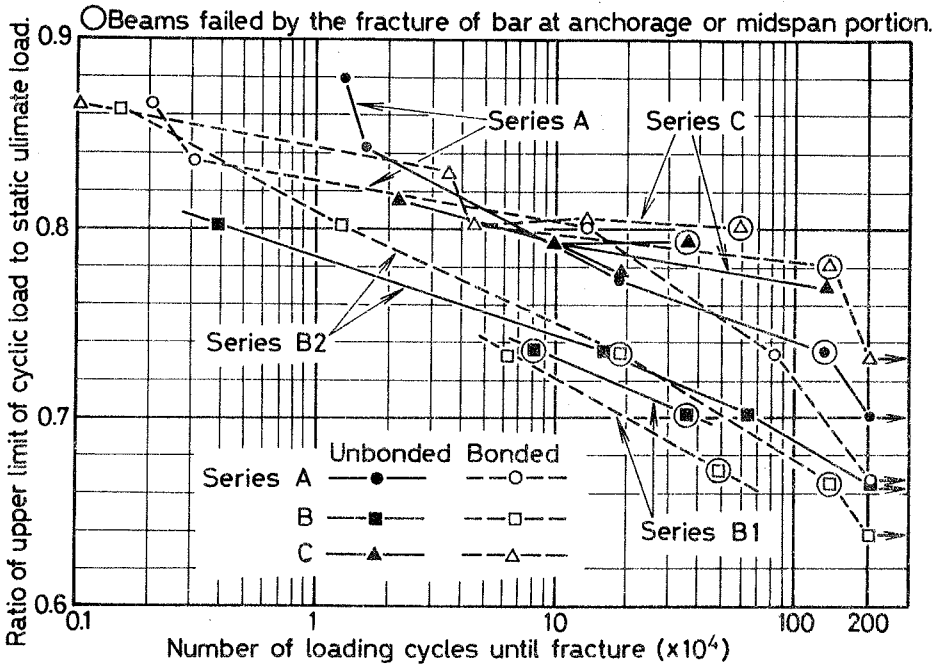

Fig. 2 Comparison of fatigue strength between bonded and unbonded beams.

As the fatigue strengths concern, the comparison of the test results illustrated in Fig. 2 shows that no obvious differences can be recognized between unbonded and corresponding bonded beams. Also, it may be interesting that the fatigue strength seems to be not governed by the fracture of bar at anchorage end or near midspan section. Thus, so far as the test results in this study it can be concluded that the unbonded beams have the structural safety against the cyclic high-over loadings as similar as bonded ones.

(b) Effects of the Shear Span Length upon the Fatigue Strength

Fatigue flexural strength of beam is much influenced by the shear span length. This can be seen from the comparison between the test results on Series A and Series B in Fig. 2, where the shear span-depth ratio is 4 in the former, and 2 and 3 in the latter. The smaller shear span-depth ratio results in the smaller endurance load cycles in this study. As a reference, the test results on unbonded and corresponding bonded beams with different shear span-depth ratio subjected to the cyclic loading with maximum load level of 74 % of static beam strength are listed in Table 3.

Table 3. Effects of the shear span length upon the fatigue strength*

Test series	Beam No.	Bonded or Unbonded	Length of beam in cm	Span length in cm	Shear span-depth ratio	Ratio of maximum load level to static beam strength in %	Loading cycles after failure	Mode of failure
A	A -3	Unbonded	164	144	4	73.2	1,300,000	Fracture of bar at anchorage end
	A' -3	Bonded				73.5	810,000	Crushing of concrete
B	B2 -3	Unbonded	126	106	3	70.2	640,000	Crushing of concrete
	B'2-3	Bonded				73.4	185,000	Fracture of bar near midspan section
C	B1 -3	Unbonded	92	72	2	73.7	80,600	Fracture of bar anchorage end
	B'1-3	Bonded				73.4	62,000	Crushing of concrete

* The concentric cyclic load was applied at midspan of each beam.

In Table 4, the test results under maximum load level of 80 % of static beam strength obtained from 3 unbonded and corresponding 3 bonded beams having various flexural span lengths in Series C are listed. It seems from Table 4 that in a case where the failure of beam takes place due to the crushing of concrete at midspan section the fatigue strength becomes smaller with increase of flexural span length (that is, with decrease of shear span length) for both unbonded and bonded beams. But Beam No. C1-1 and C'1-1 having largest flexural span length (that is, having smallest shear span length) in this study and failed in the fracture of prestressing bar at anchorage end showed excessively larger fatigue strength than Beam No. C1-2 and C'1-2. Although the reason of such test results can not be explained from the experiments, it may be noted from Table 4 that the increase of flexural span length with decrease of shear span length results in the fatigue fracture of bar at anchorage end in unbonded beam and also even in bonded beam because of the rapid bond deteriorations of prestressing bar in the shear span.

Table 4. Effects of the shear span and the flexural span lengths upon the fatigue strength

Beam No.	Bonded or Unbonded	Length of beam in cm	Span length in cm	Shear span length in cm*	Ratio of maximum load level to static beam strength in %	Loading cycles after failure	Mode of failure
C1 -1	Unbonded	164	144	36 (2)	79.4	341,000	Fracture of bar at anchorage end
C1 -2				54 (3)	79.4	97,000	Crushing of concrete
C1 -3				72 (4)	77.3	108,000	Crushing of concrete
C'1-1	Bonded	164	144	36 (2)	80.2	577,000	Fracture of bar at anchorage end
C'1-2				54 (3)	80.2	43.000	Crushing of concrete
C'1-3				72 (4)	80.2	103,000	Crushing of concrete

* The shear span-depth ratio is listed in double brackets.

(c) Fluctuation of Tensile Stress in Prestressing Bar

During the cyclic loadings, the fluctuation of tensile stress in prestressing bar was measured at anchorage end and at midspan section in each unbonded and bonded beams. Some of measured results are shown in Fig. 3 and 4, in which the values in double brackets are the ratio of maximum load level of cyclic loading to the static flexural strength of beam. In the unbonded

beams the fluctuation of tensile stress in bar at anchorage end is quite close to that at midspan section as can be seen in Fig. 3. This shows that there were no significant frictions along the unbonded prestressing bar during cyclic loadings in this study. On the contrary, the stress fluctuation of bar in bonded beams was so small at anchorage end as negligible at first load cycle. However, as shown in Fig. 4 it increased rapidly at anchorage end with considerable decrease at midspan section after the loadings less than 1000 cycles and then the steady states followed it until just before the fatigue failure of beam. This means the rapid deterioration in bond between the surface of prestressing bar and neat cement grout in a very early stage of cyclic loadings. Here, as a reference the bond deterioration defined as the difference between the tensile stress fluctuation in prestressing bar at anchorage end and at midspan section was calculated from the measurements in Fig. 4. The results obtained are shown in Fig. 5. In Fig. 5 the residual differences in stress fluctuation between anchorage end and midspan section are from 1 to 2 tons within the steady states, which correspond to the tensile stress in prestressing bar from 4.4 to 9.8 kg/mm^2. These residual differences becomes 0 to 1 ton in the bonded beams of Series B and become almost 0 in those of Series C, where the smaller value was observed in the smaller shear span length of beams. Thus, from these results it can be stated that the fatigue behaviour of bonded beams becomes quite similar as unbonded ones due to the rapid bond deterioration and also due to the resulting smaller residual differences in stress fluctuation in bar between at anchorage end and at midspan section.

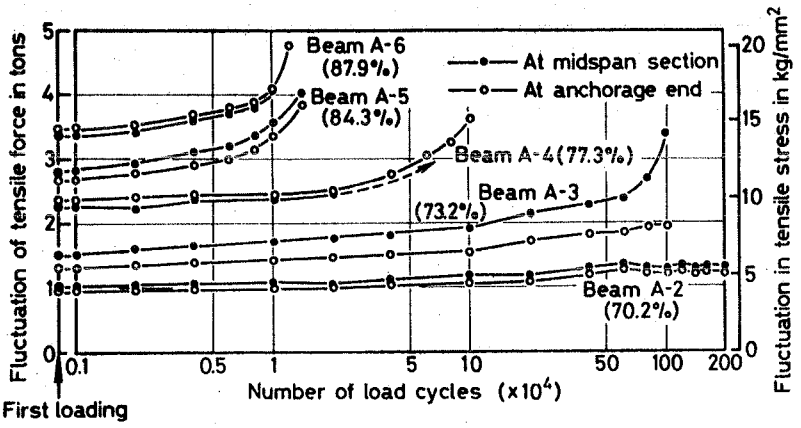

Fig.3 Fluctuation of tensile force in prestressing bar under cyclic loading.(Series A, Unbonded)

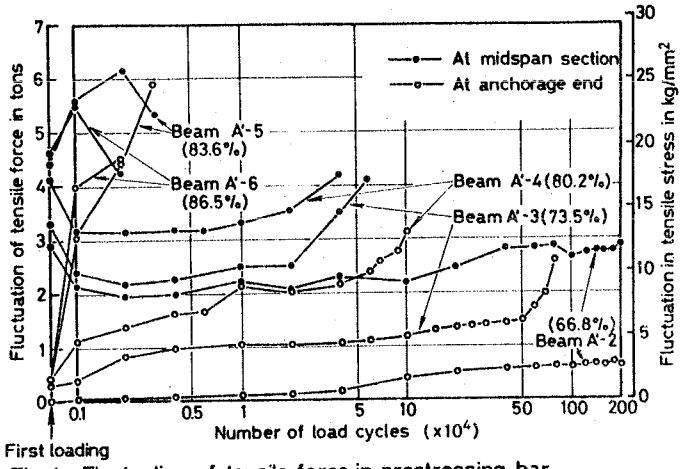

Fig.4 Fluctuation of tensile force in prestressing bar under cyclic loading.(Series A, Bonded)

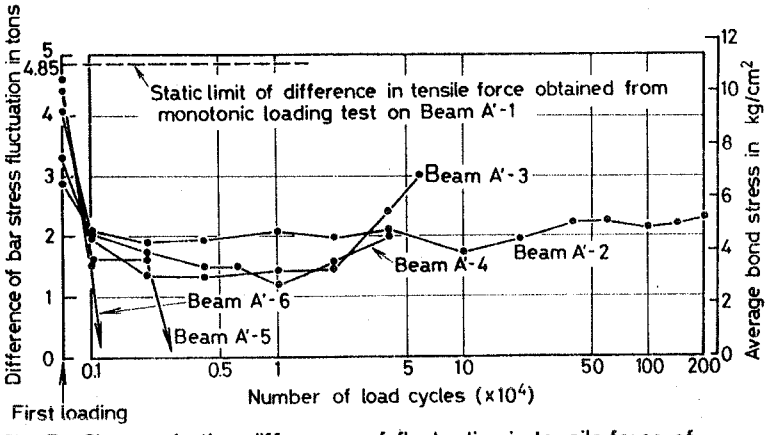

Fig.5 Change in the difference of fluctuation in tensile force of prestressing bar under cyclic loading between at the midspan and at the anchorage end.(Series A, Bonded)

(d) Fatigue Strength of Prestressing Bar

For predicting the fatigue strength of prestressing bar from the results on the beams failed in the fracture of bar at anchorage end or near midspan, the average value of stress fluctuations during cyclic loadings were obtained from the measurements at anchorage end or at midspan section in correspondence to the portion of fracture in bar. The results are summarized in Table 5.

Table 5. Average fluctuation of tensile stress in bar obtained from the beams failed by the fructure of bar.

Beam No.	Bonded or Unbonded	Effective Prestressing force in tons	Corresponding stress in kg/mm^2	Ratio of maximum load level to static beam strength in %	Average fluctuation of tensile stress in bar in kg/mm^2	Number of load cycles after failure
A - 3*	Unbonded	20.23	88.9	73.2	7.25	1,300,000
B1 - 2*	Unbonded	20.14	88.5	70.2	10.74	355,000
B1 - 3*	Unbonded	20.29	89.1	73.7	14.65	80,600
B'1 - 2	Bonded	18.75	82.4	66.8	12.30	488,000
B'2 - 3	Bonded	19.61	86.2	66.8	12.50	1,370,000
B'2 - 4	Bonded	19.40	85.2	73.4	14.72	185,000
C1 - 1*	Unbonded	20.39	89.6	79.4	12.85	341,000
C'1 - 1*	Bonded	20.02	88.0	80.2	12.85	577,000
C'2 - 3	Bonded	18.79	82.6	78.3	14.09	1,380,000

(Symbol * shows the beam failed in the fracture of bar at anchorage end. Remaining beams were failed in the fracture of bar near midspan section)

In Fig. 6, the average stress fluctuations in bar listed in Table 5 are plotted against the endurance number of loading cycles after beam failure. The tensile fatigue test results of prestressing bar itself and anchorage assembly itself are also plotted in Fig. 6, where the minimum tensile stress level of 88 kg/mm^2 is adopted in correspondence to the nominal effective prestressing force of 20 tons adopted in 17 mm dia. prestressing bar in this study. The comparison showed that the fatigue strength of bar at ordinary part or at anchorage end obtained from beam tests becomes smaller than that obtained from tensile fatigue tests on bar itself or anchorage assembly itself. This fact is also pointed out by T. Brøndum-Nielsen in the cyclic loading tests on the unbonded beams prestressed by 12 - ϕ7 mm dia. B. B. R. button head cable[5]. And further, it appears from Fig. 6 that in the beam tests the fatigue strength of bar at anchorage end becomes quite close to that at midspan section with increase of the maximum load level of cyclic loadings. On the contrary, in the tensile fatigue tests on bar itself the anchorage assembly sustained without fracture the same loading cycles in the two-third of stress amplitude in original part of bar. However, considering the test results that no evident

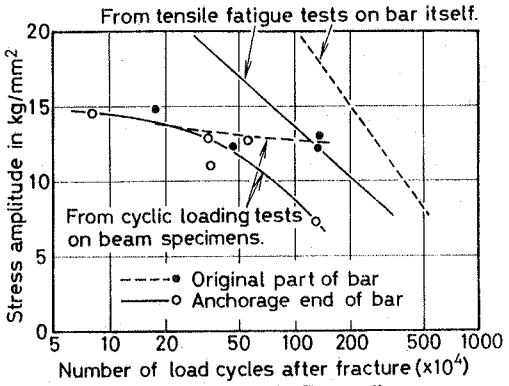

Fig.6 Fatigue strength of 17mm dia. prestressing bar predicted from the cyclic loading tests on bonded and unbonded beams.
(Lower limit of bar stress=88kg/mm^2)

differences can be recognized in the fatigue failure strength of beam itself between unbonded and corresponding bonded beams, such a decrease in fatigue strength at anchorage end in tensile fatigue tests seems to have no significant influence upon the fatigue flexural strength of beam.

5. CONCLUSIONS

High-over cyclic loading tests with various maximum load levels from 60 to 90 % of static flexural strength of beam were carried out on 22 unbonded and corresponding 22 bonded beams prestressed by 1 - ϕ17 mm dia. prestressing bar. Test results showed that the beams were failed mainly in fatigue flexure by crushing of concrete in compression zone near midspan section, while 4 unbonded and 5 bonded beams were failed in the fracture of bar at anchorage end or near midspan section. However, no obvious differences in fatigue flexural strength can be recognized between unbonded and corresponding bonded beams without regard to failure mode. Also, shear span length has much influence upon the fatigue strength of beam. Smaller shear span length results in smaller fatigue strength in this study. Measured results on stress fluctuation in prestressing bar at anchorage end and at midspan section showed no significant friction along the unbonded bar under cyclic loadings. In bonded beams, rapid bond deteriorations were observed in early stage of load cycles and consequently the bonded beams seems to become quite close to corresponding unbonded beams. Concerning to the fatigue strength of bar itself or anchorage end itself, the results obtained from beam tests were smaller than those obtained by tensile fatigue tests. However, the fatigue strength at anchorage end becomes quite similar as that of bar at midspan section in the beam tests, while the tensile fatigue test results on anchorage end itself showed the two-third of fatigue strength in original part of bar itself. Therefore, such decrease in fatigue strength at anchorage end obtained from tensile fatigue tests seems to have no obvious effects upon the fatigue flexural strength of beams,

REFERENCES

1) T. Y. Lin, Unbonded vs. Bonded Tendons for Building Construction, with Particular Reference to Flat Slab, Proc. of the FIP Symposium on Prestressed Concrete in Building, Sydney, Sept. 1976.
2) R. Part, Post-tensioned tendons in prestressed concrete- to grout or not to grout-, New Zealand Engineering, pp. 315-319, 15 Nov. 1975.
3) H. W. Chung, Unbonded Tendons in Post-Tensioned Concrete Beams under Repeated Loading, ACI Journal, Vol. 70, No. 12, pp. 814-816, Dec. 1973.
4) Y. Miyamoto, et al., Bending fatigue strength of unbonded prestressed concrete beams, Railway Technical Research Report, No. 844, Japan National Railway, 1974 (in Japanese).
5) T. Brøndum-Nielsen, Effect of Grouting on the Fatigue Strength of Post-Tensioned Concrete Beams, Final Report of the IABSE Symposium on Resistance and Ultimate Deformability of Structures Acted on by Well Defined Repeated Loads, pp. 77-82, Lisbon, 1973.

ONCE REPEATED LOADING OF PRESTRESSED CONCRETE BEAMS

Vladimir URBAN
Building Research Institute
Technical University
Prague, Czechoslovakia

SUMMARY The effect of overloading on the subsequent load carrying capacity of prestressed concrete beams was experimentally investigated for 120 specimens of four types of cross-section and reinforcement. Statistically processed data indicate changes of strength and deformations especially in the service action area. A numerical method for the nonlinear analysis of reinforced and prestressed section under bending and axial repeated load was derived. Realistic representations of stress-strain characteristics of concrete and steel were utilized in computer program to analyse the effect of initial stress distribution and prestressing reinforcement arrangement.

RESUME L'influence de surchargement sur la résistance pastérieure de pontres en béton armé a été étudié experimentalement sur 120 éprouvettes de 4 types d'armature et de sections différentes. Des dates processées statistiquement indiguent changements, de la résistance et des déformations specialment das la region de l'action. Une méthode numerique etait derivée pour l'analyse nonlineaixe d'une section armée et precontrainte des changes en flexion, et des charges axiales répétées. Des diagrammes formés realistiquement corcernant le béton et l'acier ont été utilisés pour un programme calculatrice pour analyser l'effet de la distribution de la contrainte initiale et de l'arrangement des barres précontraintes.

1. AIM OF RESEARCH

The aim was to establish the effect of one repeated load near to the ultimate load on the strength and deformations of prestressed concrete beams.

2. EXPERIMENTS

The purpose was to receive a basic information for the following theoretical analysis.

Test specimens. Each of four test series (ST1, ST2, ST3, ST4) contained 30 nominally identical beams (length 1700 mm, thickness 80 mm). The concrete of all 120 specimens had the same cube strength (40 MPa). Strands 3ØP3 mm (1700/1400 MPa) were used for pretensioned reinforcement. All specimens failed due to the concrete crushing in the compression zone. The series differed by the total depth, by the ammount and arrangement of reinforcement (Fig.1). The effective depth was the same in all series, also the prestressing force in each layer of three strands (3x25 kN). The initial stress distribution

(Fig.2) from prestressing was then different.

Load tests were performed after 3,5 years. Simply supported beams were subjected to the couple of concentrated loads applied at the midspan (Fig.3). The hydraulic loading Amsler 200 kN machine was used. The following quantities were observed automatically: time, load, deflection at the midspan, slopes at support sections, tensile, compressive and transverse strains at the midspan; visually: load and deflection, when 1.st and 2.nd crack appearance, when concrete compressive crushing initiation, when maximum. Also initiation, propagation, width of cracks etc.

Load history. Ten beams (group 1) of each series were subjected to monotonously increased load up to failure and the mean strength $\bar{F}_{u1}$ was calculated (Fig.4). The rest of the specimens was tested in two equal groups of 10 specimens each (group II or group III respectively). These beams were loaded primarily to the load $F_0=H\cdot\bar{F}_{u1}$, where H=0,86 (H=0,92) for group II (group III), then unloaded and immediately reloaded up to failure load F_{u2}^{II} (F_{u2}^{III}). The loading was controlled by constant deflection increment 1,5 mm (6 mm)/60 sec in the 1st. (2nd.) cycle.

Test results. Statistically processed experimental data indicate that the load-carrying capacity has not always been decreased by the previous overloading. The average increase of 3-5% was observed in three series, (ST1, ST3, ST4) and only one series (ST2) showed ultimate strength decrease (Tab. 1, Fig.1, Fig.2). The dispersion of strength was not effected in a systematic way.

While the ultimate total deflections corresponding to the ultimate loads were decreased in ST1, ST3 series in the 2nd. load cycle, there was an increase at ST2, ST4 observed (Tab. 2).

Repeated loading significantly decreased the bending stiffness more in ST1, ST3 then in ST2, ST4 series (Fig.5) and increased the variability of deformations especially in service action region (Fig.6). The initial prestress probably influenced also the elastic deformations and plastic strain after unloading.

3. NUMERICAL MODEL

A numerical method for the nonlinear analysis of reinforced and prestressed concrete section subjected to low cycle pure flexure or combined bending and axial load was used to analyse the phenomena observed in the experimental part of the research.

Method. A standard approach as already proved by AAS-JAKOBSEN (1970) was used to calculate stresses and strains in prestressed concrete section under repeated load. Linear strain distribution of section is assumed, corresponding stresses satisfy the equilibrium equations. Hypothesis of the unique stress-strain diagram (SINHA, GERSTLE, TULIN (1964), KARSAN, JIRSA (1969)) is taken into account. Practically arbitrary shape of loading, unloading and reloading branches of stress-strain diagrams of concrete and reinforcement (uniaxial compression and tension) can be input to the computer program. Also the reduced bond, using a reduced steel strain (BAKER (1956)). The external bending moment and normal force are described by sequential pairs of M, N values according to the development of the actual load history. The carrying capacity is exhausted when ultimate strain E_{uc} in compression of concrete or ultimate strain E_{us} in tension of steel are reached. For each pair of M, N the unknown upper and lower etreme fibre deformations are simultaneously determined by a special iteration method. A generator of random properties of material should be directly inserted in the program.

Load test simulations. Behaviour of concrete was characterized by the stress-strain diagram taken from the monotonic compression tests of prisms 150/150/450 mm as an envelope curve, all other branches were expressed by the paralel straight lines corresponding to the initial stiffness (Fig.7).

Behaviour of reinforcement was described in the same way. Sequence of pairs M, N expressed the load history as in Fig. 4.

Computed output. The computed moment-curvature diagrams qualitatively coincide the test results (Fig. 5, Fig. 9) in the work load region. Because of unique stress-strain diagram of materials assumption, the loading and reloading branches reach the same value at the lop. Program gives a material to study the changes of stress and strain distributions during repeated loading (Fig. 10).

4. CONCLUSIONS

4.1 The load carrying capacity of prestressed beams has not to be always decreased by previous overloading.

4.2 Repeated loading near to the ultimate load decreases the bending stiffness and increases variability of deformations, more in service action area than in the ultimate load region.

4.3 The nature and intensity of the mentioned effects are apparently dependent on the initial prestress distribution and on prestressing reinforcement arrangement.

4.4 Numerical model with realistic representations of the stress-strain characteristics of concrete and steel, established on the standard pressumptions and on the unique stress-strain diagram hypothesis is prepared to express the effect of the arbitrary load history.

4.5 The outputs of computer program coincide qualitatively with experimental results even linear approximation of unloading and reloading was taken into account. It is necessary to expect the considerable stress and strain redistribution after overloading in the work action range.

5. REFERENCES

AAS-JAKOBSEN, K.: Fatigue of Concrete Beams and Columns, Bull. No. 70-1, The University of Trondheim, Norway, Sept. 1970.

BAKER, A. L.: The Ultimate Load Theory Applied to the Design of Reinforced and Prestressed Concrete Frames, Concrete Publications Limited, London, 1956.

KARSAN, I. D., JIRSA, J. O.: Behaviour of Concrete under Compressive Loadings, Journal of the Struct. Div. ASCE, Dec. 1969.

SINHA, B. P., GERSTLE, K. H., THULIN, L. G.: Stress-strain Relations for Concrete Under Cyclic Loading, Journal ACI, Febr. 1964.

Tab. 1 Failure loads. Statistical characteristic.

Group	1	2	3	1	2	3
Series		ST 1			ST 2	
Number of elements	10	10	10	10	9	8
Mean value (kN)	25,31	28,24	25,39	24,65	23,19	24,31
Standard deviation (kN)	1,50	1,42	1,75	1,96	1,53	1,94
Coef. of variability (%)	6	5	7	8	7	8
Change of mean value (%)	100	111,6	100,3	100	94,1	98,6

Group	1	2	3	1	2	3
Series						
Number of elements	10	10	9	10	10	10
Mean value (kN)	43,03	45,00	41,44	35,47	37,02	37,40
Standard deviation (kN)	2,30	2,60	2,00	3,21	2,60	2,3
Coef. of variability (%)	5	6	5	9	7	5
Change of mean value (%)	100	104,6	102,6	100	104,4	105,4

Tab. 2 Limit deflections. Statistical characteristics

Group	1	2	3	1	2	3
Series		ST 1			ST 2	
Number of elements	10	8	6	10	9	8
Mean value (mm)	17,13	16,36	16,56	13,90	14,70	13,02
Standard deviation (mm)	3,199	3,028	3,539	2,277	5,225	4,774
Coef. of variability (%) (estimation)	19,7	20,1	23,4	22,6	42,8	39,2
Change of mean value (%)	100,0	95,5	96,7	100,0	105,8	93,7

Group	1	2	3	1	2	3
Series		ST 3			ST 4	
Number of elements	10	10	10	10	10	10
Mean value (mm)	14,10	13,44	12,05	9,01	10,08	9,89
Standard deviation (mm)	3,248	3,084	2,651	2,317	2,894	2,310
Coef. of variability (%) (estimation)	24,3	24,2	23,3	27,1	30,0	24,6
Change of mean value (%)	100,0	95,4	85,4	100,0	111,9	109,8

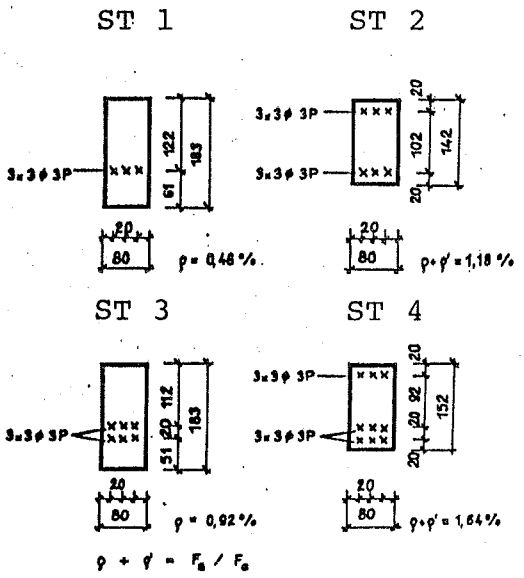

Fig.1. Cross-section of beams in series ST1 - ST4.

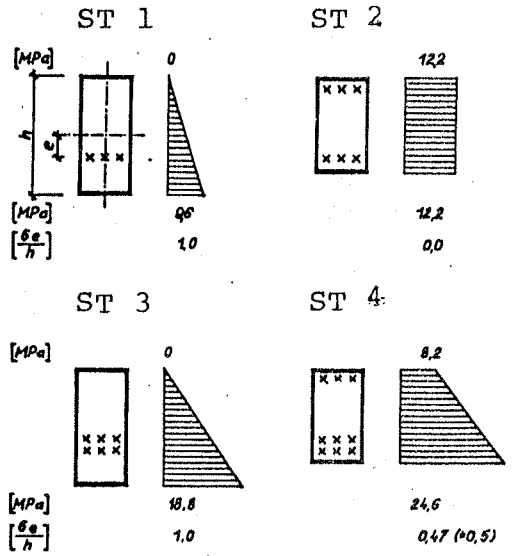

Fig.2. Stress distributions due to prestress.

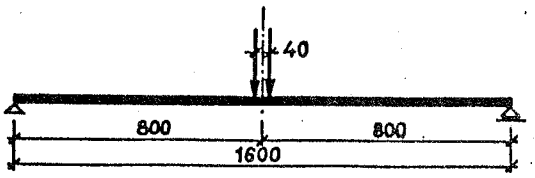

Fig.3. Test scheme.

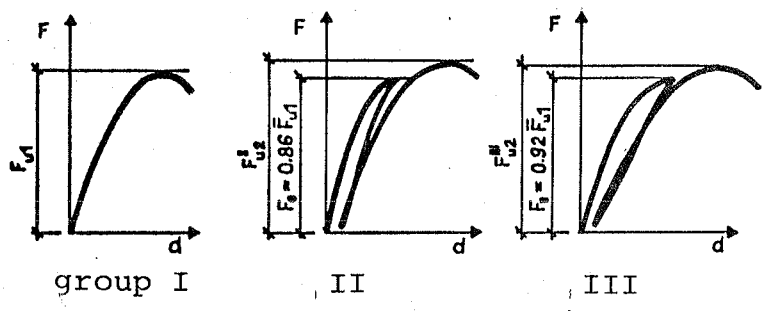

Fig.4. Loading history.

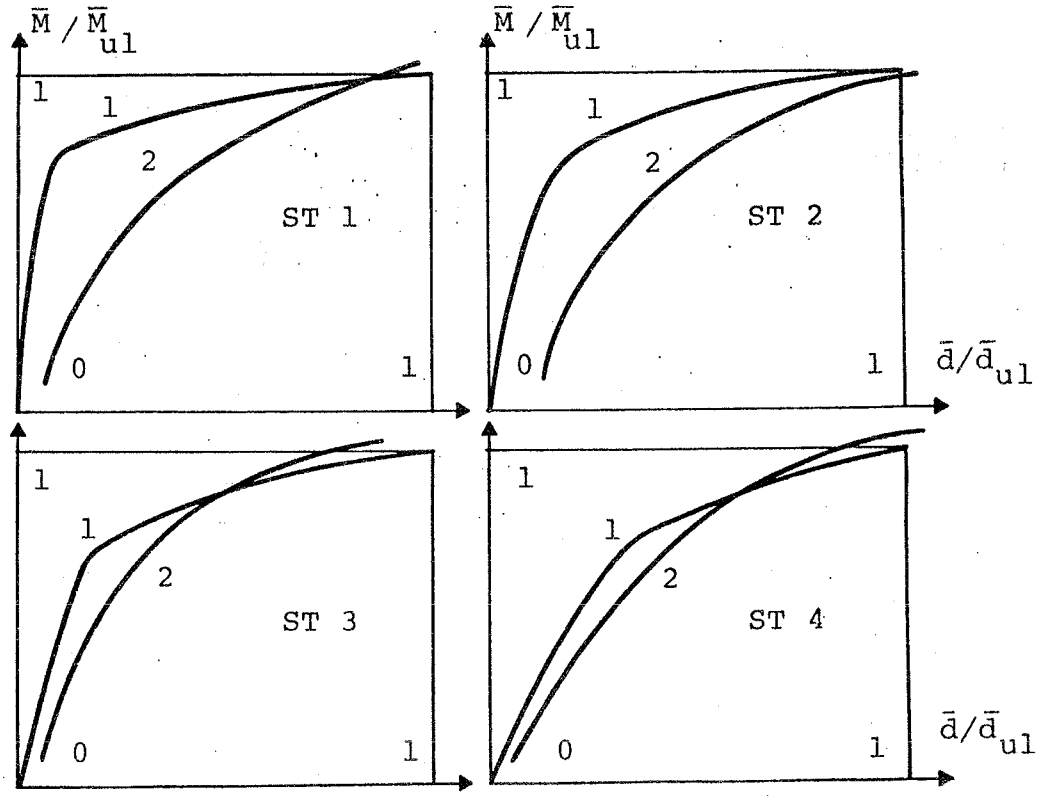

Fig.5. Bending moment - deflection at midspan diagrams during the 1st. and 2nd. load cycles. Groups III of ST1 - ST 4 series
$\bar{M}$..... mean value of bending moment in group III
$\bar{M}_{ul}$... mean value of the ultimate M in group I
$\bar{d}$..... mean value of deflection in group III
$\bar{d}_{ul}$... mean value of the ultimate d in group I

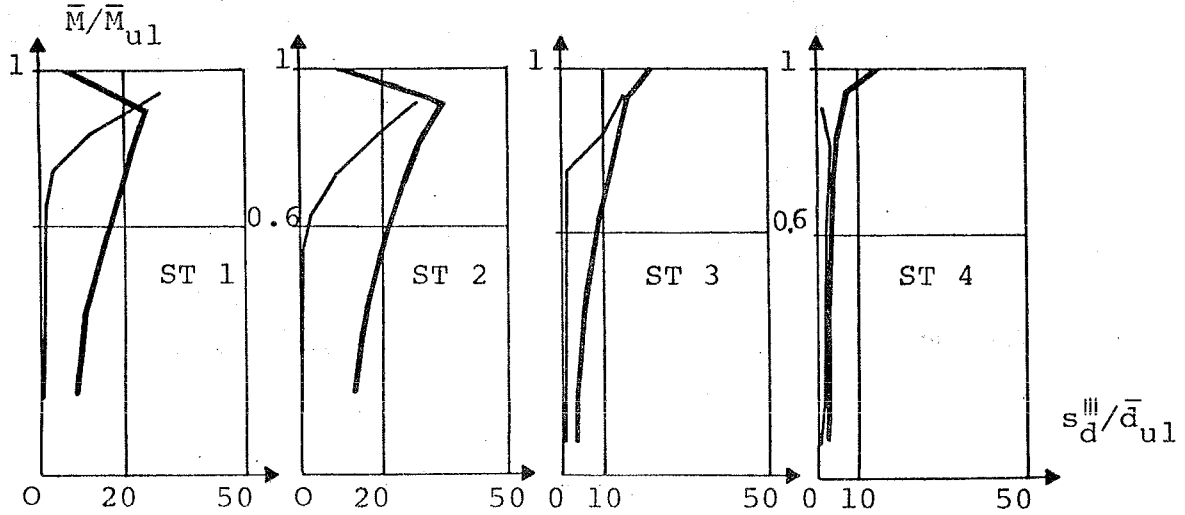

Fig.6. Changes of standard deviation of deflection during the 1st. and 2nd. load cycles. Group III of ST 1 - ST 4 series.
$\bar{M}$..... mean value of bending moment in group III
$\bar{M}_{ul}$... mean value of the ultimate M in group I
S_d^{III}. standard deviation of deflection in group III
$\bar{d}_{ul}$... mean value of the ultimate deflection in group I

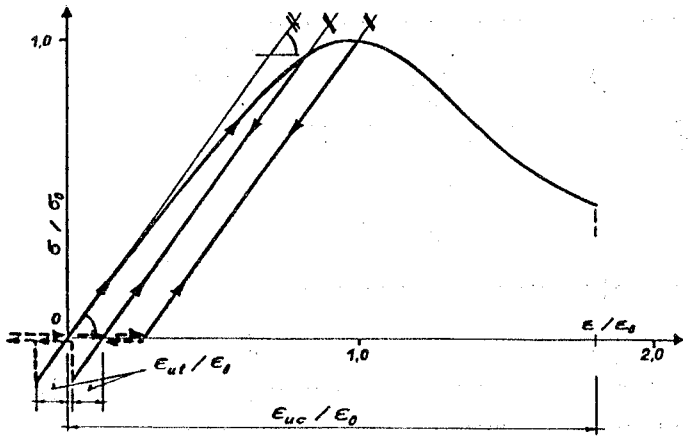

Fig.7. Stress-strain diagram of concrete used as the input approximation.

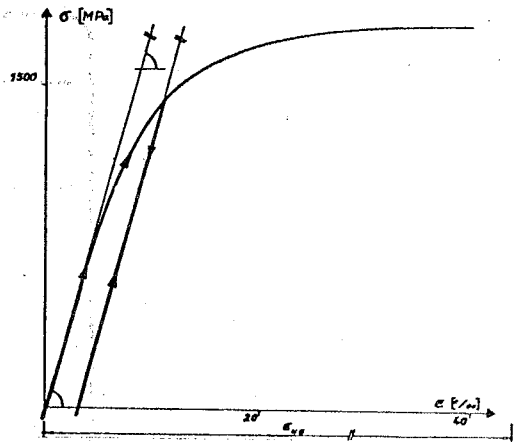

Fig.8. Stress-strain diagram of reinforcement.

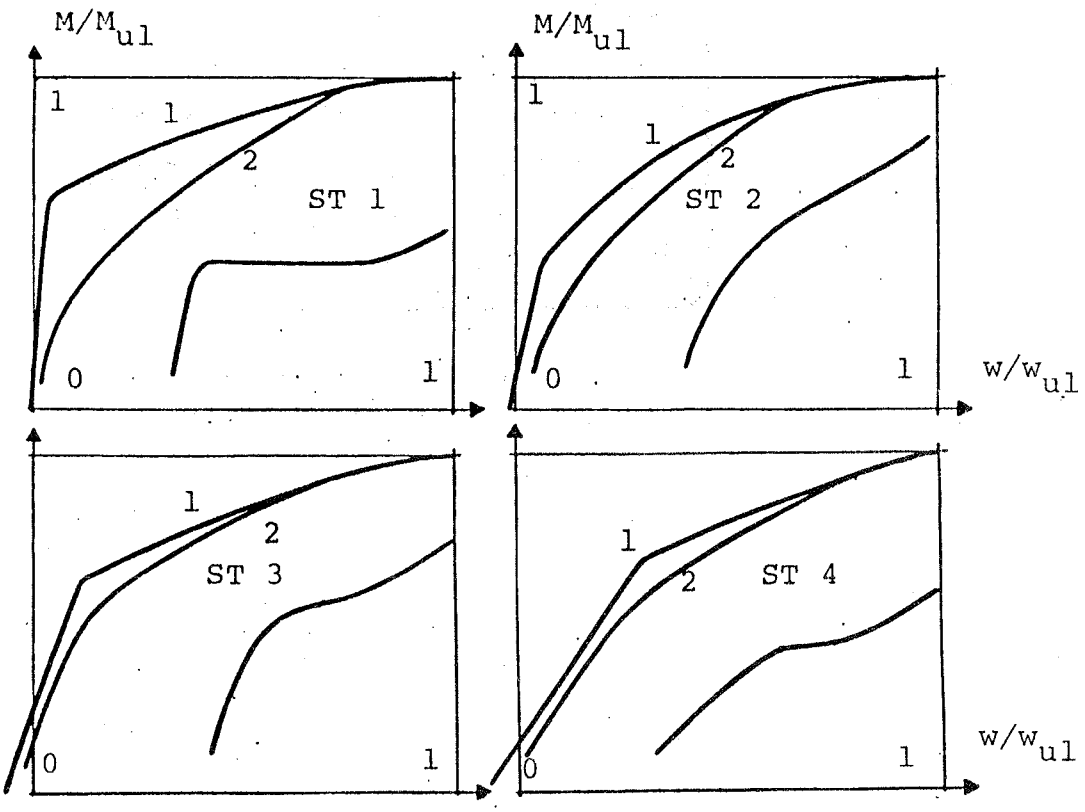

Fig.9. Computed bending moment curvature diagram during the 1st. and 2nd. load cycles. Group III of ST 1 - ST 4 series. Detail when crack initiation.

M..... bending moment in group III
M_{ul}... ultimate in group I
W..... curvature
W_{ul}... ultimate W

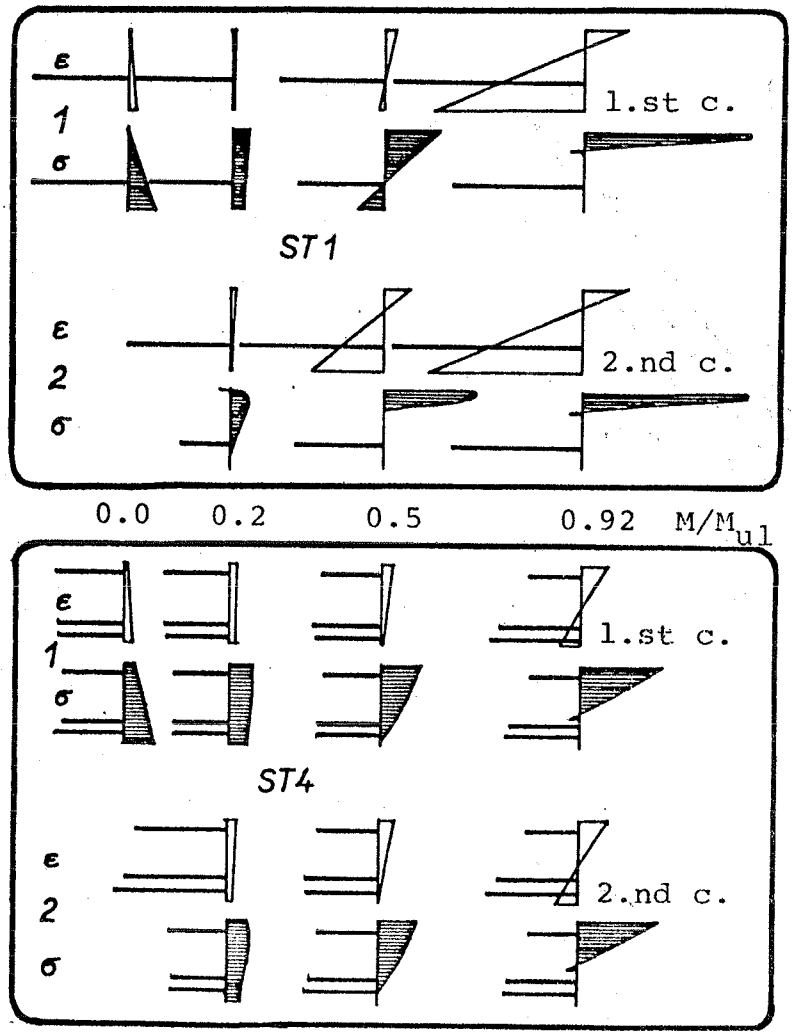

Fig.10. Stress and strain distributions at 1st. and 2nd. load cycles. Group III of ST 1 and ST 4 series.

M..... bending moment

M_{u1}... ultimate M

DUCTILITY OF PRESTRESSED LIGHTWEIGHT AGGREGATE CONCRETE

Igor TERTEA
Polytechnic Institute
of Cluj-Napoca, Romania

Vasile PACURAR
Polytechnic Institute
of Cluj-Napoca, Romania

Synopsis

The paper reports the results of a theoretical and experimental investigation concerning the ductility of prestressed lightweight (expanded clay) concrete beams in comparison with those of normal concrete. Forty-eight beams were tested, considering the degree of prestressing and the ratio of active and passive reinforcement as variables.

Résumé

On présente les résultats théoriques et expérimentaux concernant la ductilité des poutres précontraintes en béton léger par rapport à celles en béton normal. Les 48 poutres essayées ont permis d'analyser la ductilité sous l'influence du degré de la précontrainte et des pourcentages des armatures actives et passives. Pour granulat léger on a employé l'argile expansée.

ASSUMPTIONS

a) At commencement of yield of tension reinforcement the concrete compressive stresses vary with a second degree parabola (ref.Fig.1a);

b) At ultimate moment the concrete compressive stresses have the form of parabola-rectangle (ref.Fig.1b);

c) The strain in concrete may be assumed directly proportional to the distance from the neutral axis both at

yield of reinforcement and at failure (ref.Fig.1c);

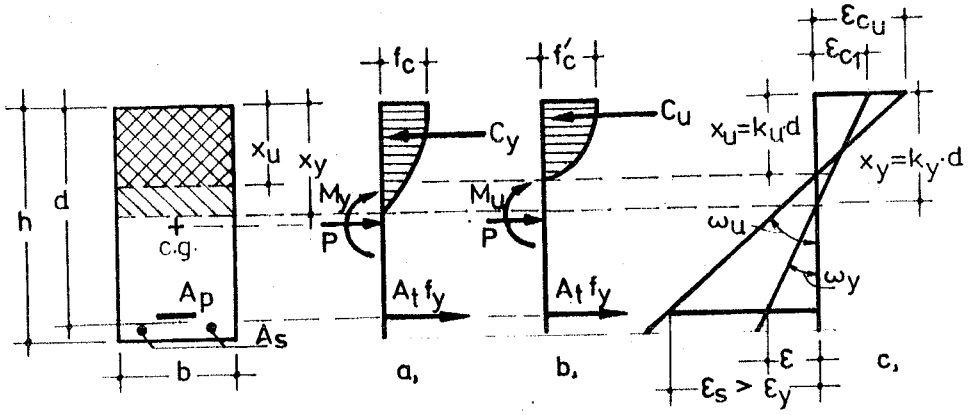

Fig.1. Conditions at yield of tension reinforcement (a) at ultimate moment (b) and strain distribution diagram (c).

d) The stress-strain curve of concrete is considered parabola-rectangle (ref.Fig.2), the limit strains having the values:

- for normal concrete : $\varepsilon_{c1} = 2\ \%$ and $\varepsilon_{cu} = 3{,}5\ \%$
- for lightweight concrete : $\varepsilon_{c1} = 2{,}5\ \%$ and $\varepsilon_{cu} = 4{,}5\ \%$

e) The stress-strain curve for both prestressed and nonprestressed reinforcement is considered bilinear, both reinforcements getting simultaneously to yield (ref.Fig.3).

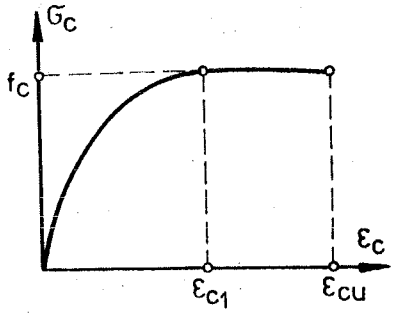

Fig.2. Stress-strain curve of concrete.

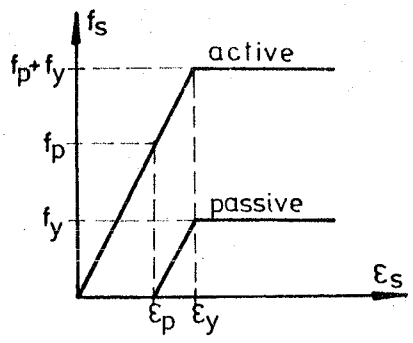

Fig.3. Stress-strain curves for prestressed (active) and nonprestressed (passive) reinforcement.

The ductility is defined as the ratio between the ultimate (ω_u) and yield (ω_y) curvatures i.e.

$$\Delta = \frac{\omega_u}{\omega_y} = \frac{\varepsilon_{cu}}{\varepsilon_y} \cdot \frac{1-k_y}{k_u} \tag{1}$$

where

$$\omega_u = \frac{\varepsilon_{cu}}{x_u} = \frac{\varepsilon_{cu}}{k_u d} \tag{2}$$

$$\omega_y = \frac{\varepsilon_y}{d-x_y} = \frac{\varepsilon_y}{(1-k_y)d} \tag{3}$$

The position of the neutral axis at yield of tension reinforcement and at ultimate moment is obtained from the equations of equilibrium and moment of internal forces, as follows:

- at commencement of yield

$$\frac{\varepsilon_y}{\varepsilon_{cl}} \left(3 + \frac{\varepsilon_y}{\varepsilon_{cl}}\right) k_y^3 - 3 \left(\frac{\varepsilon_y}{\varepsilon_{cl}} - \alpha_s - n_p\right) k_y^2 -$$

$$- 6 \left(\alpha_s + n_p\right) k_y + 3 \left(\alpha_s + n_p\right) = 0 \tag{4}$$

- at ultimate moment

$$k_u = \frac{\alpha_s + n_p}{1 - \frac{\varepsilon_{cl}}{3\,\varepsilon_{cu}}} \tag{5}$$

The meaning of the notations used above is:

$$n_p = \frac{P}{b\ d\ f_c} = p_p \frac{f_p}{f_c} \tag{6}$$

$$\alpha_s = \frac{A_t f_y}{b\ d\ f_c} = p_t \frac{f_y}{f_c} \tag{7}$$

where

$$p_p = \frac{A_p}{b\ d}\ ;\quad p_t = \frac{A_t}{b\ d}\ ;\quad A_t = A_s + A_p \frac{E_p}{E_s}$$

EFFECT OF PARTIAL PRESTRESSING ON DUCTILITY

Prestressing considered as external axial load influences the ductility of section by intensity of prestressing, expressed by n_p (given by Eq.6) and the degree of prestressing expressed by

$$\gamma = \frac{A_p f_p}{A_p f_p + A_s f_y} \qquad (8)$$

The influence of axial force on ductility of bent elements may be estimated by associating the interaction diagram for a reinforced concrete column with the diagram of inelastic curvature (ref.Fig.4). If the value of ultimate force is below balance value (P_b) the failure of concrete in compressive zone is preceded by the yield of tension reinforcement. In that situation the ductility of prestressed beam may be taken in consideration.

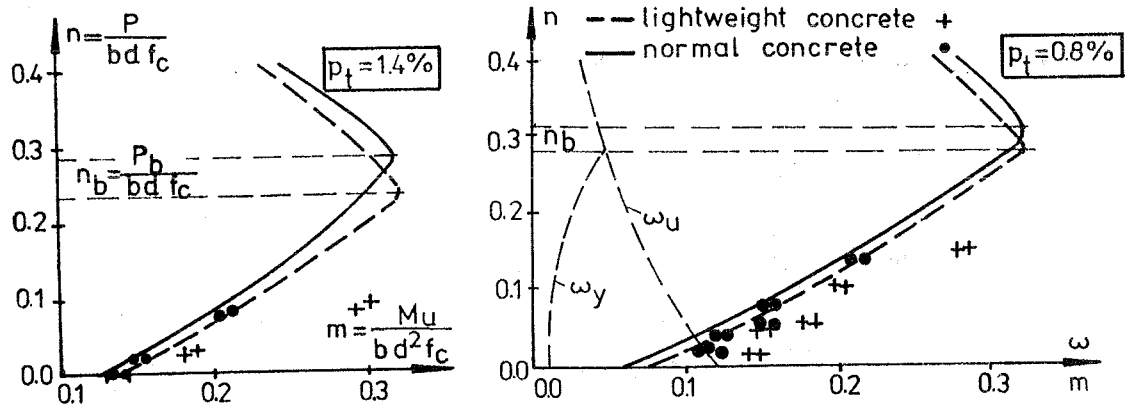

Fig.4. The place of prestressed beams in a column interaction diagram.

For total or partial prestressed beams the design codes require a maximum amount of reinforcement to determine the yielding of tension steel before reaching the ultimate moment so that the ultimate force of prestressed beams is always below balance value (P_b).

EXPERIMENTAL INVESTIGATION AND TEST RESULTS

Forty-eight simple-span rectangular beams were tested. All specimens were 15 by 30 cm in cross section and 400 cm long, with a span between supports of 300 cm. Half the number of test beams were made from lightweight aggregate concrete and the other half from normal concrete. The test beams were tested with equal loads applied at each third-point. The specimens were devided into three series corresponding to low, middle and high reinforcement ratios. Two "identical" beams for each parameter were made. The beams belonging to one group had the same ultimate moment but different prestressing degrees: 100 %, 66 %, 33 %, and 0 %. The variation of prestressing degree (defined by Eq.8) was achieved by gradual replacing of active reinforcement with a passive one.

The prestressing reinforcement represented by seven-wire tendons, having the yield strength of 1760 MPa, was anchored by bond. The nonprestressed reinforcement consisted of deformed bars having the yield strength of about 350 MPa. No stirrups or compression reinforcement were provided in the central third of the beam span.

The average of characteristic compressive strength of lightweight concrete was 24 MPa and of normal concrete 29 MPa.

In Table 1 are listed the calculated and measured values of ductility both for lightweight and normal concrete beams. The curvatures at yield and ultimate moments reffer to the central third of the beam span.

CONCLUSIONS

Ultimate axial load of prestressed beams, irrespective of the degree of prestressing, is located below the balance axial load (P_b) in the interaction diagram (ref.Fig.4). At the same reinforcement ratio the balance point for lightweight concrete is below that for normal concrete.

TABLE 1. Theoretical (Δ_c) and experimental (Δ_e) values of ductility of lightweight and normal concrete

Beam No.		γ %	Normal concrete					Lightweight concrete				
			n_p	α_s	Δ_e	Δ_c	$\frac{\Delta_e}{\Delta_c}$	n_p	α_s	Δ_e	Δ_c	$\frac{\Delta_e}{\Delta_c}$
1	a	100	0.103	0.027	6.57	8.20	0.80	0.100	0.033	7.60	8.20	0.93
	b				7.05		0.86			7.90		0.97
2	a	66	0.064	0.072	9.08	8.69	1.05	0.070	0.090	9.56	8.16	1.16
	b				8.00		0.90			9.40		1.14
3	a	33	0.029	0.113	5.48	8.29	0.66	0.022	0.137	5.70	8.21	0.69
	b				5.43		0.65			6.00		0.73
4	a	0	0.000	0.167	6.92	6.75	1.03	0.000	0.183	5.11	6.87	0.75
	b				7.14		1.06			4.64		0.67
5	a	100	0.127	0.039	6.73	6.81	0.99	0.158	0.050	5.82	5.76	1.01
	b				7.76		1.14			4.50		0.78
6	a	66	0.076	0.092	9.74	6.75	1.44	0.081	0.109	4.18	6.55	0.64
	b				6.50		0.96			4.90		0.75
7	a	33	0.037	0.145	5.51	6.06	0.91	0.038	0.176	4.35	5.50	0.79
	b				6.00		0.99			4.27		0.78
8	a	0	0.000	0.230	4.92	4.45	1.11	0.000	0.246	3.94	4.55	0,87
	b				3.61		0.81			5.17		1.14
9	a	100	0.202	0.066	4.60	3.58	1.28	0.235	0.084	2.40	3.13	0.77
	b				4.20		1.17			2.35		0.75
10	a	66	0.116	0.158	3.88	3.48	1.11	0.125	0.211	4.83	2.89	1.67
	b				3.14		0.90			2.05		0.71
11	a	33	0.058	0.278	4.09	2.60	1.57	0.054	0.333	1.78	2.31	0.77
	b				2.79		1.07			1.54		0.67
12	a	0	0.000	0.370	1.82	2.23	0.82	0.000	0.426	1.92	2.00	0.96
	b				2.21		0.99			-		-

As shown in Fig.5 at the same failure moment the ductility decreases with diminishing of prestressing degree i.e. with the increasing of the amount of reinforcement. The partial prestressed beams have a higher ductility in comparison with the reinforced concrete beams at the same ultimate moment.

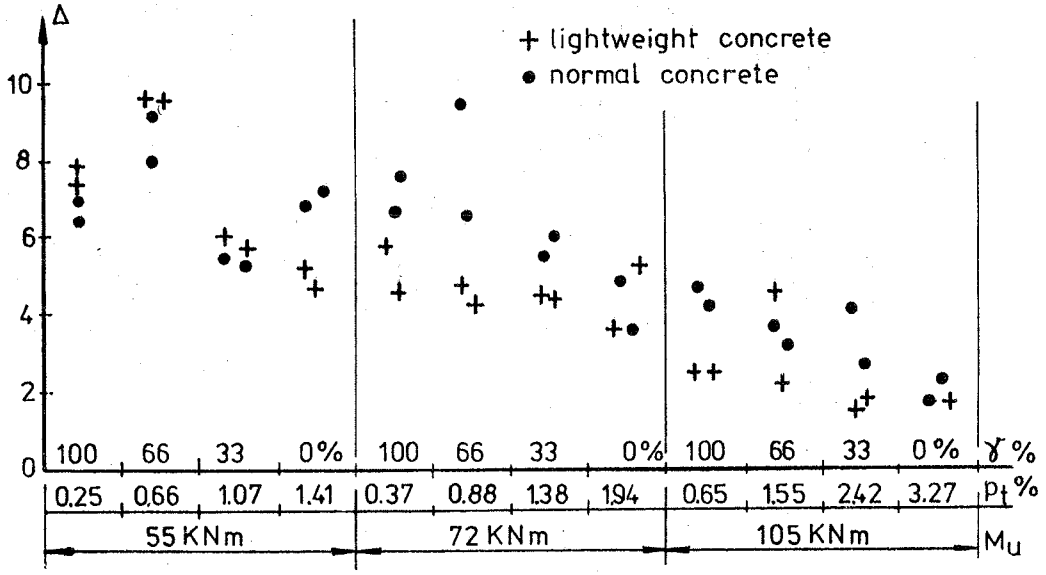

Fig.5. Variation of ductility with the degree of prestressing (γ) and the total reinforcement ratio (p_t) in beams of the same ultimate capacity

At the same amount of reinforcement (p_t) the ductility decreases with the increase of prestressing intensity (n_p). Bearing in mind that both prestressing intensity and mechanical ratio of reinforcement (α_s) influences the ductility in the same manner, it's possible to read this amount using a diagram shown in Fig.6.

As followed from test results presented in Figs.4, 5 and 6 and in Table 1, as well, the ductility of partial prestressed lightweight concrete may be considered comparable with the ductility of partial prestressed normal concrete.

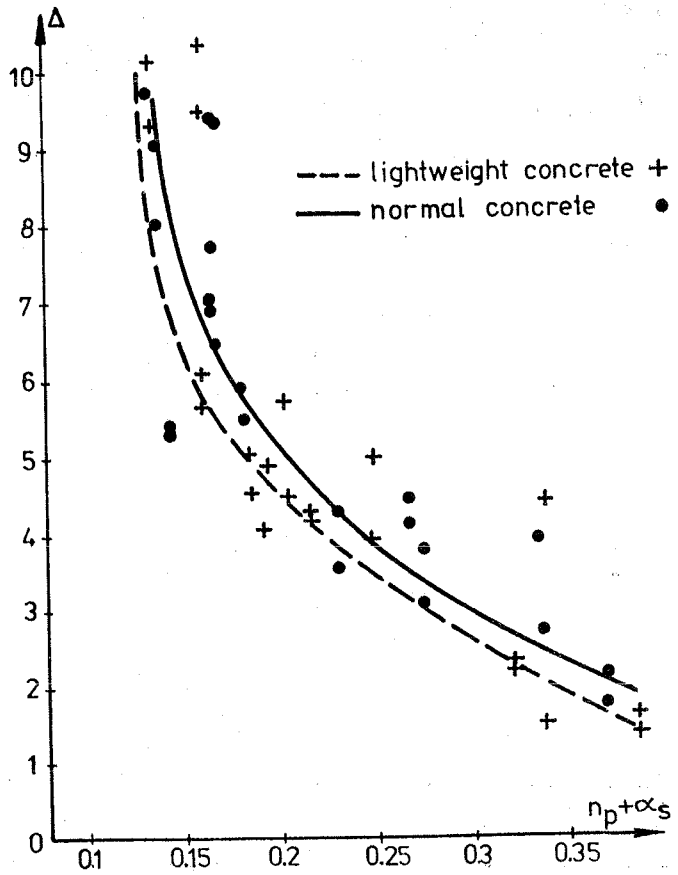

Fig.6. Variation of ductility with the intensity of prestressing (n_p) and the mechanical reinforcement ratio (α_s).

APPENDIX - Notations

A_s - area of nonprestressed reinforcement;

A_p - area of prestressed reinforcement;

f_c - compressive strength of concrete at commencement of tension reinforcement yield;

f'_c - ultimate strength of concrete;

f_p - effective stress in prestressing steel;

f_y - yield strength of nonprestressed reinforcement;

ε_{cl} - maximum concrete compressive strain at commencement of tension reinforcement yield;

ε_{cu} - maximum concrete compressive strain at ultimate strength;

E_p, E_s - modulus of elasticity of prestressed respective nonprestressed steel.

BEAM-COLUMN SUBASSEMBLAGES TESTED UNDER ALTERNATED LOADS FOR SEISMIC DESIGN

Eduardo CANSADO CARVALHO
Laboratorio Nacional de Engenharia Civil
Lisbon, Portugal

SUMMARY

In order to assess the available ductility in beam-column joints included in the structure of a large urban development in a seismic area an experimental program was carried out. Four models were constructed. The present paper describes the "T" shaped models and the tests performed. These, mainly consisted in sequences of alternated displacements applied at the beams ends inducing large non-linear incursions. General conclusion both on the models as well as on the expected real structure behavior are drawn.

SOMMAIRE

Un programe experimental a été entrepris dans le but d'evaluer la ductilité disponible dans les noeuds poutre-colonne inclus dans la structure d'un grand development urbain à construire dans une zone sismique. Quatre modèles ont été construits. La présente communication décrit les modèles en forme de "T" aussi bien que les essais. Ceux-ci ont consisté essentielment à l'application à l'extremité de la poutre des sequences de déplacements alternés induisant des grandes incursions non-linéaires. Des conclusions générales sur le comportement des modèles aussi bien que sur le comportement prévu pour la structure sont presentées

INTRODUCTION

Reinforced concrete behavior under alternated loads has been being studied for some time, but it is well recognized that further experimental research is still needed for its complete understanding, Clough (1977). Namely, beam-column joints in framed structures represent one of the areas in which there is not yet a fully understanding of its behavior. The mechanism by which shear force applied in the joint is resisted as well as the effects of such parameters as axial force in the column, confinement of concrete, spacing and arrangements of transverse steel, anchorage lengths of beam bars are examples of subjects in which there is still room for discussion.

With no intention of extensively cover the experimental data available up to now, works by Hanson and Conner (1967) Jirsa (1972) Townsend (1972), Park and Paulay (1973), Jirsa et al (1975) Bertero and Popov (1975), Lee (1976), Nascimento (1977) and Uzumeri (1977) should be mentioned.

It was exactly considering such need for experimental research that, for a large urban development in a seismic zone, an experimental program was carried out on four models reproducing two situations of external beam-column subassemblages as designed.

Typically, buildings are five to nine stories high and its structures are made up by reinforced concrete moment-resisting space frames oriented in two orthogonal directions. Girders spans are either 8,25x8,25 m or 11,0x5,5 m supporting quadrangular or rectangular waffle slabs. Due to the great extension of the building in plan a set of expansion joints were introduced dividing the structure in modules of approximately 50x50 m.

The main purpose of the experimental program referred above was to evaluate the seismic behavior of beam-column joints as designed by the author of the structural project. Tests were conducted in LNEC on what was considered to represent typical situations of external beam-column joints. The choice of external joints was imposed by the available experimental facilities. Detailed results of the experimental program carried out are presented by Carvalho (1978)

DESCRIPTION OF THE MODELS

Two pairs of models were constructed. These two pairs were extracted from a typical frame with five stories and six spans of 8,25 m. The location of the modeled zones of that frame as well as its general dimensions are present in fig. 1. The main parameter influencing the choice of these zones was the axial force acting on the column. Two situations were thus considered:

- First floor beam-column joint with the highest axial force in the column.
- Second uppermost floor beam-column joint with lower axial force in the column.

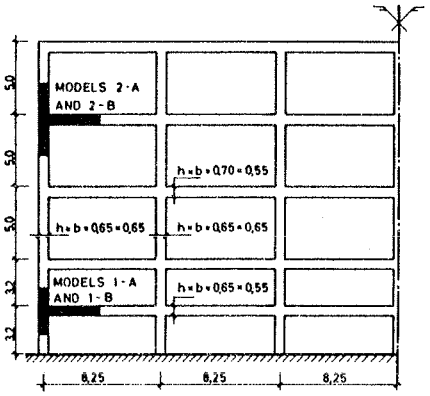

Fig. 1 - Typical frame and location of "extracted" models.

It should be noted that the column that was considered, however being an exterior one, carries loads similar to the interior ones since it supports, by short cantilevers, the girders of the adjacent structural module forming thus the expansion joint.

As usual in such cases models were extracted paying attentation to the fact that in frames under horizontal forces, zero bending moment values are present in sections approximately at mid span of its members.

The geometric scale chosen for the construction of the models took in consideration simultaneously, the need to acurately model the behavior of reinforced concrete as well as the limited space and forces available for the tests. As a balance between these two antagonic considerations a value of 1:2,5 was assigned to that scale. Four models were then constructed reproducing the corresponding details of the real structure design. Models of the first pair, representing a lower beam-column joint, are labeled 1-A and 1-B. Similarly, models of the second pair representing an upper beam-column joint are labeled 2-A and 2-B. General views and cross sections of the two types of models are presented in fig. 2.

Still in geometrical properties of the models some comments are due:

- Altough different in the real structures, the columns heights in models 1 and 2 were taken equal in order to use the same mould for the four models. The least value was considered leading to an increase in the column shear force for models 2. As expected "a priori" this increase did not show, however, any influence on the tests results.
- Special end provisions adapted to the bearing system in the testing frame were considered in the columns.
- As seen in fig. 2 top reinforcement in the beams of both types of models varied along its length. This feature was imposed by the reproduction of the real structure reinforcement curtailments and, as shall be seen later, significantly affected the experimental results. Also following the real structure design, transverse reinforcement varied along the beam and column both in steel content and spacing.
- Design drawings prescribed bar diameters in inches or fractions. For the zones of interest only 3/8", 7/8" and 1" bars were present. Reproduction of these diameters in the models was achieved approximately using 4 mm, 8 mm and 10 mm bars. The first type, being not included in the standard set of bar diameters in Portugal, had to be obtained by cold hardening plain wire of that diameter.

As far as mechanical properties are concerned, both for concrete and steel, a direct reproduction of the design specifications was envisaged. For concrete, design specification was a 28 days cylinder compressive strenght of σ_{ck} = 29,4 MPa (300 kgf/cm^2). A suitable mix was prepared limiting the aggregate maximum dimension to 1/2". The proportions adopted were as follows: Gravel-1083 kg/m^3; River sand-620 kg/m^3; Portland cement - 400 kg/m^3 and Water-198 kg/m^3. Concreting was made with the models in a horizontal position and using two mixes for each model. Pairs of cylinders, cubes and prisms were retired from each mix. Statistical data concerning the results of tests on these specimens is presented in Table I. The desired characteristic strength in cylinders was not attained but this fact was only due to an anomalous result (remark for instance the difference between standard deviations of the results in cylinders and cubes).

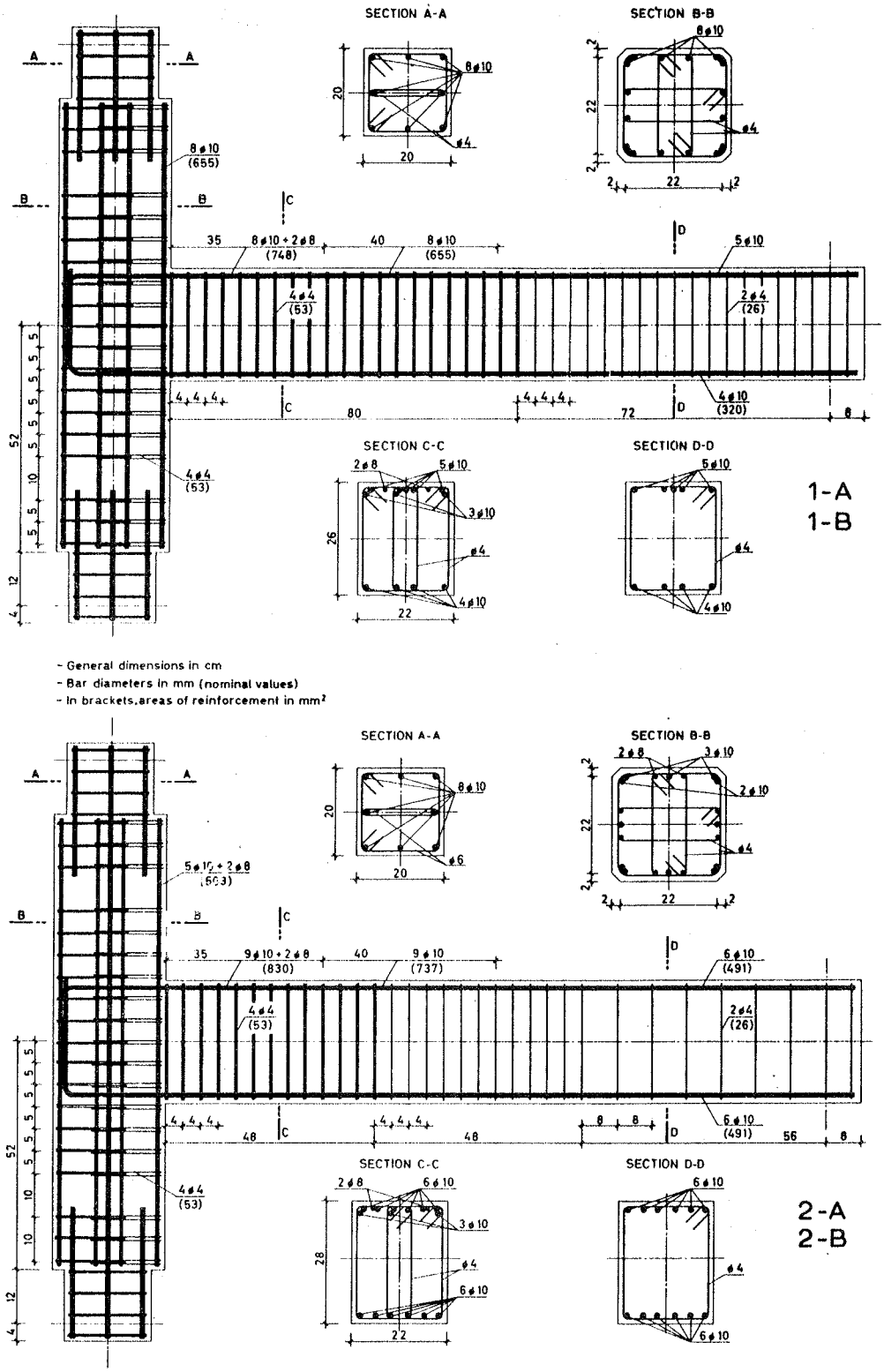

Fig. 2 - General views and cross sections of the two types of models.

TABLE I - STATISTICAL DATA ON CONCRETE SPECIMENS TESTS

SPECIMENS	TESTS AT 28 DAYS			TESTS AT DATE OF MODEL TESTS		
	σ_{cm} or σ_{ctm}	s_n	σ_{ck} or σ_{ctk}	σ_{cm} or σ_{ctm}	s_n	σ_{ck} or σ_{ctk}
CYLINDERS Comp. Strength	32,9 (336)	4,34 (44,3)	25,8 (263)	40,3 (411)	3,59 (36,6)	34,3 (350)
CUBES Comp. Strenght	39,6 (404)	1,87 (19,1)	36,6 (373)	46,7 (477)	2,53 (25,8)	42,8 (437)
PRISMS Comp. Strenght	5,44 (55,6)	0,31 (3,2)	493 (50,3)	4,98 (50,8)	0,17 (1,7)	4,70 (48,0)

σ_{cm} or σ_{ctm} - Mean compressive or tensile strength. s_n - Standard deviation.
σ_{ck} or σ_{ctk} - Characteristic compressive or tensile strength (5%). Values in MPa and (kgf/cm^2).

Design specification for steel was the ASTM Grade 60 which corresponds to a minimum or characteristic yield strenght σ_{yk} = 413 MPa (42 kgf/mm^2). Such steel was reproduced in the models longitudinal reinforcements by the use of a Portuguese steel marked SNT40. It is a high bond cold worked steel (torsion) with a characteristic strength σ_{yk} = 392 MPa (40 kgf/mm^2) (referred to $\sigma_{0,2}$ values). The same steel lot (denoted lot 1) was used throughout the construction of the four models except for the Ø10 bars in the 2-B model beam in which a new lot (denoted lot 2) had to be used. Tensile tests for several bars from these two lots were performed and mean value results are presented in fig. 3. A considerable difference between the results of the two steel lots was verified. For transverse steel, as 4 mm is not a standard diameter for construction steel, a special cold worked plain wire prepared for LNEC was used. Tests on specimens of that steel (denoted lot 3) were also performed and results are presented in fig. 3. Although one of the tests for a bar from lot 1 showed an yield strength below σ_{yk} = 413 MPa (42 kgf/mm^2), in general the steel used in the models can be considered as complying with the real structure design specification.

Considering the adopted geometric scale and the fact that mechanical properties are the same both in the model and in the real structure (prototype) numerical values for scales of forces and moments are respectively, $F_P/F_M = 2,5^2 = 6,25$ and $M_p/M_M = 2,5^3 = 15,625$.

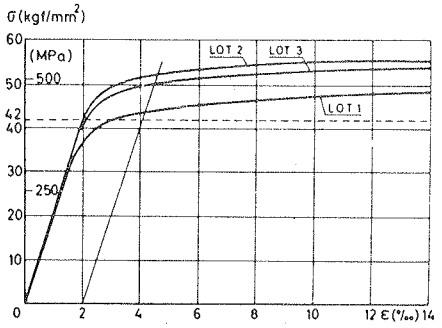

Fig. 3 - Mean value results of tensile tests on steel used in the construction of the four models

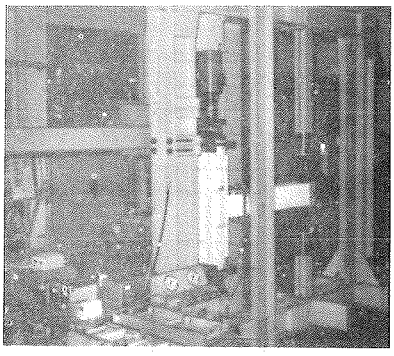

Fig. 4 - General view of the test set-up

DESCRIPTION OF THE TESTS

Tests were conducted in a testing steel frame. Columns ends were simply supported by means of adequate steel bearings which restrained horizontal displacements but permited rotations. A constant axial load was applied in the column by a manual hydraulic jacks applied alternated displacements with "a priori" defined amplitude sequences. These two jacks were manually controled allowing a certain adjustment of these displacements sequences during the tests, following the models behavior. A general view of the test set-up is presented in fig.4 and the displacements sequences applied to the four models are presented in fig. 5 (downwards for positive direction). At test dates models ages varied from 77 to 119 days. Except for the second model (1-B), amplitudes of the alternated displacements sequences continuously increased although in an asymmetrical way due to the differences between top and bottom reinforcement in the beams. For the second model (1-B) an irregular pattern was adopted based on the displacements applied in model 1-A. Due to an early rupture of the bottom reinforcement in this test, the initially defined displacements sequence with 23 cycles was not achieved.

Axial force in the column was constant throughout each test but had different values for the four models. For the first pair of models, approximately N = 700kN(70tf) were applied. This value scales the real structure axial force in the column at the foundation level due to dead load and 25% of live loads. For the second pair of models which corresponds to an upper zone of the structure lower values for the axial force were applied. For model 2-A the value

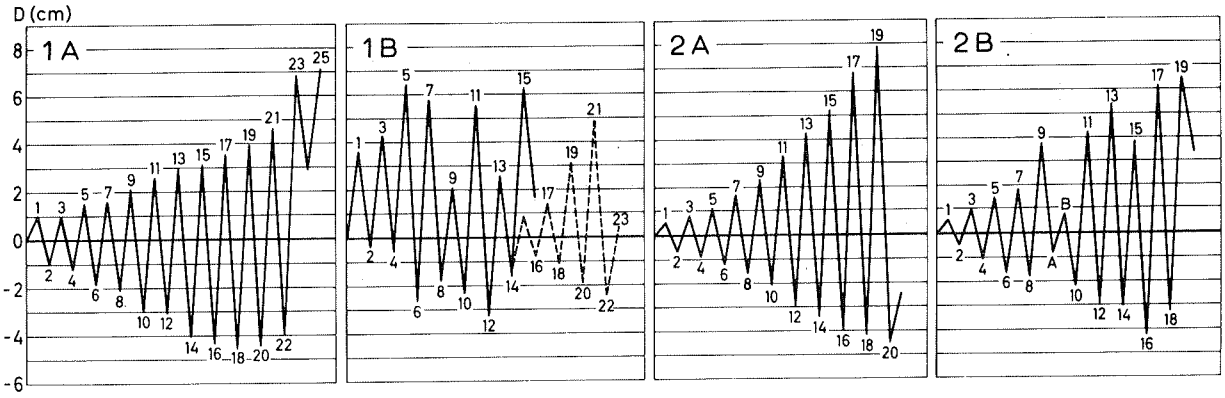

Fig. 5 - Displacements sequences for the four models

adopted was N = 300kN (30tf) whereas for model 2-B a reduced value of N = 200kN (20tf) was taken. It is stressed that for such levels of axial force this reduction in its values leads to a more severe situation both for the column and the beam column-joint.

Instrummentation of the models is general visible in fig. 4. Mainly it consisted of several inductive transducers placed in such a way as to obtain among others the following diagrams: Force - Displacements at the end of the beam; Force-Relative rotations between adjacent cross sections of the beam and Force-Lengths variations along the joint diagonals. For the relative rotation diagrams three cross sections were considered. Begining at the column's face and 20 cm apart they were named respectively A,B and C . Measurement of the joint rotation was also envisaged but since it showed very small values the used system did not work satisfatorily.

TESTS RESULTS

Some of the diagrams obtained are presented in fig. 7. In the relative rotation diagrams, further to these values, corresponding average curvatures (on a 20 cm length) are also indicated. Views of the beam-column joints at extreme load conditions are shown in fig. 6. General comments on the tests results are made in the following paragraphs.

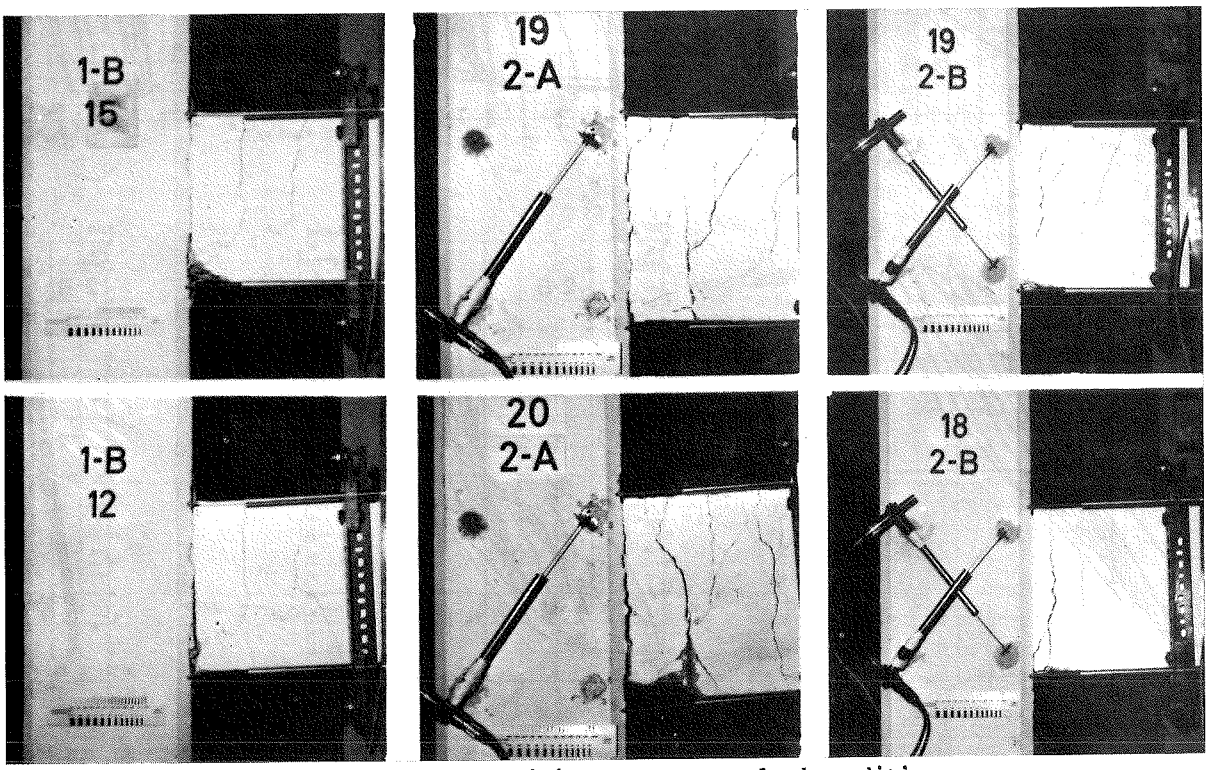

Fig. 6 - Beam-column joints at extreme load conditions.

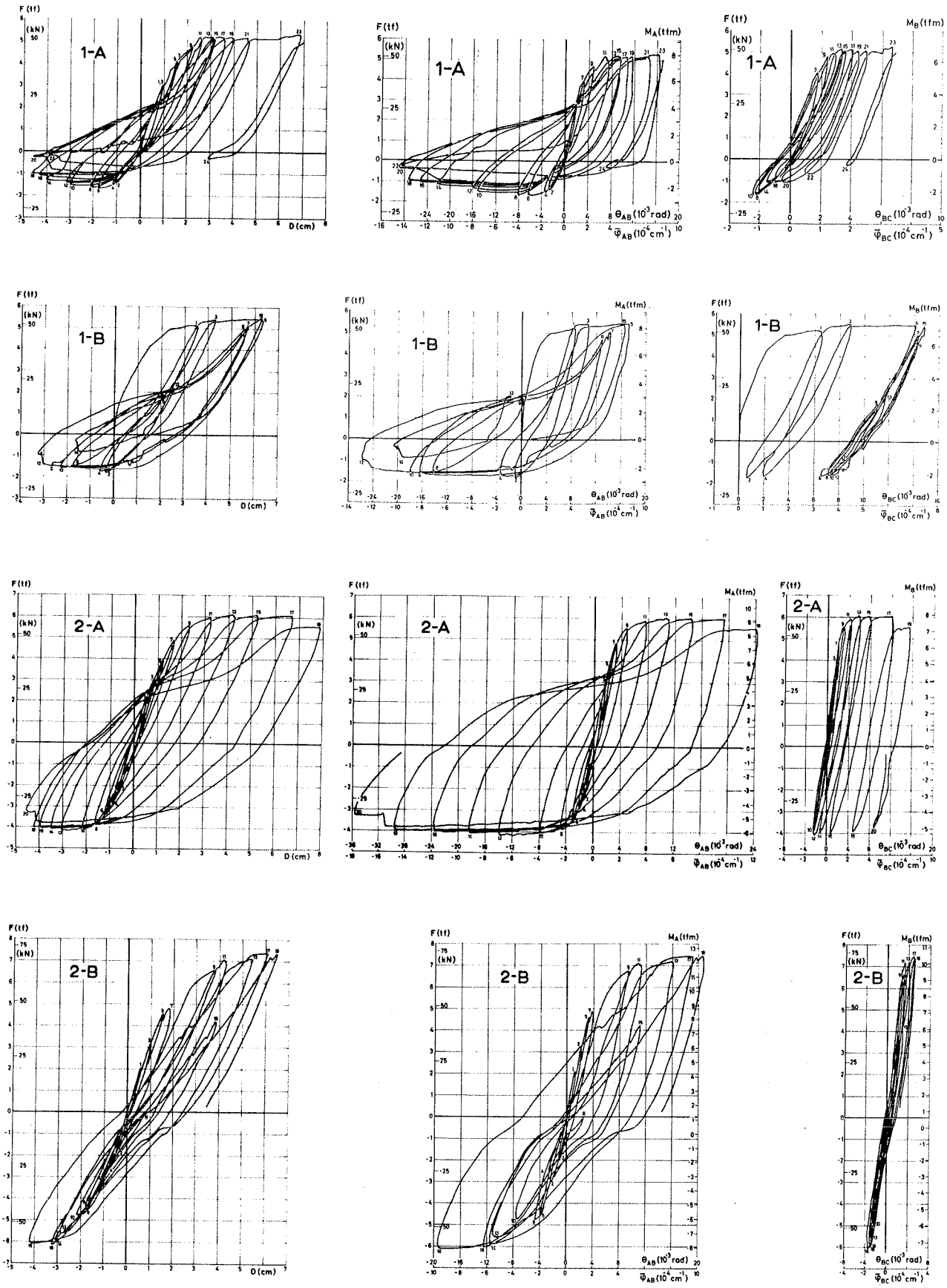

Fig. 7 - Force displacements and force relative rotation diagrams for the four models.

Models 1-A and 1-B

Being equal, these two models behaved approximately in a similar way. Ultimate load at the beam's end either downwards (positive) or upwards (negative) was controled by the resis - tant moment of the beam cross section next to the column's face. However, the behavior under positive or negative forces was completely different. Actually, for positive forces, mainly due to widespread cracking of the beam's upper face(resulting from the corresponding reinfor cement curtailments) models showed great ductility in terms of displacements at the beam's end. On the contrary, for negative forces, due to the lack of bottom reinforcement curtail - ments, non-linear behavior of the beam was established near the column's face by a single main crack. Obviously such crack pattern dramatically reduced the displacement ductility available at the beam's end. Further aggravating this situation was the fact that permanent positive cur vatures were increasingly being retained by the beam following the positive cycles (bottom reinforcement being smaller than the top one was unable to eliminate its permanent tensile yielding strains). The evolution of relative rotations between cross section B and C (fig. 7) clearly illustrates such behavior. Needless to say, an extremely severe condition was thus created for the bottom reinforcement next to the column's face. Indeed, in both models, seve - ral bottom bars collapsed when attaining strains (in a 20 cm average) with values near 4%. It is also important to note that for positive forces no strength degradation was observed while for negative forces and especially for model 1-A there was evidence of such fact. As to the effect of the irregular displacements sequence, being however certain that collapses of bottom bars for the second model (1-B) ocurred for a smaller displacement applied at the beam's end than for the first one, it is not clear that such facts are directly correlated. Being appa - rent that the main difference, relevant for the present discussion, between the two models was the behavior of the beams in theirs BC sections, it is however difficult, to establish a direct relationship connecting the greater relative rotation observed in model 1-B with the irregularity of the displacements sequence applied at the end of its beam.

Finally, it is noticed that for these two models the columns remained uncracked and the beam-column joints showed only a very thin, approximately diagonal, crack following the large amplitude positive cycles.

Models 2-A and 2-B

The two models of this pair, however being theoretically equal, presented considerably different behavior from each other. Three main reasons contributed to this fact: First, as sta ted before, bars used in the longitudinal reinforcement of the beams of both models, since coming from different steel lots, had different strengths (for model 2-B yield strength was 25% greater than for model 2-A). Secondly, for model 2-B a smaller axial force was applied in its column. Finally test procedures were considerably different in both models. In fact, for model 2-A only a variable alternating force was applied at the beam's end (originating-linear bending moment distribution) whereas for model 2-B, besides such variable force, a constant 22 kN (2,25tf) vertical force was applied on the beam at a distance of 52 cm from the column's face. This force was intended to model in the beam near the column the effects of vertical loads (dead load + 25% of five loads) both in terms of bending moment as well as in terms of shear force.

Out of the three reasons just outlined, the most relevant for the different behavior ob- served in the two models was the last one. In fact, the most striking difference was the pas- sage from a clearly assymmetrical behavior in model 2-A (as well as in models 1-A and 1-B) to- an almost symmetrical one for model 2-B. The dominant effect, as previously discussed, of the beam's reinforcement curtailments pratically disappeared leading to a sensible reduction on the "hinging length" for positive cycles. In fact this is clearly emphasized by a comparision between the behavior of the beams sections BC in both models. Tendency to retain positive per- manent curvatures in the beam also ceased thus alleviating in section AB the severe ductility demands sustained by the first three models in negative cycles. On the contrary, available dis placement ductility at the beam's end was reduced for positive cycles (forces downwards).

The other two reasons referred above as being related to the different behavior that was observed in this pair of models, however less relevant, played also a certain role distinguis- hing both models response, especially as long as the column and beam-column joint are concer - ned. In fact, for model 2-A no cracking was observed in the column and only for positive cy - cles diagonal cracks developed in the joint, whereas for model 2-B more extensive cracking was observed. For its beam-column joint, cracking along the two diagonals was observed due to for- ces applied in both directions. Also a horizontal crack in the column appeared during the grea ter amplitude positive cycles. Neverthless, general behavior of the column and the joint re - mained satisfatory in both models, no evidence being shown that either its overall strength stiffness were influenced by the joint or column.

APPLICATION OF THE RESULTS TO THE REAL STRUCTURE

Results obtained in the four tests can be extrapolated to the real structure considering the scales relating each parameter. For strengths, numerical values of these scales have already been indicated (6,25 for forces and 15,625 for moments) whereas for displacements the value is directly the geometrical scale 2,5.

Results in terms of available ductilities, which undoubtly are the most important ones, can be directly extrapolated from the model to the prototype. For displacement ductility, which is well related to interstory displacement ductility in the real frame, tests results indicated that at least a value of μ=3 was available in any of the four models. On the other hand linearrized, analysis of a typical frame indicated that, for the most severe earthquake probably possible in the area of the development, ductility demands in these terms would be at most 1,5 to 2. Furthermore it showed that non linear behavior of the frame would be chiefly established by the "hinging" of the girders. This fact matchs well the behavior of the models and as the available ductility exceeds the probable demands a satisfatory seismic response seems to be predictable.

CONCLUSIONS

Main conclusion of the four tests which were performed can be summarized as follows:

- Ultimate strengths and deformations were controled by the beams in all cases. In particular flexural strength which, very closely could be established theoretically, limited the overall strenght of the models. No evidence showed up that in any case shear strength was at stake.
- Columns and beam-column joints remained pratically uncracked for the first pair of models whereas for the second pair with lower axial forces cracking did appear although not influencing the overall behavior of the models. It can be noted that the joint shear steel content was smaller than that would be demanded by the application of the ACI-ASCE Recommendations (1976).
- Simulation of the effects of vertical loads, besides the alternated displacements applied at the beams ends, proved to be very important for the correct establishement of the real behavior of the substructure under earthquake actions.
- Bearing in mind the clear limitations of such small experimental program for a so large development, in general terms a good seismic response of the structure seems to be predictable.

REFERENCES

- ACI-ASCE Committee 352 - Recommendations for Design of Beam-Column Joints in Monolithic Reinforced Concrete Structures, ACI Journal, Proceeding V.73, No 7, July 1976, pp 375-393.
- V.V. BERTERO and E.P. POPOV - Hysteretic Behavior of Ductile Moment-Resisting Reinforced Concrete Frame Components, EERC Report 75-16, Univ. of California, Berkeley, April 1975.
- E.C.CARVALHO - Ensaios Sísmicos em Modelo das Estruturas das Areas Centrais de Morelos, La Hoyada e Carabobo, em Caracas, Final Report (in Portuguese), LNEC, Lisbon, December 1978.
- R.W. CLOUGH - Predicting the Earthquake Response of Reinforced Concrete Structures, in Reinforced Concrete Structures in Seismic Zones, ACI Publication SP-53, Detroit, Michigan, 1977, pp 59-79.
- N.W. HANSON and H.W. CONNOR - Seismic Resistance of Reinforced Concrete Beam-Column Joints, Journal of the Structural Division, ASCE, Vol. 93, No ST5, October 1967, pp 533-560.
- J.O. JIRSA - Cast-in-Place Joints for Tall Concrete Buildings, State of Art Report 3, Technical Committee 21, ASCE-IABSE Int. Conference on Tall Buildings, August 1972, pp 45-55.
- J.O. JIRSA, D.F. MEINHEIT and J.W. WOOLLEN - Factors Influencing the Shear Strength of Beam-Column Joints, Proceedings of the U.S. National Conference on Earthquake Engineering, Ann Arbor, Michigan, 1975, pp 297-305.
- D.L.N. LEE - Original and Repaired Reinforced Concrete Beam-Column Subassemblages Subjected to Earthquake Type Loading, Doctor of Philosophy Dissertation, UMEE 76R4, University of Michigan, April 1976.
- J.F.S. NASCIMENTO - Comportamento das Conexões Viga-Coluna de Betão Armado Submetidas a Esforços Repetidos, Thesis (in Portuguese), LNEC, Lisbon, February 1977.
- R. PARK and T. PAULAY - Behavior of Reinforced Concrete External Beam-Column Joints Under Cyclic Loading, Proceedings of the 5th WCEE, Vol. I, Paper 88, Rome, 1973.
- W.H. TOWNSEND - The Inelastic Behavior of Reinforced Concrete Beam-Column Joints, Doctoral Dissertation, University of Michigan, 1972.
- S.M. UZUMERI - Strength and Ductility of Cast-in-Place Beam-Column Joints, in Reinforced Concrete Structures in Seismic Zones, ACI Publication SP53, Detroit, Michigan, 1977, pp 293-350.

THE BEHAVIOUR OF BEAM-COLUMN JOINTS UNDER BIDIRECTIONAL LOAD REVERSALS

S.T. BURGUIERES
The University of Texas at Austin
Texas, U.S.A.

J. O. JIRSA
The University of Texas at Austin
Texas, U.S.A.

J. E. LONGWELL
The University of Texas at Austin
Texas, U.S.A.

SUMMARY

An experimental research program on the behavior of interior reinforced concrete beam-column joints under severe bidirectional load reversals is described. The influence of loading history on the behavior of three identical specimens is discussed.

On presente une description d'un programme de recherche experimentale au sujet du comportement des connections intérieures poutres-colonnes soumisses à un régime sévère de forces bi-latérales. Ci-dessous, trois models identiques sont presentés et discutés.

INTRODUCTION

Very little experimental work has been done on the behavior of frame elements under bidirectional seismic loading. Key frame elements such as columns and joints, however, undergo biaxial deformations as the resultant seismic excitation is skewed to the building frame's principal axes. It is likely that full system yielding may occur simultaneously in both directions several times during a major earthquake, particularly if a relatively large system ductility has been assumed in design (say 3 or 4).

Experimental work on the behavior of short rectangular columns under bidirectional shear reversals is being conducted in a parallel study with the tests on interior beam-column joint subassemblies, to provide insight into the behavior of ductile frames.

Background

All previous experimental work on interior beam-column joints reported in the literature has concerned planar joints. Several programs have used very short unloaded beams to simulate the effect of transverse framing. Information on the behavior of joints under bidirectional lateral loadings must be obtained before the influence of joints on overall frame behavior can be estimated. Past tests of planar joints and frames have established clearly that joints may control frame strength, stiffness, and ductility. Some of the critical problems in the joint regions are shear, anchorage, and bond deterioration of reinforcing, and loss of effective intersecting

member sections due to local spalling and cracking in the joint region. These problems and a review of previous literature are discussed in Refs. 1 and 2.

Scope and Objectives

The immediate objective of this report is to:

(1) Evaluate the importance of bidirectional lateral loading on the behavior of reinforced concrete beam-column joints.

The ultimate objectives of the project are to:

(2) Develop a basic model explaining the behavior observed which may be applied to different conditions, and provide information for more accurate analysis of overall frame response.

(3) Develop recommendations for the design of joints in frames subjected to several lateral loadings.

The test specimen geometry chosen is shown in Fig. 1. This geometry represents an interior beam-column joint subassembly of a frame, without a slab. The prime variable in the initial tests is the load history applied to the specimen. Loads are applied slowly, neglecting strain rate effects. Test specimens are specifically designed to exhibit joint distress.

DESCRIPTION OF TESTS

Test Specimen

Figure 1 shows the geometry and reinforcing of Specimens 1, 2, and 3. Since these tests were intended to demonstrate joint distress, the specimen was designed so that joint strength and stiffness would be critical in influencing subassembly behavior. High joint shear, reinforcing bar bond conditions, and minimal confining reinforcement in the joint were intentionally designed to ensure that these problems would affect the unidirectional versus bidirectional loading comparison.

Normal design material strengths were 28 MPa for the concrete and 420 MPa for the reinforcing steel. A 38 cm square column was chosen for ease of loading, and for direct comparison with past experimental work on planar joints. Beam reinforcing steel, with $A_{s\ bot} \approx 1/2A_{s\ top}$, was designed to develop a very high value of horizontal joint core shear when the beams yield adjacent to the column face. Figure 2 indicates the forces which develop joint core shear in the planar case. Beam steel was proportioned so that joint core shear at full beam yielding in one plane was approximately equal to the static strength of planar joints using the approach of Meinheit and Jirsa [1]. Column reinforcing was designed so that full beam yielding could occur before column yielding in the planar loading case. This was done to meet current ACI seismic design recommendations [2], which follow the weak beam-strong column frame design philosophy. Relatively large beam bars ensured that bond distress would develop and minimal joint core horizontal tie reinforcing was used. The ties were used to provide an indication of the joint core distress by monitoring strains in the tie legs. Note that all beams had the same main reinforcing, but that bars were displaced vertically as necessary to pass through the joint region.

Specimens were fabricated in the upright position, with one concrete pour including the lower column, the beams and the joint region, and the bottom 15 cm of the upper column. A second pour placed the remainder of the upper column.

Loading

A sketch of the idealized loading of an interior beam-column joint subassembly, meeting the dimensions of the specimen described above, is shown in Fig. 3. No attempt was made to exactly duplicate all the aspects of loading and restraint in a true concrete framed structure subjected to seismic loading.

Figure 4 shows a specimen situated in the loading apparatus. Specimens were tested in the upright position, braced against a floor-wall reaction system. Four vertical rods and centerhole rams applied column axial load. Four rams with spherical end attachments, attached to the reaction floor, loaded the beam stubs up or down. The upper column was effectively pin-supported at the top and braced to the reaction wall to resist upper column shear. The bottom of the lower column was semi-rigidly connected to the reaction floor. An inflection point formed a short distance above this connection to match approximately the idealized loading condition shown in Fig. 3.

Axial load applied to the column was held at a constant level of 1335 kN compression during all three tests. This value was equal to the balance load for the column. Racking loads were applied to the beam pairs, with deformation of the beam ends controlled. In order to simulate the effects of dead load on the subassembly, all four beams were deformed down 2.5 mm before beginning cyclic deformations. Cycling of beam deformation was performed about the "dead load" deflection, which cracked the beams and developed a tensile stress of approximately 83 MPa in the top beam reinforcement.

Deformations were applied to the beams in a predetermined pattern. A value of yield deformation, Δ_y, was established in the first test, with unidirectional loading of the N-S beams only. The yield deformation is defined as the beam end deformation at first flexural yield of the beam reinforcement, and was 33 mm beyond the dead load position. The deformation history applied to all specimens was 3 cycles at $1\Delta_y$, 3 cycles at $2\Delta_y$, etc., to the limit of the testing apparatus.

Instrumentation

All measurements of load, deformation, and reinforcing bar strain were made electronically by a computer-controlled VIDAR scan unit. The computer link permitted interactive data reduction as the testing progressed.

BEHAVIOR

A table of specimen names, loading history types, and basic results is shown in Fig. 5, as well as the load-deflection plots for the North beam in each test.

Specimen 1-U-C: Unidirectional

Deformations were applied to the N-S beams only. The E-W beams were held constant at the dead load deflection throughout the test. The specimen was considerably less stiff than calculated using simple elastic flexural theory, cracked sections, and a rigid joint core. Maximum column bar stress at $1\Delta_y$ was about 180 MPa. Joint shear cracking and bond distress of beam reinforcing bars were observed before $1\Delta_y$ was reached. As noted in Fig. 5a, most loss of stiffness and energy dissipative capacity was seen in the first cycle. As beam deflection was increased to $2\Delta_y$, stiffness decreased drastically, shear cracking extended well into the E and W beams, and bond deterioration became extensive. Joint tie reinforcement yielded. At $3\Delta_y$, maximum column bar stresses were near yield as column spalling above and below the beams reduced the effective column section. At $4\Delta_y$, strain gages on several column bars indicated yield stress. At the end of the test, there was severe compressive spalling of the column and North and South beams above and below the joint, with shear cracking extending 0.6 to 0.8 m into the E and W beams. Figure 6 shows crack patterns at an advanced stage of loading.

Maximum joint core shear, 1600 kN, occurred when the beams were first deformed to $2\Delta_y$. The maximum shear is approximately equal to that predicted by using the results of the work by Meinheit and Jirsa [1]. Full yield moments were developed in the beams.

Specimen 2-BS-C: Bidirectional, Simultaneous

Deformations were applied simultaneously to the N-S and E-W beams, i.e., the resultant loading or deformation was along the NW-SE 45° diagonal. The same beam deflection limits of $1\Delta_y$, $2\Delta_y$, etc., used in test 1-U-C were used in this test. Shear distress was noted very early during the first cycle to $1\Delta_y$. Corner column bars and several beam bars reached yield strains at approximately $1\Delta_y$, and joint ties exhibited stresses near yield. Strain gage readings also indicated early bond distress of both beam and column bars. A combination of shear cracking and compressive spalling appeared at the column corners above and below the joint. Again, as seen in Fig. 5b, most stiffness loss and change in shape of the hysteresis loops occurred in the first cycle of loading, and stiffness decreased drastically with increased beam deflections. Shear cracking through the joint region and into the beams and column became very pronounced with further loading. Strains well beyond yield developed in the column bars. At the end of the test, well-defined X cracking of the joint region could be observed in the NW-SE direction (direction of loading), see Fig. 7. The column above and below the joint region suffered severe compressive-shear spalling, reducing its section greatly, though axial load did not reduce significantly.

The maximum resultant joint core shear, occurring at the first peak, $2\Delta_y$, was 1760 kN and occurred at full column yielding without development of yield moment in the beams.

Specimen 3-BA-C: Bidirectional, Alternate

Deformations were applied alternately to the N-S and E-W beams. For example, one cycle to Δ_y was applied to the N-S beams while the E-W beams were held at dead load deflection and then with the N-S beams remaining at dead load deflection the E-W beams were subjected to one cycle to Δ_y, and so on. Shear and bond distress were noted before $1\Delta_y$ was reached in each

direction. Considerable nonlinearity can be seen in the load-deflection plot, Fig. 5c. Beam reinforcement reached yield and joint ties were near yield at $1\Delta_y$. Compressive spalling appeared at the junctions of the column and beam top and bottom surfaces, similar to that seen in test 1-U-C. With cycling of load, most loss of stiffness and change in shape of the hysteresis loops occurred after the first cycle of loading. Stiffness decreased drastically when beam deflections were increased to $2\Delta_y$ and shear cracking and bond deterioration became extensive. Column bar stresses gradually increased, and joint ties reached yield at $2\Delta_y$. Compressive spalling and shear cracking caused increasingly severe distress at the joint corners. Joint shear cracking progressed into all beams. Figure 8 shows crack patterns at the conclusion of the test.

Maximum joint shear, N-S, was 1510 kN and E-W was 1420 kN. These shears, like those in test 1-U-C, are approximately equal to that predicted by Meinheit and Jirsa's static strength formula. Full flexural yield of the beams was developed.

ANALYSIS AND COMPARISON OF RESULTS

The maximum loads and, therefore, joint shears sustained by the test specimens were governed by flexural yielding, either of the beams or of the column. With cycling at increased deformations, strength and stiffness reduced. The degradation can be attributed to the distress in the joint region, including shear cracking, bond distress, and accompanying shear and compressive spalling in or near the joint. Pronounced pinching of the load-deflection curves, even at low deformation levels, appears to be due to combination of joint shear and bond distress. Bond along the beam reinforcement through the joint was destroyed early in all tests, with the bars in effect sliding through the joint under continued loading. Much of the compressive distress observed in the beams and column under large deformation can be attributed to the deterioration of bond along the bars through the joint. Bars in tension were effectively anchored in the concrete compression zone of the member on the opposite side of the joint. This adds greatly to the compression in those zones.

Comparison: Unidirectional vs. Simultaneous Bidirectional

Although column yielding limited the strength of the biaxially loaded specimen (2-BS-C), the maximum resultant joint shear was 10 percent higher than that reached by the uniaxially loaded specimen (1-U-C). The rates of degradation of strength and stiffness of the two specimens were also about the same. For the specimens tested, therefore, it appears that the strength and stiffness characteristics of the joint under skew loading are approximately the same as under loading in a principal plane of the joint. Note that the specimens tested had square columns, uniform reinforcement, and nearly identical intersecting beams.

Comparison: Unidirectional vs. Alternate Bidirectional

Careful comparison of the load-deflection plots of Specimens 1-U-C and 3-BA-C shows that the strength and stiffness of the biaxially loaded specimen at any point in the loading history is approximately the same as if all of the loading had occurred in one plane only. Again, the double symmetry of the specimens tested must be noted.

CONCLUSIONS

1. Very high shears can be resisted by interior reinforced concrete beam-column joints, but strength and stiffness may deteriorate rapidly with load cycling, particularly with the first cycle at a particular amount of deformation.

2. Bond deterioration along reinforcing bars may occur early in the loading history and, combined with shear distress, may cause pinching of the load-deflection curves as well as early compressive distress in the joint region.

3. For the specimens tested, it appears that joint strength and stiffness characteristics are approximately the same for skew loading as they are for loading in the principal planes.

4. For the specimens tested, the behavior under alternating bidirectional loading appeared to be approximately the same as if all loading were applied in one direction only.

ACKNOWLEDGMENT

The support of the National Science Foundation through Grants ENV75-00192 and ENV77-20816 for this work is gratefully acknowledged.

REFERENCES

1. Meinheit, D. F., and Jirsa, J. O., "The Shear Strength of Reinforced Concrete Beam-Column Joints," CESRL Report No. 77-1, The University of Texas at Austin, January 1977.

2. ACI-ASCE Committee 352, "Recommendations for Design of Beam-Column Joints in Monolithic Reinforced Concrete Structures," Journal of the American Concrete Institute, Proc. V. 73, No. 7, July 1976.

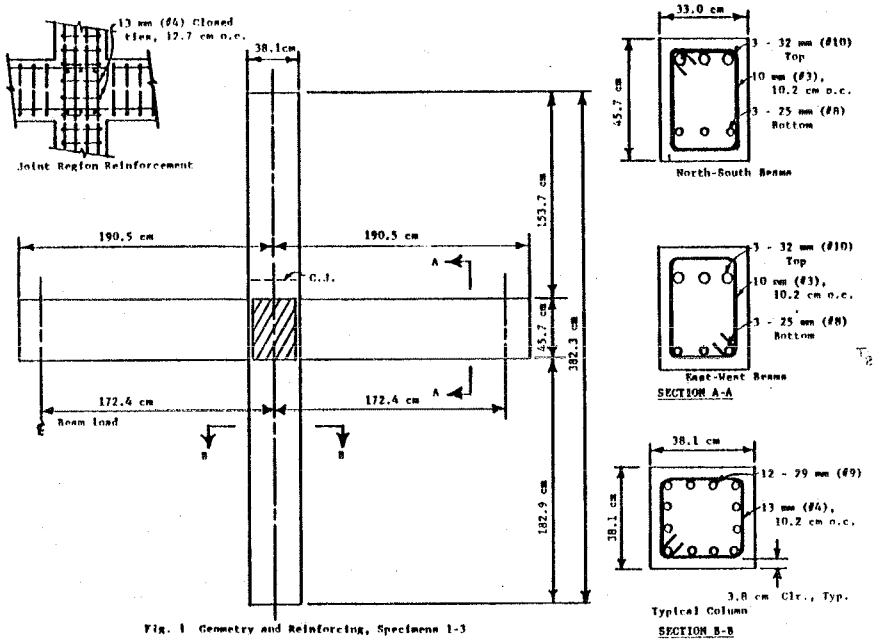

Fig. 1 Geometry and Reinforcing, Specimens 1-3

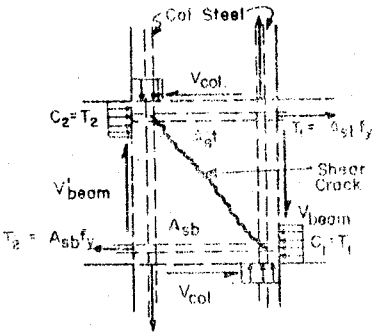

$V_{joint} = T_1 + C_2 - V_{col}$

Fig. 2 Joint Region Forces

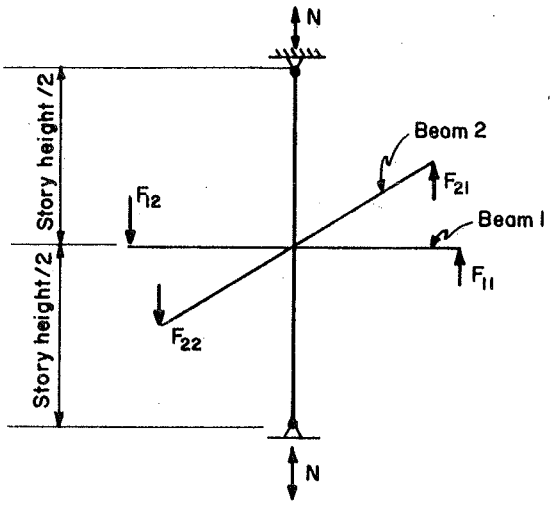

Fig. 3 Idealized Specimen Loading

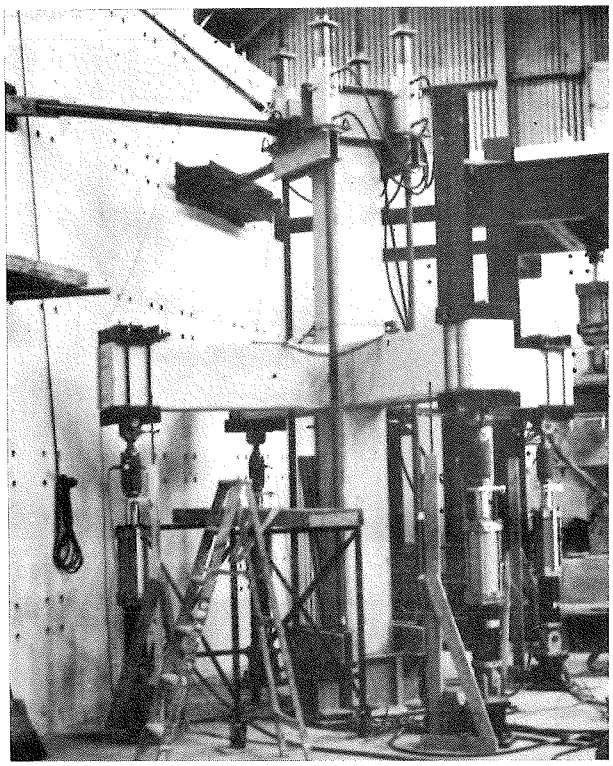

Fig. 4 Loading Apparatus

TABLE OF SPECIMENS

Specimen	f'_c, MPa	Column Axial Load, kN	Beam Loading	First Yield	Failure	Max. Resultant Jt. Core Shear
1-U-C	33	1335	Unidirectional N-S	Bms.	Jt.	1600 kN
2-BS-C	28	1335	Bidirectional Simul., NW-SE	Col.	Jt.	1760 kN
3-BA-C	30	1335	Bidirectional Alt., N-S, E-W	Bms.	Jt.	1510 kN

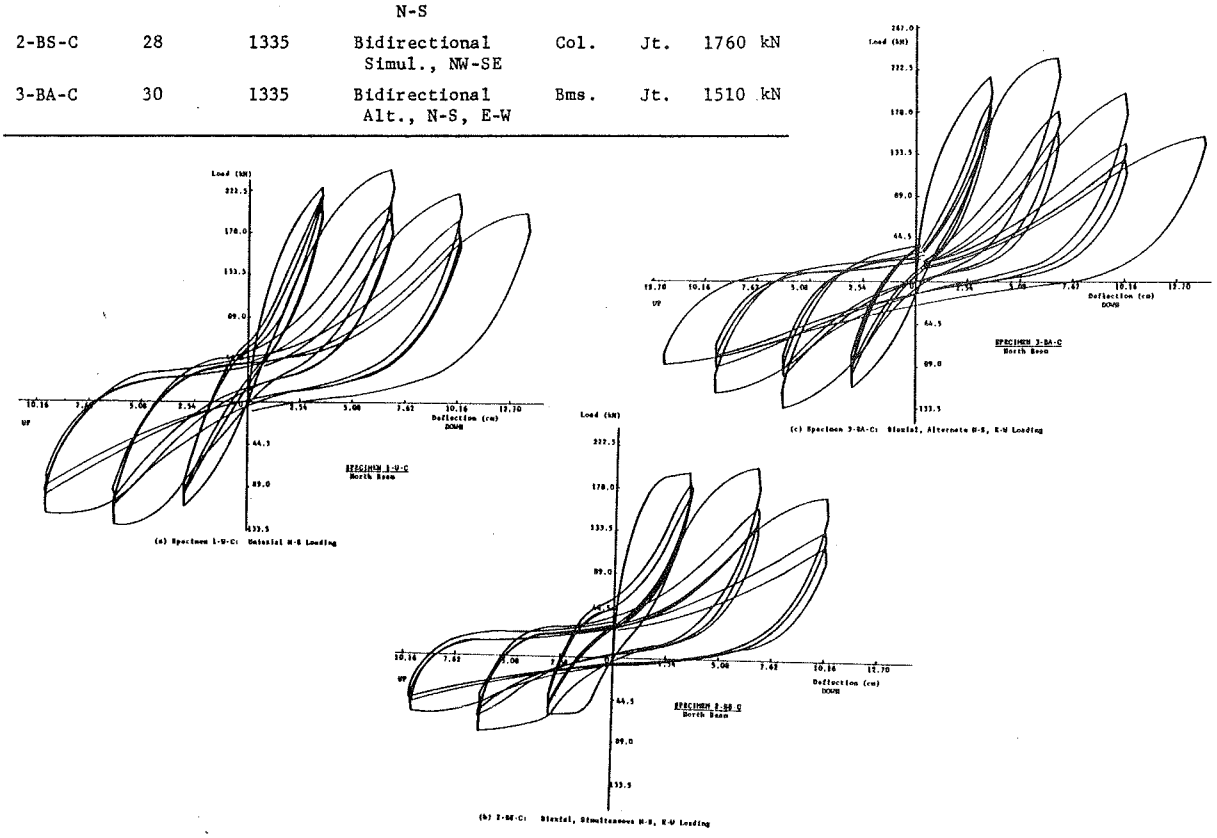

Fig. 5 North Beam Load-Deflection Plots, Specimens 1-3

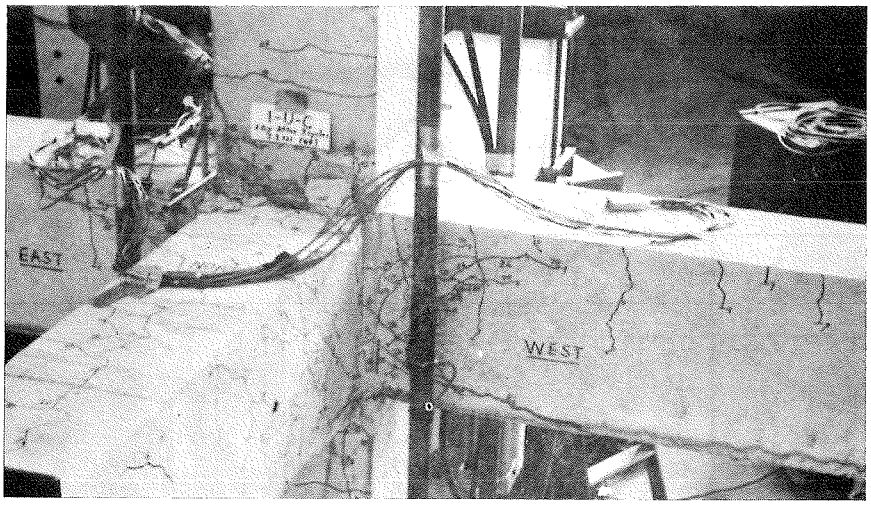

Fig. 6 Specimen 1-U-C

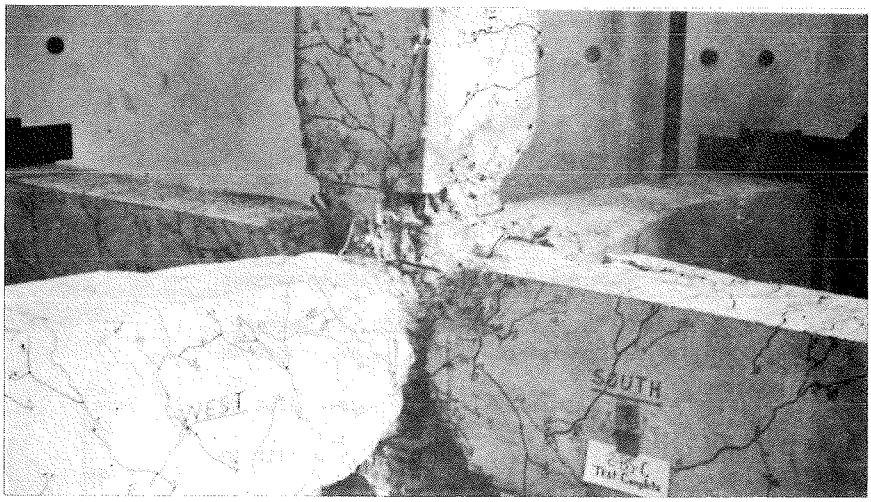

Fig. 7 Specimen 2-BS-C

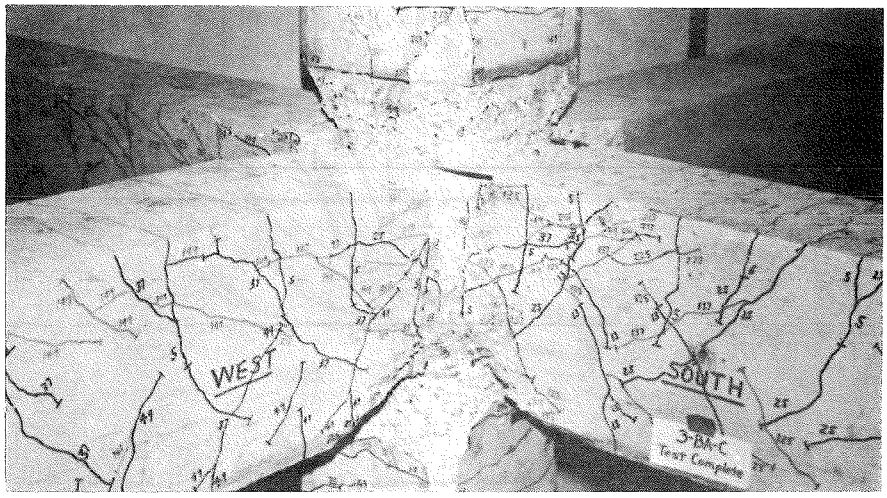

Fig. 8 Specimen 3-BA-C

DUCTILE BEHAVIOUR OF JOINTS IN PRECAST MEMBERS ASSEMBLED BY MEANS OF PRESTRESSING UNDER CYCLIC LOADING

José I. ALVAREZ BALERIOLA
Instituto Eduardo Torroja
Madrid, Spain

Hugo CORRES PEIRETTI
Instituto Eduardo Torroja
Madrid, Spain

Rafael FERNANDEZ SANCHEZ
Instituto Eduardo Torroja
Madrid, Spain

SUMMARY

Partial results are presented of an experimental program on full size prestressed precast concrete typical beam-column assemblies, under reversed cyclic loading representing severe earthquake action. The present study analyses some of the main variables of the characteristics of the mortar joint placed between the precast members.

It is concluded that, for the cases under study: the behaviour of mortar joint is satisfactory, large post-elastic deformations without a sensible loss of strength can be available, energy dissipation once structural damage has commenced may be considerable and a significant loss of stiffness is produced under cyclic loading.

RESUME

Ici sont présentés les résultats partiaux d'un programme expérimental à èchelle rèelle sur un ensemble poutre-colonne en bèton préfabriqué precontraint soumis à une charge cyclique alternèe qui représente una action sismique sévère. Les principales variables analysées dans cette étude ont été quelques caractéristiques du mortier du joint placé entre les éléments préfabriqués.

On en déduit que, pour les cas étudiés: le comportament du mortier du joint est satisfaisant, peuvent se présenter de grandes déformations post-élastiques sans perte sensible de résistance, la dissipation d'énergie, une fois commencé le dommage structural, peut être considérable et se présente une perte significative de rigidité sous charge cyclique.

INTRODUCTION

It is a well recognized fact that, if building structures are to survive strong-motion earthquakes at a low cost, they should be designed to possess ductility so as to dissipate seismic energy in the event of severe earthquakes (F.I.P., 1977).

It is also well known (Blakeley, Park, 1971),that in prestressed precast concrete building frames, the behaviour of joints is a critical factor affec-

ting the behaviour of the structures under seismic loading reversals and specially the behaviour of the joint assembly formed when precast members are post-tensioned together with mortar joints at the critical sections.

In May 1978 an experimental program on full size prestressed precast concrete typical beam-column assemblies, under reversed cyclic loading representing seismic action, was commenced at the Instituto Eduardo Torroja.

The program involves research on the behaviour of external as well as internal beam-column joints under quasi-static and dynamic reversed cyclic loading, paying special attention to ductility, energy dissipation capacity and deterioration of stiffness and strength.

The influence of a number of variable parameters is to be investigated, specially mortar joint characteristics, different levels of prestressing and amount of transverse reinforcement steel for concrete and mortar confinement. External loading will also be modified, since quasi-static and dynamic loads will be imposed on different units to observe the general behaviour from a more realistic point of view.

The program aims to develop a rational seismic desing procedure and a method for the evaluation of earthquake resistant properties for prestressed precast concrete buildings, taking into account ductility, stiffness degradation and energy dissipation considerations.

In this paper partial results corresponding to the two first units tested under quasi-static loading are presented.

OUTLINE OF TEST

General description

The beam-column test units represent, at full scale, the part of a multistory prestressed precast concrete frame. The units can be regarded as being the part of a plane frame between the points of contraflexure at a typical beam-exterior column joint.

The units were loaded by applying an axial vertical load on the columns, representing the loading due to the weight of the building above the particular assembly and the overturning moment on the structure due to the earthquake action, and by alternately repeated cyclic vertical loads on the beam ends representing the reversed shears induced by seismic loading, as shown in Fig. 1.

The constant axial force applied on the columns during the test was 861 kN which represents 0,5 of the balanced failure load for a column materials strength of f_c = 40 MPa and f_y = 420 MPa.

The column axis was held on the same vertical line during the test so that the applied beam-end loads induced reactive shears.

Beams and columns were cast separately and assembled together, with a moist pack joint of variable characteristics, placed between the elements by means of post-tensioned cables passing through the columns into an exterior anchor block before they were placed in testing position.

The longitudinal steel content was such that, for each unit, the flexural strength of the column section was greater than that of the beam section;in this way the plastic hinge was enforced in the beam rather than in the column.

Description of test units

Overall dimensions and detailing of beam and column sections are shown in Fig. 2, and described in Table 1. Material properties are also shown in Table 2. Beams were designed to possess aproximately the same strength for both units.

Prestressing tendons were formed by eight plain round high tensile wires, which were post-tensioned to aproximately 75 % of their yielding stress at transfer, and then grouted. Passive reinforcement in the beams was added for handling purposes. Columns were made of ordinary reinforced concrete.

In beams and columns, steel stirrups were placed to satisfy the shear requirements according to CEB-FIP Model Code. Special reinforcement of the beam hinge zone, the column joint core and its adjacent region was placed according to ACI-318-71.

Since one of the aims of the tests was to observe the behaviour of the moist pack mortar joint at the critical sections, the main difference between the test units were the mortar joint characteristics. Unit 1 had a 2, 5 cm thick mortar joint, while in unit 2, it was 10, 0 cm thick and had a steel stirrup placed in the middle. In both cases no attempt was made to improve the roughness of the interfaces of the precast members.

TEST PROCEDURE

Loading cycles

The test specimens were subjected to a number of series of quasi-static cyclic loadings which attempted to simulate the effect of a severe earthquake.

The loading sequence was monitored controlling the displacements at the beam ends as depicted in Fig. 3. $\delta_{y,nom}$ in this figure represents the beam end deflection corresponding aproximately to the design yield moment of the beams, this being computed using nominal strength of materials at the critical sections. The last series in test 1 and the four last series in test 2 were kept on the negative side because of the restriction of the testing apparatus.

Experimental procedure

In both units, the columns were axially loaded by means of a hydraulic jack. The variable load on the beam end was applied by means of a 50 kN double acting hydraulic jack controlled by servovalve while jack displacement and jack force were continuously registered by plotter.

Direct reading of hinge rotations was obtained from 1. v. d. t. supported

by small aluminum frameworks which were in turn attached to pins in the concrete. The rotations were continuously and intermitently registered.

The surface concrete strains in beams and columns were measured by means of mechanical and electrical resistance strain gages, deflections in beams and columns were obtained from dial gages and vertical mortar joint slipping was measured using optical devices. Induced reactive shears at the ends of the columns were registered by means of load cells.

TEST RESULTS

Fig. 4 shows measured beam moment at the critical section versus beam end deflection for both units and damage in both units at the peak of the last cycles.

During the first loading run, the opening of visible cracks were observed at the mortar joint interfaces due to the lack of tensile strength in both units, the recovery at the end of this first series of cycles was almost complete with negligible visual residual damage. Energy dissipation, measured as the area within the hysteresis loop for every cycle, stiffness and strength degradation, were also insignificant.

In the following loading series, after the moment capacities of the beams were reached and crushing of mortar and concrete had begun, that is, when the units behaviour was within the inelastic range, energy dissipation increased and degradation of strength and stiffness ocurred.

When reading the measurement devices at the end of every run, while peak deflections were maintained, a stress relaxation was observed.

Strength degradation was observed comparing the first cycles of the series whose deformation was over 2 $\delta_{y,\,nom}$, where the maximun strength was reached. This was also observed comparing the results of the different runs in any series, being more significative between the first and second cycles than between the last one.

Stiffness degradation was noticeable comparing the two firts cycles of each series, but almost inexistent between the second and the third. On the other hand, stiffness degradation was also significative when comparing the first cycles of every series.

Energy dissipation was important for large post-elastic deformations, specially during the first cycles of each series.

Moment-curvature diagrams, measured at the hinge zone are quite similar in shape to the beam moment-beam end deflection diagrams shown in Fig. 4. This may be due to the fact that most of the inelastic deformation of the assembly ocurred at the plastic hinge region.

It was observed that even though cracks in the mortar joints were wide open, over aproximately two-thirds of their section depth during the cyclic reversals, little amount of mortar was lost. Anyhow, unit 1, which had a narrower mortar joint without any binding reinforcement showed a more monolithic behaviour. In unit 2, which had a thicker mortar joint and a stirrup placed in the middle, damage was more concentrated at

the mortar joint since the spalling of mortar cover limited the progresi ve degradation of the concrete cover.

In unit 2, a noticeable vertical slip of 0,035 cm was observed in the c cracks formed between the precast beam interface and the mortar joint during the three last series of cycles. This slip was not registered in unit 1.

The columns and the column joint cores, apparently did not suffer any damage, as expected. Only the opening of very narrow flexure cracks was observed.

ANALYSIS OF TEST RESULTS

In both units aproximately the same beam flexural strength was measured at the critical section in the first loading runs into the inelastic range. The differences between these values and the theoretical flexural strengths are reasonable (6 %).

Strength deterioration, as stated above, which was observed in every series, was suppossed to be due to cyclic crushing of concrete and mortar, which led to a loss of material and a reduction in the sectional area. In order to explain the different moment value reached at the peaks of each cycle of any series, it was thought that concrete and mortar cyclic behaviour and prestressing steel Bauschinger effect were probably the most important reasons.

Stiffness deterioration mentioned above was thought to be due to the corresponding stiffness degradation of concrete and prestressing steel under inelastic cyclic deformation, and possible deterioration of bond.

During the first cycle of every series energy dissipation was far more important than for the second and third. This was probably due to the fact that during the first cycle after steel yielding was reached, a new progressive plastic deformation of prestressing steel ocurred, which did not happen for the following two cycles, and moreover stiffness deterioration of the concrete was more noticeable. In the next two cycles of any series, the prestressing steel showed a near elastic behaviour, so that area within the hysteresis loop was not enlarged because of this fact. Energy dissipation in the second and third cycles was almost identical, but always greater in the second cycles than in the thirds. This was probably due the characteristics of the cycles behaviour of the constitutive materials of the section.

It is apparent, from test results, that appreciable post-elastic deformations are available. In both units, the typical displacement ductility factors, proposed by SEAOC code and other international recommendations ranging from 3 to 5, were surpassed without significant strength degradation.

Altogether, a ductility factor based on the assumptiom of equal energy concept (Nakano, Okamoto, 1978), was obtained for both units. The results were $\mu_a = 7,0$ for unit 1 and $\mu_a = 8,3$ for unit 2.

Longitudinal strains measured on the members, allowed curvature dis-

tribution to be obtained. The equivalent plastic hinge lengths calculated as the width of the rectangle having the same area as the inelastic curvature distribution (Blakeley, Park, 1971), (Park, Paulay, 1975) were aproximately 26 cm and 22 cm for units 1 and 2 respectively, which is in good agreement with the findings of previous research (Blakeley, Park, 1971),(Park Thompson, 1977) indicating that the plastic hinge length is about one half the overall depth of the hinge region.

When deformations over 6 $\epsilon_{y,nom}$ were reached, after a considerable number of cycles, the slipping at the cracks between mortar and precast beam at the interfaces became more noticeable, which probably means that after a progressive deterioration of the friction shear resistant mechanism, dowel action seemed to become more significative.

CONCLUSIONS

1. Mortar joints between precast elements at critical sections showed a satisfactory behaviour under seismic type loading reversals.

2. Large post-elastic deformation and adequate ductility factors are available for precast concrete members assembled by means of prestrenssing even if pasive longitudinal steel at the critical sections is not available.

3. Energy dissipation is small as long as crushing of mortar and concrete and yielding of the prestressing steel are not enforced. Afterwards, during the inelastic range, a considerable increase is noticeable specially for the first cycles of every series.

4. After several series of loading cycles, a substantial stiffness degradation occurs. Strength deterioration was not important (less than 18 % at the end of test runs).

ACKNOWLEDGEMENTS

The financial assistance of the following organization is gratefully acknowledged:
Centro de Trabajos Técnicos-Stronghold, Aceros Azma, Sika.

REFERENCES

BLAKELEY, R.W.G., PARK. R.: "Seismic Resistance of Prestressed Concrete Beam-column Assemblies", ACI Journal, V. 68, Nº 9, September 1971, pp. 677-692.
NAKANO, K. and OKAMOTO, S.: "Test Results on Beam-Column Assemblies" Proceedings 8th Congress of F.I.P. Part 2, London, 1978
PARK, R. and PAULAY, T: Reinforced Concrete Structures, J. Wiley and Sons, New York, N.Y. 1975, p. 769.
PARK, R. and THOMPSON, K.:"Cyclic loand Tests on Prestressed an Partially Prestressed Beam-Column joints", ACI Journal, V. 22, Nº 5 September-October 1977, pp. 84-110.
Recommended Lateral Force Requirements and Comentary, Sismology Committee, Structural Engineers Association of California, San Francisco, 1973.

TABLE 1. TEST UNITS STEEL DETAIL

Unit	BEAN SECTION				COLUMN SECTION			
	Prestressed steel ρ_p	Non prestressed long. steel ρ_{sl}	Transverse steel ρ_{st}	Special reinf. at beam joint region ρ_{sconf}	Longitudinal steel ρ_{se}	Transverse steel ρ_{st}	Column Joint Core Reinforced	
							Longitudinal $\rho_{s,joint}$	Transverse $\rho_{s,joint}$
1	8 Ø 7 (0,273)	4 Ø 10 (0,279)	Ø 8-200[a] (0,2)	Ø 8-55[a] (0,731)	8 Ø 12 (0,861)	Ø 8-200[a] (0,2)	2 Ø 12	Ø 8-100[a] (0,4)
2	8 Ø 7 (0,273)	4 Ø 10 (0,279)	Ø 8-200[a] (0,2)	Ø 8-55[a] (0,731)	8 Ø 12 (0,861)	Ø 8-200[a] (0,2)	2 Ø 12	Ø 8-100[a] (0,4)

TABLE 2. MATERIAL PROPERTIES OF UNITS

Unit	Concrete compresiver cylinder strength at time of testing MPa	Mortar Compresiver strength at time of testing MPa	Prestressed Steel Ø mm	Prestressed Steel 0,2% Proof stress MPa	Prestressed Steel Tensile strength MPa	Non prestres. long st Ø mm	Non prestres. long st Yield strength MPa	Beam stirrups Ø mm	Beam stirrups Yield strength MPa	Column stirrups Ø mm	Column stirrups Yield strength MPa	Joint Core stirrups Ø mm	Joint Core stirrups Yield strength MPa
1	44,2	53,7	7	1.440	1.800	10 12	420	8	420	8	420	8	420
2	43,3	51,3	7	1.440	1.800	10 12	420	8	420	8	420	8	420

Fig. 2 Dimensions of the test units and detail of sections (cm)

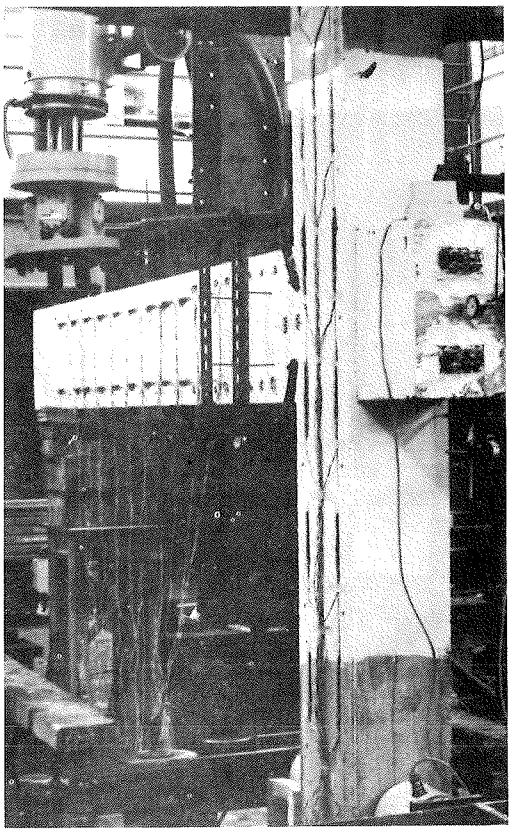

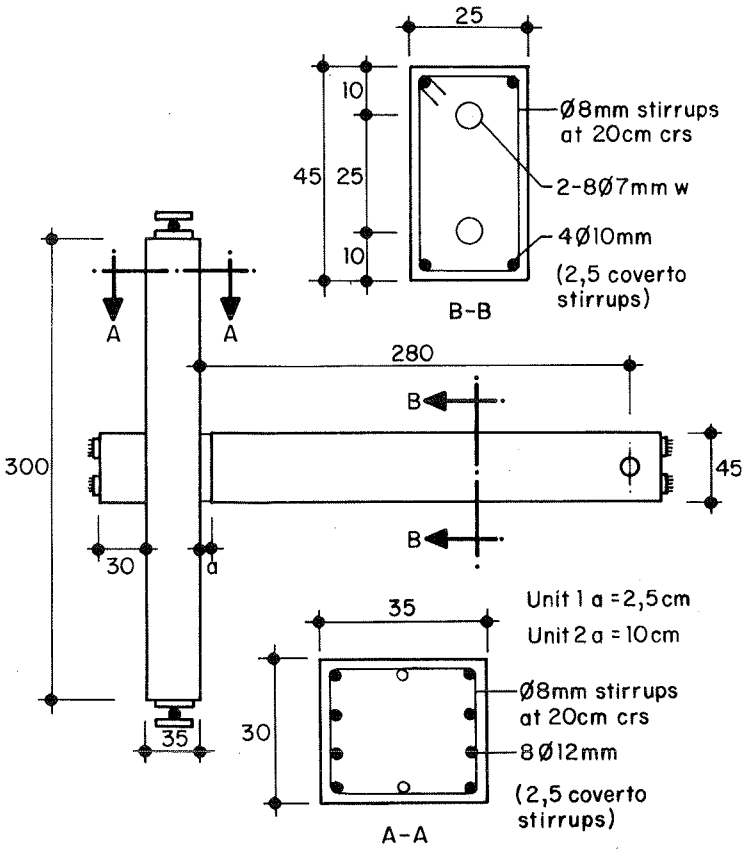

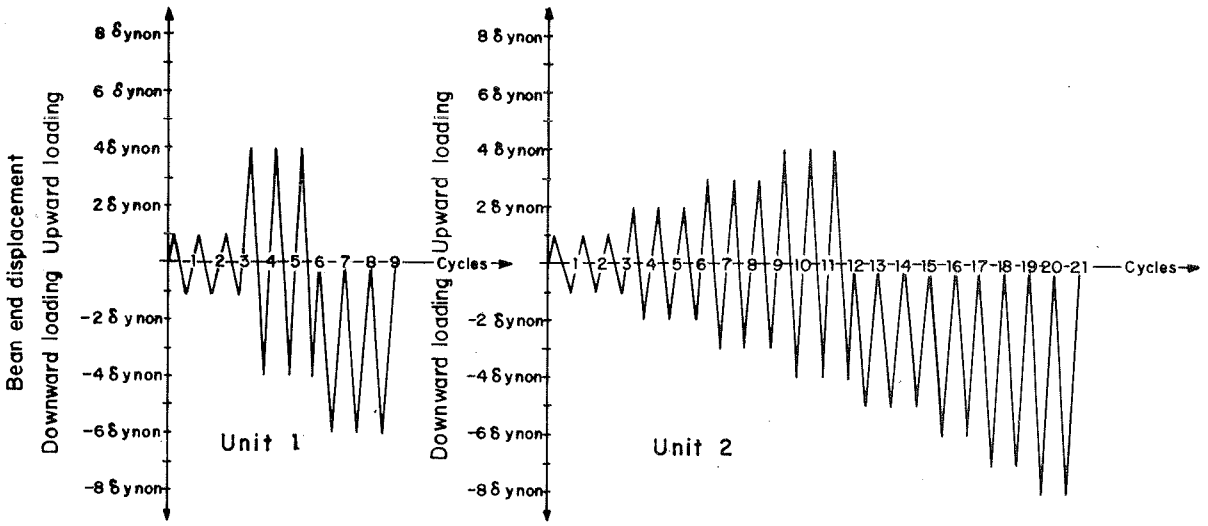

Fig. 3 Earthquake loading sequences.

Fig. 1 Unit under testing

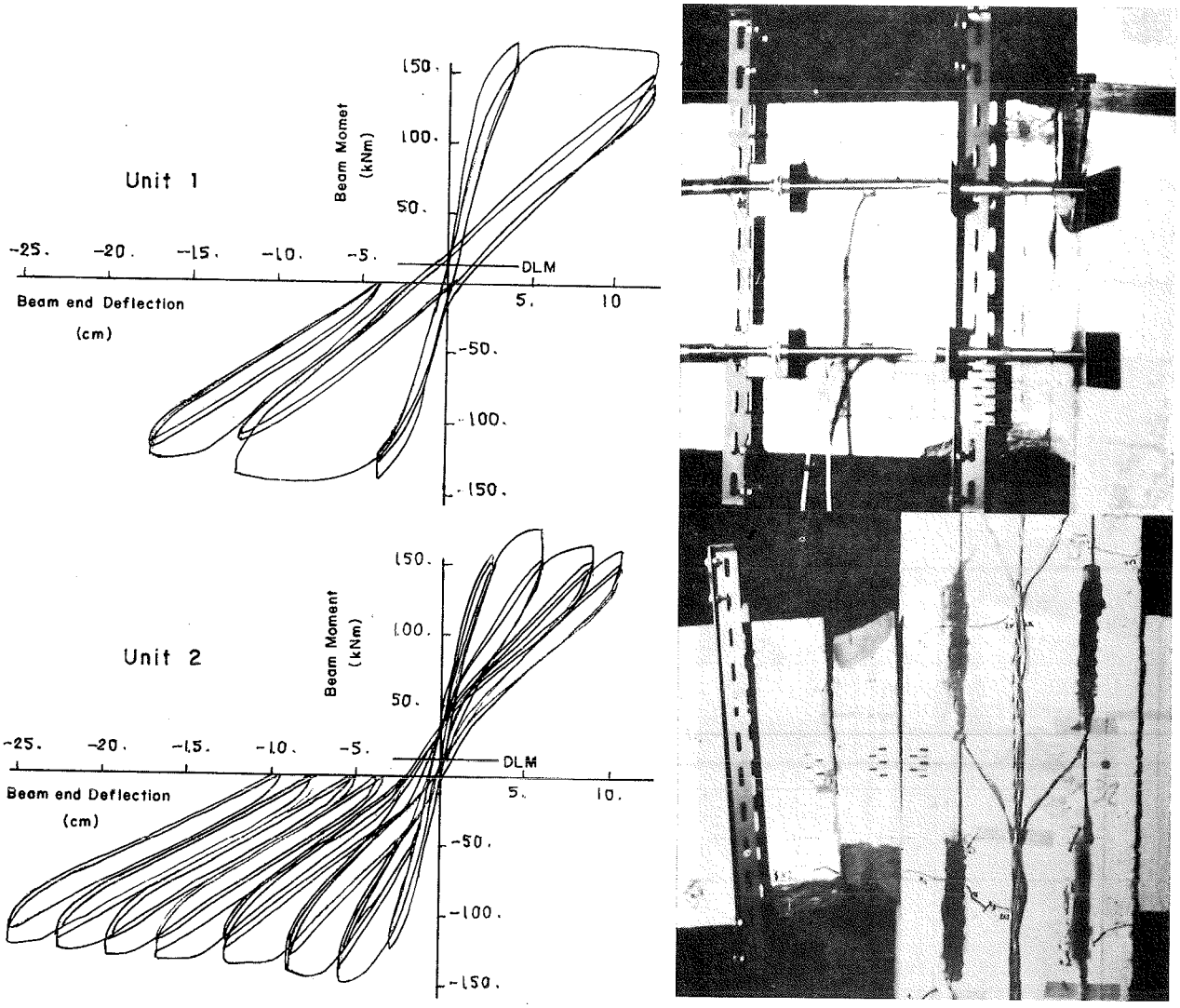

Fig. 4 Beam moment at the critical section versus beam end deflection and state of damage.

EXPERIMENTAL STUDY ON THE BEHAVIOUR OF REINFORCED CONCRETE BRIDGE PIERS UNDER SEISMIC ALTERNATING LOADS

Yoshio OZAKA
Tohoku University
Sendai, Japan

Minoru OHTA
Ministry of Construction
Tokyo, Japan

SUMMARY

The results of investigations of the influences of spacing and configuration of hoops on behaviour of bridge piers under seismic alternating loads using 6 single column bridge pier specimens of cross-sectional dimensions 40×80 cm and height of 155 cm are reported.

Les resultats d'etude exparimentale mené sur six modéles en béton armé avec la section 40×80 cm et la hauteur 155 cm sont reportés. L'etude s'est effectuée afin de préciser des effets du ecartement et de la configuration des armature transversales sur le comportement de la pile du pont en béton armé soumise à l'action alternative sismique.

1. BACKGROUND OF STUDY

Experiments to clarify behaviours of reinforced concrete columns during earthquake have chiefly been conducted concerning those in building structures. In experiments in the past, members with certain properties indicated in Row (1) in Table 1 have mainly been treated reflecting properties for columns in actual buildings. In contrast, ordinary single-column bridge piers are almost all of the properties given in Row (2) of Table 1, and differ considerably from building columns both structurally and mechanically. Experimental studies on such members have seldom been made.

Table 1. Comparison of Properties for Building Columns and Bridge Piers

	Structure	Shear Span Ratio	Steel Ratio (%) Tension Bar, p_t	Steel Ratio (%) Hoop p_w	σ_N = N/Ac (N/mm^2)	Remarks
(1)	Building Column	1~3	1~2	o.2~1.2	2~12	Principal ranges in past experiments
(2)	Bridge Pier	>3	<1	<0.1	1~2	Values for most actual bridge piers

It has been thought that evaluations of safety against earthquake of ordinary bridge piers are made satisfactorily by the seismic coefficient method, but in view of the fact that in recent earthquakes damages have frequently occurred to reinforced concrete bridge piers, particularly,

those of relatively low height, it is thought necessary to reexamine the earthquake resistance of structures of this type.

The study reported here has been made with the purpose of investigating the fundamental behaviours under cyclic loading of column members such as described above.

2. EXPERIMENT METHOD

(1) Specimens

The properties of specimens were determined as indicated in Fig. 1 refering to those of single-column bridge piers with a shear span ratio of about 4 Which are frequently used for bridges. The hoop ratio was selected as 0.04, 0.08 and 0.16 %. The configurations of hoops were the three varieties (single hoop, double hoop, and combined single hoop and cross ties) indicated in Fig. 1. It is specified in the standards of the Japan Society of Civil Engineers that hoop spacing should be not more than the minimum lateral dimension of the column. The hoop spacing of Specimen F corresponds to the maximum value (40 cm) according to this provision.

Materials used are as given in Table 2.

(2) Loading Method

Loading apparatus in Fig. 2 was used. Horizontal cyclic loading was performed under a condition of a constant axial force applied by a constant loading apparatus. In order not to restrict horizontal displacement of the column, a sliding plate using rollers was provided between the loading plate of the constant loading apparatus and the top surface of the column.

The horizontal load was applied at the height of 140 cm from the column base. Load was increased, at first, up to the theoretical yeild point of the column (load Py = 220 kN, displacement δy) based on the yeild point of longitudinal reinforcing steel, subsequent to which one-direction cyclic loading (Spacimen A) and cyclic loading (Spacimens B~F) with $2\delta y$, $3\delta y$..... as displacement amplitudes were performed. The number of repetitive loadings for δy, $2\delta y$, $3\delta y$..... was 10 times for each amplitude level.

(3) Measurements

Horizontal displacements of columns were measured by strain gauge-type displacement meters and extensions from footings of longitudinal bars at column bases by dial gaugetype displacement meters. Strains in longitudinal bars and concrete at column bases, and strains in the hoops nearest the column bases (the second hoop also in case of Spacimen C) were measured by wire strain gauges.

3. EXPERIMENTAL RESULTS

(1) Strength and Deformation Capacity

The hysteresis loops of all of the specimens are shown in Fig. 3, and the envelopes of the loops in Fig. 4.

Specimens B to E showed stable loops up to loading to $3\delta y$, but strengths dropped drastically during cyclic loading to $4\delta y$ and the ultimate states were reached. Specimen F indicated stable loops up to loading to $2\delta y$, but strength dropped while loading to $3\delta y$, and after 10 cycles of the

loading, decreased to approximately one half of Py, and nearly reached the ultimate state. Specimen A loaded in one direction, reached a maximum load (261 kN) during loading to 7δy, subsequently dropping to Py while loading to 11δy, and after 10 cycles of loading to 12δy, fell to approximately o.7Py.

With the envelopes in Fig. 4, the maximum displacement corresponding to the strength being maintained at the level not less than Py is defined as ultimate displacement δu, and the ratio to δy, δu/δy, is defined as ductility factor. Then the ductility factor was 3 for specimens B to E and 2 for Specimen F, while that for Specimen A was 11. This result indicates that ductility factor is greatly lowered in case of load reversals as compared with one-direction loading.

The theoretical value (1) indicated in Fig. 4 is a value, δ_1, determined by elasto-plastic calculations of horizontal displacement due to bending deformation of the column. The theoretical value (2) was obtained considering δ_1 and the displacement accompanying rotation of the column due to extension, Δ, of longitudinal bars from footings. In this case a triangular distribution of bond stresses in the footings was assumed. The theoretical value (3) is a value considering 2Δ as the extension of reinforcement under cycling loading referring to the suggestion by Krawinker and Popov [1], in addition to δ_1. The theoritical values of ultimate displacement (points U_1, U_2 and U_3 in Fig. 4) are corresponding to the strain of concrete 0.35 %.

Measured displacements differed greatly from theoretical value (1) and indicate a trend closest to theoretical value (3). The extension of reinforcement measured after loading at δy reached close to 2Δ. As for horizontal displacements measured at mid-heights of columns, the values were close to the half of the displacements at the loading point in loadings to δy and 2δy. These facts indicate that the influence of the fixed end rotation due to the extension of reinforcing bars on yielding displacement of a column is extremely great.

The energy absorbing capacity of columns under load reversals were examined by the equivalent viscous damping coefficients, heq, obtained from the loops for the second cycles in Fig. 3, and the results as shown in Fig. 5 were obtained. In Fig. 5, it may be seen that heq is greater the larger the displacement amplitude with all specimens within limits of deformation not more than 4δy, and that Specimens C (closely spaced single hoops) and D (double hoops) have greater energy absorbing capacity than other specimens, while the capacity of Specimen F with wide hoop spacing is extremely small.

(2) Modes of Failure

The cracked states of columns after loading to 3δy are shown in Fig. 6. With Specimen A loaded in one direction, bending cracks produced during loading to δy grew in a slightly diagonal direction while loading to 2δy and 3δy. In Specimens B to E subjected to load reversals, in addition to bending cracks produced during loading to δy, diagonal cracks were developed from the longitudinal bar locations at column bases during loading to 2δy and 3δy, and during loading to 4δy, shear distortions gradually became greater and the ultimate states were reached. In Specimen F, when shear distortions suddenly increased during loading 3δy, simultaneously indicated development of cracks along longitudinal bars and reached the ultimate state.

With specimens subjected to load reversals, cracks went completely through at column bases, during loading to δy, and it was observed that crack opening were enlarged as displacement amplitudes were increased.

For example, in the case of Specimen C, the average crack openings after loading to 2δy and 3δy were 1.30 mm and 1.67 mm, respectively. From this fact, it is considered that cracks which are opened during loading to δy could not close in the earlier stage of each cycle of loading to 2δy, so that the shear force carried only by the dowel actions of the longitudinal bars, then the diagonal cracks described above were developed.

As described above, in the cases of the columns considered here, the modes of failure differed for one-direction cyclic loading and load reversals, and in case of load reversals, it is clear that diagonal cracks which develop more prominently the larger the deformation have a dominant influence on strength and ductility of columns. Therefore when the safety against earthquake of such columns are to be examined through calculations based on the P-δ model of one-direction loading, it is necessary to consider the influence of reduction in strength and ductility under load reversals.

(3) Strain of Reinforcing Steel

As illustrated in Fig. 7, strains in longitudinal bars at column bases indicated, stable historys during loading to δy, and the strains suddenly increased during the first cycle of loading to 2δy.

The strains in legs parallel to the direction of horizontal load of rectangular hoops are indicated in Fig. 8. Strains in outer legs of the hoop at a height of 20 cm from the column base in Specimen C and of the hoop at the same position in Specimen D, during loading to 3δy, were gradually increased up to the yielding strain (approximately 1.5×10^{-3}) with development of diagonal cracks and they reached to yielding at the earlier stage of loading to 4δy. In Specimens B and E, the strains remain roughly below 1×10^{-3} during loading to 3δy, and they drastically increased to the yielding during loading to 4δy. On comparison with the hysteresis loops in Fig. 3, it may be clearly seen that the sudden decreases in column strength during to 4δy corresponds with yielding of hoops.

With Specimen F, since the positions of hoops are distant from the diagonal cracking zone, the strains at hoops are extremely small compared with the other specimens.

On comparisons of the 3 specimens of C, D and E with identical hoops ratios, it may be said that double hoops (D) or closely spaced single hoops (C) are more effective than a combination of single hoops and cross ties (E).

The strains in legs perpendicular to the horizontal load increased suddenly after the rapid increases in strains at legs parallel to the horizontal load occured. This was clearly due to pressure brought about by deterioration of concrete surrounded by hoops, and it was observed that legs which were straight at the beginning had been considerably bent at the ultimate stage.

4. CONCLUSION

From the results of cyclic loading tests of reinforced concrete column having cross sections of 40 × 80 cm, shear span ratio of 3.5, longitudinal steel ratio of 0.82 %, and varying ratios and shapes of hoops, the following may be pointed out as suggestions for examining earthquake resistance of such columns:

1) The influence of the extension of longitudinal bars from footings on the lateral displacement of single-column-bridge piers under load reversals is extremely great.

2) The ductility factors of the columns under load reversals are greatly decreased as compared with the case of one-direction loading. It is necessary to consider the influence of the reduction in strength and ductility under load reversals when the safety against earthquake of such columns are to be examined through calculations based on the P~δ model of one-direction loading.

3) In so far as the strength of a column is adequately maintained, the energy absorbing capacity of the column tends to be greater the larger the displacement amplitude.

4) The hoop spacing not less than the minimum lateral dimension of the column may not be adequate for this type of columns. The maximum spacing may be desirable to be not more than half of the minimum lateral dimension of the column. With regard to the shapes of hoops, double hoops or closely spaced single hoops seem to be more effective rather than combined single hoops and cross ties, if the hoop ratio is to be constant.

5) It is necessary hereafter to further aim for accumulation of experimental data with respect to cases where specifications of columns are differed in various ways. Still further, it will be necessary for more detailed investigations to be carried out on the behaviours of anchorage zones in footings of longitudinal bars of columns.

REFERENCE

1 H. Krawinkler and E. P. Popov: Hysteretic Behaviour of Reinforced Concrete Rectangular and T-Beams, 5th World Conference on Earthquake Engineering, 1973.

TAB.-2 MATERIALS

REINFOR-CING BAR		GRADE	σ_{sy} (N/mm^2)	σ_{su} (N/mm^2)	ELONGATION (%)				
	MAIN BAR	SD-30, D19	373	540	28				
	HOOP	SR-24, ø9	380	500	33				
CONCRETE	MATERIAL	Cement : High-early-Strength Portland Cement Aggregate : Natural Sand and Gravel							
	MIX	M.S. OF GRAVEL	SL.(cm)	W/C (%)	S/a (%)	MATERIAL (N/m^3)			
						C	W	S	G
		25	8±2	65	45	2.49	1.62	8.56	10.76
	STRENGTH	σ_c = 28.4~31.0 N/mm^2, AVE. 29.2 N/mm^2 (6 Specimens)							

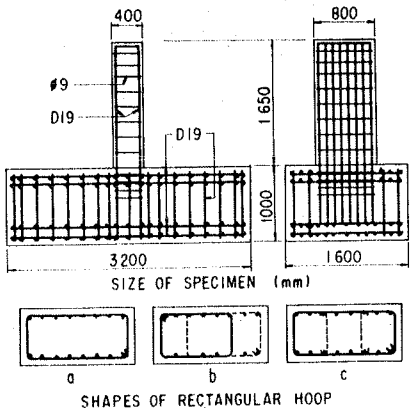

SPECIMEN	SHEAR SPAN RATIO	HOOP SPACING (cm)	HOOP RATIO p_w(%)	SHAPE OF HOOP	LONGITUDINAL BAR RATIO p_t (%)	LOADING HISTORY*	LOADING $\sigma_N = N/Ac$ (N/mm²)
A	3.5	20	0.08	a	0.82	I	1.0
B		20	0.08	a		II	
C		10	0.16	a			
D		20	0.16	b			
E		20	0.16	c			
F		40	0.04	a			

* LOADING I : ONE DIRECTION: 10 CYCLES AT $\delta_y, 2\delta_y, 3\delta_y, \cdots$
LOADING II : REVERSAL : 10 CYLES AT $\delta_y, 2\delta_y, 3\delta_y, \cdots$

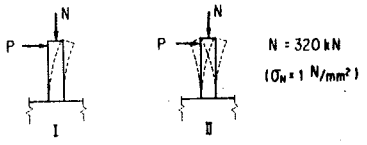

Fig.-1 Test Specimens

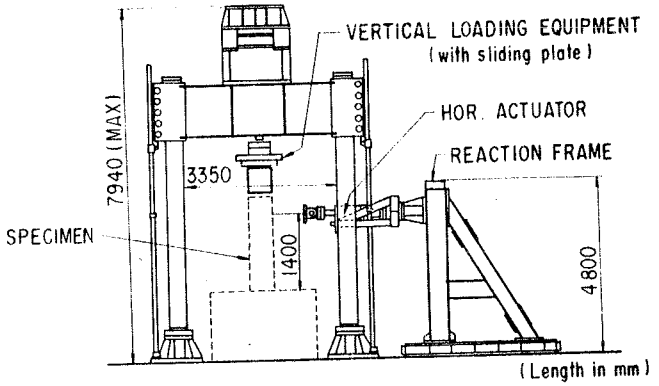

Fig.-2 Test Set-up

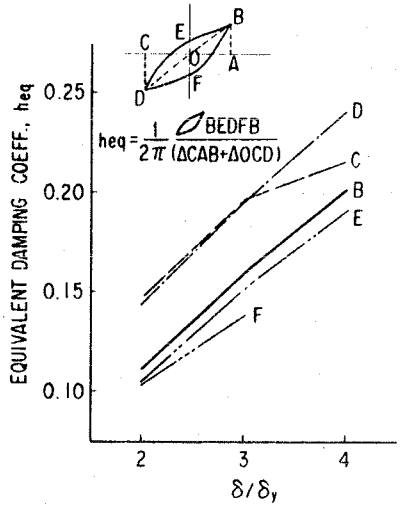

Fig.-5 Equivalent Damping Coefficient

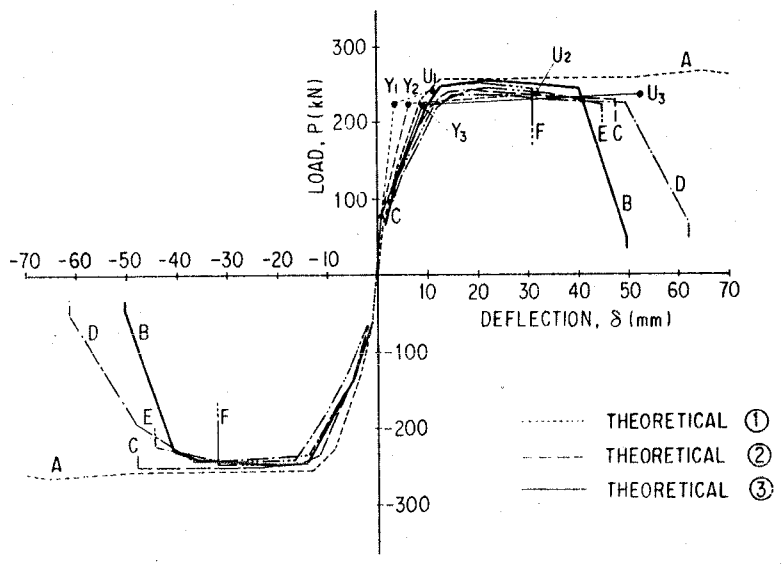

Fig.-4 Envelop of P~δ Diagram

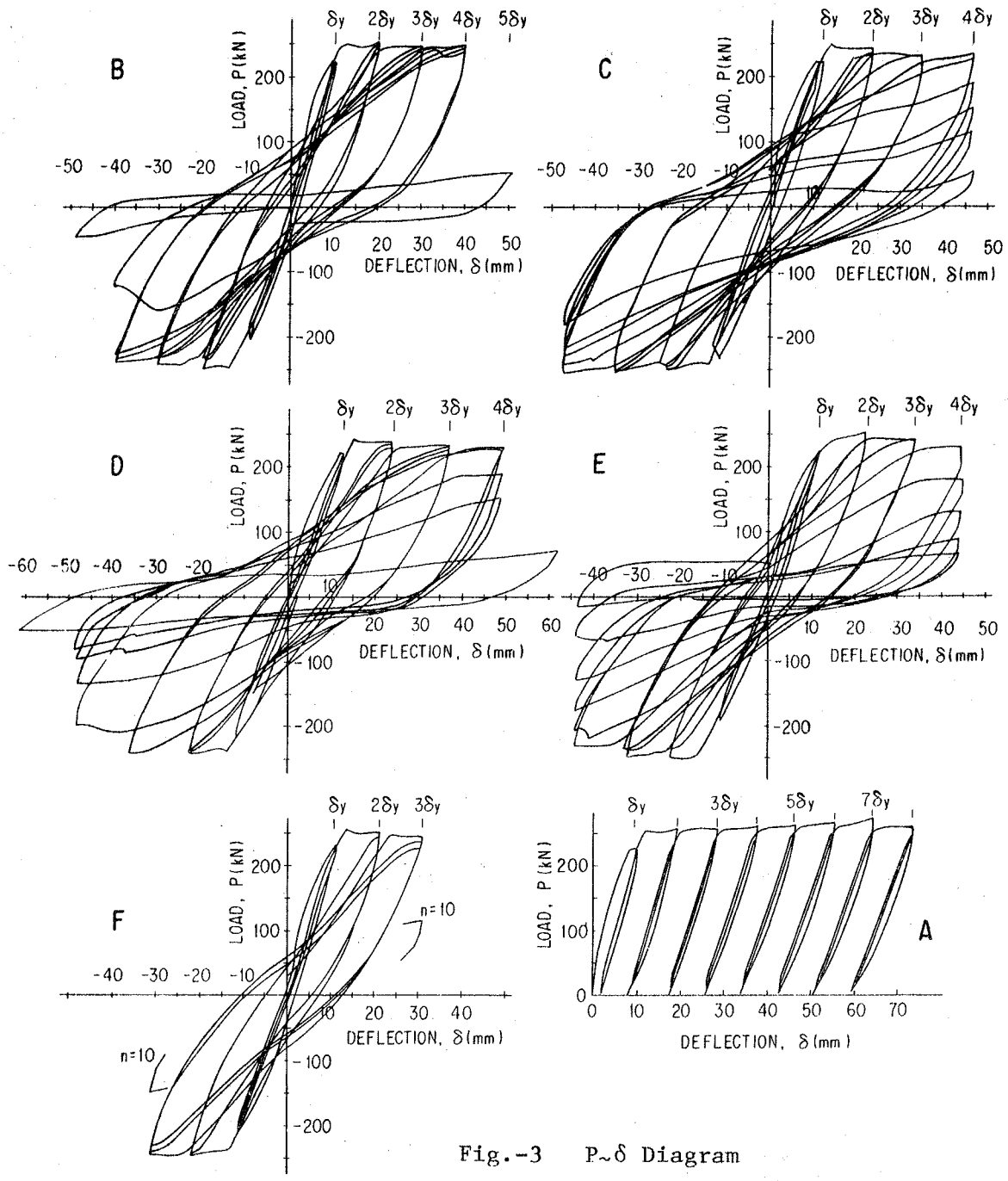

Fig.-3 P~δ Diagram

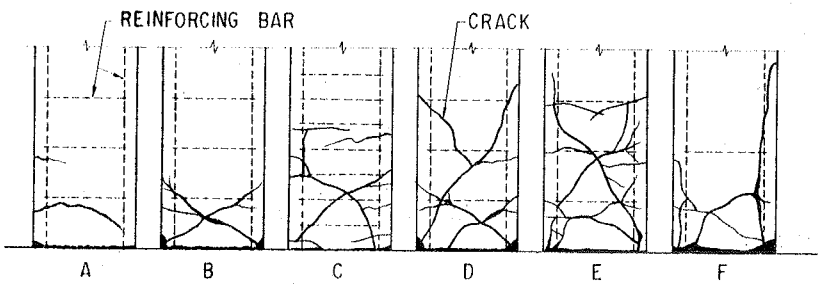

Fig.-6 Cracks after 10 cycles at 3δy

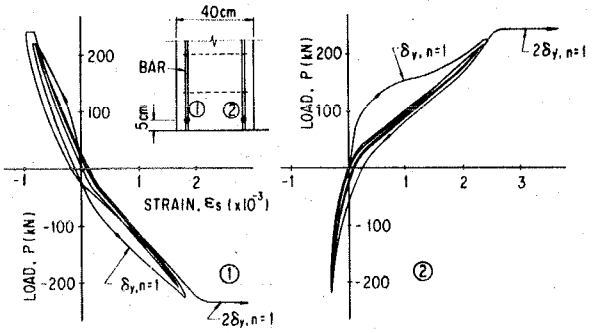

Fig.-7 Main Bar Strain
(Spe.-C Reversal at δy)

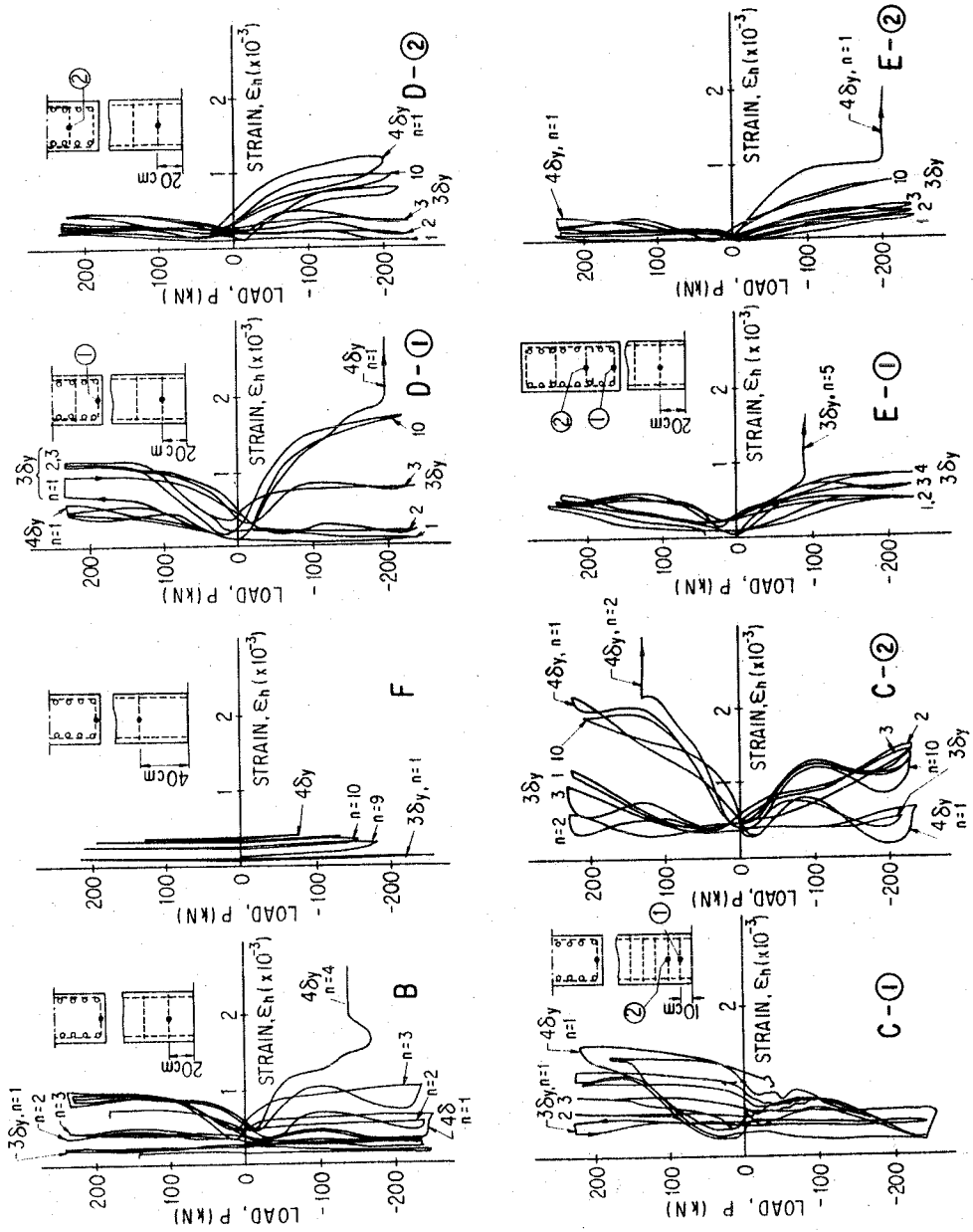

Fig.-8 Hoop Strain

TEST ON REINFORCED CONCRETE MEMBERS REPAIRED FOLLOWING DIFFERENT TECHNIQUES AFTER HEAVY DAMAGE

A. SAMUELLI FERRETTI
Istituto di Scienza delle Costruzioni
Roma, Italy

SUMMARY

Reinforced concrete members, kept under constant axial load during their whole test-history, were subjected to a first series of alternate bending cycles; a repair followed, and a second series of bending cycles. The bending was pushed well beyond yielding of steel and first crushing of concrete, as it happens during violent earthquakes.

Three different repair techniques were employed:

I) adequate lengths of longitudinal bars and stirrups were added around the damaged zone, and embedded in new concrete.

II) Short sections of bars were welded to the damaged ones, and the damaged zone was restored by means of new stirrups and cement plaster.

III) The damaged zone was restored by means of epoxy mortar.

The first technique behaved rather poorly, because the imposed rotation concentrated in a short zone and collapse followed after three cycles; the best results were given by the epoxy mortar, while the second technique gave intermediate results.

RESUME

Une charge axiale constante a été maintenue sur chaque spécimen an cours de tout l'essai; on a appliqué une prémière série de cycles de flexion jusqu'a l'étirage de l'acier et l'écrasement du béton, c'est a dire des dégâts tels qu'on a en suite de séismes violents.

On a réparé les dégâts, et l'on a ensuite appliqué une deuxième série de flexions.

Trois techniques de réparatios ont été appliquées.

I) Placement d'armatures longitudinales et transversales, suivi par remplissage en béton autour de la zone endommagée.

II) Soudure d'armatures longitudinales, placement d'étriers et application d'enduit en mortier de ciment.

III) Placement d'enduit en mortier epoxy.

La prémiere technique a donné de mauvais résultats, car la déformation s'est concentrée sur une courte étendue de la poutre et le spécimen n'a pu survivre que 2-3 cycles de flexion. La deuxième technique montra une meilleure resistance à la fatigue, et la troisième une résistance presque égale a celle de la poutre originaire.

The test specimens have been studied for a previous series of tests on plastic fatigue [1] - [2] of prismatical columns of concrete under axial load and alternate bending.

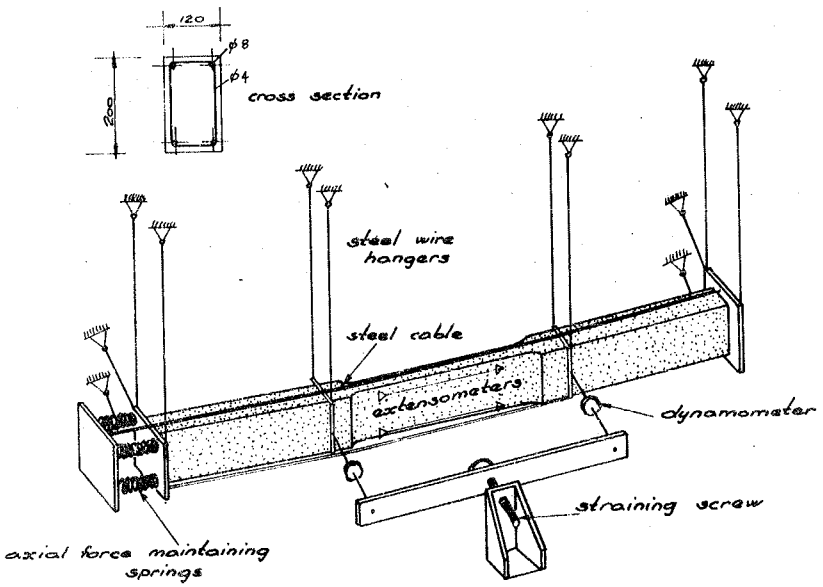

Fig.1 – Testing setup.

The testing arrangement is the usual one, of a beam subjected to two equal loads symmetrically placed about the middle section; the lateral parts subjected to shear have a stronger cross section with respect to the central part, in which the bending moment is constant. The specimen is instrumented in the central section of this part. The axis is placed horizontally while the beam is suspended on vertical hangers whose upper ends are free to move, following the large displacements imposed to the beams by means of an hand operated screw. The reacting forces are measured by means of inductive dynamometers, as shown in the figure (1.).

The cross section of the beam is 120 x 200 mm, the flexure is applied along the weak axis; longitudinal reinforcement consists of four 8 mm deformed bars, whose σ-ϵ diagram is shown in figure (2).

Stirrups of 4 mm diameter are placed at 50 mm spacings. Strength of concrete has an average value of 35,0 MPa, so that a mechanical reinforcement percentage of 15,7% is attained, while the geometrical one is of 0,83%.

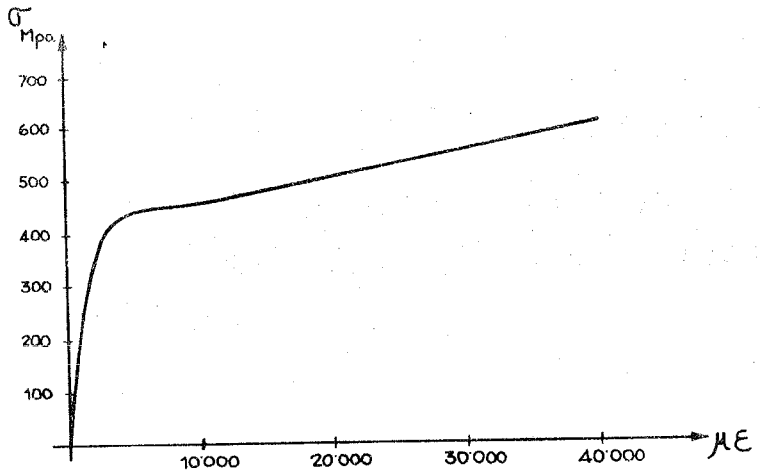

Fig.2 – Stress-strain diagram of the steel.

Axial force has been applied in the form of an external prestressing, by means of two steel cables co-axial to the beam, and kept in tension by the interposition of four helical springs. Loss of axial forced due to shortening of the specimen during the fatigue cycles did not reach 6% of the original value, which was of 96.000 N, corresponding to a stress of 4,0 MPa over the concrete section.

Measuring of deformation was made by means of two groups of inductive displacement transducers, placed at the central part of the specimen over a 360 mm base. The first group (four transducers at the corners of the cross-section) gives the different digital values of the single strains, recorded on tape, while the second group of two, placed along the flexure plane of the beam, gives directly the curvature on the abscissas of an analogue plotter. The output of the dynamometers placed on the stressing arm gives the ordinates on the same plotter.

The axial load has been applied at the beginning of the testing of each specimen, and its value controlled both trough the measure of the shortening of the springs and directly by means of a couple of dynamometers placed in series with the stressing cables. It is worth noticing that the axial force applied is 1,10 times larger than the one necessary to bring to yielding the longitudinal reinforcement; this value seems to have a definite meaning on the behaviour of the columns [2].

The series of cycles of alternate bending is therefore applied as follows:

– three cycles up to the maximum curvature, determined by the ratio:

$$\frac{\text{depth of the cross-section}}{\text{radius of curvature}} = \frac{h}{R} = \frac{120}{5000} = 0{,}024,$$

– Three cycles up to a curvature:

$$\frac{h}{R} = 0{,}012.$$

– Twenty cycles up to the maximum service bending moment, which, computed following the italian building code based on the allowable stresses, has a value of 2500 Nm.

After this first series of bending cycles, the measuring devices are disassembled and repairs take place, while the axial force is maintained.

It has to be pointed out that, as it can be seen from the photographs, the situation of the damaged zone is quite similar to that observed in columns of structures damaged by violent earthquakes.

It can be said, as a matter of fact, that the three well known stages of bending in reinforced concrete are observed, followed by a fourth one.

After the first stage (uncracked), the second (cracked) and the third (steel yielding), the last having the feature of a flattening out of the moment-curvature diagram, the fourth stage shows a well distinct falling branch, due mainly to crushing and spalling of the unconfined concrete, in spite of strain hardening of steel.

The maximum compressive strain of the concrete, measured locally by means of resistance strain gages, lies between 2000 and 3000 $\mu\epsilon$; at such values the strain ceases to increase, the concrete shows crushing, and spalling takes place, while the strain gage, if undamaged, comes back to zero strain.

As far as the steel in concened, the maximum strains are in the range of 17'000 $\mu\epsilon$. Cracks are formed at 100 - 120 mm spacings, and reach a maximum width of about 3 mm.

During the first cycle of curvature, maximum bending moment reaches values of about 8500 - 9500 N m, in good agreement with the theoretical one, which, computed following the C.E.B. recommendations, assuming a rectangular stress block, equals 8800 Nm.

Spalling of concrete reaches a depth of a little more than 20 mm; that means that between stirrups the remaining core is less than the confined one; thus, the cross sectional area of concrete is about halved.

Compressed bars are buckled, with a displacement of 1 ÷ 1,5 times their diameter.

During the cycles of imposed moment of service value no appreciable decay of the beam was observed; the maximum curvature reached was from 15 to 20 times larger than the one of the first cycle, in the uncracked stage.

Having thus completed the first series of bending cycles, repairs were provided, following three different techniques. A total of six specimens were tested, that is two for each technique.

I Technique. After an accurate cleaning of the exposed concrete, with removal of detached parts, four longitudinal 10 mm bars of 400 mm length were applied around the damaged zone, with new stirrups of 4 mm diameter and 30 mm spacing.

The characteristics of the embedding new concrete were as follows, per cubic metre of mix:

natural gravel 1 ÷ 8 mm,	0,800 m^3,
natural sand 0,3 ÷ 1,5 mm,	0,400 m^3,
cement of 425 kg/cm^2 type:	500 kg
water	250 kg

This concrete, vibrated, reached the strength of 17,2 MPa after three days, 26,0 MPa after 8 days. The sclerometric index (Schmidt) was of 38,5 at the time of the second series of bending cycles.

The repair resulted in a concrete "casing" having the overall dimensions of 179 x 240 x 480 mm.

After hardening of concrete the second series of bending cycles was imposed, up to the value of h/R = 0,024, that is the maximum one reached during the first series.

The resisting bending moments of the first cycle were larger than the ones of the first cycle during the first series, but their value decayed rapidly; during the third cycle failure in tension of the previously buckled bars took place, and the testing was stopped. As it could be easily foreseen, the deformation and the damage took place in short sections outside the reinforced "casing".

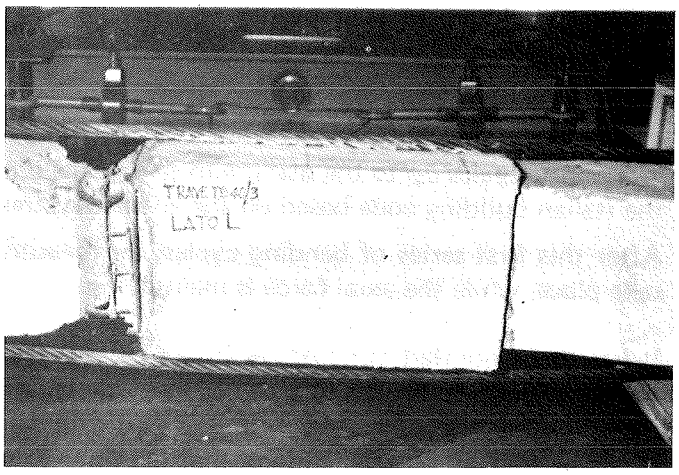

Fig.3 – I Technique.

II Technique. The repairs consisted of four lengths (150 mm) of 8 mm bars, welded on place along the buckled ones, and new 4 mm stirrups at 20 mm spacing. The new steel reinforcement was then embedded in mortar plaster. This mortar was the plastic one employed in quality control of the strength of

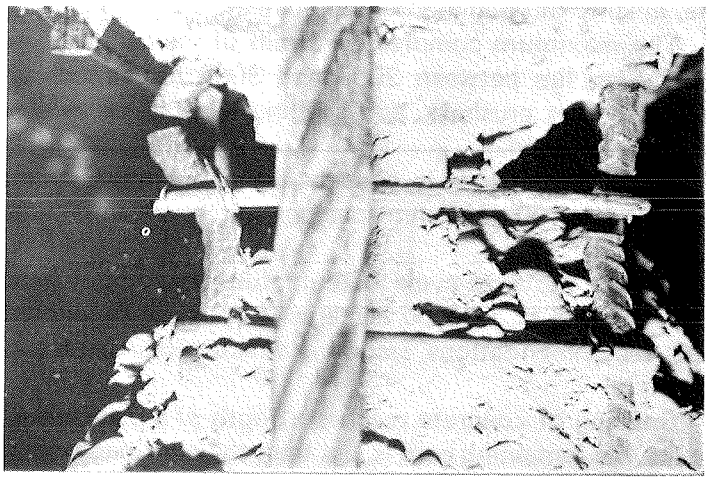

Fig.4 – I technique, after second series. Failure of a bar is visible.

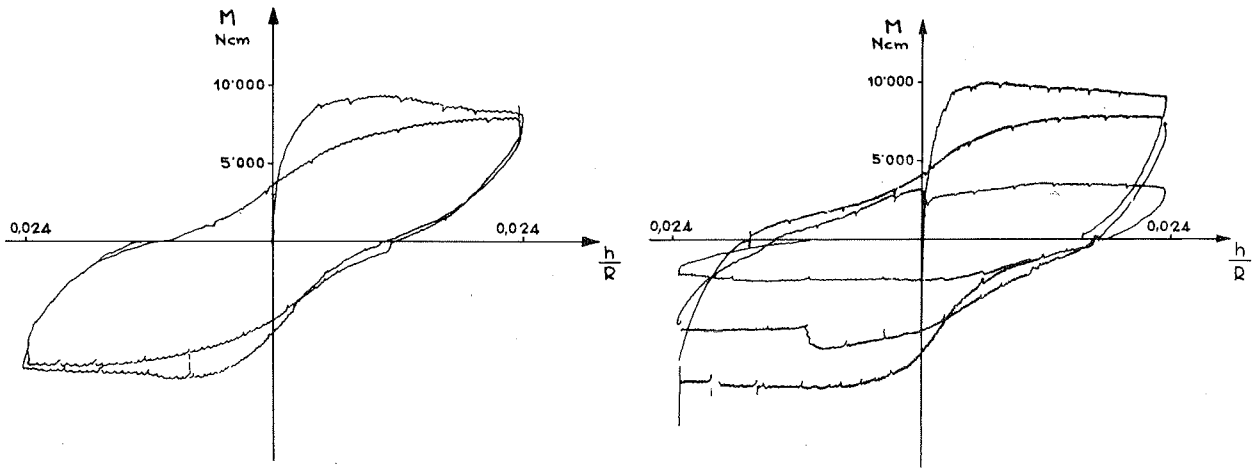

Fig.5 – I technique. Recorded moment-curvature cycles before and after repairs.

cements, that is a three to one mix of special sand (0,5 ÷ 1,5 mm) with 425 concrete, and a W/C ratio of 0,5. Average strength at 8 days was of 25,5 MPa, with a sclerometric index of 33,2.

The second series of bending consisted of three 0,024 h/R cycles, followed by twenty 2500 Nm cycles, and by as many 0,024 h/R cycles as it was possible. Damages took place at the ends of the repaired zone.

III Technique. A plaster of epoxy mortar was applied at the damaged zone, which had been previously cleaned and covered by a thin film of epoxy primer, still fresh when the plastering took place.

The mortar mix was as follows:

6 parts in weigth of quartz sand, composed by a fine (0,2 mm) and a coarse one (1,5 mm).

1 part in weigth of epoxy resin.

The resin was prepared by mixing 100 parts in weigth of CIBA BY 154 resin, with 35 parts of HY 2995 hardener. Average strength was of 68,5 MPa.

The stress strain diagram is given in Fig.11.

After repair strain history followed, equal to the one applied to the specimens repaired with the II technique.

In the figures 12 and 13 maximum resisting bending moments 0,24 h/R curvature are plotted against the number of cycles.

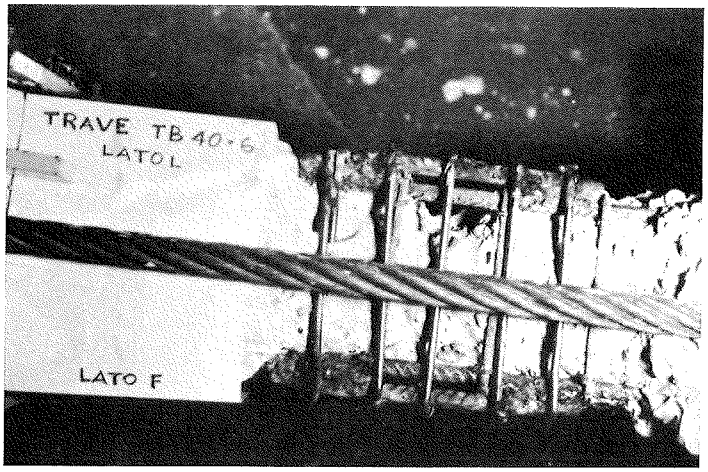

Fig.6 – II Technique. Welded bars and new stirrups are shown.

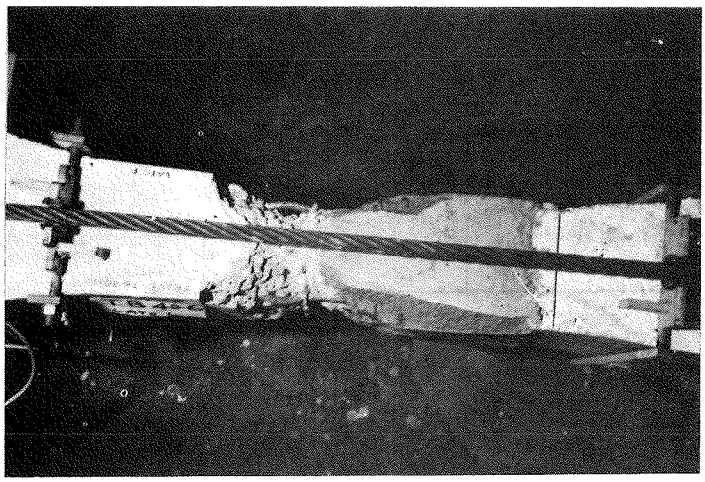

Fig.7 – II Technique. Damages after the second series of bending cycles.

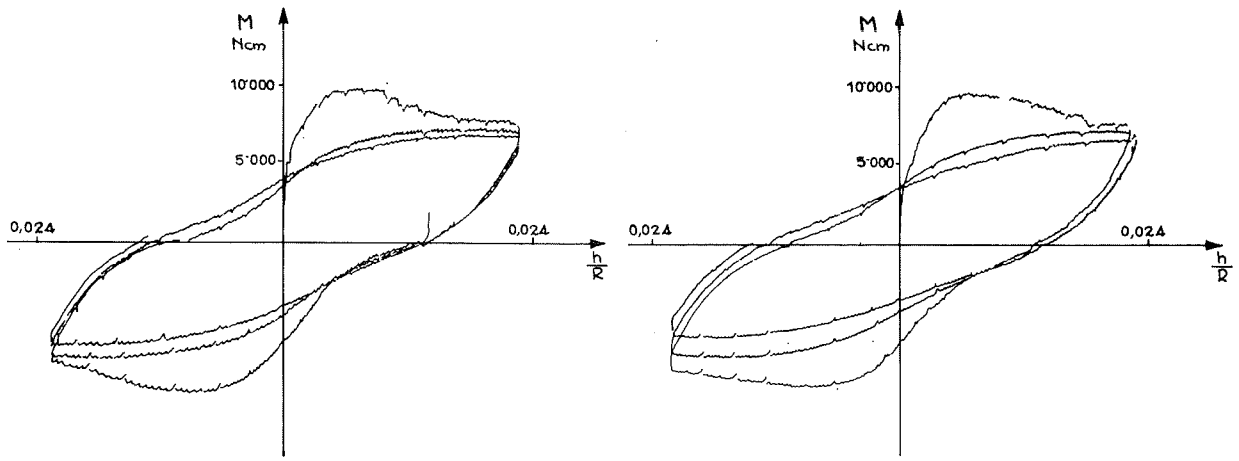

Fig.8 — II technique. Recorded moment-curvature cycles before and after repairs.

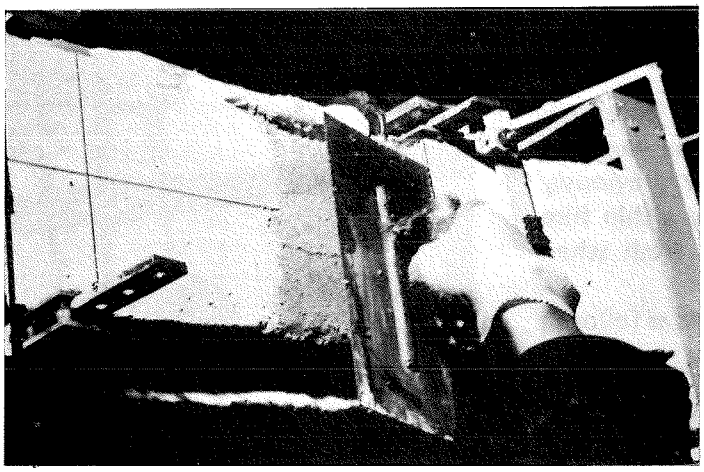

Fig.9 — III Technique. Plastering by means of epoxy mortar.

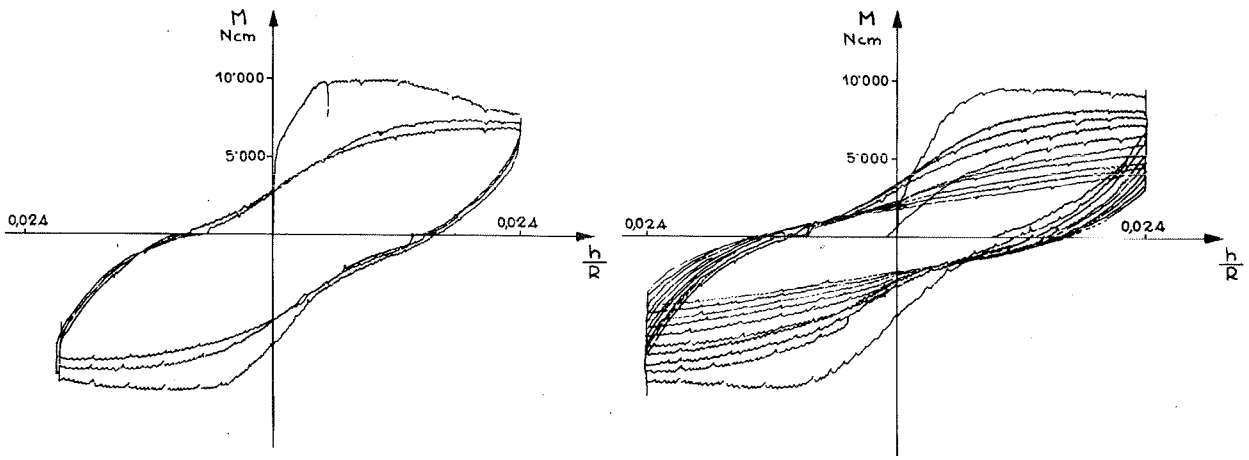

Fig.10. — III Technique. Recorded moment-curvature cycles before and after repairs.

It can easily be seen that the first technique is not apt to give a good resistance against fatigue; after three cycles the flexural strength has fallen to less than 1/3 of the original one.

The second technique shows a valuable improvement of behaviour, because as many as 6 cycles are possible; it has also the advantage of needing only a welding equipment and an usual cement plaster, that is simple means usually available in building yards.

The third technique is by far the best one as long as results are concerned; it needs special means, but no reinforcement is added. The spalled parts of concrete are simply replaced by the epoxy mortar. Also curing is very rapid, because sufficient strength is obtained after 12 hours.

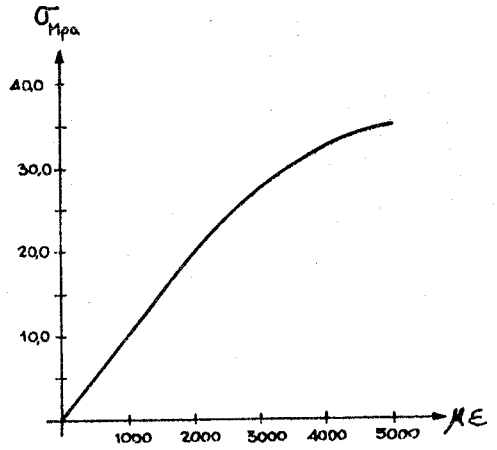

Fig. 11 – Stress-strain diagram of the epoxy mortar.

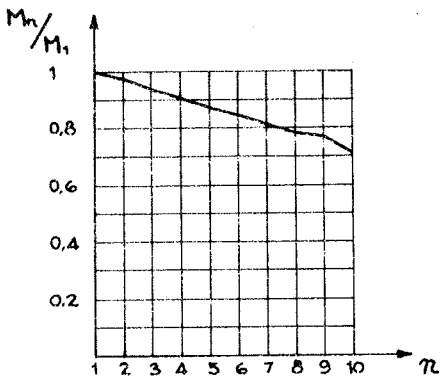

Fig. 12 – Decaying of unrepaired specimen.

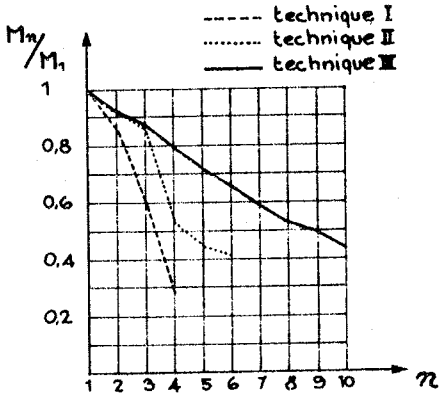

Fig. 13 – Decaying of repaired specimens.

It is of the utmost importance, anyway, to avoid a sharp increase of the cross section, because the strain concentration causes a rapid decaying of the strength.

AKNOWLEDGEMENTS

The author wishes to thanks all the technicians of the laboratory, who carried out efficiently the various chores of the testing, and especially M. Camilli, M. Cortella, M. Purgatorio, M. Umile and M. Zambenedetti.

REFERENCES:

[1] A. Parducci – A. Samuelli Ferretti
Prismatic reinforced concrete members: alternate bending beyond the yielding of the reinforcement under axial loads. Vth world conference on earthquake engineering, Rome 1973.

[2] A. Parducci – A. Samuelli Ferretti
Flessione alternata su elementi di cemento armato sottoposti a carico assiale. Indagine sperimentale. Report of the Istituto di Scienza delle Costruzioni. Fac. di Ingegneria - Roma 1974.

Rome, jannuary 1979

REPEATED-LOADING EXPERIMENTS ON R.C. ELEMENTS REHABILITATED WITH RHEOPLASTIC MORTAR

G. AUGUSTI
University of Florence
Florence, Italy

F. FOCARDI
University of Florence
Florence, Italy

E. MANZINI
University of Florence
Florence, Italy

M. VALENTE
Mac Mediterranea S.p.A.
Treviso

SUMMARY

Out of a series of 24 full scale models of a r.c. column and its joint to a rigid beam, the first four specimens have been tested under constant axial load and a cycling horizontal displacement process, simulating strong earthquake action, which produced heavy damage and a marked reduction of the load-carrying capacity. Then, the specimens were repaired, by means of a special premixed rheoplastic concrete (EMACO S 88), without variation of dimensions, but otherwise adopting different details; and tested under the same loading process. The responses of the virgin and repaired specimens are discussed and compared.

RESUME'

On expose les résultats experimentaux des essais sur quatre (les premiers d'une suite de 24 modèles) piliers en beton armé, encastrés à l'extrémité inférieure dans une poutre rigide, chargés par une force axiale constante et soumis à un déplacement horizontal assimilable à un fort tremblement de terre. Ces sollicitations causaïent de graves dommages et une considérable réduction de la capacité portante. Enfin les modèles étaient réparés par un beton spécial preconfectionné (Emaco S 88), sans augmenter leurs dimensions originales, adoptant différentes méthodes de reparation pour l'acier, et étaint de nouveau soumis au méme essai. On compare enfin les résultats sur les modèles neufs et sur ceux soumis à la reparation.

1. INTRODUCTION.

In the last few years, a number of reinforced concrete structures, severely damaged by earthquakes or other exceptional loads, have been repaired by the reconstruction of the damaged zones: some laboratory tests (e.g. Gulkan, 1977; Lee et al., 1977; Tassios et al., 1977) have shown that in this way it is possible to obtain resistances of the repaired structure comparable to those of the original one, with respect to both static and repeated loads.

Among the most successfull materials used for this type of rehabilitation, there are special premixed rheoplastic concretes, which, thanks to their specific chemical and mechanical properties, allow a quick and easy treatment, and a rapid restoration of strength: also, the original structural dimensions can be maintained, if so required by architectural and/or functional reasons. This specific technique has been recently applied in Friuli,

where many buildings, repaired after the May 1976 shocks, survived satisfactorily the strong September shocks (Il Calcestruzzo oggi, 1976-77).

However, it appears that the reliability of repairs with rheoplastic concretes has never been substantiated by laboratory experiments, nor the advantages, difficulties and problems connected with different alternative repair and rehabilitation techniques have ever been systematically compared. Therefore, in the Structural Laboratory of the Civil Engineering Department - University of Florence, a systematic experimental investigation on the techniques of repair of r.c. structures has been started.

The results of the first group of tests, performed on r.c. portal frames repaired by rheoplastic concrete without addition of reinforcement and loaded by a sinusoidal horizontal force, have already been reported (Augusti et al., 1978): they can be regarded as a preliminary confirmation of the effectiveness of the investigated repair technique. However, apart from the small number of tests performed, the writers feel that the practical validity and significativeness of the results obtained is limited by the fact that the axial loads in the specimen columns were much smaller than in actual buildings: indeed, the details observed in the experimental rupture zones are remarkably different from those observed in many real instances (in particular, because of the absence of buckling waves in the longitudinal reinforcement). Moreover, the four beam-column joints in each frame did not fail simultaneously and behaved differently one from another, which does not allow a clear distinction between primary and secondary phenomena. Also, the loading history (a number of slow oscillations at constant amplitude, then other cycles at a larger amplitude, and so on up to heavy damage of the specimen), although of the same type used in most similar experiments,

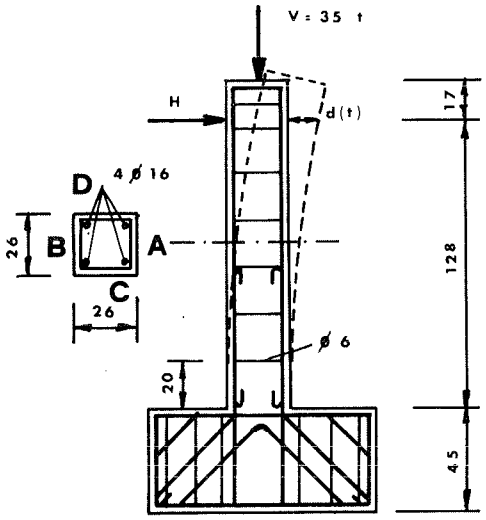

FIG. 1: Test specimens.

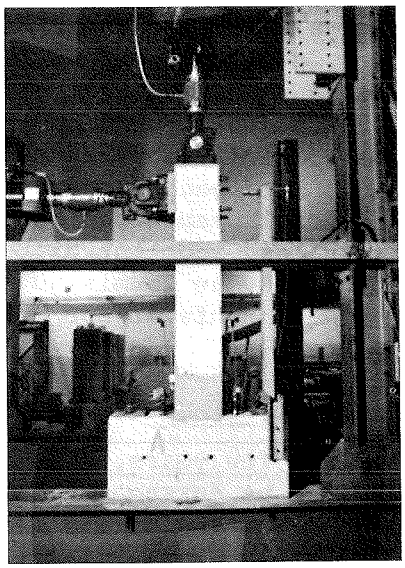

FIG. 2: Test set up.

is not felt to be the best schematization of earthquake actions in structural elements.

Therefore, a new series of 24 specimens has been prepared, each representing a simple full-size half-column and its joint to a rigid beam (Figs.1-2). This paper reports on the tests of the first four specimens in this series.

2. DESCRIPTION OF SPECIMENS.

The new specimens are as shown in Fig. 1. Thery are intended to simulate realistic conditions: for instance, in 12 specimens out of 24, the reinforcing bars are not continuous, but joined by superposition, as in practice it often occurs at the bottom end of concrete columns. All specimens have the same geometrical dimensions, while the nominal diameter of the four longitudinal bars is either 12, 16 or 20 mm: Feb 44 k steel was used for the bars. Each specimen is denoted by a letter (A in case of interrupted bars, B in case of continuous bars), followed by the diameter of the bars (12,16 or 20) and a number (1 to 4): the present paper reports the tests of specimens A 16/1,2,3,4. The 28-day concrete characteristic cubic strength of the A specimens was 515 kgf/cm^2 (52.5 MPa); the dynamic elastic modulus 483500 kgf/cm^2.

The length of the specimen columns is about half the most usual free length is actual buildings. Thus, a transverse force at the top of the specimen gives approximately the same bending moment/shear ratio in the bottom section as in real buildings with rigid beams, subjected to horizontal actions.

3. LOAD HISTORY AND REPAIR PROCEDURES.

The "beam" stub was rigidly fixed to the testing bench, and two hydraulic double-effect jacks were applied at the top of the specimen (Fig. 2): the vertical jack maintained a constant force of 35 t (corresponding to 50 kgf/cm^2 approximately) throughout each test, while the horizontal jack applied a pre-programmed displacement whose typical record, symmetric about the initial position, is shown in Fig. 3: this load history was intended to simulate the most damaging part of the actions during a strong earthquake shock which, apart from the number of cycles, shows roughly the same general shape, as confirmed by many numerical investigations (e.g. Matteuzzi, 1978; Fig. 4). Also, this history, being independent of the specimen response, should allow significative comparisons of the behaviours. (Only in the first test of specimen A 16/1, the horizontal displacement was applied statically; cf. Fig. 9). The reactive force in the horizontal jack was also recorded (Fig.5), and showed that the amplitude of the applied displacement was such that the

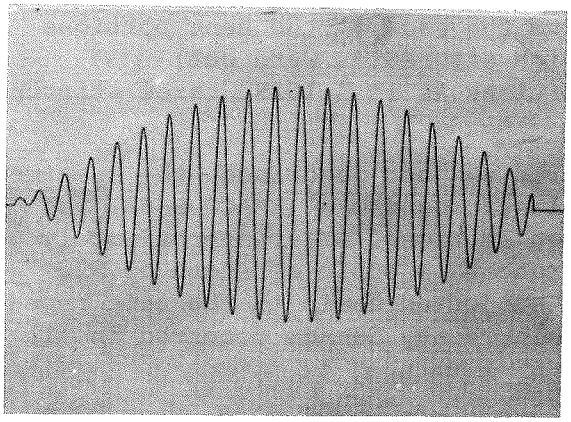

FIG. 3: Typical record of the experimentally applied displacement.

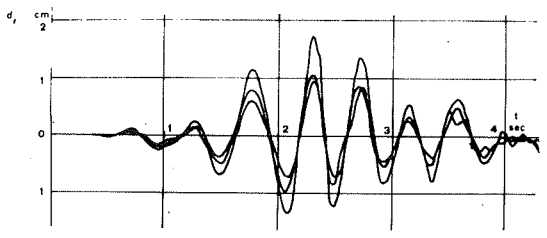

FIG. 4: Typical storey displacements, calculated from the El Centro record.

strength begun deteriorating before the maximum displacement had been reached. Indeed, at the end of the test, heavy damage was evident in the bottom zone of each speciment column: the concrete had cracked and spalled, and the longitudinal bars buckled with permanent waves (Fig. 6).

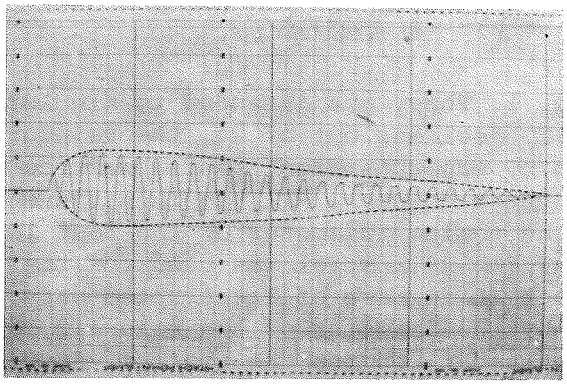

FIG. 5: Record of force in the horizontal jack.

FIG. 6: Specimens A 16/2 after first test (sides B and C of bottom end of column, cf. Fig. 1).

After the first test, the concrete was demolished for a depth of 4-5 cm all around the perimeter of the damaged zone of specimens A 16/1, A 16/2 and A 16/3; in the case of A 16/4, in which the core had been more severely damaged, all concrete was demolished (Fig. 7); then, the reinforcement was repaired in four different ways, namely:

A 16/1: the longitudinal bars were flame-heated and straightened;
A 16/2: besides straightening, three 6-mm-dia. stirrups have been added at 5 cm intervals;
A 16/3: stubs of virgin bars were welded to the ends of the bent portions of the original reinforcement, which afterwards were cut;
A 16/4: besides substition of bent bar portions as in A 16/3, three stirrups were added as in A 16/2.

After the reinforcement had been repaired as just described, the specimens were soaked, and a special premixed rheoplastic concrete (EMACO S-88) was poured, so to restore the original specimen sections. After approximately 28 days (in which the repairing concrete reached a cubic strength of 920 kgf/cm^2 approximately), each specimen was subjected again to the same repeated-load history as in the first test: again, heavy damage occurred in all specimens (Fig. 8).

4. TEST RESULTS AND DISCUSSION.

The forces in the jacks, and the displacements of the specimen top end were recorded with continuity in each test (cf. Figs. 1, 3 and 5); the force recorded in the horizontal jack was then corrected to take account of the relevant component of the vertical force (dotted line in Fig. 5). The strains in the concrete and in the reinforcing bars were also recorded by inductive

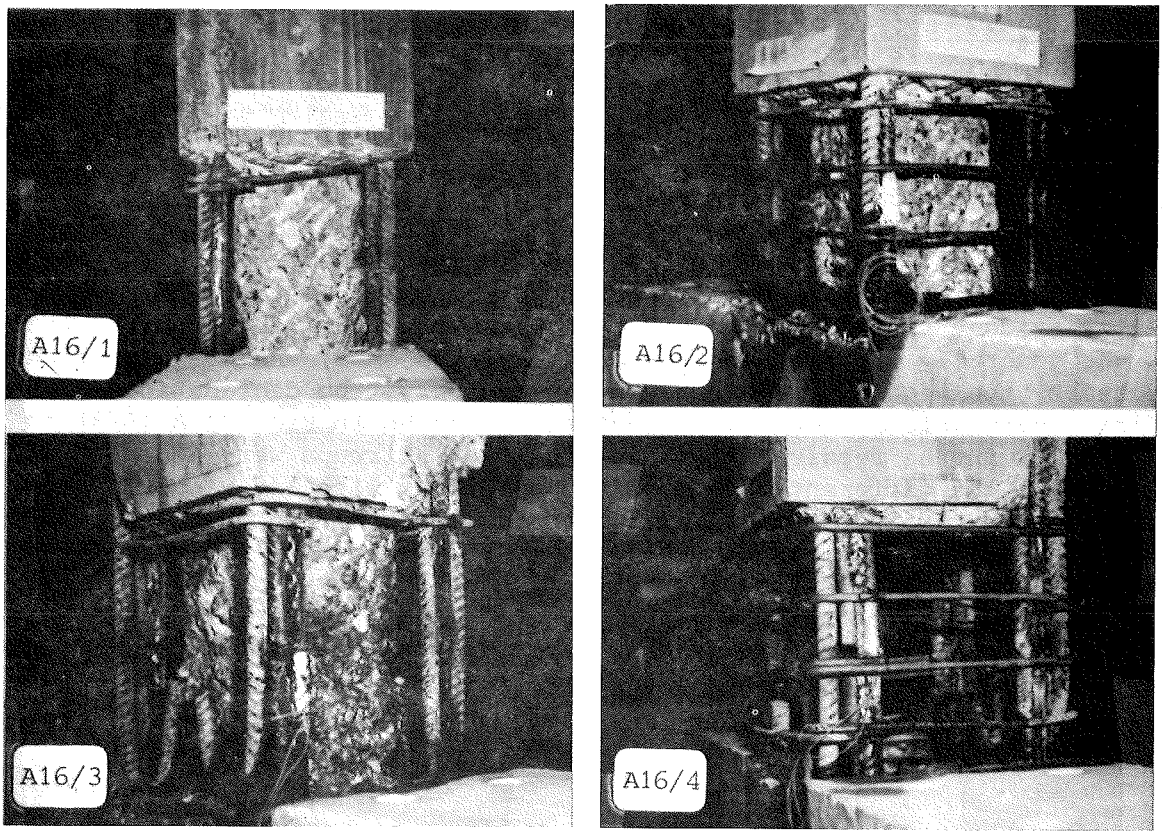

FIG. 7: Repaired specimens, before concreting.

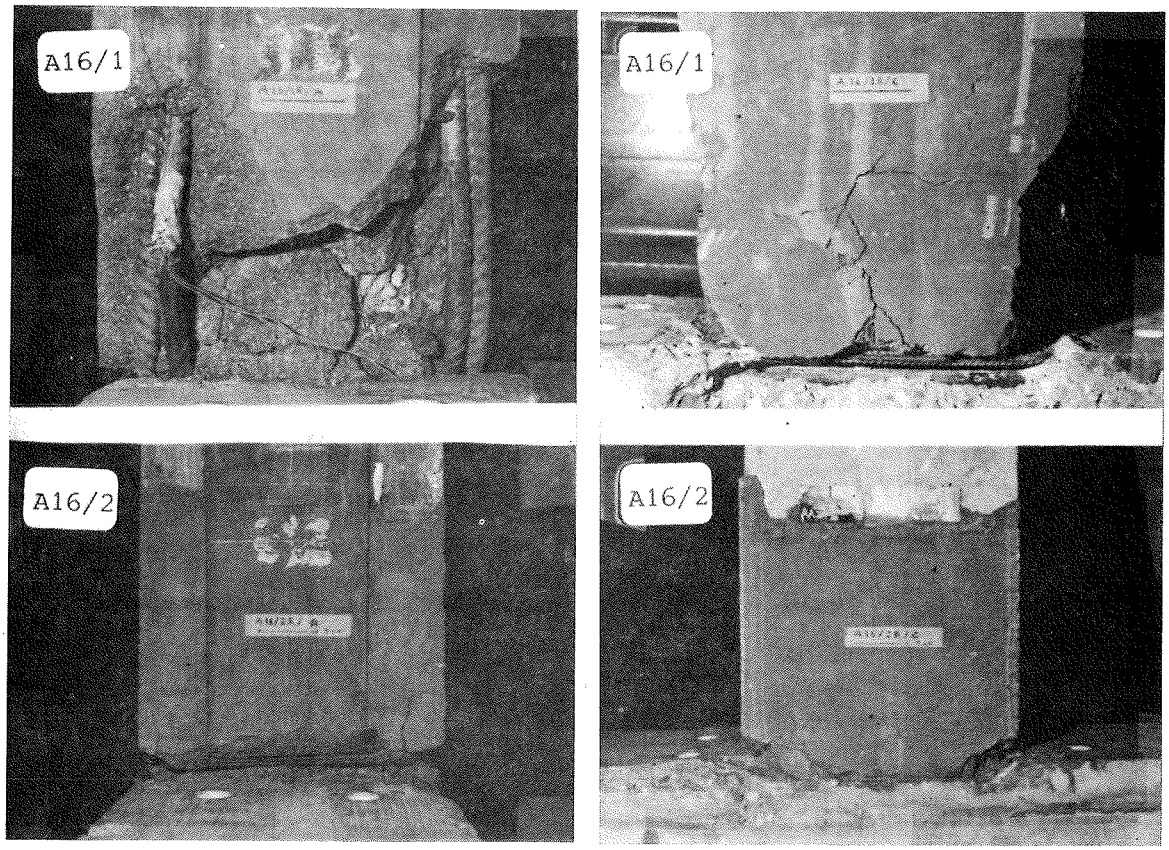

FIG. 8: Specimens A 16/1 and A 16/2 after second test (sides A and C, cf. Fig. 1).

transducers and electric-resistance gauges respectively, but are not reported in the present paper.

The most significative plots are those of the peak corrected horizontal force vs. peak displacement of specimen top end in each loading cycle. The plots for the virgin and repaired specimens are shown in Fig. 9; while Fig. 10 compares the plots of the four repaired specimens.

It is evident from Fig. 9 and 10 that the strength of the repaired specimens was generally higher than that of the virgin ones, and not significantly affected by the repair procedures. On the contrary, the degradation during loading (measurable by vertical segments such as AB in Fig. 9, A 16/3) is much smaller in the repaired specimens in which stirrups were added (A 16/2 and A 16/4): the different aspect of the specimens with and without added stirrups after testing is also remarkable (cf. Fig. 8). On the other hand, it is not possible (at least at the present stage) to distinguish between the effects of straightening or substitution of the buckled bars.

The planned future tests will further investigate these tentative indications. However, it seems already fair to state that the simplicity and effectiveness of the rehabilitation with rheoplastic concrete has been again confirmed.

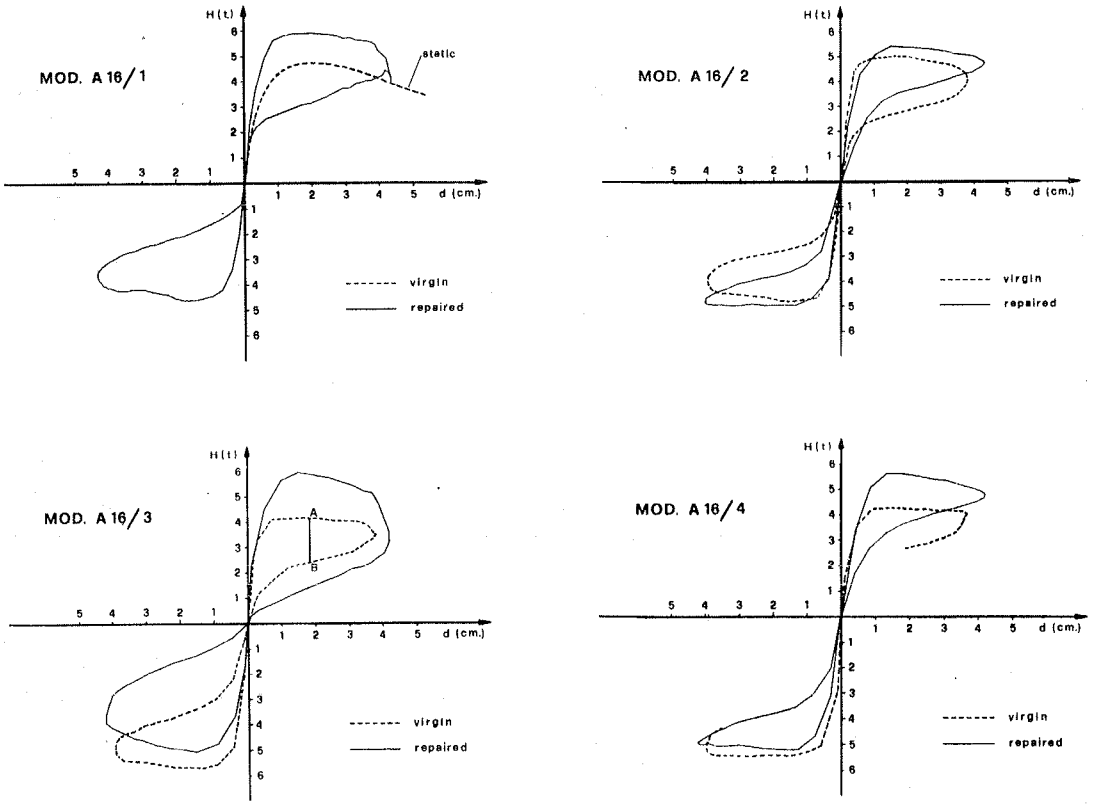

FIG. 9: Peak horizontal force (corrected) H vs. peak horizontal displacement d.

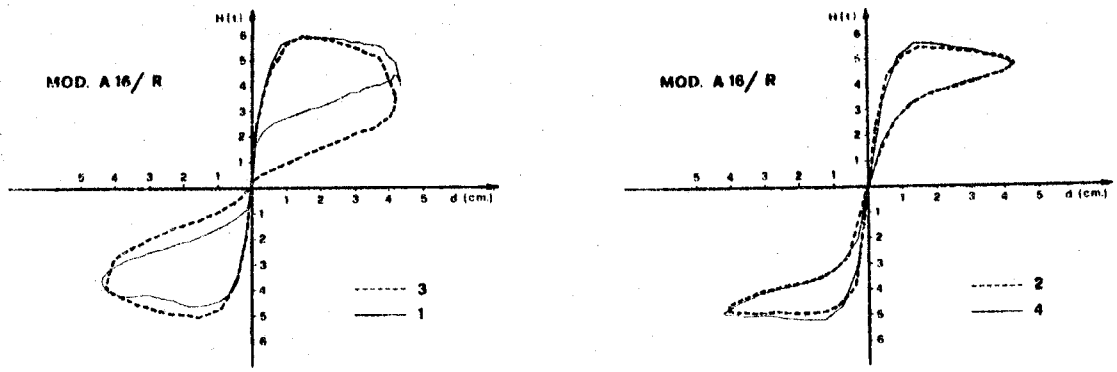

FIG. 10: Peak horizontal force (corrected) vs. peak displacement; repaired specimens.

REFERENCES.

Augusti, G., Avramidou-Maio, N., Focardi, F., and Manzini, E.; 1978: "Tests of R.C. structural components subjected to Repeated Loads and Repaired"; 6. E.C.E.E., Dubrovnik, Vol.1 (p.143).

Gulkan, P.; 1977: "The inelastic response of Repaired R.C. Beam-column connections"; 6. W.C.E.E., New Delhi, Vol.7(55).

Lee, D., Wight, J., and Hanson, R.; 1977: "Repair of Damaged R.C. Frame structures"; 6. W.C.E.E., New Delhi, Vol.7(67).

Matteuzzi, M.; 1978: Dr.Ing. Thesis; Dept. of Civil Engineering, Università di Firenze.

Tassios, T., Vassiliou, G., and Plainis, P.; 1977: "Mechanical behaviour of Repaired R.C. structures under Static and Dynamic load"; 6. W.C.E.E., New Delhi, Vol.7(109).

-; 1976-77: "Malte speciali per ripristini strutturali"; Il Calcestruzzo oggi; Vol.9, nn.1-2.

ACKNOWLEDGEMENTS.

This research is supported, in parts, by grants from the Italian National Research Council (C.N.R.). The original specimens, and the materials and workmanship for repairs, were provided by the courtesy of Mc Mediterranea s.p.a., Treviso.